2014-01-01

Depositional And Sequence Stratigraphic Framework Of An Exposed Neoproterozoic Suprasalt Minibasin At Patawarta Diapir, Flinders Ranges, South Australia

Cora Evelyn Gannaway
University of Texas at El Paso, cegannaway@miners.utep.edu

DEPOSITIONAL AND SEQUENCE STRATIGRAPHIC FRAMEWORK OF AN EXPOSED NEOPROTEROZOIC SUPRASALT MINIBASIN AT PATAWARTA DIAPIR, FLINDERS RANGES, SOUTH AUSTRALIA

CORA EVELYN GANNAWAY

Department of Geological Sciences

APPROVED:

Katherine A. Giles, Ph.D., Chair

Richard P. Langford, Ph.D.

Geoffrey B. Saupe, Ph.D.

Charles H. Ambler, Ph.D.
Dean of the Graduate School

Dedication

To Roscoe P. Brown, who never fails to put a smile on my face when I need it most and who is always excited to see me, whether I have been gone for five hours or five weeks.

DEPOSITIONAL AND SEQUENCE STRATIGRAPHIC FRAMEWORK OF AN EXPOSED NEOPROTEROZOIC SUPRASALT MINIBASIN AT PATAWARTA DIAPIR, FLINDERS RANGES, SOUTH AUSTRALIA

by

Cora Evelyn Gannaway, B.S.

THESIS

Presented to the Faculty of the Graduate School of

The University of Texas at El Paso

in Partial Fulfillment

of the Requirements

for the Degree of

MASTER OF SCIENCE

Department of Geological Sciences

THE UNIVERSITY OF TEXAS AT EL PASO

December 2014

Acknowledgements

First and foremost, I wish to thank my parents, Jim and Cass, for supporting me through thick and thin and for giving me every opportunity to succeed regardless the challenges that present themselves. I also owe so much to my sisters and brothers, Marion, James, Callie, and Jackson, who are never more than a phone call away and provide me with never-ending love, support, and encouragement when I need it most.

I owe a tremendous debt of gratitude to Dr. Katherine Giles for the expertise, guidance, and opportunities provided to me through the duration of this project. I thank you for the constant motivation to be a better geologist, educator, and person, and most importantly, to never let the curiosity die.

The numerous sponsors of the Institute of Tectonic Studies Salt-Sediment Interaction Research Consortium at The University of Texas at El Paso are graciously thanked for funding this research project. Current sponsors BHP-Billiton, BP, Chevron, ConocoPhillips, ExxonMobil, Hess, Kosmos Energy, Repsol, and Shell are thanked for their financial support. Additional funding was kindly provided by the American Association of Petroleum Geologists Sherman A. Wengerd Memorial Grant and the Geological Society of America Research Grant.

The many colleagues and friends who have contributed to this project deserve an indescribable amount of thanks. I would like to thank Rachelle Kernen, Thomas Hearon, Mark Rowan, and Carl Fiduk for their technical guidance, knowledge, and feedback throughout course of this research. While we may bicker and banter back and forth during the process, I feel strongly that without your tremendous insight, our conclusions and this final product would be severely lacking. Eric Stautberg also deserves enormous thanks for being a steadfast field companion through sun, wind, rain, and even hail. Nila Matsler is due special thanks for her massive contributions in both logistical and emotional support over the course of this project.

Landowners Keith and Lisa Slade of Moolooloo Station and Stony and Gina Steiner of Warraweena Conservation Park are graciously thanked for unlimited access to the Patawarta area. The extended Fargher family is also thanked for taking care of our research group in Adelaide and the South

Australian outback on innumerable occasions in recent years. The staff at the Adelaide School of Petroleum at the University of Adelaide is thanked for their logistical support over the past several years.

I would like to thank Drs. Rip Langford, Tim Lawton, and Greg Mack for the immense amount knowledge about geology and life that they imparted in both the classroom and the field during my time at UTEP and NMSU. I am lucky to have worked with such exceptional geologists and educators. Additionally, I would like to thank my internship mentor, Aaron Berger, for pushing me beyond my comfort zone, and the rest of the ConocoPhillips Western Gulf of Mexico exploration team for their technical expertise and support during my internship. Lastly, I wish to thank my undergraduate professors at the University of the South, Drs. Martin Knoll, Bran Potter, and Steve Shaver, who sparked my initial interest in the field of geology, educated and challenged me every day in the Snowden classrooms, and ultimately inspired me to become the geologist I am today.

To all of my dear friends at Sewanee, NMSU, and UTEP, I want to thank you all for the laughter, companionship, and good company. I have no doubt that all of these friendships, forged in the field and the classroom over many late nights and early mornings, will last for many years to come.

Abstract

Outcrops of mixed carbonate/siliciclastic strata comprise the Neoproterozoic (Marinoan) Wilpena Group at Patawarta diapir in the Flinders Ranges, South Australia. Patawarta diapir is a ramping allochthonous salt sheet flanked by suprasalt and subsalt minibasin strata. The stratal and structural attributes of the coeval minibasin fills afford a unique perspective on lateral and vertical salt migration and the impacts of salt-modified bathymetry in shallow marine depositional environments. This study documents the depositional and diagenetic facies, stratal thickness trends, and structural style and stratal geometries of the suprasalt minibasin fill and correlates it to the previously studied subsalt minibasin fill. The goal is to develop a predictive model utilizes stratigraphic and structural relationships of suprasalt strata to effectively identify potential characteristics of correlative subsalt strata. Enhanced understanding of potential relationships adjacent to allochthonous salt will allow for improved pre-drill prediction of minibasin reservoir attributes, thereby limiting the risks involved with subsalt petroleum exploration.

The stratigraphic units of interest for this study include the Bunyeroo Formation, Wonoka Formation, and Patsy Hill Member of the Bonney Sandstone, which form parts of two 3rd-order depositional sequences. The Bunyeroo Formation records deposition in a deep, offshore basin to outer shelf environment during the Transgressive Systems Tract of the lower depositional sequence. The formational contact between the Bunyeroo Formation and overlying Wonoka Formation is interpreted as the maximum flooding surface. The Wonoka Formation represents a regional regressive sequence deposited in a storm-dominated carbonate shelf environment, whereby the lower, middle, and upper limestone, and green mudstone members reflect upward-shallowing outer shelf to shoreface, foreshore, lagoonal, and subtidal to intertidal settings. The Patsy Hill Member, which includes the lower dolomite, sandstone, and upper dolomite beds, records deposition in a barrier bar-lagoonal complex. The lower dolomite beds of the Patsy Hill Member reflect ongoing normal regression from the underlying Wonoka Formation to an intertidal setting, whereas the sandstone and upper dolomite beds document a non-Waltherian shift to more basinward deposition in the barrier bar-lagoonal complex. Therefore, the Wonoka Formation and Patsy Hill lower dolomite beds comprise the Highstand Systems Tract of the lower depositional sequence, while the Patsy Hill sandstone and upper dolomite beds form the Lowstand

Systems Tract of the upper depositional sequence. An erosional unconformity between the Patsy Hill lower dolomite and sandstone beds is interpreted as the sequence boundary separating the lower and upper depositional sequences.

Suprasalt Bunyeroo, Wonoka, and Patsy Hill strata thin gradually, but dramatically towards Patawarta diapir from ~3500 to 20 m over distances of 3-6 km, primarily by low-angle onlap and depositional thinning with local angular stratal truncations. Flanking suprasalt Wilpena Group strata form a broad, open fold above the allochthonous salt body with significant thinning, but only minor halokinetic upturn, which represents minibasin-scale folding and thinning. The local angular stratal truncations documented at the basal contact of the Wonoka middle limestone member and at the sequence boundary within the Patsy Hill Member are interpreted as tapered composite halokinetic sequence boundaries adjacent to the suprasalt margin.

Correlation of suprasalt strata to the previously studied subsalt strata utilizes the depositional sequence stratigraphy to evaluate characteristic stratigraphic, geometric, and halokinetic relationships in coeval minibasin fills. Wonoka strata reflect consistent trends in depositional facies and interpreted depositional settings between the suprasalt and subsalt minibasins with the exception of the uppermost green mudstone member. Patsy Hill strata vary significantly in regards to depositional facies and interpreted depositional settings in the suprasalt and subsalt minibasins. Subsalt Bunyeroo, Wonoka, and Patsy Hill strata form two stacked tapered composite halokinetic sequences, whereby significant folding and thinning occurred within 560 m of the subsalt-sediment interface. Because halokinetic sequence boundaries developed in different stratigraphic levels in the coeval minibasins despite presumably analogous sedimentation rates, it is concluded that halokinetic deformation cannot be correlated from one side of an allochthonous salt body to another. The stratigraphic and structural analysis of suprasalt strata flanking Patawarta diapir and correlation to coeval subsalt strata reveal that, despite many similarities in the shallow marine environment, the depositional and halokinetic history of coeval minibasin fills do not display characteristic, predictable relationships. Although this does not allow for a predictive model of the characteristics of subsalt minibasin fill based on correlative suprasalt strata, it does contribute to a growing catalogue of petroleum system possibilities that ideally reduce exploration risks.

Table of Contents

List of Figures

List of Plates

Chapter 1: Introduction

Current models of salt tectonics are derived primarily from the analysis of subsurface geophysical datasets and scaled laboratory and computer modeling (Jackson, 1995). The geophysical datasets are almost exclusively from offshore salt basins with current petroleum exploration, such as the Gulf of Mexico, the North Sea, and the South Atlantic conjugate margins of offshore Brazil (e.g. Campos and Santos Basins) and offshore West Africa (Jackson and Talbot, 1991; Hudec and Jackson, 2011). In the past, these data were two-dimensional (2-D) surveys, but now consist primarily of higher quality three-dimensional (3-D) surveys. Despite advances in both acquisition and processing, there is often poor resolution adjacent to salt structures. This is particularly true in subsalt environments associated with allochthonous salt sheets (Figure 1). Subsalt settings have potentially large hydrocarbon accumulations (Jackson and Talbot, 1991; Schultz-Ela and Jackson, 1996), but image very poorly due to the overlying salt. In contrast, seismic resolution of suprasalt minibasins is typically very high (Jackson and Talbot, 1991).

Pre-drill prediction of the geometry and continuity of subsalt minibasin reservoirs is essential to successful exploration strategies in these complex trap styles (Hart and Albertin, 2001; Hart et al., 2004). However, the lack of outcrop documentation of allochthonous salt structures and their adjacent suprasalt and subsalt minibasin stratigraphic architecture means predictive models for this type of salt tectonics remain inadequate (Moore et al., 1995; Schultz-Ela and Jackson, 1996; Dyson and Rowan, 2004). This study explores the nature and relationship of basin fill architecture between outcropping subsalt and suprasalt minibasins adjacent to allochthonous salt. It remains unclear to what extent the depositional and halokinetic stratigraphic history of adjacent subsalt and suprasalt minibasins are related or completely independent. However, detailed outcrop study of growth strata adjacent to allochthonous salt sheets allows for interpretations and constraints on potential stratigraphic and geometric relationships expected between suprasalt and subsalt settings that may be applied to both ancient and modern salt systems around the world.

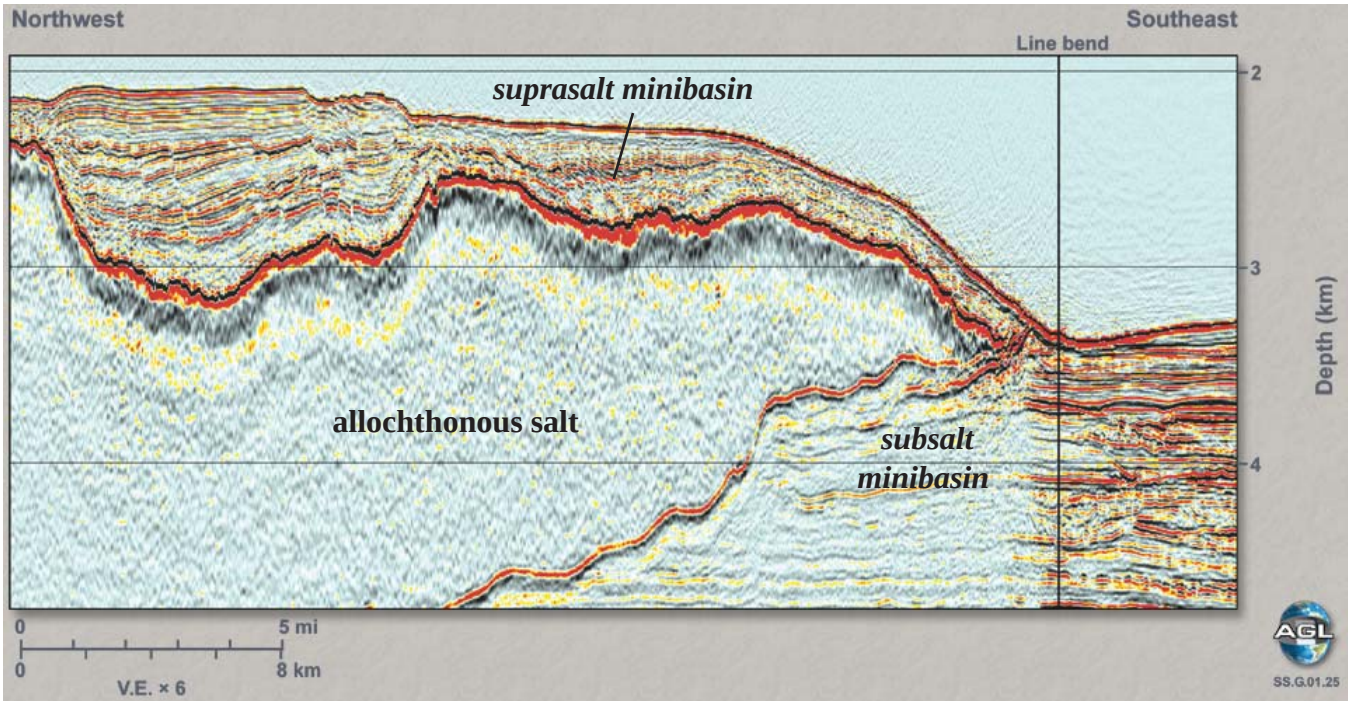

Figure 1. Seismic image of an allochthonous salt body with associated suprasalt and subsalt minibasin strata; note that subsalt structure and stratal geometries are difficult to discern near the salt-sediment interface due to the proximity of overlying salt (from Hudec and Jackson, 2011).

1.1 Allochthonous Salt

Allochthonous salt sheets are most recently defined by Hudec and Jackson (2006) as "subhorizontal or moderately dipping, sheetlike salt diapirs emplaced at stratigraphic levels above the autochthonous source layer." Due to the ramping nature of an advancing allochthonous salt sheet, synkinematic minibasins develop in subsalt and suprasalt positions (Figure 1; Jackson and Talbot, 1991; Hart et al., 2004). Outcrop examples of allochthonous salt bodies have been documented in the Flinders Ranges of South Australia, Katangan Copperbelt of Zambia, Sivas Basin of Turkey, Sverdrup basin of northern Canada, and Zagros Ranges of southern Iran (Dyson, 1996; Jackson et al., 2003; Sherkati et al., 2005; Jackson and Harrison, 2006; Giles and Rowan, 2012; Kernen et al., 2012; Ringenbach et al., 2013; Callot et al., 2014; Hearon et al., 2014).

1.2 Stratal Geometries of Minibasin Fill

Recently, growth strata associated with passively rising salt diapirs and associated allochthonous salt sheets have been categorized into unconformity-bound stratigraphic packages termed 'halokinetic sequences' (Giles and Lawton, 2002, Rowan et al., 2003, Giles and Rowan, 2012). Halokinetic sequences are fundamental components of salt-related growth strata and are commonly present in salt basins containing near-surface diapiric or extrusive salt bodies (Giles and Lawton, 2002). These unconformity-bound stratal packages are genetically influenced by salt movement and are characterized by two end-member types, termed hook and wedge halokinetic sequences (Giles and Lawton, 2002; Giles et al., 2004; Giles and Rowan, 2012). The two types are distinguished by distinct drape-folding geometries, scale of deformation, and degree of discordance of bounding angular unconformities (Figure 2). Hook halokinetic sequences display tight drape-fold geometries, narrow zones of deformation, bed rotation up to 90°, and high-angle bounding unconformities that become conformable within approximately 200 m of the diapir. Wedge halokinetic sequences display open drape-fold geometries, broad zones of deformation, minor rotation of beds, and low-angle bounding unconformities that become conformable between 0.5-1.5 km from the diapir margin. When stacked stratigraphically, halokinetic sequences form composite halokinetic

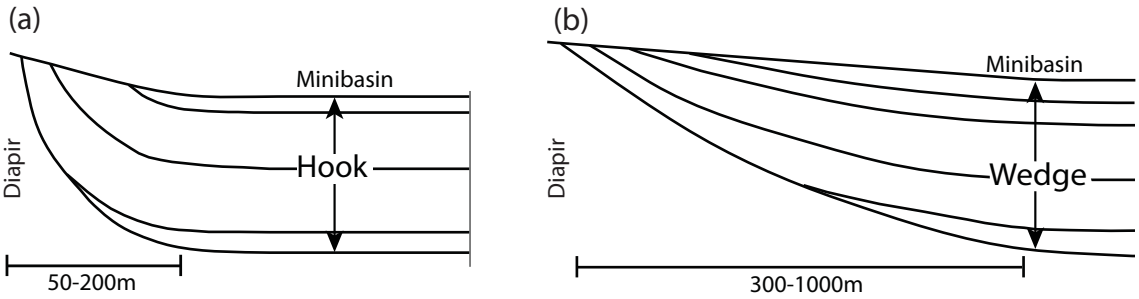

- Drape folding 50-200m from diapir.
- ≤ 90 degree angular unconformities.
- Near-diapir abrupt facies changes.

- Drape folding 300-1000m from diapir.
- <30 degree angular unconformities.
- Broad zone of gradational facies changes.

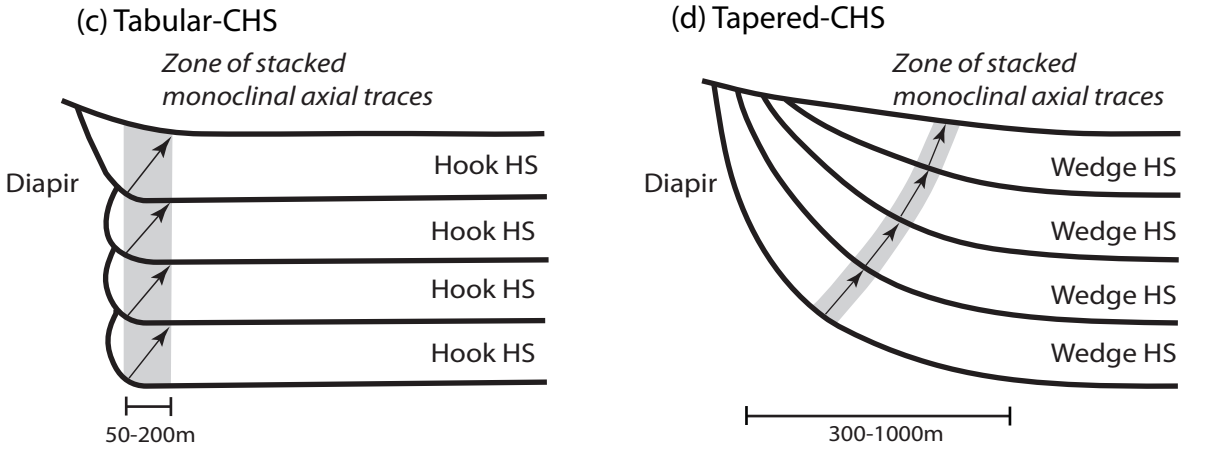

- Subparallel base and top boundaries.
- Narrow zone of thinning near diapir.
- Axial trace of monocline near diapir & forms zone parallel to diapir margin.

- Convergent base and top boundaries.
- Broad zone of thinning toward diapir.
- Axial trace of monocline progressively inclined from diapir.

Figure 2. Halokinetic sequences, (a) hook and (b) wedge, and composite halokinetic sequences, (c) tabular and (d) tapered (modified from Giles and Rowan, 2012).

sequences; stacked hook and wedge halokinetic sequences form tabular and tapered composite halokinetic sequences, respectively (Figure 2; Giles and Rowan, 2012).

Generation of halokinetic sequences adjacent to passive diapirs is driven by variations in net diapir rise rate relative to local sediment accumulation rate (Giles and Lawton, 2002; Rowan et al., 2003). The interplay of salt rise and sediment accumulation results in fluctuations of topographic relief over the diapir. Hook halokinetic sequences form when the relative diapir rise rate outpaces the rate of sediment accumulation, producing high topographic relief and associated abrupt near-diapir facies changes. In contrast, wedge halokinetic sequences form when the local sediment accumulation rate exceeds the relative rate of diapir rise, which results in low topographic relief and associated gradual and broad facies changes (Giles and Rowan, 2012).

Stratal folding and thinning in salt-withdrawal minibasins can occur over broader zones (>1.5 km) than those defined for halokinetic sequences. Minibasin-scale folding and thinning forms stratal packages with shallow dips and less angular discordance. Differential loading and minibasin subsidence into an underlying salt layer or salt body can drive withdrawal and/or inflation of salt. The various resulting geometries, including synclinal minibasins, turtle or half-turtle structures, expulsion rollovers, and megaflaps, all exhibit minibasin-scale folding and thinning (Figure 3; Giles and Rowan, 2012).

1.3 Lateral Caprock at Minibasin Margins

Passive salt diapirs and allochthonous salt sheets may also develop diagenetic caprock assemblages, which become incorporated through time into the minibasin fill and associated growth strata by analogous processes of salt inflation and halokinetic drape-folding. Diagenetic caprock forms when an evaporite body is exposed to undersaturated waters. It is a laminar to irregular, zoned mantling of anhydrite, gypsum, and/or carbonate that forms at the salt-sediment boundary on top of salt diapirs (Figure 4; Enos and Kyle, 2002). The anhydrite zone forms as an insoluble residue after the dissolution of halite by undersaturated, typically meteoric pore waters. As diapirism continues, compaction and cementation follow and produce a thick section of dense, laminated anhydrite (Kyle and Posey, 1991; Enos and Kyle, 2002; Warren, 2006). Numerous dissolution and compaction cycles accumulate over time in

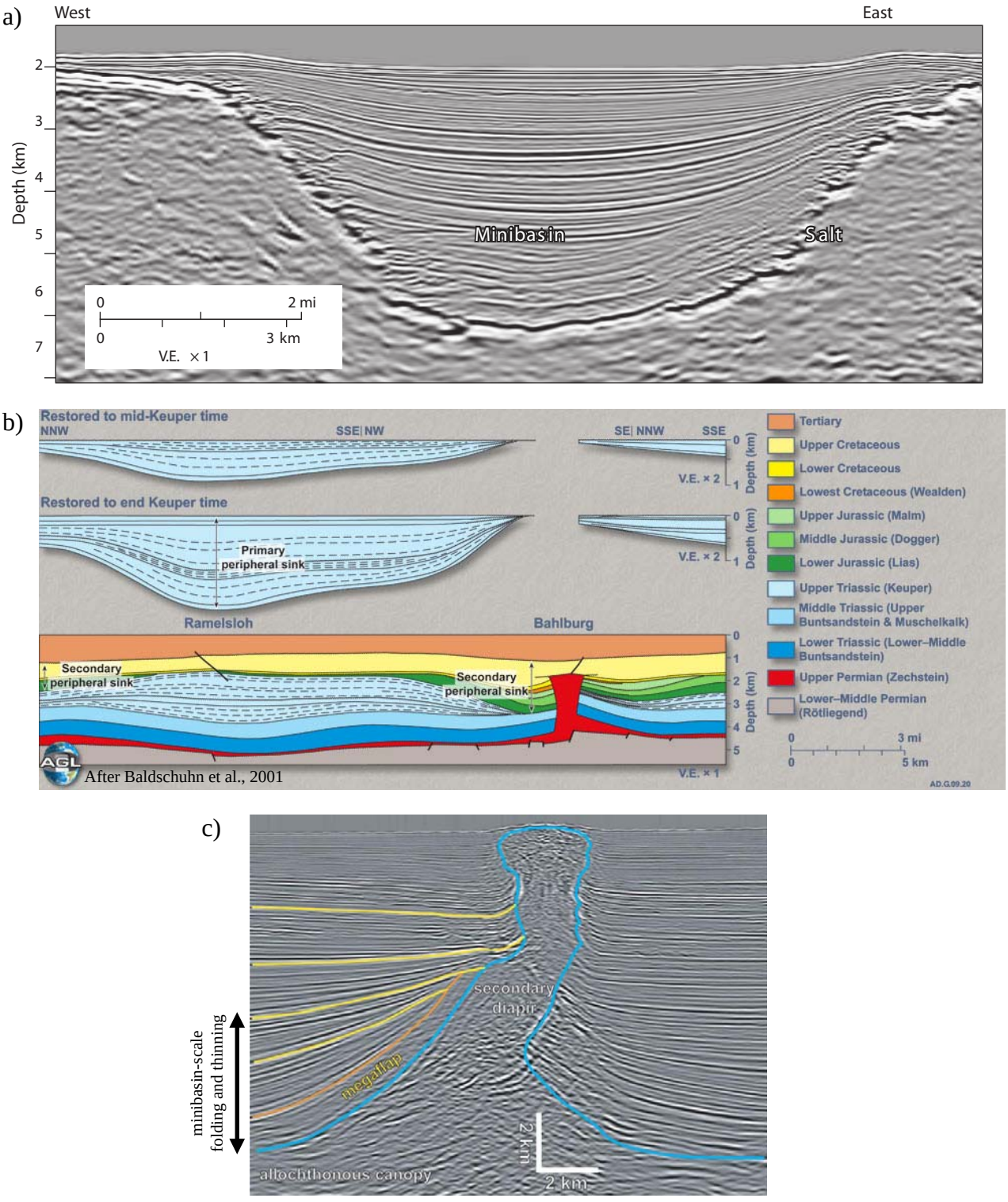

Figure 3. Differential loading and minibasin subsidence into underlying salt may result in various geometries exhibiting minibasin-scale folding and thinning: a) synclinal minibasin subsiding into thick allochthonous salt, northern Gulf of Mexico (from Hudec et al., 2009); b) turtle structure developed in primary minibasin, North German Basin (from Hudec and Jackson, 2011); c) megaflap and onlapping stratal wedge adjacent to secondary diapir, northern Gulf of Mexico (from Giles and Rowan, 2012).

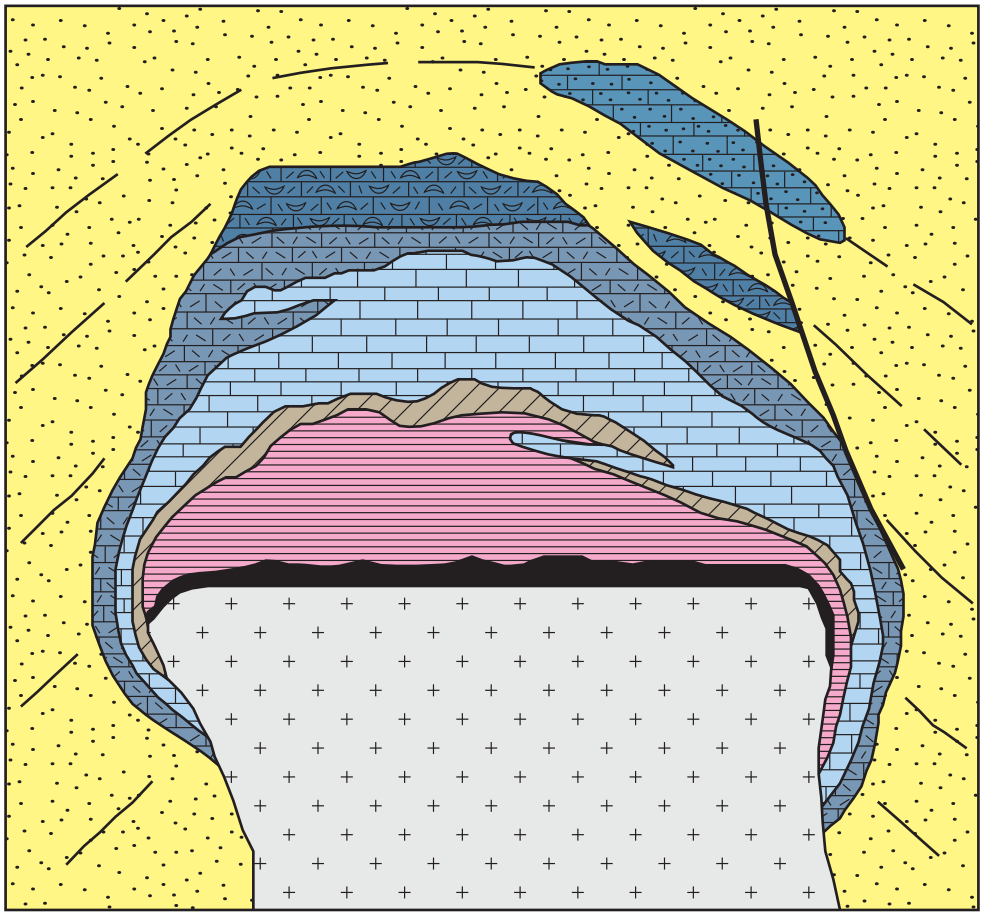

EXPLANATION

- Cenozoic sediments
- False calcite caprock
- Marine calcite caprock
- Variegated calcite caprock
- Banded calcite caprock
- Gypsum (transitional) caprock
- Anhydrite caprock
- Salt dissolution zone
- Salt stock

Figure 4. Cross-sectional view of a Gulf Coast salt dome with generalized caprock lithologic zonation (modified from Enos and Kyle, 2002).

stratigraphically reversed position, whereby the youngest layers are located at the anhydrite caprock-halite diapir contact (Enos and Kyle, 2002). Rehydration of the upper part of the anhydrite zone can result in irregular pods of gypsum (Warren, 2006). In the presence of hydrocarbons, anhydrite and gypsum may be converted to carbonate by dissolution and anaerobic bacterial sulphate reduction (Kyle and Posey, 1991; Enos and Kyle, 2002; Warren, 2006). With continued diapiric rise, caprock may also halokinetically drape-fold and rotate off the top of the diapir into a position on the diapir flank and minibasin margin, where it is termed 'lateral caprock' (Giles et al., 2012).

1.4 Research Objectives

Patawarta diapir is a ramping allochthonous salt sheet in the Flinders Ranges of South Australia that affords a unique perspective on lateral and vertical salt migration and the sedimentary processes that fill adjacent subsalt and suprasalt minibasins (Figure 5; Dyson, 1996; Giles and Rowan, 2012; Hearon et al., 2014). Because of the oblique plane of section exposed at Patawarta diapir, both subsalt and suprasalt geometries are visible flanking the allochthonous salt body (Kernen, 2011; Kernen at al., 2012; Hearon, 2013; Hearon et al., 2014). Although only two-dimensional exposures are present, outcrop examples such as Patawarta diapir allow for the analysis of multiple factors controlling the variable depositional settings, stratal thicknesses and geometries, and styles of structural deformation associated with coeval suprasalt and subsalt minibasins flanking ramping allochthonous salt sheets.

This study is an outcrop-based investigation designed to identify characteristics of suprasalt minibasin fill associated with a ramping allochthonous salt sheet. The goal is to test the hypothesis that stratal and structural relationships present in a suprasalt minibasin can be used to predict the characteristics of the poorly imaged, correlative subsalt minibasin strata. If valid, a predictive model for coeval depositional facies, stratal thickness trends, and structural styles and stratal geometries will be developed. The specific objectives include the following: (1) document depositional facies types and distribution, depositional settings, unit thicknesses, stratal geometries, and structural style of suprasalt minibasin fill, (2) correlate to the previously studied subsalt stratigraphy within both a depositional and halokinetic sequence stratigraphic framework, (3) generate a depositional model that accounts for vertical and lateral

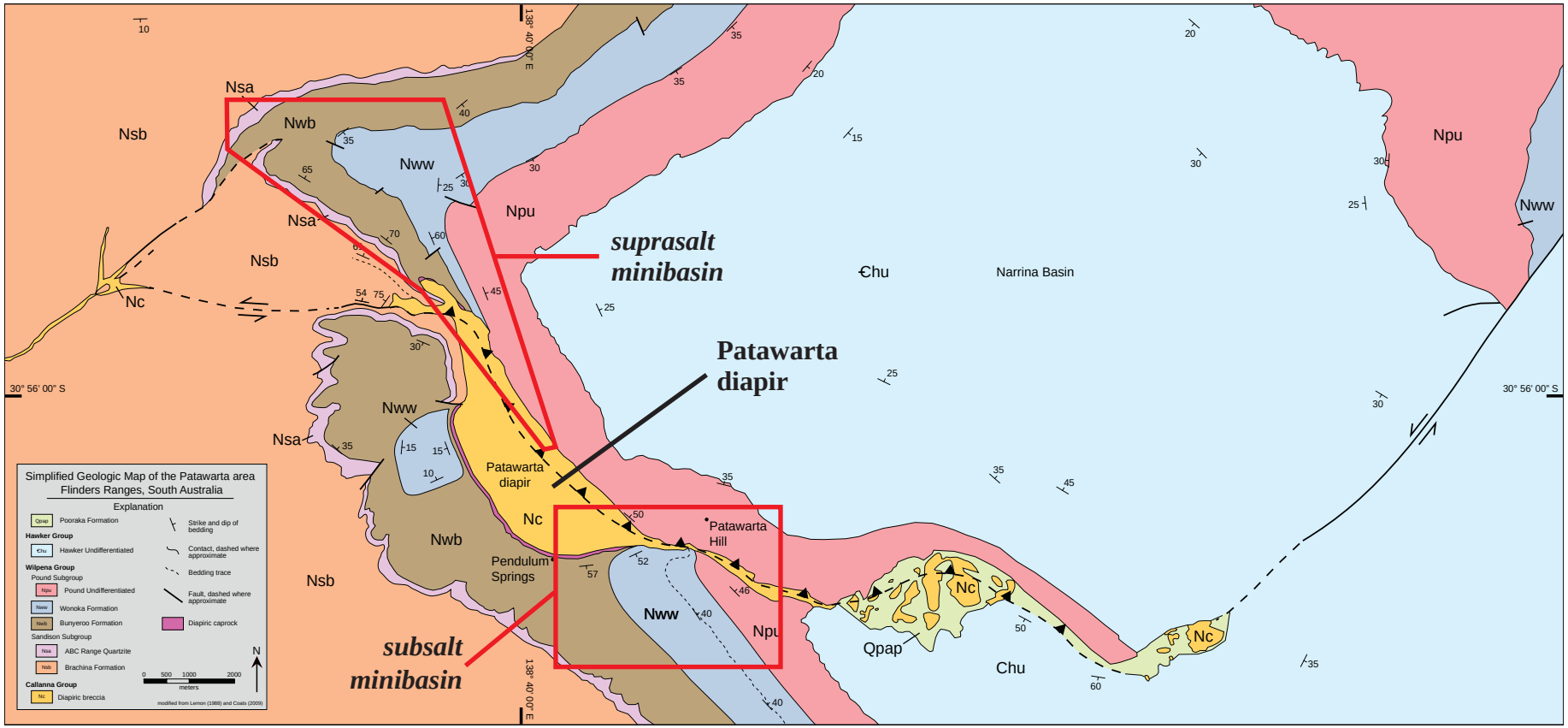

Figure 5. Simplified geologic map of Patawarta diapir in the Flinders Ranges, South Australia; flanking subsalt and suprasalt minibasins are designated by red boxes; map view of the Patawarta area is an oblique cross-section (modified from Hearon, 2013).

salt migration, (4) determine impacts of allochthonous salt-modified bathymetry on shallow marine depositional environments, and (5) determine occurrence and correlatability of lateral caprock units in minibasin successions. A better understanding of potential stratigraphic and geometric relationships adjacent to allochthonous salt will reduce exploration risk by allowing for more successful pre-drill prediction of subsalt minibasin reservoir characteristics.

Chapter 2: Geologic Setting of Patawarta Diapir

Patawarta diapir is located in the Flinders Ranges of South Australia (Figure 6). The Flinders Ranges contain Neoproterozoic to Cambrian strata that were deposited in the northern part of a north-south trending, deeply subsiding rift basin complex variously referred to as the Adelaide Geosyncline, Adelaide Fold Belt, or Adelaide Basin (e.g. Sprigg, 1952; Preiss, 1987; Jenkins, 1990; Preiss, 2000). Bounded by the Gawler Craton to the west and Curnamona Province to the east, the Adelaide Fold Belt developed as an aulocogen through at least five significant cycles of continental rifting as western Laurentia and Australia separated during the breakup of the Neoproterozoic Rodinian supercontinent (Figure 7; Sprigg, 1952; Dyson, 1996; Preiss, 2000). A thick succession (>15 km) of Neoproterozoic to Middle Cambrian strata comprises the sedimentary fill as the failed rift basin underwent deep subsidence during early rifting followed by thermal subsidence (Figure 8; Sprigg, 1952; Preiss, 2000).

Following the cessation of rifting in the Sturtian, a major episode of crustal shortening known as the Delamerian Orogeny deformed and inverted the rift basin (Figure 8; Preiss, 2000). Although the generally accepted timing of deformation places the orogeny in the Late Cambrian to Ordovician (~500 Ma) (e.g. Preiss, 1987, 2000), some researchers suggest an earlier initiation in the latest Neoproterozoic or early Cambrian (e.g. Jenkins, 1990; Rowan and Vendeville, 2006). Delamerian deformation of the Adelaide Fold Belt has been subdivided into three tectono-stratigraphically distinct zones (Figure 6). The Northern Flinders Ranges is an arcuate zone of tight east-west oriented folding. The Central Flinders Ranges contains broad open folds with a generally north-south orientation. The Mt. Lofty-Olary fold belt is the southernmost zone and includes the Southern Flinders Ranges, Houghton Anticlinal Zone, Inner Nackara Arc, and Outer Fleurieu Arc, where distinct tectonic signatures define each sub-zone (Haines, 1987; Preiss, 1987). Preiss (1987) attributes the overall dome-and-basin geometry that developed in the Flinders Ranges to three phases of shortening with variable orientations: northwest/southeast, north/south, and north-northwest/south-southeast. Alternatively, Rowan and Vendeville (2006) suggest that Delamerian shortening of an inherited morphology of weak salt diapirs and strong sedimentary minibasins resulted in these dome-and-basin structures.

Figure 6. Generalized map of the Adelaide Fold Belt showing tectono-stratigraphic zones and the location of Patawarta diapir in the north-central Flinders Ranges; inset map of Australia indicates the approximate location of the Flinders Ranges (modified from Preiss, 1987 and Hearon, 2013).

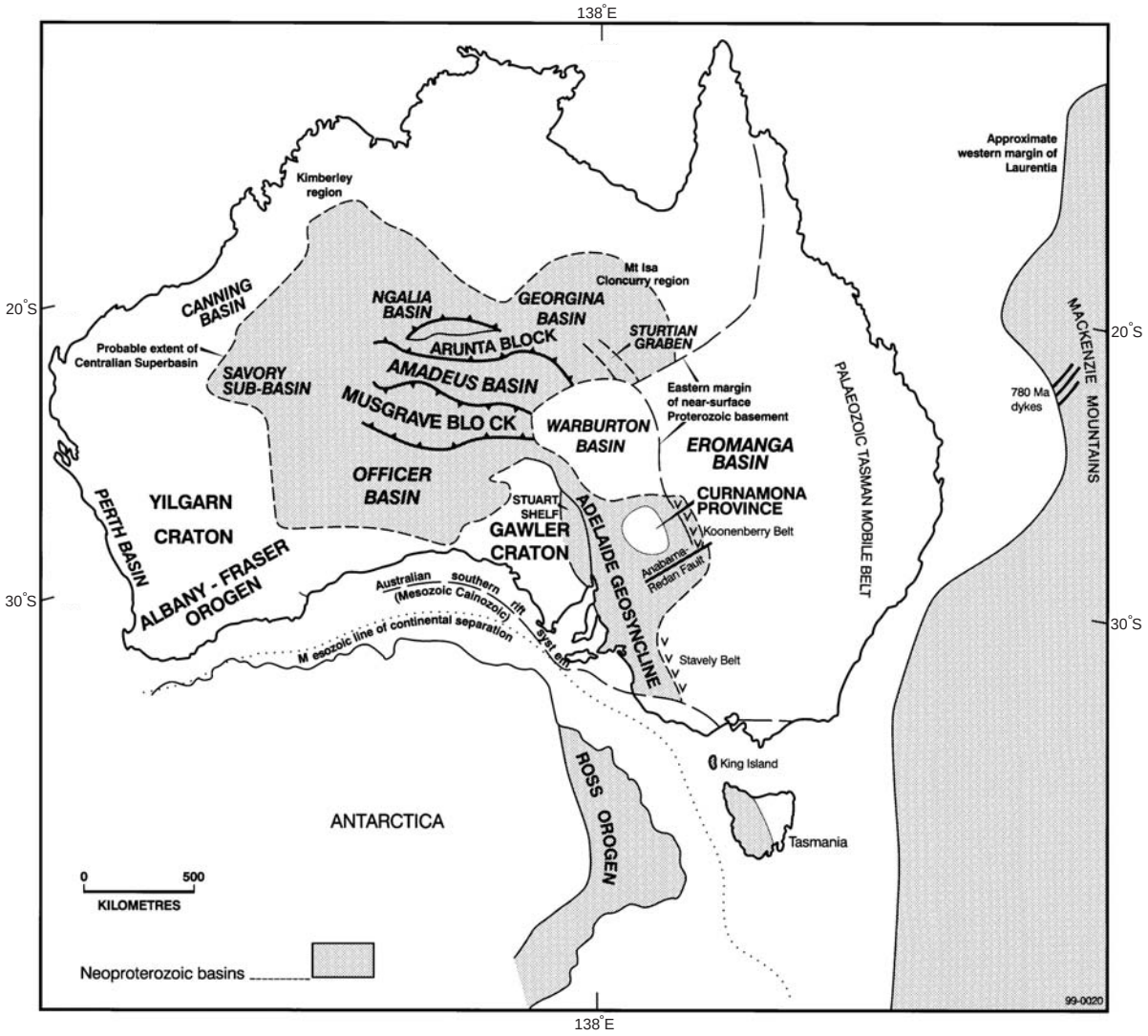

Figure 7. Location of the Adelaide Geosyncline and rift-bounding features of the Gawler Craton and Curnamona Province with regard to western Laurentia and Antartica and other Neoproterozoic basins formed during the continental breakup of Rodinia; longitudes and latitudes reflect present-day location of Australia (from Preiss, 2000).

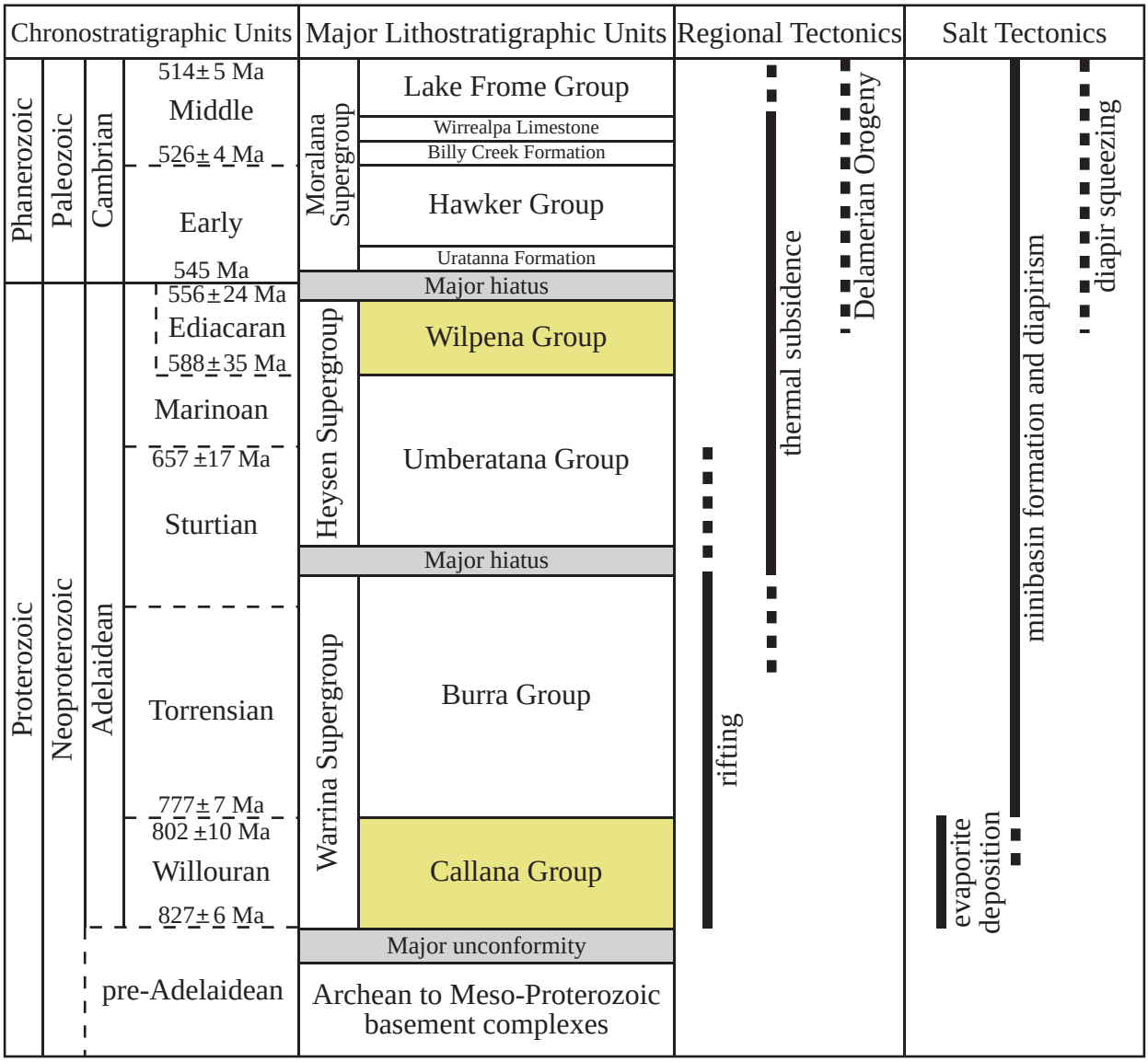

Figure 8. Generalized timing of Neoproterozoic and Cambrian chronostratigraphic and lithostratigraphic units in relation to major regional and salt tectonic events of the Adelaide Fold Belt (modified from Preiss, 1987, Kernen et al., 2012, and Hearon et al., 2014). Light yellow boxes designate major lithostratigraphic units of interest for this study.

The sedimentary rift basin fill was deposited contemporaneously with long-lived (>250 m.y.), widespread passive diapirism (Preiss, 1987; Dyson, 1996). Major diapiric structures in the Flinders Ranges are derived from evaporites of the Callana Group (Figure 8), a layered sequence of incompetent detrital, carbonate, and evaporite sediments and mafic igneous rocks that are now represented by megabreccia bodies (Dyson, 1996; Preiss, 2000; Dyson and Rowan, 2004). Forming the base of the Adelaidean succession, the Callana Group was deposited from approximately 850-800 Ma unconformably above metamorphic and igneous rocks of the Archean and Meso-Proterozoic basement complexes. The Callana Group is overlain by the late Neoproterozoic (Adelaidean) Burra, Umberatana, and Wilpena groups and early Cambrian Hawker Group (Figure 8; Preiss, 1987, 2000). Mobilization of the Callana layered evaporite sequence and initiation of passive diapirism is documented by at least the time of Burra Group deposition (Dyson, 1996, 2004; Rowan and Vendeville, 2006), but some evidence suggests halokinetic deformation may have even begun during deposition of Callana strata (Dyson, 2004). The Callana non-evaporite layers were subsequently fragmented and mixed by entrainment within the more mobile evaporite bodies. No evaporite sediments remain at the surface today, and instead Callana-derived diapiric structures are characterized by a megabreccia, referred to as diapiric breccia. It consists of carbonate matrix surrounding heavily altered detrital, carbonate, and igneous clasts, which range in size from centimeters to several hundred meters (Coats, 1964; Preiss, 1987, 2000; Hearon, et al., 2014).

Patawarta diapir is a ramping allochthonous salt sheet in the northern Central Flinders Ranges and one of more than 180 exposed diapirs in the Adelaide Fold Belt (Figure 6; Dyson, 1996; Lemon, 1988, 2000; Hearon et al., 2014). It is a 15 km^2 elongate body of diapiric breccia (Figure 5) located approximately 15 km to the northeast of the town of Blinman (Figure 6). Basin inversion related to the Delamerian Orogeny tilted the Patawarta area to expose an oblique plane of section, whereby both subsalt and suprasalt stratal geometries are visible adjacent to the allochthonous salt body (Figure 5; Kernen, 2011; Hearon et al., 2014). Flanking stratigraphic units at Patawarta diapir (Figures 8 and 9) comprise the Marinoan Wilpena Group and include, in ascending stratigraphic order, the Brachina Formation, ABC Range Quartzite, Bunyeroo Formation, Wonoka Formation, Bonney Sandstone, and Rawnsley Quartzite (Preiss, 1987, 2000). The stratigraphic units of primary interest for this study are the Bunyeroo Formation,

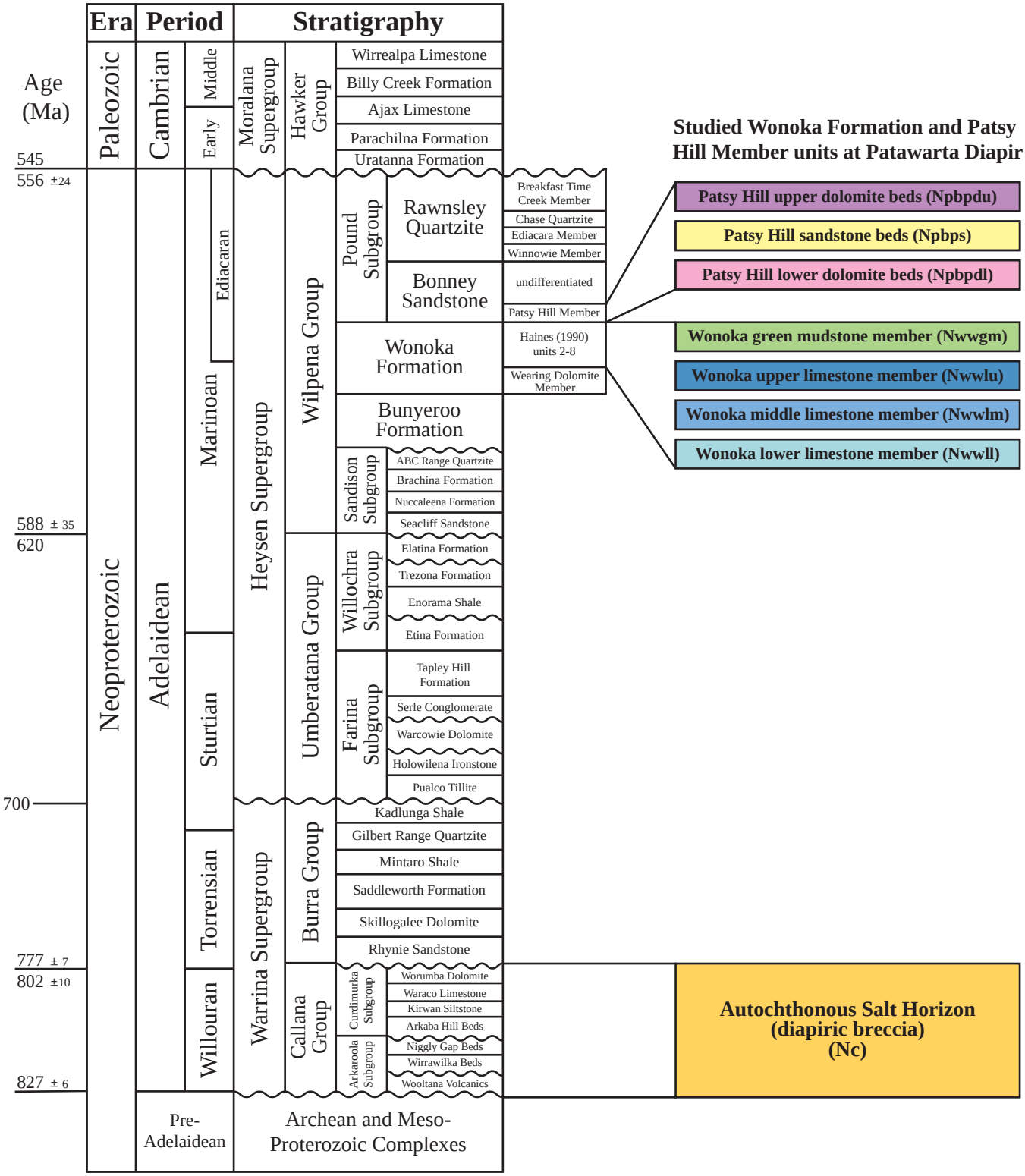

Figure 9. Stratigraphy of the Adelaide Fold Belt with relevant nomenclature, subdivisions, and associated map units highlighted (adapted from Kernen et al., 2012; modified from Preiss, 1987).

Wonoka Formation, and basal Bonney Sandstone (Patsy Hill Member), which are exposed in the suprasalt minibasin at Patawarta diapir.

2.1 Stratigraphy

Wilpena Group stratigraphic nomenclature and subdivisions have varied significantly since initially described by Selwyn (1860) as "olive-brown and blue sandy shales, and thin calcareous shales lying beneath thick sandstones and quartzites" (Figure 10). Following Mawson's (1938, 1939, 1941) initial definitions, numerous workers have described, interpreted, and redefined the Wilpena Group stratigraphy in the Flinders Ranges (e.g. Dalgarno and Johnson, 1964, 1966; Gostin and Jenkins, 1983; Haines, 1987, 1990; Reid and Preiss, 1999; Preiss, 2000). Recent work at Patawarta diapir by Kernen (2011) and Kernen et al. (2012) on diapir-adjacent subsalt stratigraphy redefined units within the Marinoan Wonoka Formation and Patsy Hill Member of the Bonney Sandstone. This study adopts the nomenclature of Kernen et al. (2012) for consistency purposes (Figure 10).

2.1.1 Bunyeroo Formation

The Marinoan Bunyeroo Formation maintains an average thickness of 400 m in the Central Flinders Ranges and comprises dominantly maroon to red shale to siltstone with minor intercalated green shale and rare basal sandy beds (Haines, 1990; Preiss, 2000). Initial depositional environment interpretations by Mawson and Segnit (1949) cited the homogeneity, significant thickness, grain size, and lack of sedimentary structures as evidence for deposition as a loessite. Subsequent reinterpretation by Gostin and Jenkins (1983) invoked deposition as an offshore, deep-water basinal shale that was generally starved of coarse-grained sediment input (Haines, 1990). The Bunyeroo Formation unconformably overlies the ABC Range Quartzite, which is a progradational shallow marine sandstone (Figure 9; Haines, 1987, 1990; Preiss, 2000).

2.1.2 Wonoka Formation

The Marinoan Wonoka Formation conformably overlies the Bunyeroo Formation (Figure 9; Reid and Preiss, 1999; Preiss, 2000). At Bunyeroo Gorge in the Central Flinders Ranges, the Wonoka

<table>
<tr><th>Selwyn (1860)</th><th>Mawson (1938)</th><th>Dalgarno & Johnson (1964)</th><th>Gostin & Jenkins (1983)</th><th colspan="2">Haines (1990)</th><th colspan="2">Reid & Preiss (1999)</th><th>Kernen et al. (2012) & Gannaway (2014)
subsalt & suprasalt strata</th></tr>
<tr><td>unit 2</td><td>Pound Quartzite unit 19</td><td>lower Pound Quartzite</td><td>Bonney Sandstone</td><td colspan="2">Bonney Sandstone</td><td rowspan="2">Bonney Sandstone</td><td>undifferentiated</td><td>undifferentiated</td></tr>
<tr><td rowspan="3">unit 3</td><td rowspan="3">unit 18</td><td rowspan="6">Wonoka Formation</td><td rowspan="6">Wonoka Formation</td><td rowspan="12">Wonoka Formation</td><td>unit 11</td><td rowspan="3">Patsy Hill Member</td><td>upper dolomite beds</td></tr>
<tr><td>unit 10</td><td>sandstone beds</td></tr>
<tr><td>unit 9</td><td>lower dolomite beds</td></tr>
<tr><td rowspan="6">unit 4-5</td><td>unit 17</td><td>unit 8</td><td rowspan="11">Wonoka Formation</td><td rowspan="10">undifferentiated</td><td>green mudstone member</td></tr>
<tr><td>unit 16</td><td>unit 7</td><td rowspan="2">upper limestone member</td></tr>
<tr><td rowspan="2">unit 10-15</td><td>unit 6</td></tr>
<tr><td>unit 5</td><td>middle limestone member</td></tr>
<tr><td rowspan="3">unit 9</td><td rowspan="3">Bunyeroo Formation</td><td rowspan="3">Bunyeroo Formation</td><td>unit 4</td><td rowspan="5">lower limestone member</td></tr>
<tr><td rowspan="3">unit 8</td><td>unit 3</td></tr>
<tr><td>unit 2</td></tr>
<tr><td>unit 7</td><td colspan="2">Bunyeroo Formation</td><td>unit 1</td><td>Wearing Dolomite</td></tr>
<tr><td colspan="6"></td><td colspan="2">Bunyeroo Formation</td><td>Bunyeroo Formation</td></tr>
</table>

Figure 10. Stratigraphic nomenclature and subdivisions of the Bunyeroo and Wonoka formations and Bonney Sandstone that have evolved from Selwyn (1860) to Gannaway (2014) time; colored boxes shown on Kernen et al. (2012) and Gannaway (2014) subdivisions reference map unit colors for subsalt and suprasalt minibasin stratigraphy at Patawarta diapir.

Formation is approximately 620 m thick and is interpreted as a mixed carbonate/siliciclastic regressive sequence deposited on a storm-dominated carbonate shelf with a possible north-facing transition from shelf to slope in the proximity of Patawarta diapir (Figure 11; Haines, 1990; Kernen et al., 2012). Throughout the Central and Southern Flinders Ranges, Haines (1990) identified eleven mappable units of the Wonoka Formation (Figures 10 and 11). Reid and Preiss (1999) later subdivided the Wonoka Formation into the basal Wearing Dolomite Member (unit 1), undifferentiated Wonoka Formation (units 2-8), and the Patsy Hill Member of the Bonney Sandstone (units 9-11) (Figure 10).

Kernen et al. (2012) identified four lithostratigraphic units of the Wonoka Formation preserved in a subsalt minibasin adjacent to Patawarta diapir (Figure 12). The four informal map units comprise, in ascending stratigraphic order, the lower, middle, and upper limestone, and green mudstone members, which record regional regression from outer wave-dominated shelf to coastal plain depositional environments (Figure 13). The following paragraphs are a brief summary of the detailed depositional facies and depositional environment interpretations for subsalt Wonoka stratigraphy at Patawarta diapir as defined by Kernen et al. (2012) with correlations to regional interpretations of Wonoka Formation units 1-8 from Haines (1990).

Lower limestone member (Nwwll)

Kernen et al. (2012) correlated the lower limestone member of the Wonoka Formation to units 1-4 of Haines (1990) (Figure 10). Units 1-4 are approximately 319 m thick in the Central Flinders Ranges (Figure 11). Unit 1 is a thin, finely laminated dolomicrite interbedded with green to maroon dolomitic mudstone. Unit 2 comprises fine-grained, brown calcareous and dolomitic sandstone to siltstone with minor maroon mudstone. Unit 3 consists of finely laminated, red calcareous mudstone with thin-bedded, pink micritic limestone. Unit 4 contains thin-bedded, green silty to fine-grained sandy limestone with interbedded green mudstone, as well as brown calcareous siltstone, pink limestone, and maroon to brown mudstone. Haines (1990) interpreted the depositional environment of units 1-4 as a shallowing upward, outer shelf setting that transitioned from below to near storm wave base through time (Figure 11). This also marked the transition from siliciclastic-dominated sedimentation of the underlying Bunyeroo

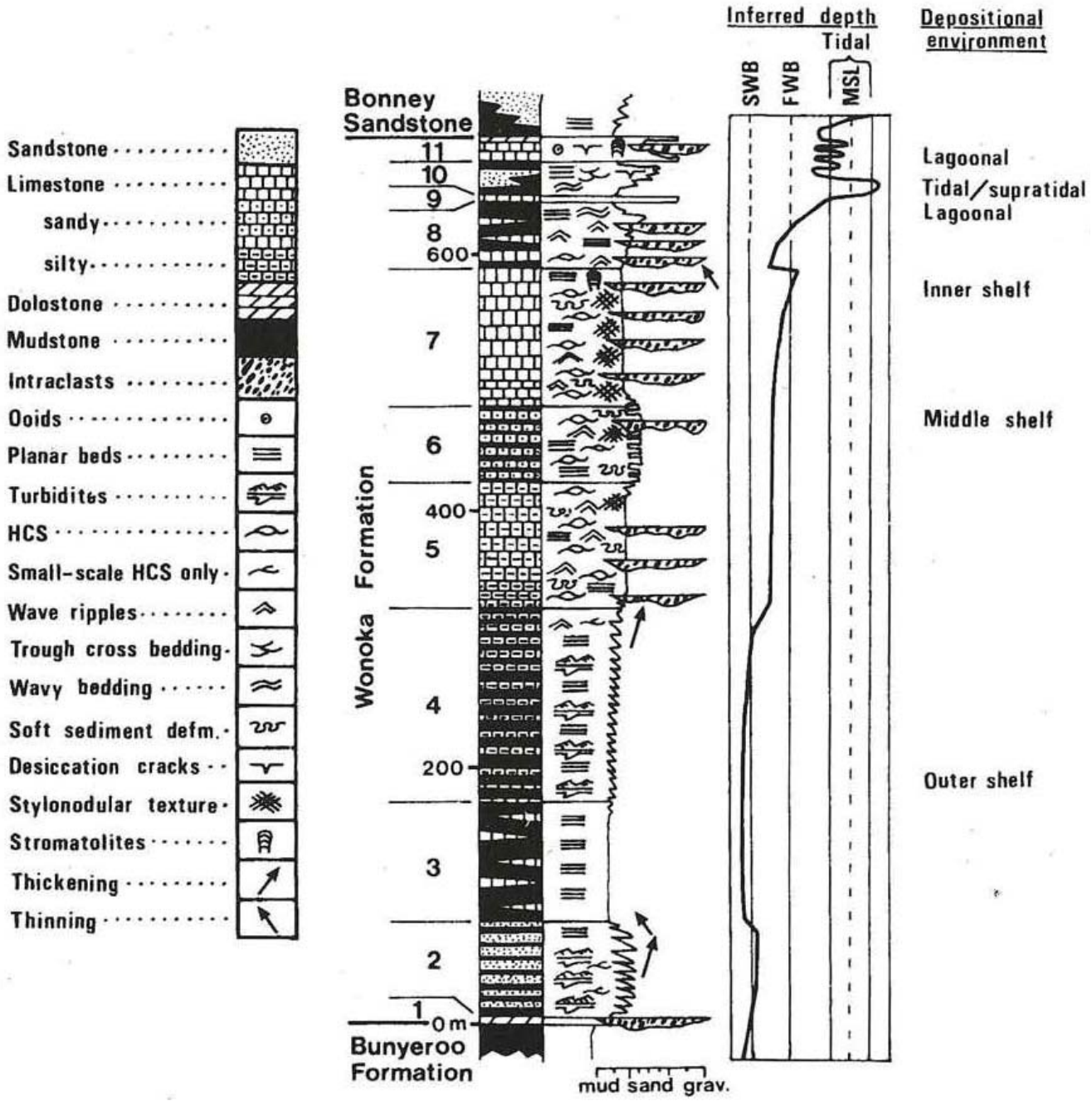

Figure 11. Haines' (1990) measured reference section of the Wonoka Formation at Bunyeroo Gorge in the Central Flinders Ranges with lithologic subdivisions and depositional environment interpretations.

Stratigraphy			Map Unit	Depositional Environment	Depositional Sequence Stratigraphy	Halokinetic Sequence Stratigraphy
Bonney Sandstone			Npb	middle shelf lower shoreface	**Transgressive-Highstand Systems Tracts**	
Bonney Sandstone	Patsy Hill Member	unit 11	Npbpdu	lagoon/bay	*Transgressive Surface*	*Sequence Boundary*
Bonney Sandstone	Patsy Hill Member	unit 10	Npbps	barrier bar flood tidal delta	**Lowstand Systems Tract**	
Bonney Sandstone	Patsy Hill Member	unit 9	Npbpdl	main tidal channel inlet		
Wonoka Formation		unit 8	Nwwgm	coastal plain	*Sequence Boundary*	**Tapered Composite Halokinetic Sequence**
Wonoka Formation		units 6-7	Nwwlu	upper shoreface foreshore	**Highstand Systems Tract**	
Wonoka Formation		unit 5	Nwwlm	lower to upper shoreface foreshore		
Wonoka Formation		units 1-4	Nwwll	outer shelf lower shoreface	*Maximum Flooding Surface*	*Sequence Boundary*

Figure 12. Compilation of depositional environments and depositional and halokinetic sequence stratigraphy for subsalt minibasin strata at Patawarta diapir; correlative regional stratigraphy from Haines' (1990) Wonoka Formation units 1-11 are shown (modified from Kernen et al., 2012).

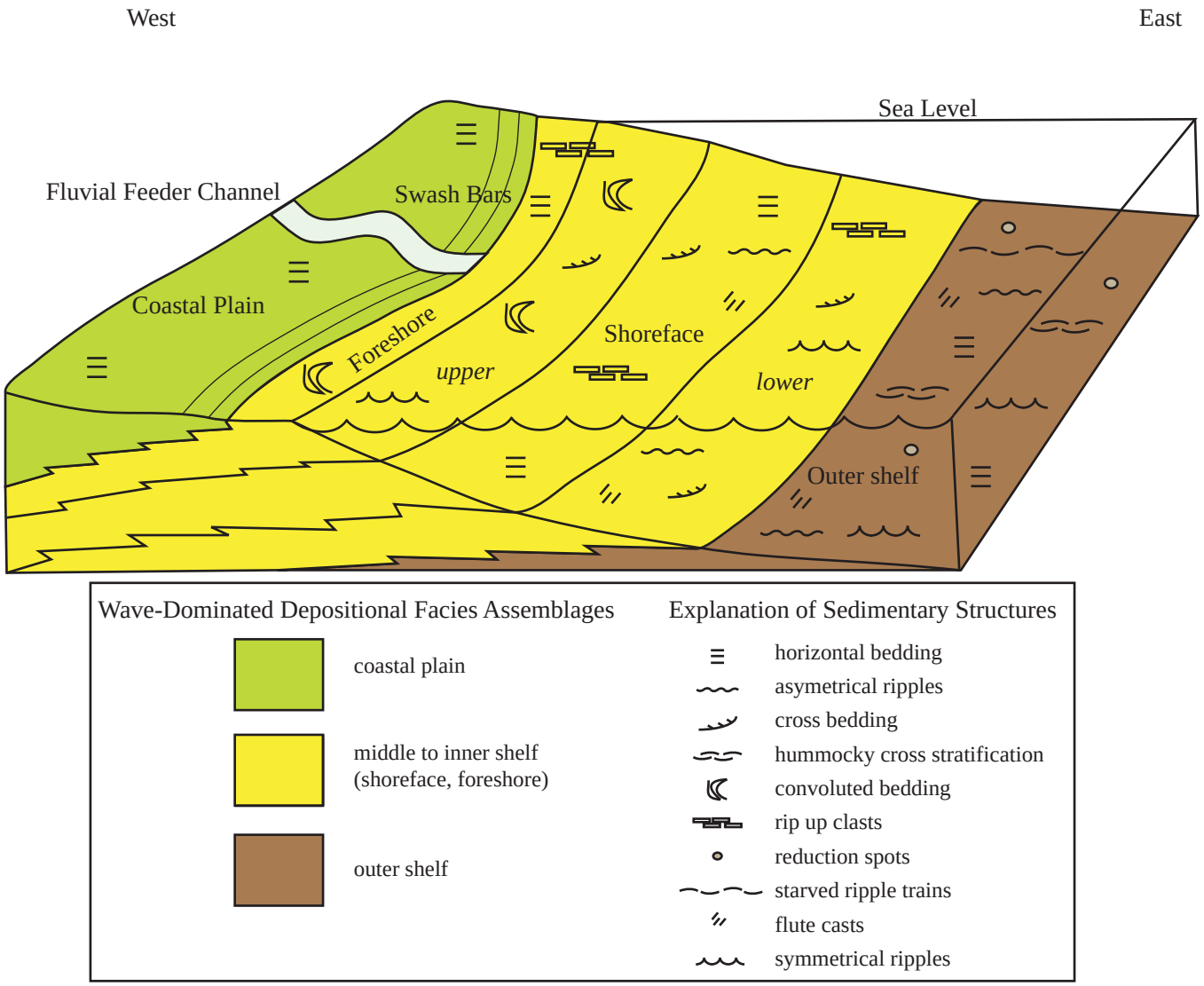

Figure 13. Depositional settings of subsalt Wonoka Formation that record regional regression from outer wave-dominated shelf to coastal plain environments as interpreted by Kernen et al. (2012).

Formation to an increasingly carbonate-rich system during deposition of the Wonoka Formation with the development and progradation of a gently inclined carbonate ramp (Haines, 1990).

The subsalt Wonoka lower limestone member thins towards Patawarta diapir from 550 m to 70 m over a lateral distance of 457 m. It comprises lime mudstone, silty-lime mudstone, micaceous siltstone, and rare lithic arkosic sandstone near the base. The thinly laminated, red, purple, and light-green lime mudstone has horizontal laminations, mud drapes, flute casts, and reduction spots. The thin-bedded silty-lime mudstone and micaceous siltstone display hummocky cross-stratification, dolomitized starved ripple trains, low angle cross-bedding, symmetrical and asymmetrical ripple laminations, climbing ripple laminations, flute clasts, and lime mudstone rip-up clasts. The lithic arkose is fine- to medium-grained, poorly sorted, and consists of primarily angular quartz and orthoclase feldspar grains with lithic clasts of lime mudstone, siltstone, and chert. Kernen et al. (2012) interpreted the depositional environment of the subsalt Wonoka lower limestone member as an outer shelf setting below storm wave base that shallowed through time into a lower shoreface setting (Figures 12 and 13).

Middle limestone member (Nwwlm)

Kernen et al. (2012) correlated the middle limestone member of the Wonoka Formation to unit 5 of Haines (1990) (Figure 10). Unit 5 is approximately 105 m thick and comprises medium- to thick-bedded, green silty limestone with minor interbedded mudstone (Figure 11). Haines (1990) interpreted the depositional environment of unit 5 as an outer to middle shelf setting above storm wave base during the progradation of a gently inclined carbonate ramp (Figure 11).

The subsalt Wonoka middle limestone member thins towards Patawarta diapir from 215 m to 20 m over a lateral distance of 457 m. It consists of lime mudstone, calcareous siltstone, and quartz arenite. The blue-gray to red lime mudstone is thin- to medium-bedded, decreasing to thinly laminated at the top of the unit, and displays horizontal laminae and mud drapes. The calcareous siltstone displays planar laminations, hummocky cross-stratification, symmetrical and asymmetrical ripple laminations, flute casts, and lime mudstone rip-up clasts. The quartz arenite is medium-grained, well-sorted, and consists of sub-angular to sub-rounded quartz grains with less than 10% lithic clasts of calcareous siltstone. It displays horizontal laminations, low-angle cross-bedding, symmetrical and asymmetrical ripple laminations, and

lime mudstone rip-up clasts. Kernen et al. (2012) interpreted the depositional environment of the subsalt Wonoka middle limestone member as primarily an upper to lower shoreface setting with some foreshore component (Figures 12 and 13).

Upper limestone member (Nwwlu)

Kernen et al. (2012) correlated the upper limestone member of the Wonoka Formation to units 6 and 7 of Haines (1990) (Figure 10). Units 6 and 7 are approximately 153 m thick in the Central Flinders Ranges (Figure 11). Unit 6 comprises fine-grained, brown calcareous sandstone and coarse-grained siltstone with interbedded brown and gray mudstone, as well as minor green and red limestone. Unit 7 consists of gray-green, argillaceous and silty micritic limestone and red glauconitic limestone. Haines (1990) interpreted the depositional environment of units 6 and 7 as a middle to inner shelf setting that transitioned upward from above storm wave base to fair weather wave base during the progradation of a gently inclined carbonate ramp (Figure 11).

The subsalt Wonoka upper limestone member thins towards Patawarta diapir from 80 m to 20 m over a lateral distance of 457 m. It is composed of lime mudstone and litharenite. The blue-gray to purple lime mudstone is thin- to medium-bedded and displays soft-deformation with overlying sandstones. The litharenite, which is medium-grained, well-sorted, and contains well-rounded lime mudstone lithic grains, forms stylonodular bedding (Haines, 1987) and displays low-angle cross-bedding. Kernen et al. (2012) interpreted the depositional environment of the subsalt Wonoka upper limestone member as an upper shoreface to foreshore setting (Figures 12 and 13).

Green mudstone member (Nwwgm)

Kernen et al. (2012) correlated the green mudstone member of the Wonoka Formation to unit 8 of Haines (1990) (Figure 10). Unit 8 is approximately 54 m thick in the Central Flinders Ranges and is characterized by upward thinning packages of medium- to thin-bedded, gray limestone interbedded with and capped by green calcareous mudstone with cyanobacterial laminations near the top (Figure 11). Haines (1990) interpreted the depositional environment of unit 8 as an inner shelf setting below fair weather wave base that transitioned upward to a lagoonal setting (Figure 11).

The subsalt Wonoka green mudstone member thins towards Patawarta diapir from 130 m to 7 m over a lateral distance of 323 m. It dominantly comprises calcareous siltstone and lime mudstone with local conglomeratic litharenite and sublitharenite beds. The green to yellow calcareous siltstone is thinly laminated and lacks any current or wave sedimentary structures. The lime mudstone is interbedded with the calcareous siltstone at the base of this unit, whereas upsection it is interbedded with the conglomerate beds. Kernen et al. (2012) documented twelve intercalated conglomeratic litharenite to sublitharenite beds composed of lithic clasts of lime mudstone, dolomitic mudstone, quartz arenite, and calcareous siltstone. Kernen et al. (2012) interpreted the depositional environment of the subsalt Wonoka green mudstone member as a coastal plain environment (Figures 12 and 13). Based on a diapir-proximal distribution of the conglomeratic beds and that these lithologies could have only been derived from the underlying Wonoka upper and middle limestone members, Kernen et al. (2012) interpreted them as a diapir unroofing sequence when deposition in the coastal plain environment was influenced by erosion of the local bathymetric high of Patawarta diapir.

2.1.3 Patsy Hill Member

The Marinoan Patsy Hill Member is the basal member of the Bonney Sandstone, which forms the lower Pound Subgroup (Figure 9). At Bunyeroo Gorge in the Central Flinders Ranges, the Patsy Hill Member is approximately 47 m thick and comprises two shallow-water carbonate intervals separated by an entirely siliciclastic interval (Figure 11; Haines, 1990; Kernen et al. 2012). Formerly defined by Haines (1990) as Wonoka Formation units 9-11, the Patsy Hill Member was most recently redefined by Reid and Preiss (1999) and is unconformably overlain by undifferentiated Bonney Sandstone (Figures 9 and 10).

Kernen et al. (2012) identified three lithostratigraphic units of the Patsy Hill Member of the Bonney Sandstone preserved in a subsalt minibasin adjacent to Patawarta diapir (Figure 12). The three informal map units consist of, in ascending stratigraphic order, the lower dolomite, sandstone, and upper dolomite beds, which record deposition in a tidally-dominated barrier bar complex environment (Figure 14). The following paragraphs are a brief summary of the detailed depositional facies and depositional environment interpretations for subsalt Patsy Hill stratigraphy at Patawarta diapir as defined by Kernen et

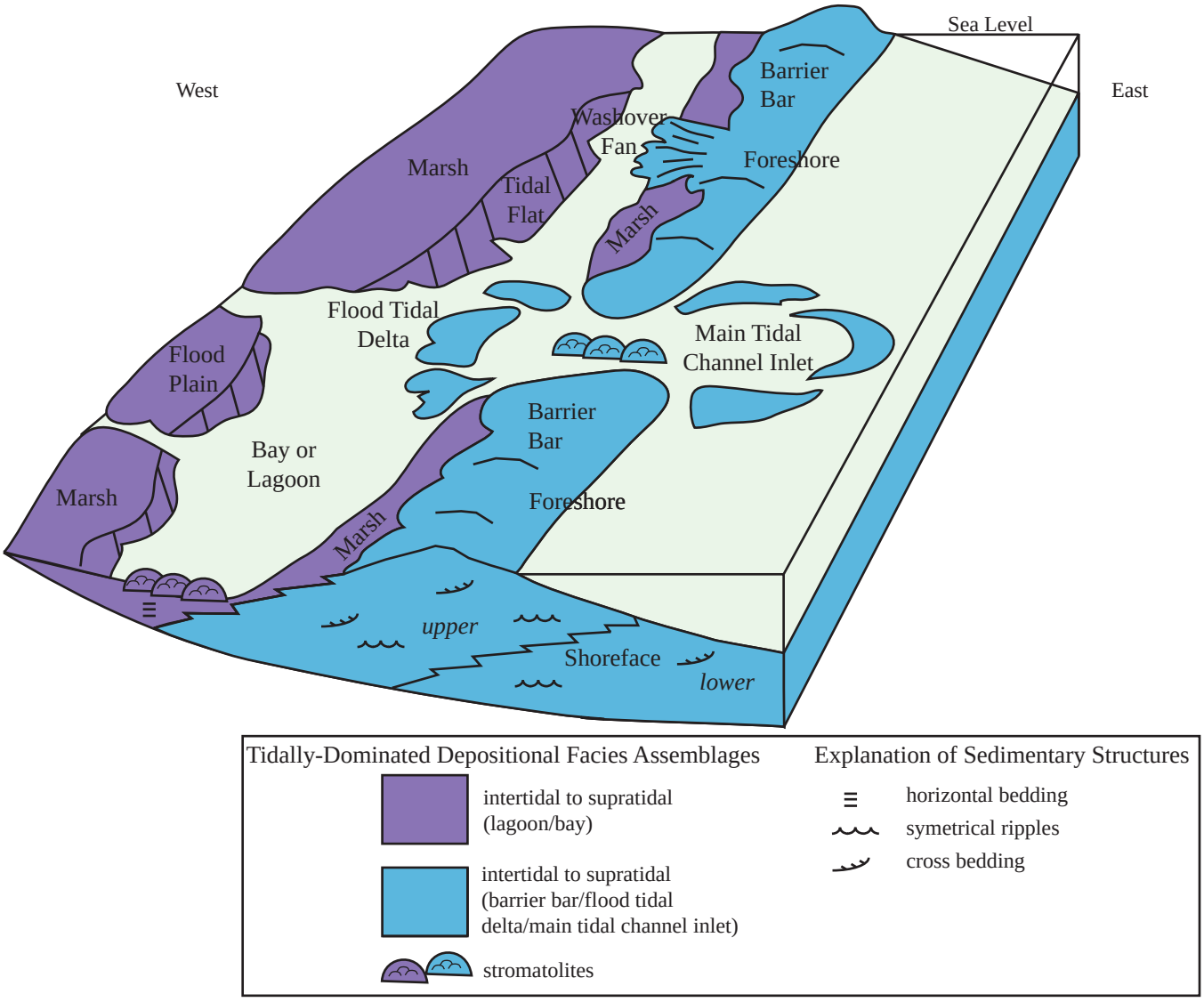

Figure 14. Depositional settings of subsalt Patsy Hill Member of the Bonney Sandstone in a tidally-dominated barrier bar complex environment as interpreted by Kernen et al. (2012).

al. (2012) with correlations to regional interpretations of Wonoka Formation units 9-11 from Haines (1990).

Lower dolomite beds (Npbpdl)

Kernen et al. (2012) correlated the lower dolomite beds of the Patsy Hill Member to Wonoka Formation unit 9 of Haines (1990) (Figure 10). Unit 9 ranges in thickness from 1 m in the Central Flinders Ranges to at least 40 m in the Northern Flinders Ranges (Figure 11). It contains thin-bedded, cyanobacterial-laminated, gray limestone with interbedded thicker, black calcarenites that are massive to cross-bedded. Haines (1990) interpreted the depositional environment of unit 9 as a shallow subtidal lagoonal setting (Figure 11).

The subsalt Patsy Hill lower dolomite beds range in thickness from 18 m to 40 m and pinch out to the northwest and southeast, developing a lenticular geometry interpreted as the fill of an erosional surface. They comprise dark-gray dolomite, dolomitic crypt-algal laminite, black fetid shale, litharenite to subarkose, and caprock-derived pebble conglomerate. The dark-gray dolomite is rhythmically interbedded with black fetid shale and contains round to irregular, stacked concretions. Pink caprock-derived pebble clasts are locally imbricated and overlie erosional scour surfaces. The crypt-algal laminite is interbedded with caprock-derived pebble conglomerate horizons and litharenite to subarkose sand stringers. The pebble conglomerate beds are derived from exposure and erosion of the diagenetic caprock developed on top of Patawarta diapir. Kernen et al. (2012) interpreted the depositional environment of the subsalt Patsy Hill lower dolomite beds as a main tidal channel inlet setting (Figures 12 and 14).

Sandstone beds (Npbps)

Kernen et al. (2012) correlated the sandstone beds of the Patsy Hill Member to Wonoka Formation unit 10 of Haines (1990) (Figure 10). Unit 10 is approximately 30 m in the Central Flinders Ranges and is dominated by red, micaceous silty sandstone with thin-bedded, green sandstone and mudstone at the base and laminated, olive green, calcareous mudstone at the top (Figure 11). Haines (1990) interpreted the depositional environment of unit 10 as a shallow water setting that ranged from subtidal through intertidal and supratidal (Figure 11).

The subsalt Patsy Hill sandstone beds thin towards Patawarta diapir from 40 m to 9 m over a lateral distance of 590 m, with a distinct pinch and swell geometry in map view. They consist of conglomeratic red subarkose to arkose. The subarkose contains poorly sorted, sub-rounded to sub-angular, fine-grained sand to granule and pebble clasts and displays normal grading. The arkose contains moderately well-sorted, sub-angular to sub-rounded, fine- to medium-grained sand and displays symmetrical ripple laminations and low-angle cross-bedding. Kernen et al. (2012) interpreted the depositional environment of the subsalt Patsy Hill sandstone beds as a tidally-dominated barrier bar or flood-tidal delta setting (Figures 12 and 14).

Upper dolomite beds (Npbpdu)

Kernen et al. (2012) correlated the upper dolomite beds of the Patsy Hill Member to Wonoka Formation unit 11 of Haines (1990) (Figure 10). Unit 11 is approximately 16 m in the Central Flinders Ranges and is characterized by cyclic gray and black limestone packages (Figure 11). A typical, upward coarsening cycle consists of thin-bedded, lenticular and wavy, gray to black, fine-grained peloidal grainstone with interbedded silty micritic limestone in the lower half of the cycle and calcarenite in the upper half. The silty micritic limestone is thin-bedded, planar, and gray. The calcarenite is coarse-grained, cross-bedded, and contains abundant ooids, large peloids, and intraclasts. Cycles in the lower part of this unit are frequently capped by stromatolites. Haines (1990) interpreted the depositional environment of unit 11 as a subtidal lagoon that periodically shallowed to develop ooid shoal and beach settings (Figure 11).

The subsalt Patsy Hill upper dolomite beds thin towards Patawarta diapir from 55 m to 15 m over a lateral distance of 134 m and are present as two isolated outcrops that onlap subjacent Patsy Hill sandstone beds. They comprise dolomitic stromatolitic boundstone with caprock-derived pebble conglomerate horizons and rare sand stringers of calcareous litharenite. The boundstone is dark-gray, light-gray, pink, and tan, develops wavy laminations, and forms laterally linked stromatolites with up to 3 cm of relief. The caprock-derived pebble conglomerate horizons, which contain tabular, well-rounded, well-sorted, pink caprock granule to pebble clasts derived from the exposure of Patawarta diapir, occur

only locally and are not imbricated. Kernen et al. (2012) interpreted the depositional environment of the subsalt Patsy Hill upper dolomite beds as a tidally-dominated lagoon or bay setting (Figures 12 and 14).

2.1.4 Bonney Sandstone

The Bonney Sandstone forms the lower part of the Pound Subgroup, and undifferentiated Bonney Sandstone is approximately 255 m thick in the Central Flinders Ranges (Figure 9). It consists of fine- to medium-grained, red silty sandstone with occasional coarse-grained horizons and interbedded siltstone and limestone (Forbes, 1971; Preiss, 2000). It locally displays trough and planar cross-bedding, lenticular and wavy bedding, ripple laminations, parting lineations, soft-sediment deformation, and mud cracks (Forbes, 1971; Kernen, 2011). Forbes (1971) interpreted the depositional environment of the undifferentiated Bonney Sandstone as marginal marine with tidal influence and local estuary-type settings, while Gehling (1982) suggested deposition by a tidal mud flat to delta sand ridge complex that transitioned upward into an alluvial plain setting.

2.1.5 Suprasalt Carapace Interpretation and Correlation at Patawarta Diapir

Hall et al. (1986) and Lemon (1988) identified a thin section of Wonoka Formation on the northeast side of Patawarta diapir (Figure 15). Kernen (2011) interpreted this section as a condensed carapace that formed in a suprasalt position on top of the allochthonous Patawarta salt sheet. The significantly thinner suprasalt section is separated from the subsalt minibasin section by approximately 3.8 km of diapiric breccia (Figure 16a). Kernen (2011) documented 14 m of interbedded limestone and conglomerate in the suprasalt Wonoka strata, which lies depositionally but unconformably above the Patawarta salt sheet and lacks wedge-shaped drape folding. The sedimentology and lithology of this section is distinct from equivalent strata in the adjacent subsalt minibasin (Figure 16b). Kernen (2011) and Kernen et al. (2011) suggested the Wonoka suprasalt section formed a condensed carapace based on the model proposed by Hart et al. (2004), which defined suprasalt carapace as sequences of “strata that are deposited in sub-parallel layers over salt-induced sea floor highs, and which lie semi-conformably atop diapiric salt or its relic weld.” The Patsy Hill Member of the Bonney Sandstone was not documented in this suprasalt stratigraphy (Kernen, 2011; Kernen et al., 2011). The condensed section of interpreted Wonoka Formation

(a)

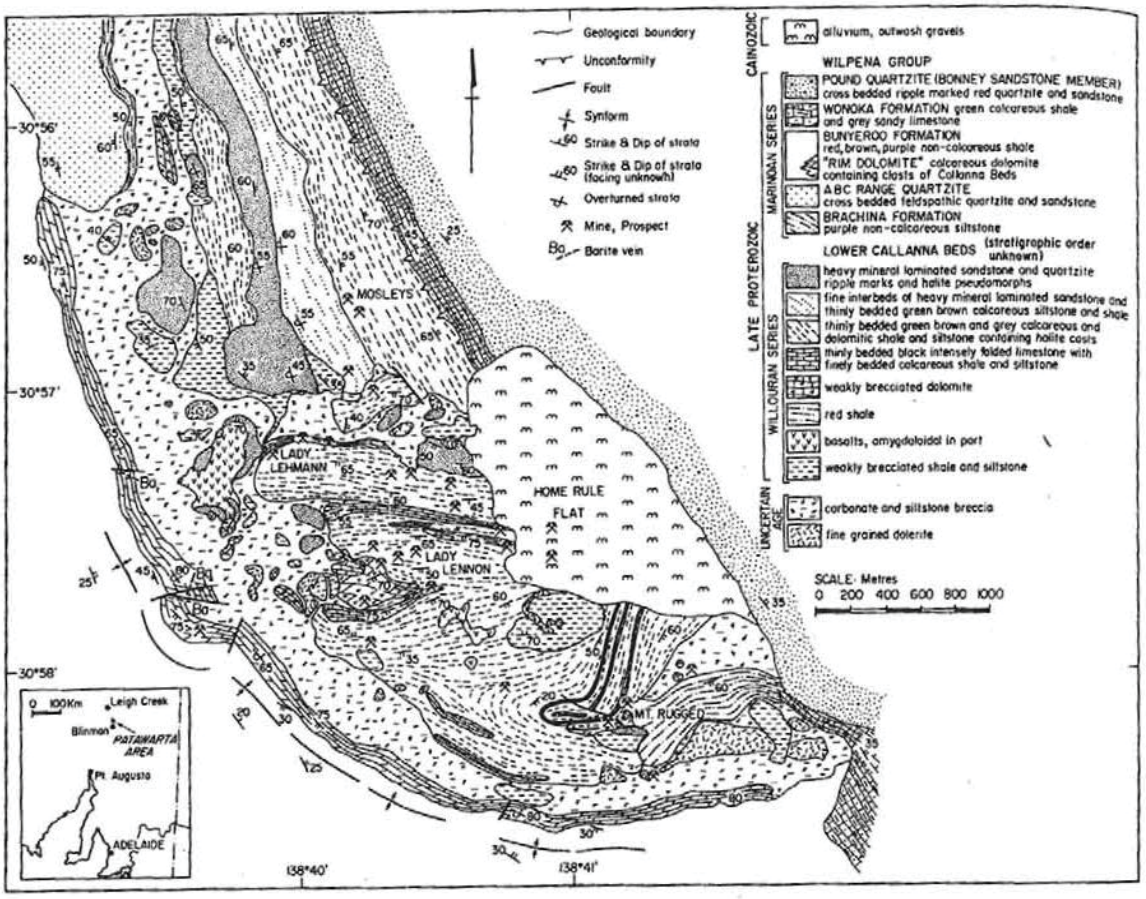

(b)

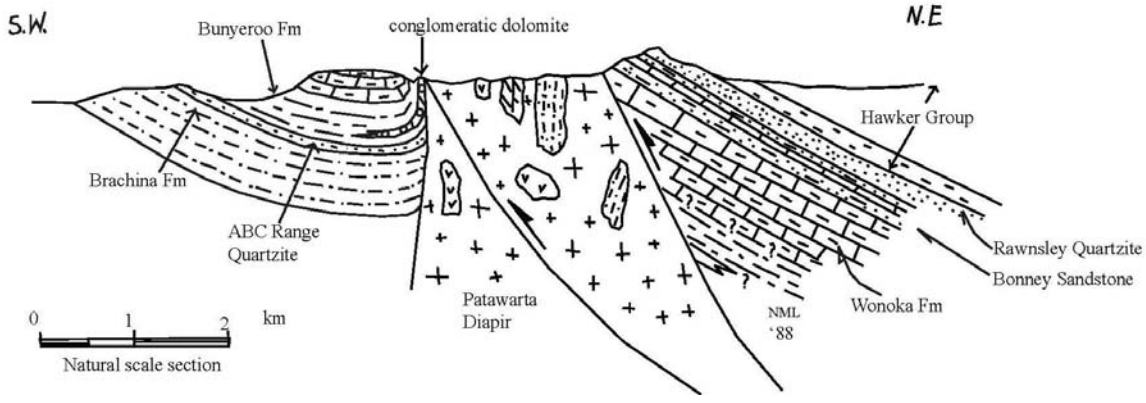

Figure 15. (a) Geologic map (Hall et al., 1986) and (b) cross-section (Lemon, 1988) representing previous work conducted at Patawarta diapir that documented subsalt and suprasalt stratigraphy of the Bunyeroo and Wonoka formations and Bonney Sandstone.

(a)

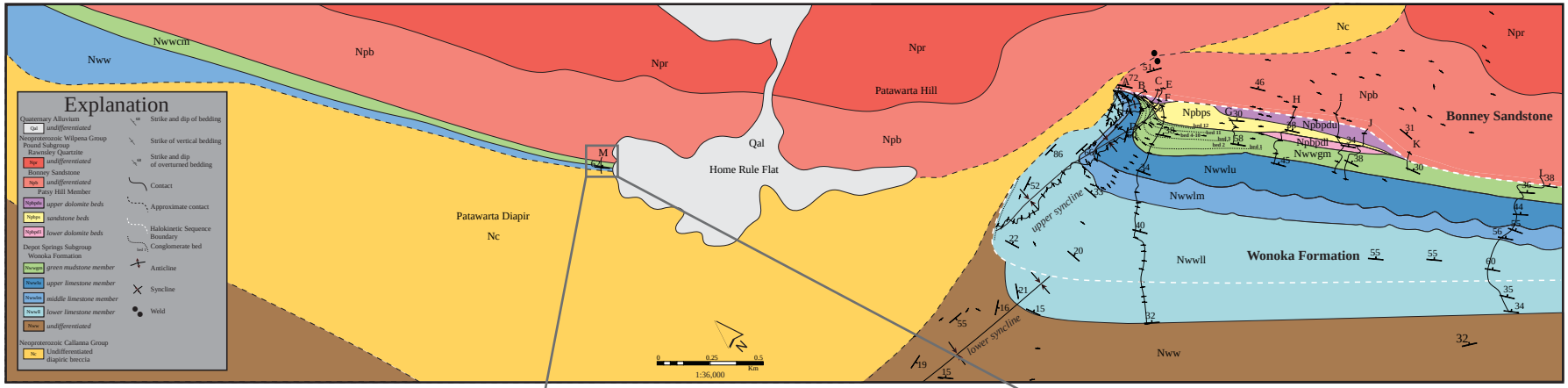

(b)

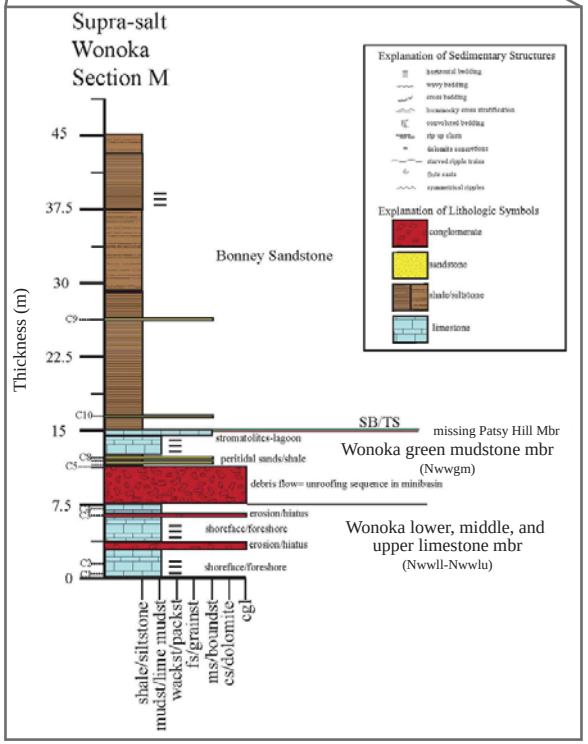

Figure 16. (a) Geologic map and (b) measured stratigraphic section of interpreted suprasalt Wonoka Formation carapace at Patawarta diapir (modified from Kernen, 2011 and Kernen et al., 2011).

carapace is instead unconformably overlain by undifferentiated Bonney Sandstone (Coats, 1973; Hall et al., 1986; Kernen, 2011; Kernen et al., 2011).

2.2 Depositional Sequence Stratigraphy

The Wilpena Group comprises two major regressive cycles in the Adelaide Fold Belt (Haines, 1990; Christie-Blick et al., 1995). The lower cycle contains, in ascending stratigraphic order, the Nuccaleena and Brachina formations and ABC Range Quartzite. The upper cycle contains, in ascending stratigraphic order, the Bunyeroo and Wonoka formations and Bonney Sandstone (von der Borch et al., 1988; Haines, 1990). Within the upper cycle, the Bunyeroo and Wonoka formations and Patsy Hill Member of the Bonney Sandstone form parts of two distinct 3rd-order depositional sequences (Coats, 1964; von der Borch et al., 1982, 1988; Preiss, 1987, 2000).

The lower depositional sequence is bound at the base by an interpreted sequence boundary (SB) at the formational contact of the ABC Range Quartzite and Bunyeroo Formation based on the abrupt non-Waltherian facies shift from progradational shoreface shallow marine sandstones of the ABC Range Quartzite to overlying offshore basinal shales of the Bunyeroo Formation (Christie-Blick et al., 1988; von der Borch, et al., 1988; Haines, 1990; Posamentier et al., 1992; Preiss, 2000). Haines (1990) and Preiss (2000) interpret a maximum flooding surface (*mfs*) at the Wearing Dolomite Member of the overlying Wonoka Formation, whereby Wonoka facies progressively shallow upward from the deep-water Wearing Dolomite, which records sediment starvation in the basin. Therefore, the Bunyeroo Formation forms the Transgressive Systems Tract (TST) of the lower depositional sequence (Catuneanu, 2006).

The overlying Wonoka Formation records regional progradation of a storm-dominated carbonate shelf from west to east (Haines, 1990). The lower, middle, and upper limestone and green mudstone members of the Wonoka Formation in the subsalt minibasin comprises a normal regressive succession from outer shelf to shoreface, foreshore, and coastal plain (Figure 13; Kernen, et al., 2012). This progressively shallowing upward succession denotes a progradational depositional system with high sedimentation rates. Therefore, the Wonoka Formation forms the Highstand Systems Tract (HST) of the

lower depositional sequence in the subsalt minibasin at Patawarta diapir (Figure 12; Catuneanu, 2006; Kernen, et al., 2012).

The sharp and erosional contact between the Wonoka Formation and the Patsy Hill Member of the Bonney Sandstone is interpreted as the sequence boundary (SB) between the lower and upper depositional sequences in the subsalt minibasin (Figure 12; Kernen, et al., 2012). The overlying Patsy Hill Member, which consists of the lower dolomite, sandstone, and upper dolomite beds in the subsalt minibasin, records an abrupt non-Waltherian facies shift to deposition in a tidally-dominated barrier bar system that depositionally filled an incised valley (Figure 14; Kernen et al., 2012). Therefore, the Patsy Hill lower dolomite, sandstone, and upper dolomite beds form the Lowstand Systems Tract (LST) of the upper depositional sequence in the subsalt minibasin at Patawarta diapir (Figure 12; Catuneanu, 2006; Kernen et al., 2012).

The formational contact between the Patsy Hill Member and the undifferentiated Bonney Sandstone in the subsalt minibasin represents a transition in the depositional system from a mixed carbonate and siliciclastic lagoonal setting to a siliciclastic-dominated shallow marine environment (Figure 12; Forbes, 1971; Kernen et al., 2012). This major flooding surface is interpreted as a transgressive surface (ts) and a transgressive lag is recorded in the subsalt minibasin by a sandy conglomeratic arkose (Figure 12; Kernen et al., 2012). The undifferentiated Bonney Sandstone represents the Transgressive Systems Tract (TST) to Highstand Systems Tract (HST) of the upper depositional sequence (Figure 12; Catuneanu, 2006; Kernen et al., 2012).

2.3 Halokinetic Sequence Stratigraphy

The base of Patawarta allochthonous salt sheet displays a ramp-flat geometry at the southeastern end of the field area, which preserves adjacent subsalt minibasin strata of the Bunyeroo and Wonoka formations and Patsy Hill Member of the Bonney Sandstone (Plate 1; Kernen et al., 2012; Hearon et al., 2014). These subsalt stratal units form two stacked tapered composite halokinetic sequences each containing convergent lower and upper boundaries, a broad zone (approximately 560 m) of folding and thinning toward the diapir, and offset fold axial traces trending approximately east-west (Kernen, 2011;

Kernen et al., 2012). Steep to near vertical strata comprise the northwest monoclinal limb of the drape folds and parallel the margin of Patawarta diapir. The original salt-sediment interface in this subsalt setting had a base of salt dipping 62° inward, whereby the adjacent vertical to overturned strata represent the halokinetic drape folding of original roof as the top salt rotated into a base salt ramp position (Kernen et al., 2012; Hearon et al., 2014). A minor amount of roof strata preserved in the upper monoclinal fold limb is then truncated by a steep salt-sediment interface (72°) through lower undifferentiated Bonney Sandstone strata that lacks halokinetic folding, which represents allochthonous salt breakout at Patawarta diapir by piston-like rise (Hearon et al., 2014).

2.4 Caprock

The Rim Dolomite at Patawarta diapir is a locally silicified dolomite unit present as laterally extensive outcrops along the salt sheet margin in both subsalt and suprasalt positions (Figure 15; Coats, 1973, 2009; Hall et al., 1986; Giles et al., 2012). It is present at the salt-sediment interface separating Callana Group diapiric breccia from Bunyeroo Formation maroon shales and siltstones. In the subsalt position, the unit thins from 100 to 3 m and extends for >10 km along the western margin of Patawarta diapir. It terminates at the tapered composite halokinetic sequence bounding unconformity at the contact between the Bunyeroo Formation and overlying Wonoka Formation in the subsalt minibasin (Plate 1). Attitudes in the Rim Dolomite parallel the steep to vertical salt-sediment interface and there is a lack of interfingering into adjacent Bunyeroo strata (Giles et al., 2012). In the suprasalt position, the Rim Dolomite is mapped as a thin, discontinuous unit present along the northeastern margin of Patawarta diapir (Coats, 1973, 2009).

The origin of the Rim Dolomite has been interpreted as a diapir-proximal facies change within the Bunyeroo Formation (Hall et al. 1986; Lemon, 1988), but more recently Giles et al. (2012) have reinterpreted the Rim Dolomite as a lateral carbonate caprock assemblage currently in a subsalt position. Giles et al. (2012) postulated that the caprock developed in a crestal position on top of Patawarta diapir during deposition of the Bunyeroo Formation. Continued salt sheet inflation and advance resulted in the rotation and drape-folding of both the roof strata and the caprock into a diapir-flanking position in the

subsalt minibasin (Figure 17). Following erosional truncation of the Bunyeroo Formation and Rim Dolomite caprock, deposition of the Wonoka Formation initiated another composite halokinetic sequence. The overlying tapered composite halokinetic sequence of subsalt Wonoka Formation did not develop caprock (Giles et al., 2012).

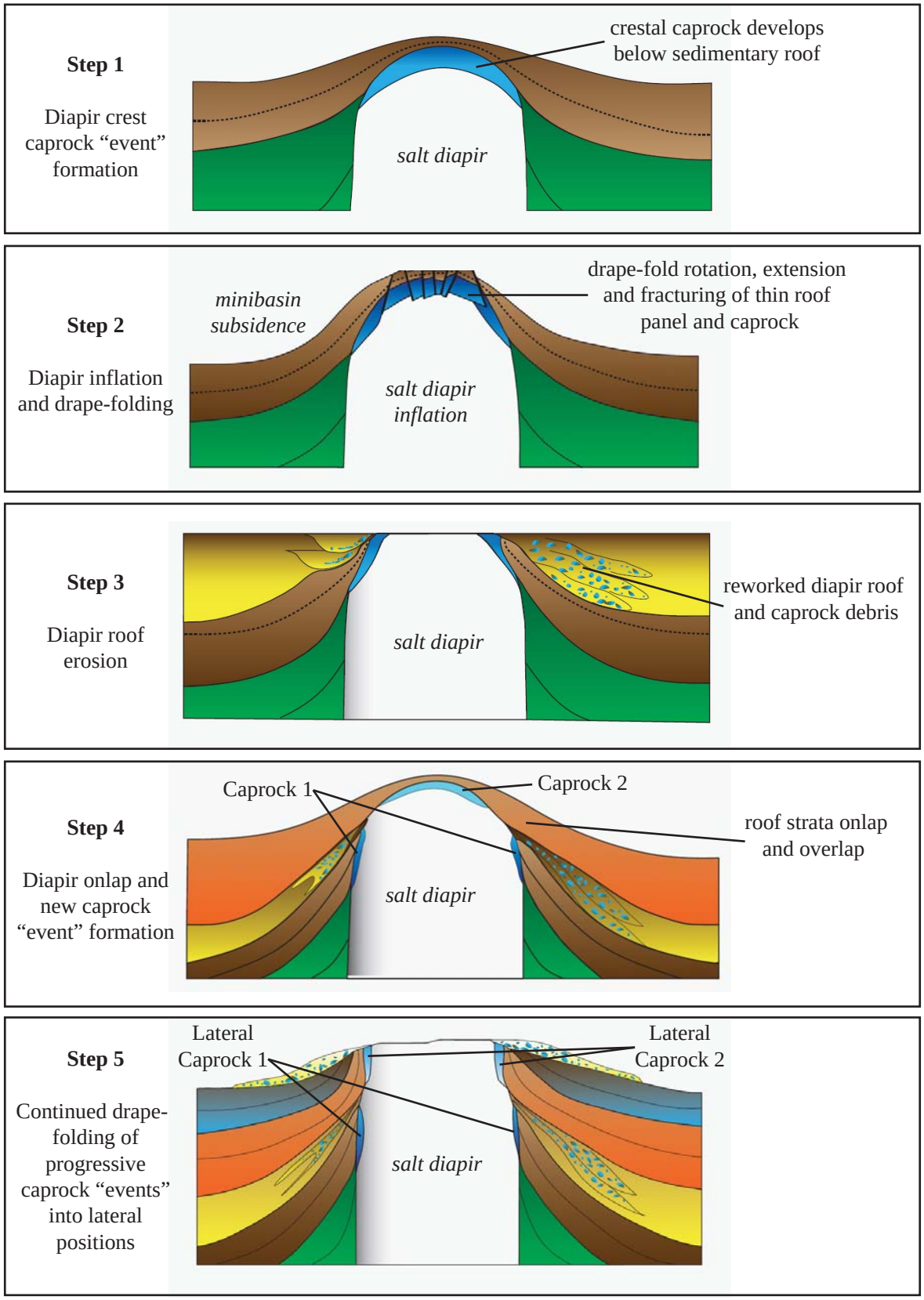

Figure 17. Halokinetic drape-fold model for emplacement of lateral caprock at passively rising salt diapirs (modified from Giles et al., 2012).

Chapter 3: Methods

A thin suprasalt section of Wonoka strata was documented by Kernen (2011) 3.8 km northwest of the subsalt minibasin at Patawarta diapir (Figure 16). Kernen (2011) interpreted this interval as carapace on top of the allochthonous salt sheet. Using this data as a starting point, a complete stratigraphic and structural analysis of the suprasalt minibasin was conducted at Patawarta diapir beginning at the carapace section and working northward toward the synclinal axis of the minibasin.

Extensive field mapping was conducted to create a geologic map of northwestern end of Patawarta diapir and adjacent Wilpena Group stratigraphy (Plate 1). Quickbird aerial imagery with 60 cm resolution was used as the primary base material for the geologic map. Structural data was collected using a Brunton compass and Garmin Vista GPS. A digital geologic map was constructed with Global Mapper 13 and Adobe Illustrator CS4 and merged with the previously published geologic map by Kernen et al. (2012) detailing the subsalt minibasin. Along with the Quickbird aerial imagery and ANGEPENA 1:100,000 and COPLEY 1:250,000 map sheets (Coats, 1973, 2009), the digital geologic map was geo-rectified and projected on WGS84.

Twelve stratigraphic sections were measured in order to document the lithofacies, thickness, distribution, and geometry of the Bunyeroo and Wonoka formations and Patsy Hill Member of the Bonney Sandstone in the suprasalt minibasin (Appendix A). The sections (Section 1-12) were measured from the diapir margin through the adjacent suprasalt minibasin to the base of the undifferentiated Bonney Sandstone along a diapir-proximal (east) to diapir-distal (west) transect. Observations of lithology, grain size, color, sedimentary structures, bed thickness, lateral variation and relationships with adjacent strata were recorded. The measured sections were completed using a 1.5m Jacob staff, Brunton compass, hand lens, and grain size chart. Bunyeroo, Wonoka, and Patsy Hill strata were traced laterally in the suprasalt minibasin and mapped with a Garmin Vista GPS to identify facies distribution, halokinetic sequence boundaries, and angular unconformities.

Seven informal map units as defined by Kernen et al. (2012) were identified in the suprasalt minibasin. Formational contacts were used as a basis for correlation of subsalt and suprasalt Wonoka and Patsy Hill stratigraphy (Figure 10). The seven map units are, in ascending stratigraphic order, the lower,

middle, and upper limestone, and green mudstone members of the Wonoka Formation and the lower dolomite, sandstone, and upper dolomite beds of the Patsy Hill Member of the Bonney Sandstone. A correlation diagram was constructed from measured section data (Plate 2) to compare depositional environments and depositional and halokinetic sequence stratigraphy laterally across the suprasalt minibasin, as well as to the subsalt minibasin (Kernen et al., 2012). Because the undifferentiated Bonney Sandstone lacks evidence of diapir growth or halokinetic stratal upturn (Lemon, 1988), the base of this unit was used as a datum for the correlation diagram. In addition, approximately 200 samples were collected for thin sections for detailed petrographic analysis to correlate facies and determine differences in diagenetic history between minibasins (Appendix B).

The original orientation of the suprasalt-sediment interface was calculated using stereonet analysis of bedding attitudes and assumptions related to the halokinetic drape-fold theory. According to Hearon (2013), this analysis hinges on the reasonable assumption that "the fold axis of a halokinetic drape fold is parallel to the associated salt face because the edge of the rising or advancing salt is controlling the geometry of the 'draped roof'" (Figure 18). Two-dimensional map-view relationships were used to derive the three-dimensional orientation of the salt-sediment interface and the direction of salt emplacement. Complete methodology for the structural analysis of a salt-sediment interface can be found in Hearon (2013).

Using the ANGEPENA 1:100,000 map sheet (Coats, 1973, 2009) as a guide, Rim Dolomite exposures mapped in suprasalt positions were also investigated. The detailed outcrop geometries as well as lateral and vertical facies variations were documented as part of ongoing research into a potential caprock origin for the Rim Dolomite at Patawarta diapir and other analogous but anomalous dolomite beds at salt diapir margins throughout the Flinders Ranges (Giles et al., 2012).

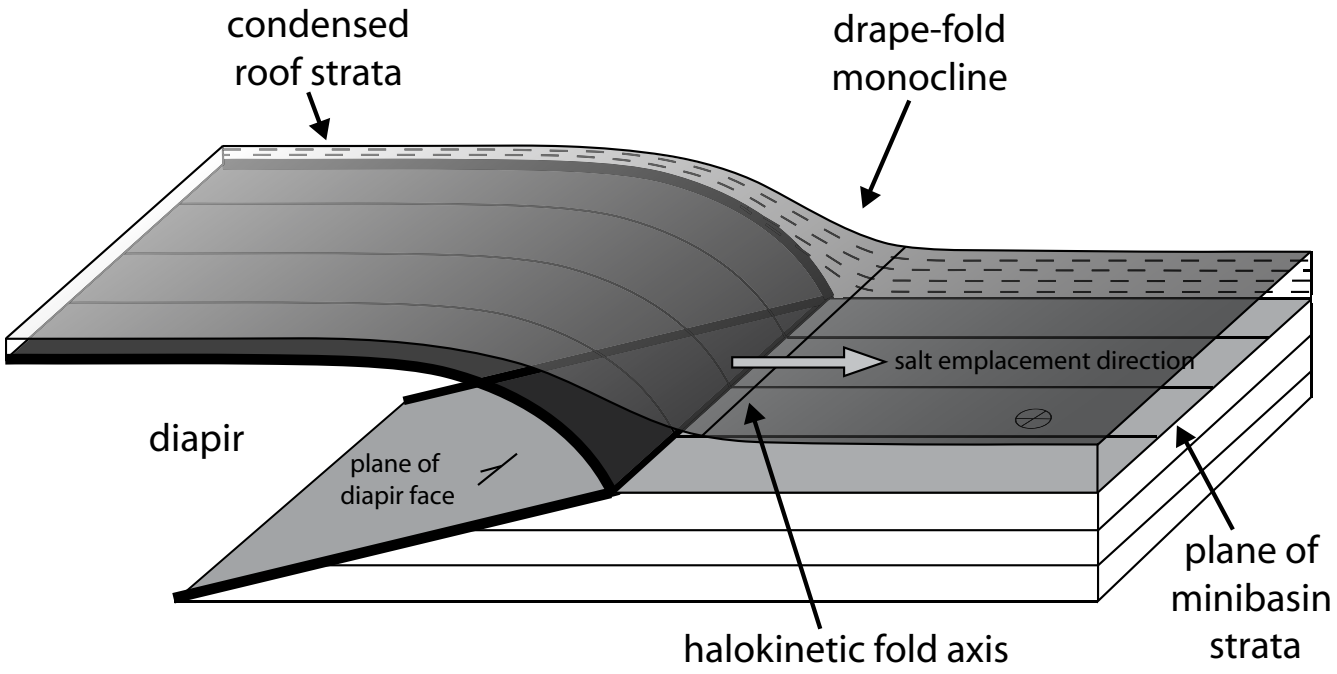

Figure 18. Three-dimensional block diagram of a ramping salt sheet and associated halokinetic drape-fold that denotes the key lines and planes used when deriving three-dimensional orientations of the salt-sediment interface from map view relationships (Hearon, 2013). See text and Hearon (2013) for further explanation of the structural analysis.

Chapter 4: Suprasalt Minibasin Analysis

The stratigraphic and structural analysis of the suprasalt minibasin at Patawarta diapir consisted of documentation and interpretation of the following: depositional and diagenetic facies, stratal thickness trends, structural style and stratal geometries, depositional sequence stratigraphy, and halokinetic sequence stratigraphy of diapir-flanking Wilpena Group stratigraphy. The Wilpena Group stratigraphy of the suprasalt minibasin was correlated to the subsalt minibasin based on lithofacies and depositional sequence stratigraphy. Using this correlation framework, a comparison of depositional facies, stratal thickness trends, structural style and stratal geometries, and halokinetic sequence stratigraphy was made between the suprasalt and subsalt minibasins at Patawarta diapir.

4.1 Depositional Facies

Stratigraphic units of the Wilpena Group analyzed in the suprasalt minibasin adjacent to Patawarta diapir include the Bunyeroo and Wonoka formations and the Patsy Hill Member of the Bonney Sandstone (Plate 1). The suprasalt Bunyeroo Formation comprises outer shelf shale facies. The suprasalt Wonoka Formation contains four informal lithostratigraphic units (lower, middle, and upper limestone, and green mudstone members) and is composed of outer shelf to foreshore mixed carbonate and siliciclastic facies. The suprasalt Patsy Hill Member consists of three informal lithostratigraphic units (lower dolomite, sandstone, and upper dolomite beds) and comprises marginal marine mixed carbonate and siliciclastic facies. Depositional facies of the Bunyeroo and Wonoka formations form broad linear facies belts, whereas depositional facies of the Patsy Hill Member form a spatially variable facies mosaic (Plate 2)

4.1.1 Bunyeroo Formation (Nwb)

The Bunyeroo Formation crops out in the suprasalt minibasin at the northwestern end of Patawarta diapir to the north of measured stratigraphic Section 4 (Plate 1; Appendix A). In diapir-distal exposures, it has a sharp basal contact with the underlying ABC Range Quartzite, whereas in diapir-proximal exposures, it onlaps Patawarta diapiric breccia and diagenetic caprock (Plate 1). It comprises shale and siltstone with rare, locally interbedded lenses of conglomerate to conglomeratic sandstone confined to the basal part of the formation (Figure 19). The shale and siltstone is dominantly red/maroon but may be

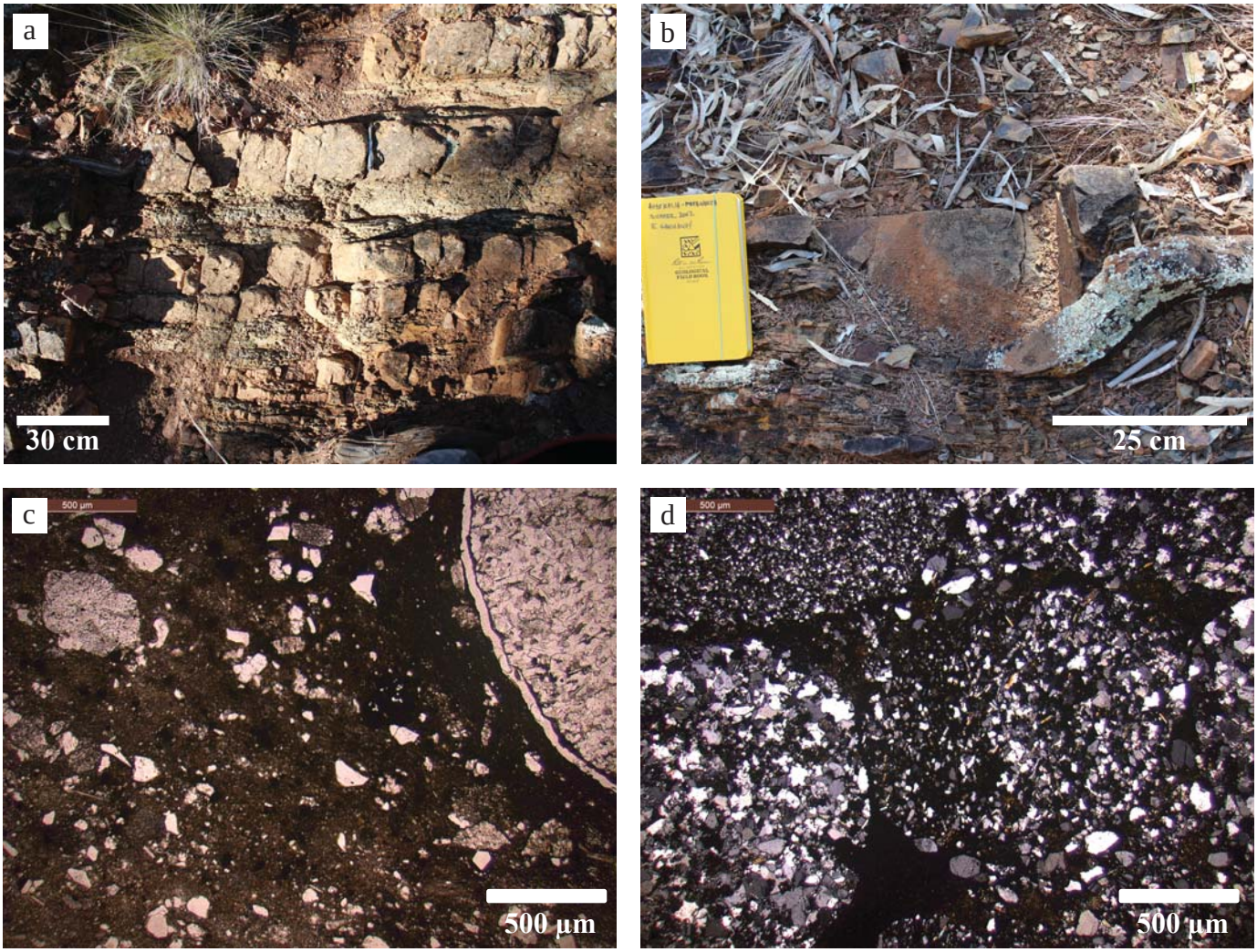

Figure 19. Photographs of the Bunyeroo Formation (Nwb) from the suprasalt minibasin adjacent to Patawarta diapir: (a) outcrop photograph of interbedded siltstone with conglomeratic sandstone in basal Bunyeroo Formation; (b) outcrop photograph of conglomerate lense in maroon siltstone; (c) thin section photomicrograph of sand to pebble-sized lithic clasts in shale matrix (ppl); (d) thin section photomicrograph of pebble conglomerate (xp).

locally green, yellow, tan, or orange-brown. It is thin-bedded (0.5-10 cm thick) and lacks sedimentary structures besides lamination. The orange-brown conglomerate to conglomeratic sandstone beds are thin-bedded, dominantly clast-supported, and contain coarse-grained sand with granule and pebble clasts (Figure 19a,b). The rounded, moderately well-sorted sand component consists of quartz with minor feldspar grains. The granule to pebble fraction includes rounded, elongate to tabular clasts of siltstone, chert, quartzite, shale, silicified carbonate, and meta-igneous clasts. (Figure 19c,d). Conglomerate beds were documented at the base of the Bunyeroo Formation in the most diapir-proximal measured stratigraphic section only (Section 9) directly adjacent to the northern domain of diapiric breccia at the northwestern end of Patawarta diapir. They occur as broad, lense-like outcrops that thin away from the diapir and grade into the more dominant shale and siltstone (Figure 19a,b).

The depositional environment of the Bunyeroo Formation in the suprasalt minibasin is interpreted as a deep basinal to outer shelf setting below fair-weather and storm wave base (Figure 20) based on the minimal coarse-grained sediment input and the absence of sedimentary structures in the thick, homogenous stratal package. These observations are consistent with the regional depositional interpretation as an offshore, deep-water basinal shale generally starved of coarse-grained sediment input (Gostin and Jenkins, 1983; Haines, 1990). The local conglomerates and conglomeratic sandstone lenses present in this stratal unit (Figure 19), which contain meta-igneous and silicified carbonate clasts, record periods of exposure and erosion of the diapir and diapir caprock during storm events.

4.1.2 Wonoka Formation

The four informal lithostratigraphic units of the Wonoka Formation as originally defined for the subsalt stratigraphy at Patawarta diapir by Kernen et al. (2012) are recognized in the suprasalt minibasin, but vary in internal lithofacies, stratal thickness, stratal geometry, and halokinetic upturn (Plate 1). The units comprise, in ascending stratigraphic order, (1) lower limestone member, Nwwll; (2) middle limestone member, Nwwlm; (3) upper limestone member, Nwwlu; and (4) green mudstone member, Nwwgm (Figure 10). The informal members correspond to Wonoka Formation units 1-8 of Haines (1990) as follows: (1) Wonoka lower limestone member corresponds to units 1-4; (2) Wonoka middle limestone

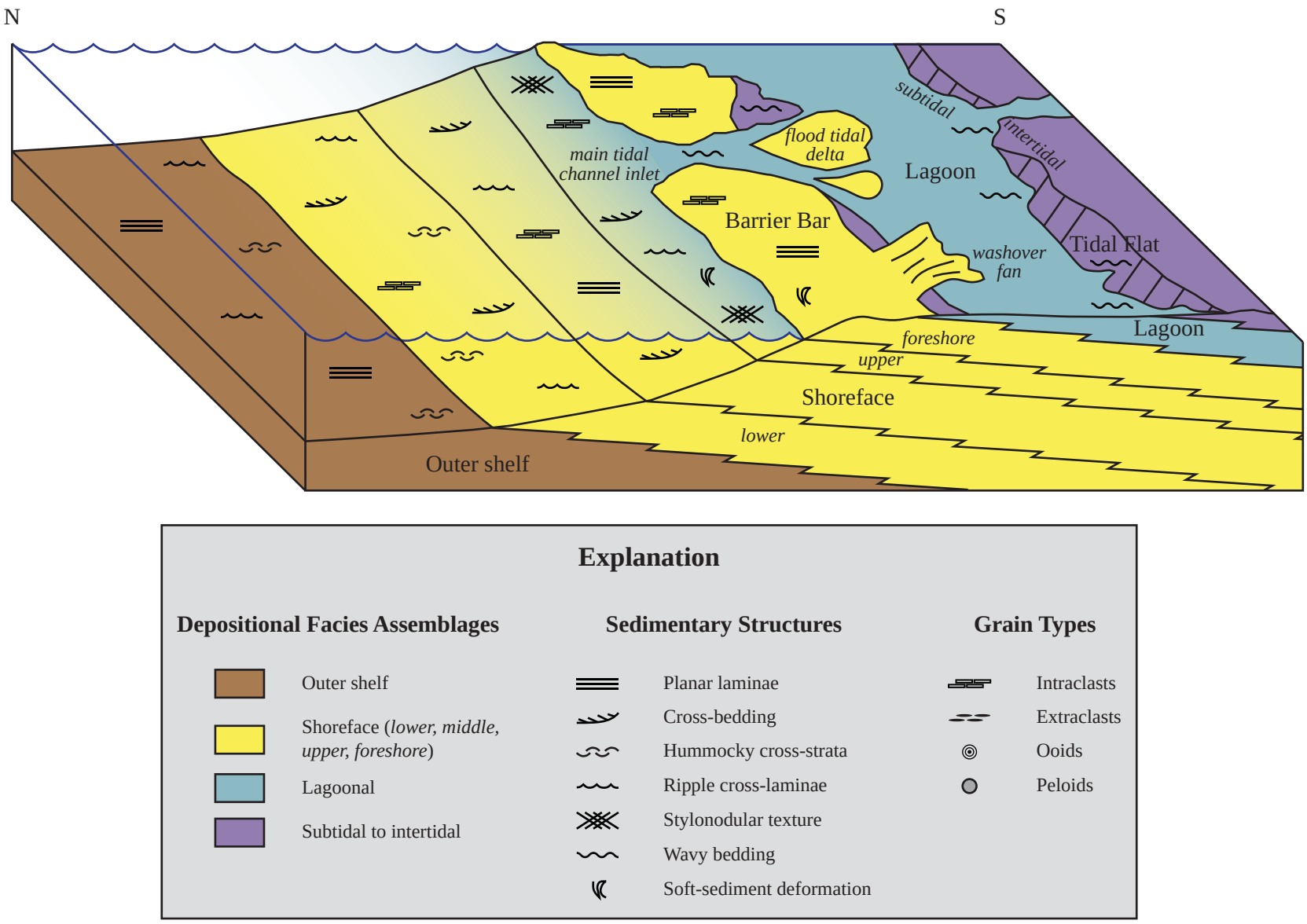

Figure 20. Interpreted depositional profile for Bunyeroo, Wonoka, and Patsy Hill strata in the suprasalt minibasin at Patawarta diapir in overall shallowing upward outer shelf to shoreface and barrier bar-lagoon complex environments (adapted from Kernen, et al., 2012; modifed from Coe, 2002).

member corresponds to unit 5; (3) Wonoka upper limestone member corresponds to units 6-7; and (4) Wonoka green mudstone member corresponds to unit 8 (Figure 10).

Lower limestone member (Nwwll)

The lower limestone member of the Wonoka Formation crops out in the suprasalt minibasin at the northwestern end of Patawarta diapir to the north of measured stratigraphic Section 6 (Plate 1; Appendix A). Throughout the minibasin, the contact with the underlying Bunyeroo Formation is sharp and demarcated by the first occurrence of carbonate-rich sediments. The lower limestone member comprises lime mudstone, silty-lime mudstone, and calcareous siltstone (Figure 21).

The lime mudstone is red-pink, purple, and green-gray (weathered and fresh) and displays horizontal laminae, reduction spots, and sole marks (Figure 21a,b). The silty-lime mudstone is red, purple, and green (weathered and fresh) and displays horizontal laminae, low-angle cross-bedding, hummocky cross-stratification, oscillation and asymmetric ripples, fine-grained turbidites (dominantly Bouma B and C subdivisions; Bouma, 1962), and rare reduction spots (Figure 21c,f). The lime mudstone and silty-lime mudstone beds are typically thin- to medium-bedded (avg. 3 mm - 10 cm thick, rare up to 40 cm thick) and have thin intraclast conglomerate horizons containing lime mudstone and silty-lime mudstone rip-up clasts (Figure 21d). The red, purple, and green (weathered and fresh) calcareous siltstone is thin-bedded (5 mm - 5 cm thick), commonly micaceous, and displays horizontal laminae, low-angle cross-bedding, oscillation and current ripples, and hummocky cross-stratification. Cyclically interbedded packages of silty-lime mudstone (10-50 cm) and calcareous siltstone (0.5-3 m) dominate the middle and upper zones of the lower limestone member (Figure 21e). Slumping and convolute bedding are present throughout this stratal unit, but are more prevalent in diapir-distal settings.

The depositional environment of the Wonoka lower limestone member in the suprasalt minibasin is interpreted as an outer shelf setting, which shallowed upward to a lower shoreface setting in the more diapir-proximal locations (Figure 20). Both turbidity currents and storm waves strongly influenced deposition of this stratal unit, particularly in diapir-distal settings. These interpretations are based on the horizontal laminae of the lime mudstone, silty-lime mudstone, and calcareous siltstone, the hummocky cross-stratification of the silty-lime mudstone and calcareous siltstone, the fine-grained turbidites in the

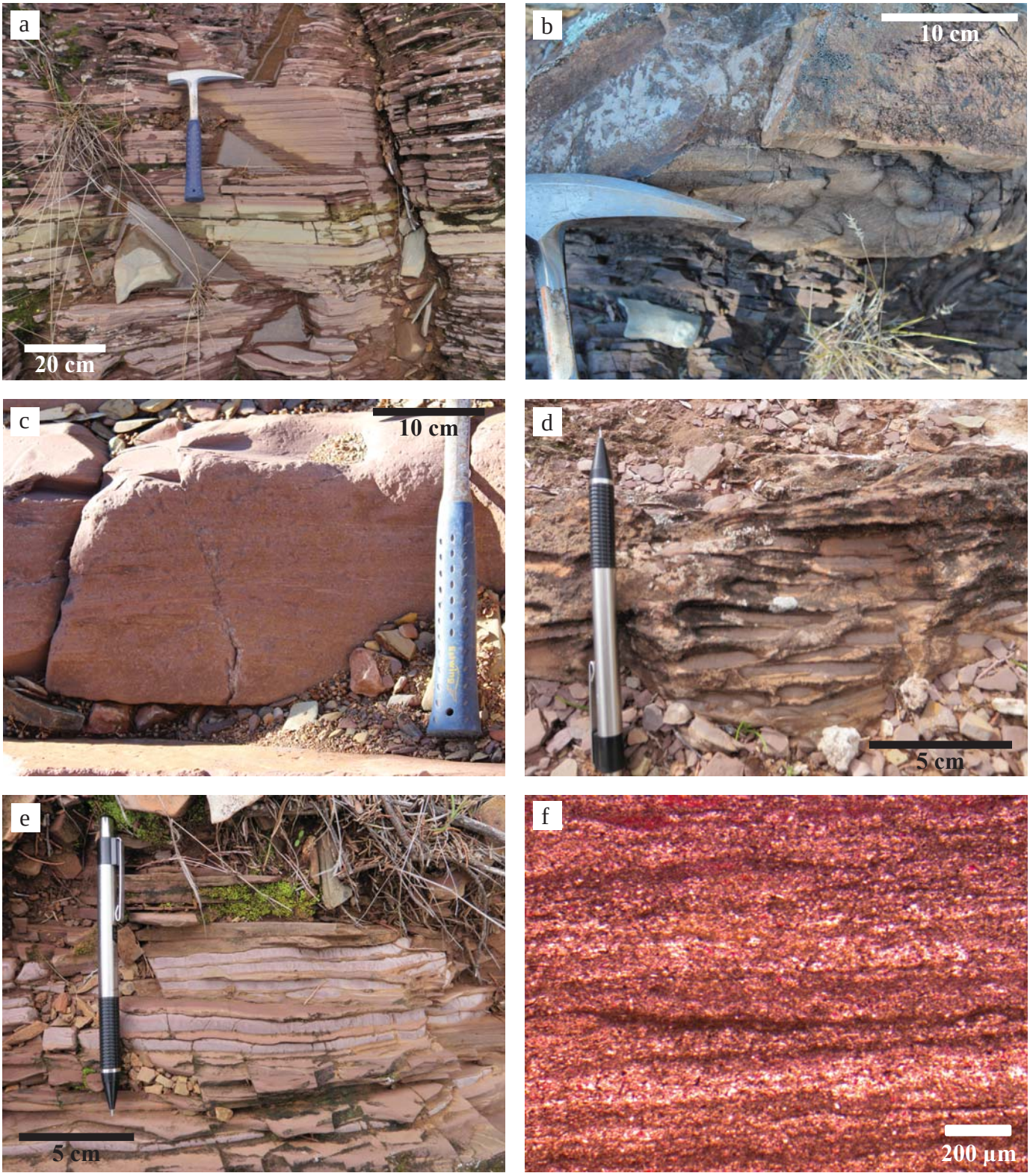

Figure 21. Photographs of the lower limestone member of the Wonoka Formation (Nwwll) from the suprasalt minibasin adjacent to Patawarta diapir: (a) outcrop photograph of horizontal laminae in lime mudstone; (b) outcrop photograph of sole marks in lime mudstone; (c) outcrop photograph of faint hummocky cross-stratification in silty-lime mudstone; (d) outcrop photograph of intraclast conglomerate horizon; (e) outcrop photograph of interbedded lime mudstone and calcareous siltstone; (f) thin section photomicrograph of horizontal laminae in silty-lime mudstone (ppl).

silty-lime mudstone, and the convolute bedding throughout the unit (Haines, 1990; Coe, 2002; Plint, 2010). These observations are consistent with the regional depositional interpretation by Haines (1990) of Wonoka Formation units 1-4 in an outer shelf environment near storm wave base.

Middle limestone member (Nwwlm)

The middle limestone member of the Wonoka Formation crops out in the suprasalt minibasin at the northwestern end of Patawarta diapir to the north of measured stratigraphic Section 4 (Plate 1; Appendix A). The contact with the underlying Wonoka lower limestone member is gradational. In the most diapir-proximal locations (Sections 5 and 6), the lower limestone member is not present and the middle limestone member directly onlaps the Bunyeroo Formation (Plate1). The middle limestone member comprises silty-lime mudstone, calcareous siltstone, and minor lime mudstone (Figure 22).

The gray, blue-gray, and red-gray (weathered and fresh) silty-lime mudstone is thin-bedded (1-10 cm thick) and displays horizontal laminae, hummocky cross-stratification, low-angle cross-bedding, oscillation ripples, and convolute bedding (Figure 22a). Intraclast conglomerate horizons within the silty-lime mudstone intervals are composed of lime mudstone and silty-lime mudstone rip-up clasts and increase in frequency and bed thickness (8 cm - 1.5 m thick) from the diapir-proximal to diapir-distal position (Figure 22c). The thin-bedded, gray-green (weathered and fresh) calcareous siltstone displays horizontal laminae. The silty-lime mudstone and calcareous siltstone frequently occur as thinly interbedded mudstone (1-5 cm thick) and thinly laminated siltstone (3 mm - 2 cm thick) throughout this unit (Figure 22b). However, thicker overall packages of dominantly silty-lime mudstone (1.5-15 m thick) and calcareous siltstone (2.5-7.5 m thick) are identifiable with a general increase in mudstone content upsection.

The depositional environment of the Wonoka middle limestone member in the suprasalt minibasin is interpreted as lower and middle shoreface settings above fair-weather wave base in diapir-distal and diapir-proximal locations, respectively, which shallow upward to an upper shoreface environment throughout the suprasalt minibasin (Figure 20). These interpretations are based on the hummocky cross-stratification, low-angle cross-bedding, and oscillation ripples present within the silty-lime mudstone and horizontal laminae of the silty-lime mudstone and calcareous siltstone (Haines, 1990; Coe, 2002; Plint,

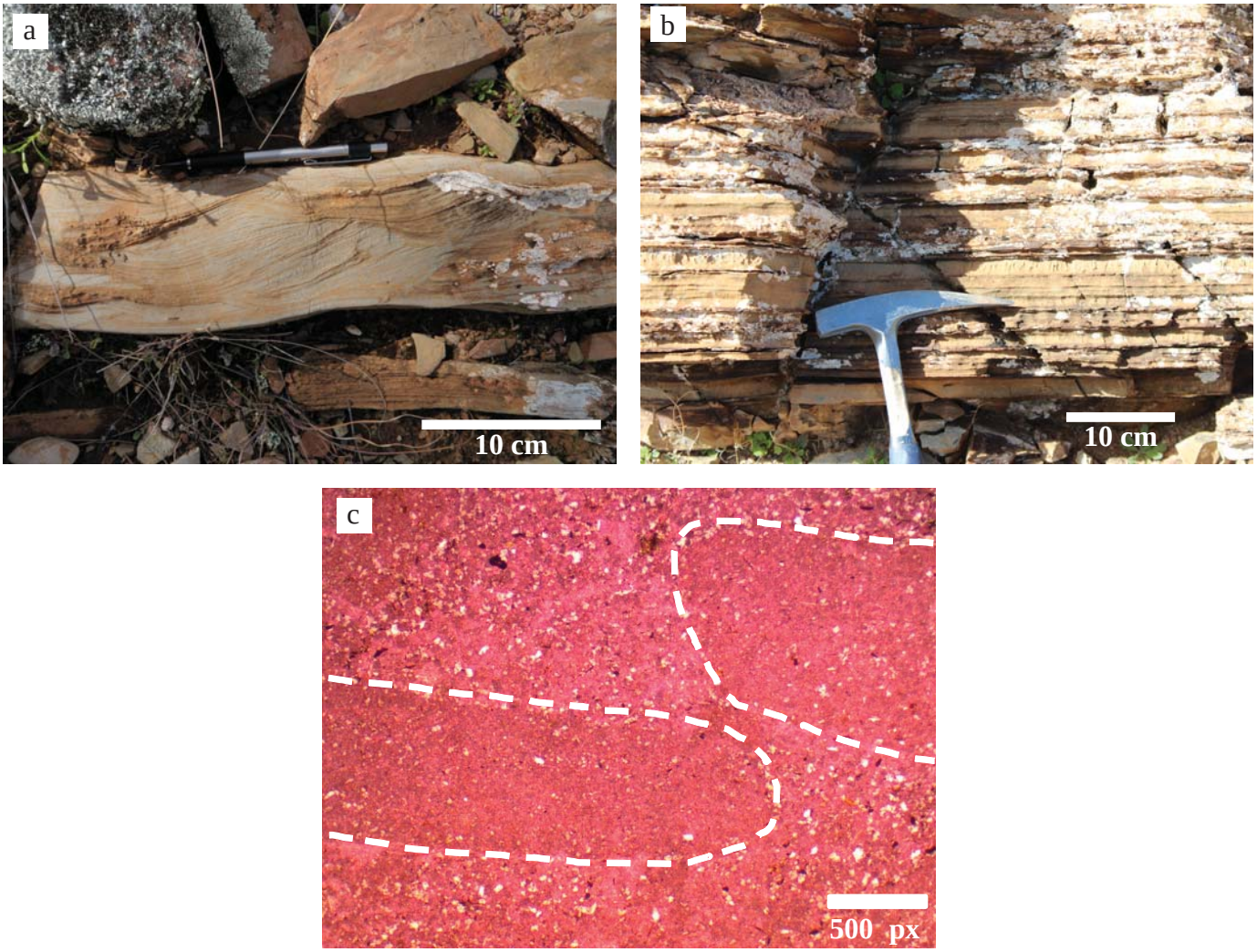

Figure 22. Photographs of the middle limestone member of the Wonoka Formation (Nwwlm) from the suprasalt minibasin adjacent to Patawarta diapir: (a) outcrop photograph of hummocky cross-stratification in silty-lime mudstone; (b) outcrop photograph of thinly interbedded silty-lime mudstone and calcareous siltstone; (c) thin section photomicrograph of intraclast conglomerate horizon in silty-lime mudstone (ppl).

2010). These observations are consistent with the regional depositional interpretation by Haines (1990) of Wonoka Formation unit 5 as an outer to middle shelf environment above storm wave base.

Upper limestone member (Nwwlu)

The upper limestone member of the Wonoka Formation crops out in the suprasalt minibasin at the northwestern end of Patawarta diapir to the north of measured stratigraphic Section 5 (Plate 1; Appendix A). The contact with the underlying Wonoka middle limestone member is gradational. The upper limestone member comprises lime mudstone to silty-lime mudstone, litharenite, calcareous siltstone, and rare cyanobacterial laminite (Figure 23).

The green-gray to blue-gray, red, and purple (weathered) and green-gray to dark gray (fresh) lime mudstone to silty-lime mudstone is thin- to medium-bedded (2 cm - 1 m thick) and displays hummocky cross-stratification, climbing wave ripples, soft-sediment deformation, and stylonodular bedding (see Haines, 1987 for description and interpretation of this sedimentary structure; Figure 23a,d) . Thin intraclast conglomerate beds (max. 10 cm thick) occur within the lime mudstone to silty-lime mudstone intervals and are composed of lime mudstone and silty-lime mudstone rip-up clasts (Figure 23a). The red (weathered and fresh) litharenite is composed of moderately well-sorted, sub-rounded to rare sub-angular, very fine- to fine-grained lithic grains of recrystallized lime mudstone with minor quartz (Figure 23b,e). It is thin-bedded (1-5 cm thick) and displays horizontal laminae, low-angle cross-bedding, hummocky cross-stratification, and dewatering structures (Figure 23b). The green (weathered and fresh) calcareous siltstone is thin-bedded (2-5 mm thick) and displays horizontal laminae. A thin interval of interlaminated dense, dark micrite and coarse-grained calcite spar is present near the top of the upper limestone member in the diapir-distal synclinal basin and is interpreted as a cyanobacterial laminite horizon (Figure 23c,f).

The depositional environment of the Wonoka upper limestone member in the suprasalt minibasin is interpreted as an upper shoreface to foreshore setting (Figure 20). This interpretation is based on the presence of climbing wave ripples and stylonodular bedding of the lime mudstone and silty-lime mudstone, horizontal laminae and low-angle cross-bedding of the litharenite, and the presence of the cyanobacterial laminite horizon (Haines, 1990; Coe, 2002; Plint, 2010). These observations are consistent with the regional depositional interpretation by Haines (1990) of Wonoka Formation units 6-7 in a middle

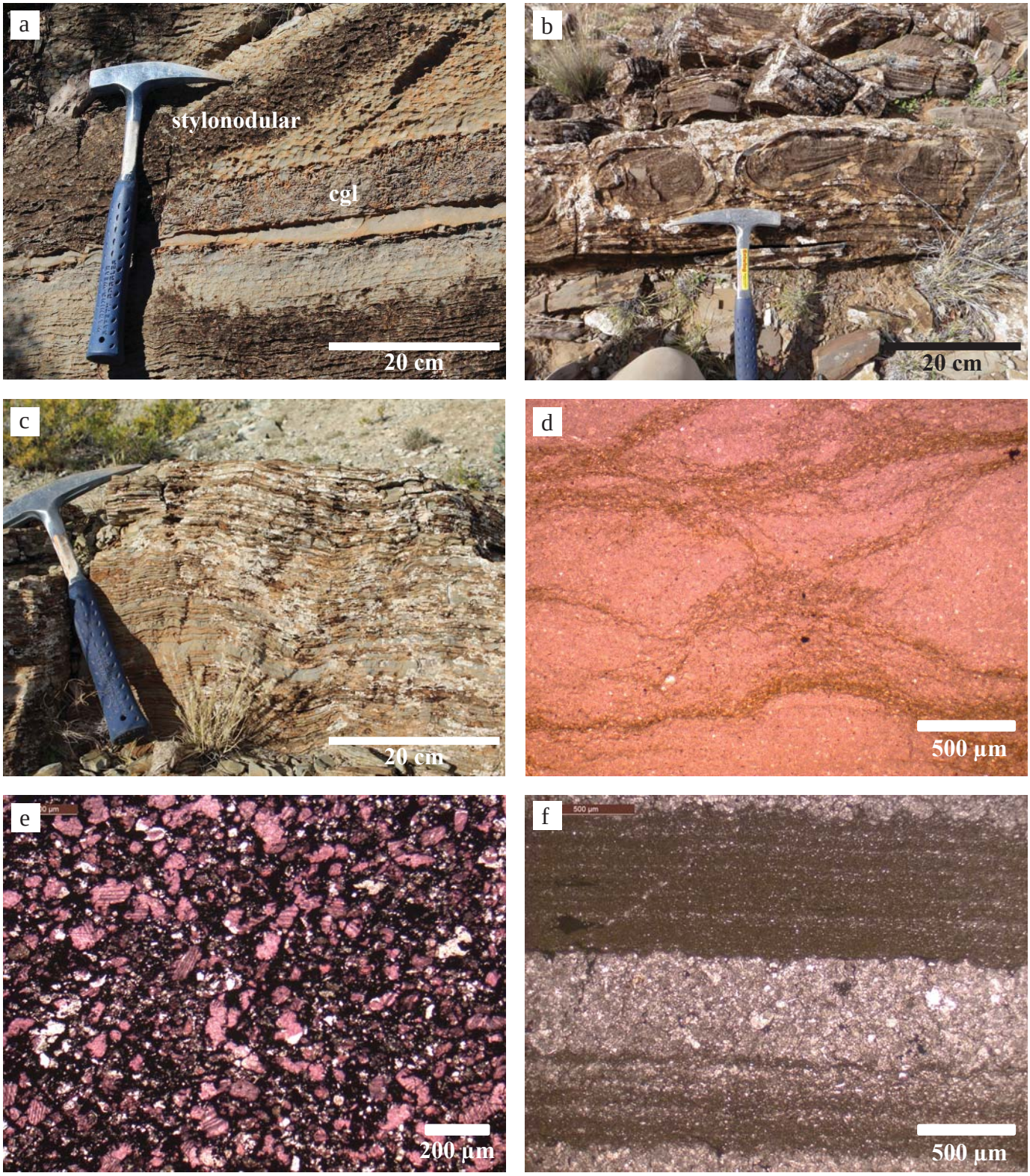

Figure 23. Photographs of the upper limestone member of the Wonoka Formation (Nwwlu) from the suprasalt minibasin adjacent to Patawarta diapir: (a) outcrop photograph of stylonodular bedding and intraclast conglomerate horizon in lime mudstone; (b) outcrop photograph of horizontal laminae and dewatering structures in litharenite; (c) outcrop photograph of cyanobacterial laminite horizon; (d) thin section photomicrograph of stylonodular bedding in lime mudstone (ppl); (e) thin section photomicrograph of litharenite (ppl); (f) thin section photomicrograph of cyanobacterial laminite horizon (ppl).

shelf environment above storm wave base that shallowed upward to an inner shelf environment at fair weather wave base.

Green mudstone member (Nwwgm)

The green mudstone member of the Wonoka Formation crops out in the suprasalt minibasin at the northwestern end of Patawarta diapir to the north of measured stratigraphic Section 5 (Plate 1; Appendix A). The contact with the underlying Wonoka upper limestone member transitions from sharp and abrupt in diapir-proximal settings to gradational in diapir-distal settings. The green mudstone member comprises calcareous siltstone to shale with subordinate interbedded lime to silty-lime mudstone, stromatolitic boundstone, lithoclastic wackestone, and calcareous subarkose to sublitharenite, as well as rare conglomeratic litharenite and oolitic (-peloidal) packstone to grainstone (Figure 24).

The yellow-green (weathered and fresh), fine-grained calcareous siltstone in the lower and middle part of this unit is thin-bedded (5 mm – 8 cm thick) and displays fine horizontal laminae, low-angle cross-bedding, and oscillation ripples (Figure 24a). It is interbedded with the various thin-bedded carbonate facies and grade distally into yellow-green shale (Figure 24e). It transitions at the top of this unit to green to brown (weathered) and green to light tan (fresh) shale to shaley siltstone and red, red-purple, and brown (weathered) and red to gray (fresh) siltstone. The shale to shaley siltstone is thin-bedded (avg. 1 cm thick) and displays fine, horizontal laminae. The siltstone is thin-bedded (1-3 cm thick), displays horizontal laminae and rare oscillation ripples, and may be micaceous, calcareous, or locally dolomitic (Figure 24b).

The green-gray (weathered) and light to dark gray (fresh) lime mudstone to silty-lime mudstone is thin-bedded (1-5 cm thick) with low-angle cross-bedding and rare hummocky cross-stratification. The lime to silty-lime mudstone is interbedded with siltstone and shale at the base of this unit and bedsets increase in frequency from diapir-proximal to diapir-distal locations.

Stromatolitic boundstone form alternating dark gray and light gray (weathered and fresh)layers containing wavy laminations with minor relief (<3cm) and are partially to completely dolomitized in diapir-proximal locations (Figure 24c,f). Rare litharenite stringers are present and consist of poorly sorted, sub-angular silt to coarse-grained sand and rare pebble clasts. Lithic grains include quartz, calcite,

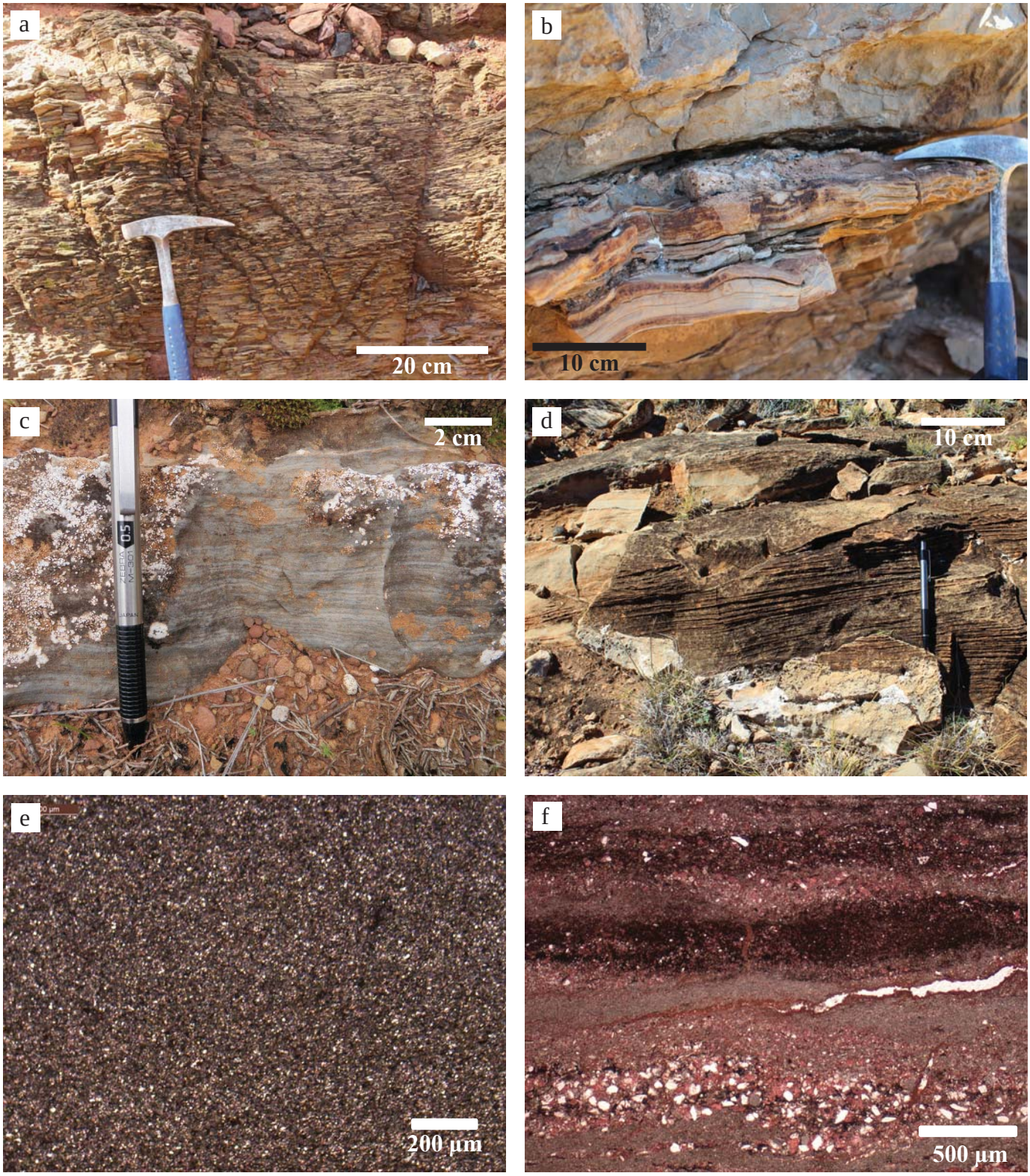

Figure 24. Photographs of the green mudstone member of the Wonoka Formation (Nwwgm) from the suprasalt minibasin adjacent to Patawarta diapir: (a) outcrop photograph of yellow-green calcareous siltstone to shale; (b) outcrop photograph of oscillation ripples in calcareous siltstone; (c) outcrop photograph of wavy laminae in stromatolitic boundstone; (d) outcrop photograph of horizontal laminae and low-angle cross-bedding in lithoclastic wackestone; (e) thin section photomicrograph of yellow-green shaley siltstone (xp); (f) thin section photomicrograph of interbedded stromatolitic boundstone (ppl).

dolomite, siltstone, chert, quartzite, and shale. Thin intraclast conglomerate horizons (max. 10 cm thick) of elongate rip-up clasts of cyanobacterial mat also occur within the stromatolitic boundstone intervals.

The lithoclastic wackestone is light to dark gray and locally tan, pink, green and purple (weathered and fresh). It is thin- to medium-bedded (1-20 cm thick), and displays low-angle cross-bedding, wavy bedding, and horizontal laminae, but may also be completely homogenous (Figure 24d). The sub-angular silt to sub-rounded coarse-grained sand and granule lithic component is dominantly quartz with minor feldspar, calcite, dolomite, siltstone, chert, and peloids. The stromatolitic boundstone and lithoclastic wackestone with subordinate interbedded siltstone and shale dominates the middle of this unit, but are present less frequently towards the top of this unit.

The pink-gray to red-gray (weathered) and pink to light gray (fresh) subarkose to sublitharenite contain moderately sorted, sub-rounded to sub-angular, medium-grained quartz sand with feldspar and lithic siltstone and chert grains. It is thin- to medium-bedded (2-30 cm thick) and displays horizontal laminae, oscillation and current ripples, and low-angle cross-bedding. It typically forms coarsening-upward packages with the shale and siltstone in the upper part of this unit but with variable proportions of fine- to coarse-grained material.

Conglomeratic litharenite is rare but present in the middle of this unit and contains poorly sorted, coarse-grained sand to granule-sized quartz and lithic extraclasts and intraclasts. The sub-angular to angular, polymict extraclasts include siltstone, chert, quartz sandstone, and strained quartz, while the sub-rounded intraclasts include lime mudstone, dolomudstone, and crystalline dolomite. The rare yellow-tan (weathered) to gray (fresh) oolitic (-peloidal) packstone to grainstone occur in diapir-distal locations and contain a poorly sorted mixture of ooid types including normal, superficial, composite, and deformed ooids, as well as peloids. The ooid cores are typically recrystallized calcite or dolomite spar, but concentric growth lines in the micritic grain coatings are often identifiable.

The depositional environment of the Wonoka green mudstone member in the suprasalt minibasin is interpreted as an upper shoreface to foreshore setting that transitioned upward to lagoonal and subtidal to intertidal settings (Figure 20). These interpretations are based on the horizontal laminae of the shale, siltstone, and sandstone, the low-angle cross-bedding of the siltstone, sandstone, and lime to silty-lime

mudstone, the diverse ripples of the subarkose and sublitharenite, and the interbedded stromatolitic boundstone (Scholle, et al, 1983; Haines, 1990; Coe, 2002; Plint, 2010). These observations are consistent with the regional depositional interpretation by Haines (1990) of Wonoka Formation unit 8 in inner shelf environment below fair weather wave base that transitioned upward to a lagoonal environment at the top.

4.1.3 Patsy Hill Member

The three informal lithostratigraphic units of the Patsy Hill Member of the Bonney Sandstone as originally defined for the subsalt stratigraphy at Patawarta diapir by Kernen et al. (2012) are recognized in the suprasalt minibasin, but vary in internal lithofacies, stratal thickness, and stratal geometry (Plate 1). The units are, in ascending stratigraphic order, (1) lower dolomite beds, Npbpdl; (2) sandstone beds, Npbps; and (3) upper dolomite beds, Npbpdu (Figure 9). The informal units correspond to Wonoka Formation units 9-11 of Haines (1990) as follows: (1) Patsy Hill lower dolomite beds correspond to unit 9; (4) Patsy Hill sandstone beds correspond to unit 10; (5) Patsy Hill upper dolomite beds correspond to unit 11 (Figure 10).

Lower dolomite beds (Npbpdl)

The lower dolomite beds of the Patsy Hill Member crop out in the suprasalt minibasin at the northwestern end of Patawarta diapir to the north of measured stratigraphic Section 8 (Plate 1; Appendix A). The contact with the underlying Wonoka green mudstone member is conformable but abrupt. The lower dolomite beds comprise lithoclastic wackestone to packstone with subordinate interbedded stromatolitic boundstone (Figure 25).

The gray to dark gray (weathered and fresh) lithoclastic wackestone to packstone is thin- to medium-bedded (2 cm – 1 m thick) and consists of sand-sized grains of quartz, calcite, dolomite, and lithic siltstone and rare dolomicrite (Figure 25b). The dark gray to tan, dolomitized stromatolitic boundstone contains thin, wavy laminae (Figure 25c) and forms cyclic, thin interbeds (max. 5 cm thick) with the lithoclastic wackestone to packstone (Figure 25c). The lower dolomite beds occur as generally tabular stratigraphic units that do not display channelization. The entire unit is heavily karsted, brecciated, and disrupted, particularly near the top, which results in yellow-tan to orange, weathered outcrops.

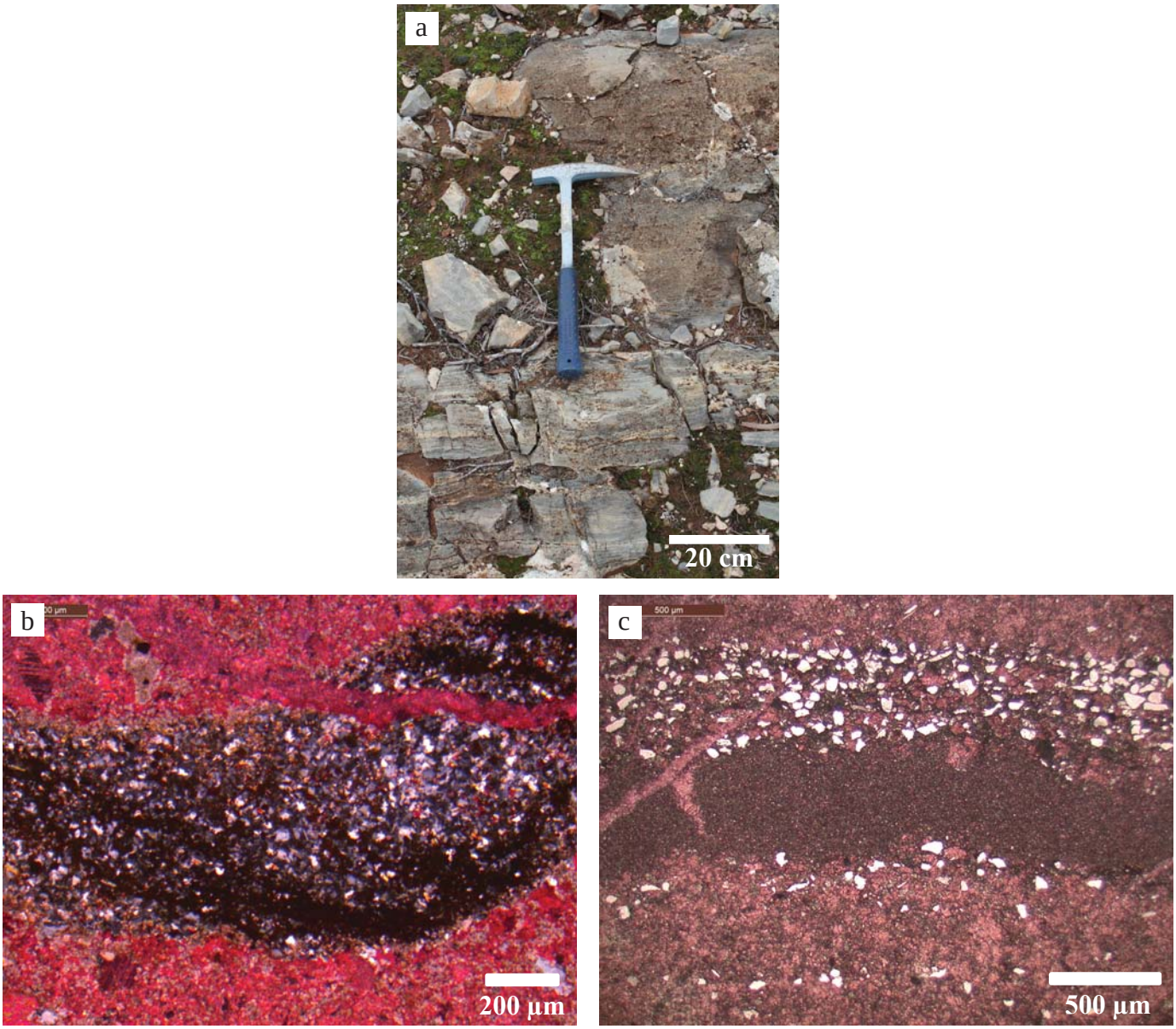

Figure 25. Photographs of the lower dolomite beds of the Patsy Hill Member of the Bonney Sandstone (Npbpdl) from the suprasalt minibasin adjacent to Patawarta diapir: (a) outcrop photograph of lithoclastic wackestone to packstone with interbedded stromatolitic boundstone at base; (b) thin section photomicrograph of lithoclastic wackestone to packstone (xp); (c) thin section photomicrograph of stromatolitic boundstone with possible mudcrack (ppl).

The depositional environment of the Patsy Hill lower dolomite beds in the suprasalt minibasin is interpreted as a tidal flat setting within the intertidal zone (Figure 20) based on the lack of channel development in this unit and the cyclically interbedded lithoclastic wackestone to packstone and thin stromatolitic boundstone (Scholle et al., 1983; Haines, 1990; Coe, 2002). These observations are consistent with the regional depositional interpretation by Haines (1990) of Wonoka Formation unit 9 in a shallow subtidal lagoonal environment.

Sandstone beds (Npbps)

The sandstone beds of the Patsy Hill Member crop out in the suprasalt minibasin at the northwestern end of Patawarta diapir only in the most diapir-distal locations (Section 11) in the synclinal axis of the minibasin (Plate 1; Appendix A). The contact with the underlying Patsy Hill lower dolomite beds is sharp and erosional. Approximately 30º of angular discordance was documented between the sandstone beds and underlying lower dolomite beds, which suggests Patsy Hill sandstone beds onlapped an erosional basal unconformity following rotation of the underlying lower dolomite beds. The sandstone beds comprise interbedded shale and fine-grained sandstone and minor lithoclastic wackestone to packstone (Figure 26).

The yellow-green (weathered and fresh) shale is thin-bedded and displays horizontal laminae. The pink to yellow (weathered and fresh) sandstone is fine-grained and thin-bedded with horizontal laminae and low-angle cross-bedding (Figure 26). A thin- to medium-bedded lithoclastic wackestone to packstone bed with horizontal laminae separates the more common lower and upper packages of interbedded shale and sandstone.

The depositional environment of the Patsy Hill sandstone beds in the suprasalt minibasin is interpreted as a barrier island or flood tidal delta setting (Figure 20) based on the onlapping geometry, restricted distribution in the minibasin syncline axis, low-angle cross-bedding of the sandstone, and horizontal laminae of the shale and sandstone (Scholle et al., 1983; Haines, 1990; Coe, 2002). These observations are consistent with the regional depositional interpretation by Haines (1990) of Wonoka Formation unit 10 in a shallow water environment varying from subtidal to intertidal and supratidal.

Figure 26. Outcrop photograph of the sandstone beds of the Patsy Hill Member of the Bonney Sandstone (Npbps) from the suprasalt minibasin adjacent to Patawarta diapir: Cross-bedding in calcareous sandstone.

Upper dolomite beds (Npbpdu)

The upper dolomite beds of the Patsy Hill Member crop out throughout the suprasalt minibasin at the northwestern end of Patawarta diapir in all measured stratigraphic sections (Plate 1; Appendix A). The abrupt but conformable contact with the underlying Patsy Hill sandstone beds is only preserved in the diapir-distal synclinal axis. In more diapir-proximal locations, the Patsy Hill upper dolomite beds have an unconformable basal contact and overlie progressively older Patsy Hill and Wonoka strata from distal (northwest) to proximal (southeast) settings. The most diapir-proximal exposures of Patsy Hill upper dolomite beds sit unconformably above Callana Group breccia of Patawarta diapir. The upper dolomite beds comprise stromatolitic boundstone, lithoclastic wackestone, oolitic-lithoclastic-peloidal packstone to grainstone, pebble conglomerate to conglomeratic sandstone, calcareous siltstone, and minor dolomite (Figure 27).

The tan-yellow (weathered) and gray (fresh), lenticular stromatolitic boundstone has wavy laminae with cm-scale relief and is commonly partially to entirely dolomitized (Figure 27c). It is thin- to thick-bedded and decreases in abundance away from the diapir. Litharenite stringers are commonly interlaminated with irregular to disrupted stromatolitic laminae and consist of polymict, poorly sorted, quartz silt to lithic pebble clasts, ooids, and peloids clusters. Lithic clasts include siltstone, chert, quartzite, shale, and intraclasts of lithoclastic wackestone, crystalline dolomite, and dolomudstone. Significant disruption of the stromatolitic laminae is common in the most diapir-proximal settings.

The dark gray (weathered and fresh) lithoclastic wackestone is thin-bedded (<10 cm thick) with wavy bedding. It contains rounded to sub-angular silt and sub-rounded to rounded coarse-grained sand to pebble-sized clasts of dominantly quartz with lithic siltstone, chert, and quartzite, and minor feldspars. This facies is often partially dolomitized (Figure 27a) and becomes finer-grained away from the diapir.

The oolitic-lithoclastic-peloidal packstone to grainstone is yellow-tan to red-purple (weathered) and dark gray, pink, and tan-white (fresh) (Figure 27d). It is variably thin- to medium-bedded with oscillation ripples and wavy bedding or thick-bedded to massive and homogenous. The coarse-grained detrital component consists of variable proportions of normal, superficial, and composite ooids, small peloids, and lithic siltstone, chert, quartzite, and silicified carbonate clasts, as well as quartz and feldspar. The ooid cores are typically recrystallized calcite or dolomite spar, and concentric growth lines in the

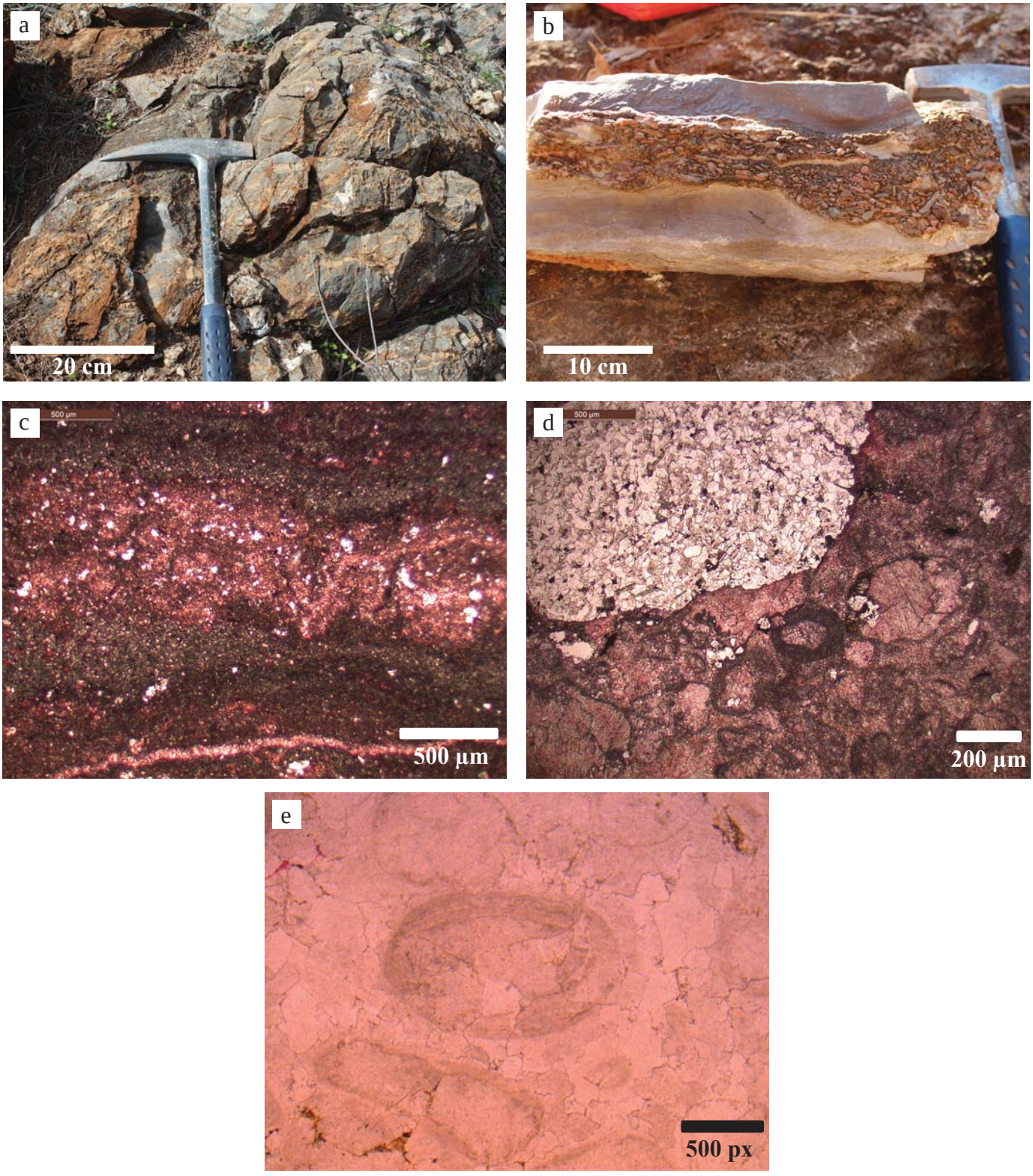

Figure 27. Photographs of the upper dolomite beds of the Patsy Hill Member of the Bonney Sandstone (Npbpdu) from the suprasalt minibasin adjacent to Patawarta diapir: (a) outcrop photograph of partially dolomitized lithoclastic wackestone; (b) outcrop photograph of pebble conglomerate bed with scoured base; (c) thin section photomicrograph of stromatolitic boundstone (ppl); (d) thin section photomicrograph of oolitic-lithoclastic-peloidal grainstone with lithic siltstone clast (upper left) and mixed ooid types showing overcompaction (center and lower right) (ppl); (e) thin section photomicrograph of oolitic grainstone with mixed ooid types as “ghosted” grains in coarse-grained dolomite spar (ppl).

micritic grain coatings are often identifiable. This facies may be completely dolomitized resulting in "ghosted" ooids and peloids preserved in coarse-crystalline dolomite spar (Figure 27e) (Haines, 1987).

The pebble conglomerate is typically clast-supported but may be locally matrix-supported and contains poorly sorted, rounded elongate to tabular granule to large pebble clasts with subordinate fine- to medium-grained sand (Figure 27b). The coarse-grained detrital component includes ooids, small peloids, and lithic granule to pebble clasts of siltstone, chert, quartzite, silicified carbonate, shale, strained quartz, and meta-igneous clasts, while the sand fraction is dominantly quartz with feldspar grains. Distally, the conglomerate beds decrease in abundance and thickness and grade into conglomeratic sandstone away from the diapir.

The red to dark red, green, and purple (weathered) and pink gray, green, and purple (fresh) calcareous siltstone is thin-bedded (0.5-3 cm thick), displays horizontal laminae and rare oscillation ripples, and is locally dolomitic. The tan to yellow (weathered) and light to dark gray and rare yellow (fresh) dolomite is medium-bedded and variably micritic to coarsely crystalline with no discernable original fabric.

The depositional environment of the Patsy Hill upper dolomite beds in the suprasalt minibasin is interpreted as a lagoonal setting with preservation of washover fan and flood tidal delta deposits (Figure 20) based on the presence of stromatolitic boundstone and the horizontal laminae and rare oscillation ripples of the calcareous siltstone (Scholle et al., 1983; Haines, 1990; Coe, 2002). These observations are consistent with the regional depositional interpretation by Haines (1990) of Wonoka Formation unit 11 in a subtidal lagoonal environment that periodically shallowed to develop ooid shoals and beach settings. The pebble conglomerates present in this stratal unit (Figure 27b), which contain meta-igneous and silicified carbonate clasts, record periods of exposure and erosion of the diapir and diapir caprock.

4.2 Diagenetic Facies

The Rim Dolomite crops out as thin, laterally discontinuous exposures along the northeastern margin of Patawarta diapir (Plate 1; Appendix A). The Rim Dolomite comprises silicified dolomite that ranges from 0 to 50 m in thickness along the salt-sediment interface for >2 km in the suprasalt minibasin.

It occurs as irregular, isolated exposures that separate the Patawarta diapiric breccia from Bunyeroo Formation shale and siltstone. Orientations of layering in the Rim Dolomite parallel the adjacent, steep to vertical Bunyeroo strata (Figure 28a). In the most diapir-proximal position, the Bunyeroo Formation is missing at the salt-sediment interface, and the Rim Dolomite is locally overlain by the upper dolomite beds of the Patsy Hill Member.

The microcrystalline dolomite is blue-gray to gray, yellow-tan, and pink (weathered and fresh) and displays variable massive, laminated, brecciated, and/or silicified fabrics (Figure 28b,c,d). Locally the Rim Dolomite appears conglomeratic with pink, tabular silicified pebble clasts floating in a dolomitic matrix. These fabrics transition abruptly both vertically and laterally within this unit with little consistency.

The Rim Dolomite is interpreted as a diagenetic carbonate caprock assemblage that developed on top of Patawarta diapir in a suprasalt position during deposition of the Bunyeroo Formation (Figures 4 and 17). This interpretation is based on the spatially variable dolomite fabrics and the irregular and zoned carbonate mantle that parallels the diapir margin and overlying stratigraphy (Kyle and Posey, 1991; Enos and Kyle, 2002; Warren, 2006; Giles et al., 2012; Shock, 2012). Ongoing inflation of the allochthonous salt sheet resulted in attenuation of the suprasalt carbonate caprock interval into laterally discontinuous outcrops along >2 km of the top salt-sediment interface. Subsequent stripping of the Patawarta roof strata in the diapir-proximal settings exposed the diagenetic caprock assemblage to erosion as well. This resulted in the incorporation of caprock-derived, silicified carbonate pebble clasts in the significantly younger Patsy Hill Member of the Bonney Sandstone (e.g. Figure 27b).

4.3 Stratal Thickness Trends

The stratal thickness variations of the map units in the suprasalt minibasin were compiled to establish trends in accommodation and deposition of Wilpena Group stratigraphy through time (Figures 29 and 30). When compared to correlative regional thicknesses (Haines, 1990), all suprasalt Wonoka and Patsy Hill stratal units are consistently thicker in the diapir-distal settings than regionally and locally thin dramatically, but variably towards the diapir (Figure 31). In diapir-proximal settings, suprasalt Wonoka

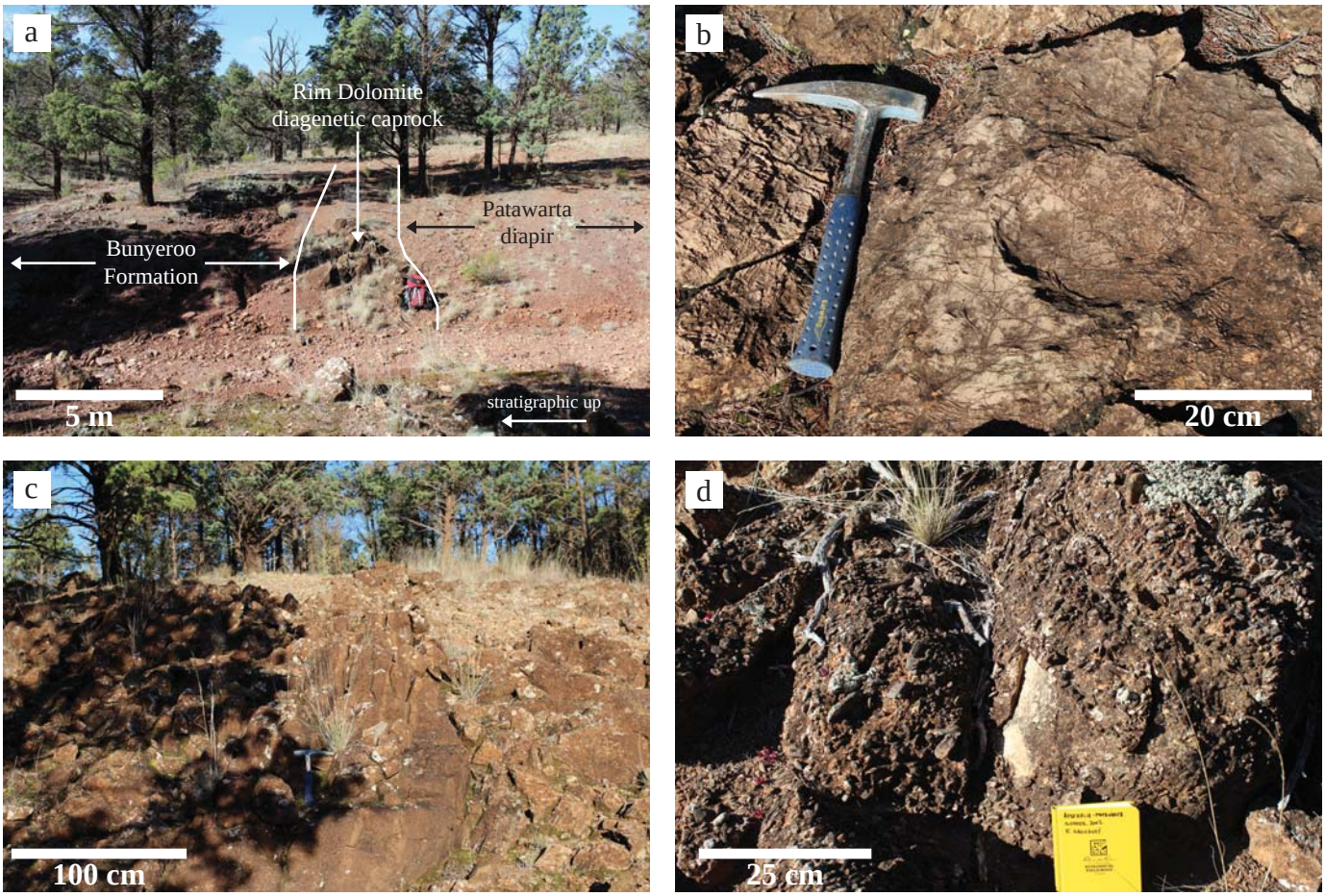

Figure 28. Outcrop photographs of diagenetic caprock fabrics of the Rim Dolomite from the suprasalt minibasin adjacent to Patawarta diapir: (a) salt-sediment interface with irregular contact of Patawarta diapiric breccia, Rim Dolomite diagenetic caprock, and Bunyeroo Formation maroon siltstone to shale; (b) brecciated dolomite; (c) laminated dolomite; (d) silicified, brecciated, and "conglomeratic" dolomite.

Stratigraphy		Map Unit	Thickest Section (m)	Location of Thickest Section	Thinnest Section (m)	Location of Thinnest Section	Lateral Distance of thinning toward diapir	Percentage of thinning
Bonney Sandstone	Patsy Hill Member	Npbpdu	105	11	20	1	5.8 km	81
		Npbps	156	12*	69	11	isolated lens	56
		Npbpdl	43	11	19	9	2.1 km	55
Wonoka Formation		Nwwgm	230	12	97	4	3.0 km	58
		Nwwlu	246	12	36	6	3.3 km	85
		Nwwlm	383	12	30	6	3.8 km	92
		Nwwll	779	12	247	9	4.2 km	96
Bunyeroo Formation		Nwb	1588	12	32	5	5.0 km	98

Figure 29. Stratigraphic unit thicknesses and locations relative to Patawarta diapir with calculated percentages of thinning for suprasalt stratal units; *indicates estimated thickness at Sec. 12 based on projected attitudes.

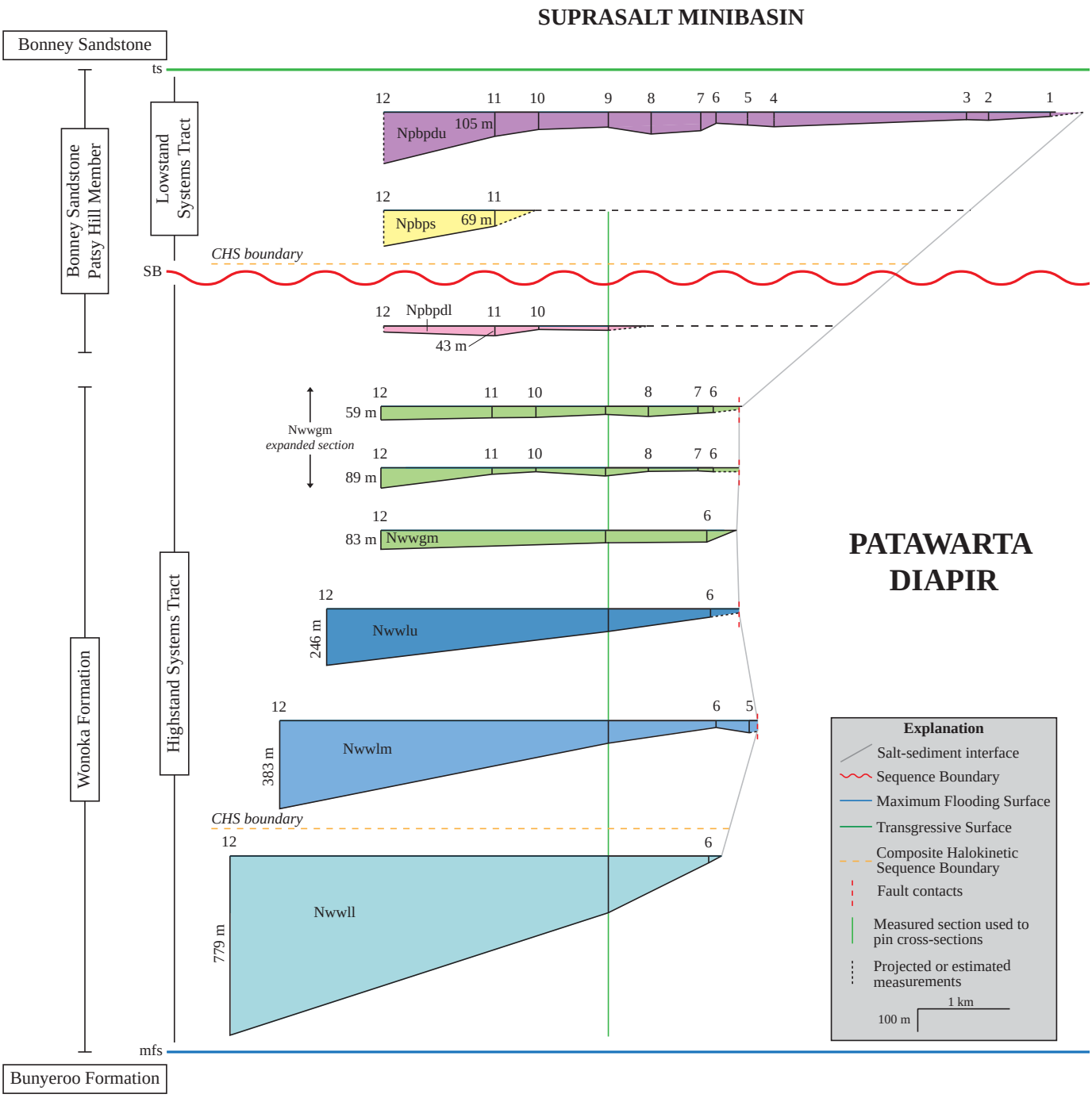

Figure 30. Interval thickness cross-sections of individual Wonoka and Patsy Hill stratal units constructed for the suprasalt minibasins; note that distances over which strata thin are ~3-6 km; meters represent thickest section measured for stratal units (see Figure 29).

Stratigraphy		Map Unit		Maximum Thicknesses (m)			Comparison of Thicknesses (%)		
				Bunyeroo Gorge (Haines, 1990)	Suprasalt Minibasin (Gannaway, 2014)	Subsalt Minibasin (Kernen et al., 2012)	Suprasalt to Regional	Subsalt to Regional	Suprasalt to Subsalt
Bonney Sandstone	Patsy Hill Member	Npbpdu	unit 11	80*	105	55	132	69	192
		Npbps	unit 10	30	69	40	230	133	173
		Npbpdl	unit 9	40*	43	40	108	100	108
Wonoka Formation		Nwwgm	unit 8	54	230	130	426	241	177
		Nwwlu	units 6-7	153	246	80	161	52	307
		Nwwlm	unit 5	105	383	215	365	205	178
		Nwwll	units 1-4	319	779	550	244	172	142

Figure 31. Comparison of regional thicknesses of the Wonoka Formation and Patsy Hill Member to maximum stratal thicknesses in suprasalt and subsalt minibasin strata at Patawarta diapir; * indicates regional thickness variations from the Haines' (1990) type section at Bunyeroo Gorge in the Central Flinders Ranges, where units 9 and 11 thicken to the north closer to Patawarta diapir.

stratal units are consistently thinner than their regional counterpart, whereas suprasalt Patsy Hill stratal units are approximately equivalent or slightly thicker (Haines, 1990).

Stratal units of the Bunyeroo and Wonoka formations display an upward decreasing trend in the percentage of thinning of individual map units through time (Figures 29 and 30). Stratal units of the Patsy Hill Member do not show a consistent trend in thinning through time. Thinning of the suprasalt stratal units occurs by a combination of dominantly low-angle onlap with subordinate local truncation (Figure 32). Minor angular discordance indicating stratal truncation was documented at two significant surfaces and formational contacts: 1) basal contact of the Wonoka middle limestone member (Nwwlm) with underlying Bunyeroo Formation (Nwb) and Wonoka lower limestone member (Nwwll) and 2) basal contact of the Patsy Hill Member upper dolomite beds (Npbpdu) with the underlying Wonoka (Nwwlm, Nwwlu, and Nwwgm) and Patsy Hill strata (Npbpdl and Npbps) (Figure 32; Plates 1 and 3).

4.3.1 Bunyeroo Formation (Nwb)

In the Patawarta suprasalt minibasin, the Bunyeroo Formation thins towards the diapir from 1588 m (Section 12) to 32 m (Section 5) over a lateral distance of 5.0 km (Figures 29 and 30), which represents a 98% decrease in intrabasinal stratal thickness. However, the suprasalt minibasin shows a nearly four-fold local increase in stratal thickness when compared to the regional thickness of the Bunyeroo Formation derived from the Bunyeroo Gorge area, which is approximately 400 m (Gostins and Jenkins, 1983). This trend is continued through the Wonoka Formation and is interpreted to be the result of increased accommodation in the minibasin center relating to subsidence into a thick underlying allochthonous salt sheet.

4.3.2 Wonoka Formation

The individual informal map units of the Wonoka Formation preserved in the suprasalt minibasin at Patawarta diapir thin dramatically toward the diapir or minibasin margin over distances of 3-4 km (Figures 29 and 30). The percentages of thinning of each stratal unit decrease steadily upward. Wonoka stratal units are consistently thicker in diapir-distal locations towards the center of the minibasin than regionally based on correlations to Wonoka units 1-8 of Haines (1990) (Figure 31). Conversely, Wonoka stratal units are consistently thinner in diapir-proximal locations than regionally.

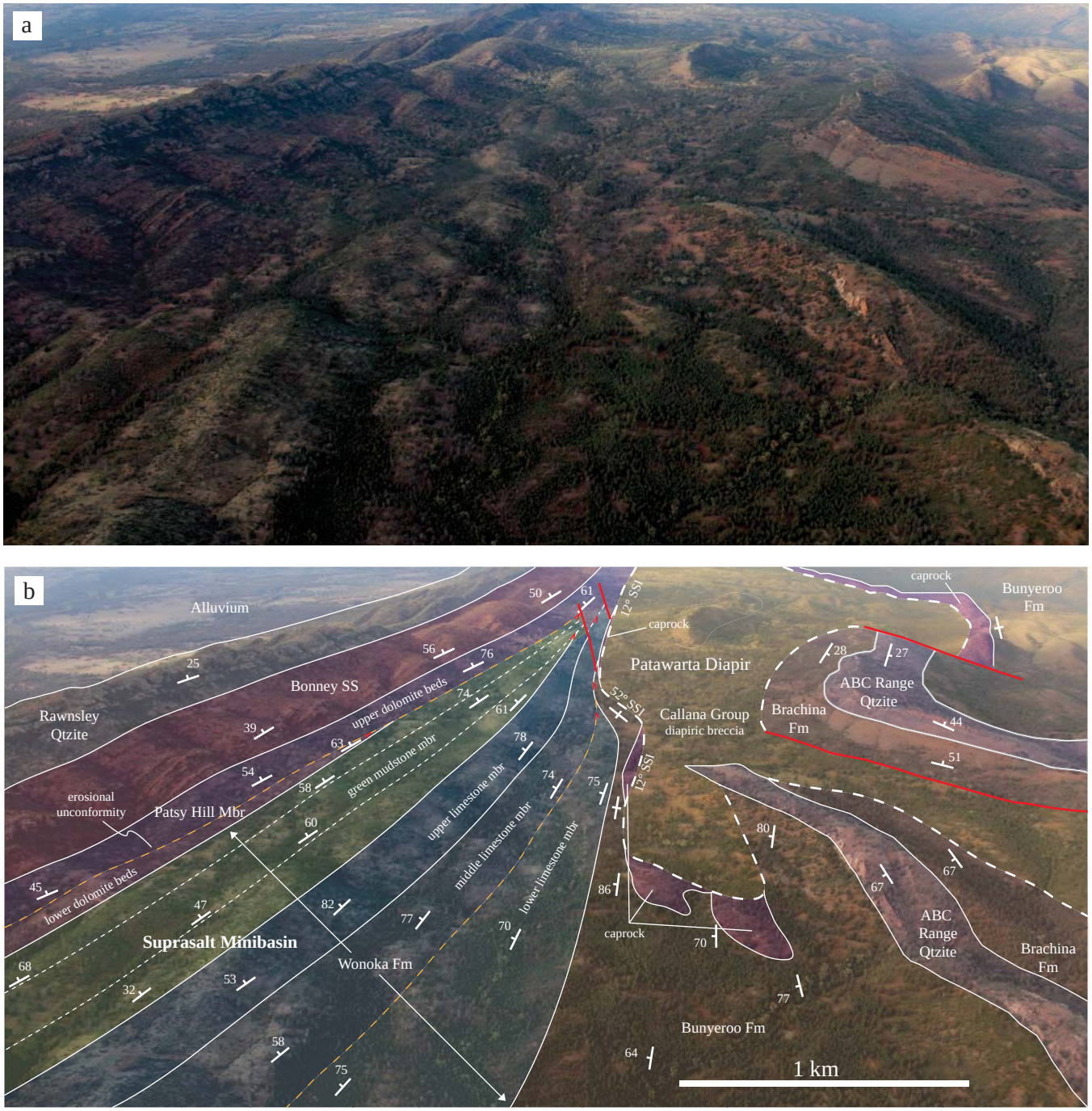

Figure 32. (a) Uninterpreted and (b) interpreted oblique aerial photograph of suprasalt stratal geometries flanking Patawarta diapir showing gradual thinning of Bunyeroo, Wonoka, and Patsy Hill strata by low-angle onlap and local stratal truncations; thick dashed white lines represent the boundaries of the Patawarta diapiric breccia, solid white lines are lithostratigraphic unit contacts, dashed orange lines are interpreted tapered CHS boundaries, thin dashed lines represent bedding traces, small red arrows are local stratal truncations, and solid red lines are faults; map unit colors match explanation from Plate 1; view is to the south-southeast.

The lower limestone member (Nwwll) of the Wonoka Formation thins towards the diapir from 779 m (Section 12) to 247 m (Section 9) over a lateral distance of 4.2 km (Figures 29 and 30). The percentage of thinning of the lower limestone member is 96% within the suprasalt minibasin. The regional thickness of the correlative Wonoka Formation units 1-4 from the type section at Bunyeroo Gorge is 319 m (Haines, 1990), which reflects a more than two-fold local increase (244%) in stratal thickness into the suprasalt minibasin (Figure 31).

The middle limestone member (Nwwlm) of the Wonoka Formation thins towards the diapir from 383 m (Section 12) to 30 m (Section 6) over a lateral distance of 3.8 km (Figures 29 and 30). The percentage of thinning of the middle limestone member is 92% within the suprasalt minibasin. The regional thickness of the correlative Wonoka Formation unit 5 from the type section at Bunyeroo Gorge is 105 m (Haines, 1990), which reflects a more than three-fold local increase (365%) in stratal thickness into the suprasalt minibasin (Figure 31).

The upper limestone member (Nwwlu) of the Wonoka Formation thins towards the diapir from 246 m (Section 12) to 36 m (Section 6) over a lateral distance of 3.3 km (Figures 29 and 30). The percentage of thinning of the upper limestone member is 85% within the suprasalt minibasin. The regional thickness of the correlative Wonoka Formation units 6-7 from the type section at Bunyeroo Gorge is ~153 m (Haines, 1990), which reflects an almost two-fold local increase (161%) in stratal thickness into the suprasalt minibasin (Figure 31).

The green mudstone member (Nwwgm) of the Wonoka Formation thins towards the diapir from 230 m (Section 12) to 97 m (Section 6) over a lateral distance of 3.0 km (Figures 29 and 30). The percentage of thinning of the green mudstone member is 58% within the suprasalt minibasin. The regional thickness of the correlative Wonoka Formation unit 8 from the type section at Bunyeroo Gorge is 54 m (Haines, 1990), which reflects a more than four-fold local increase (426%) in stratal thickness into the suprasalt minibasin (Figure 31).

The percentages of thinning of each stratal unit within the Wonoka Formation decreases steadily upward from 98% to 58% (Figure 29). This suggests that the amount of depositional relief over Patawarta diapir decreased from a maximum during Bunyeroo Formation deposition. The steady decrease in stratal

thickness of each unit in the suprasalt minibasin when compared to the regional suggests that differential subsidence into the allochthonous Patawarta salt sheet decreased throughout deposition of the Wonoka Formation (Figure 31).

4.3.3 Patsy Hill Member

The individual informal map units of the Patsy Hill Member of the Bonney Sandstone preserved in the suprasalt minibasin at Patawarta diapir thin dramatically toward the diapir or minibasin margin over distances of 2-6 km (Figures 29 and 30). The percentages of thinning of each stratal unit increase upward. Patsy Hill stratal units are consistently thicker in diapir-distal locations towards the minibasin center than regionally based on correlations to units 9-11 of Haines (1990). They thin toward the diapir to thicknesses roughly equivalent to or slightly thicker than their regional counterparts. It is important to note that these units display major regional thickness changes (Haines, 1987), and therefore regional thickness values were compiled from Bunyeroo Gorge as well as the Northern Flinders Ranges to better reflect patterns in stratal thinning (Haines, 1990).

The lower dolomite beds (Npbpdl) of the Patsy Hill Member thin towards the diapir from 43 m (Section 11) to 19 m (Section 9) over a lateral distance of 2.1 km (Figures 29 and 30). The percentage of thinning of the lower dolomite beds is 55% within the suprasalt minibasin. The regional thickness of the correlative Wonoka Formation unit 9 from the type section at Bunyeroo Gorge is 1 m, but thickens to 40 m in the Northern Flinders Ranges (Haines, 1990), which reflects a minor increase (108%) in stratal thicknesses into the suprasalt minibasin (Figure 31).

The sandstone beds (Npbps) of the Patsy Hill Member occur as an isolated wedge that thins from a projected thickness of 159 m (Section 12) to 69 m (Section 11) before abruptly pinching out towards the diapir (Figures 29 and 30). The percentage of thinning of the sandstone beds is 56% within the suprasalt minibasin. The regional thickness of the correlative Wonoka Formation unit 10 from the type section at Bunyeroo Gorge is 30 m, but thickens to 73 m in the Southern Flinders Ranges (Haines, 1990), which reflects a more than two-fold (230%) increase in stratal thickness into the suprasalt minibasin (Figure 31).

The upper dolomite beds (Npbpdu) of the Patsy Hill Member thin towards the diapir from 105 m (Section 11) to 20 m (Section 1) over a lateral distance of 5.8 km (Figures 29 and 30). The percentage of

thinning of the upper dolomite beds is 81% within the suprasalt minibasin. The regional thickness of the correlative Wonoka Formation unit 11 from the type section at Bunyeroo Gorge is 16 m, but thickens to 80 m in the Northern Flinders Ranges (Haines, 1990), which reflects a minor increase (132%) in stratal thickness into the suprasalt minibasin (Figure 31).

The percentages of thinning of each stratal unit within the Patsy Hill Member increase upward from 55% to 81% (Figure 29). This suggests that the amount of depositional relief over Patawarta diapir increased during deposition of the Patsy Hill Member due to pinned salt inflation prior to allochthonous breakout (Hearon, 2014), while the suprasalt minibasin center experienced a relative sea-level rise as it subsided into a thick underlying salt sheet. No consistent stratigraphic trend is reflected in the stratal thickness in the suprasalt minibasin when compared to regional thicknesses.

4.4 Structural Style and Stratal Geometry

Hearon (2013) and Hearon et al. (2014) defined two structural domains or prongs (southern and northern) related to the diapir edge with complex map-view relationships at the northwestern end of Patawarta diapir flanked by Wilpena Group stratigraphy (Figure 33). The southern margin of the southern prong is an east-west trending tear fault (Lemon, 1988) that offsets the main allochthonous salt body against the Brachina Formation to the south. The southern prong is depositionally flanked to the west and north by the Brachina Formation and ABC Range Quartzite (Figure 33). Detailed analysis of the structural development of the southern prong at Patawarta diapir can be found in Hearon (2013) and Hearon et al. (2014).

The southwestern margin of the northern prong cuts shallowly upsection in Bunyeroo Formation strata at a low angle of 5° (Hearon, 2013). The northern prong and the main allochthonous salt body of Patawarta diapir are depositionally flanked to the north by suprasalt stratigraphy of the Bunyeroo and Wonoka formations and Patsy Hill Member of the Bonney Sandstone. Stereonet analysis of the salt-sediment interface for suprasalt Bunyeroo, Wonoka, and Patsy Hill strata indicate an overall shallow inclination to the top salt surface (12°) with a locally steeper portion (52°) near the termination of the

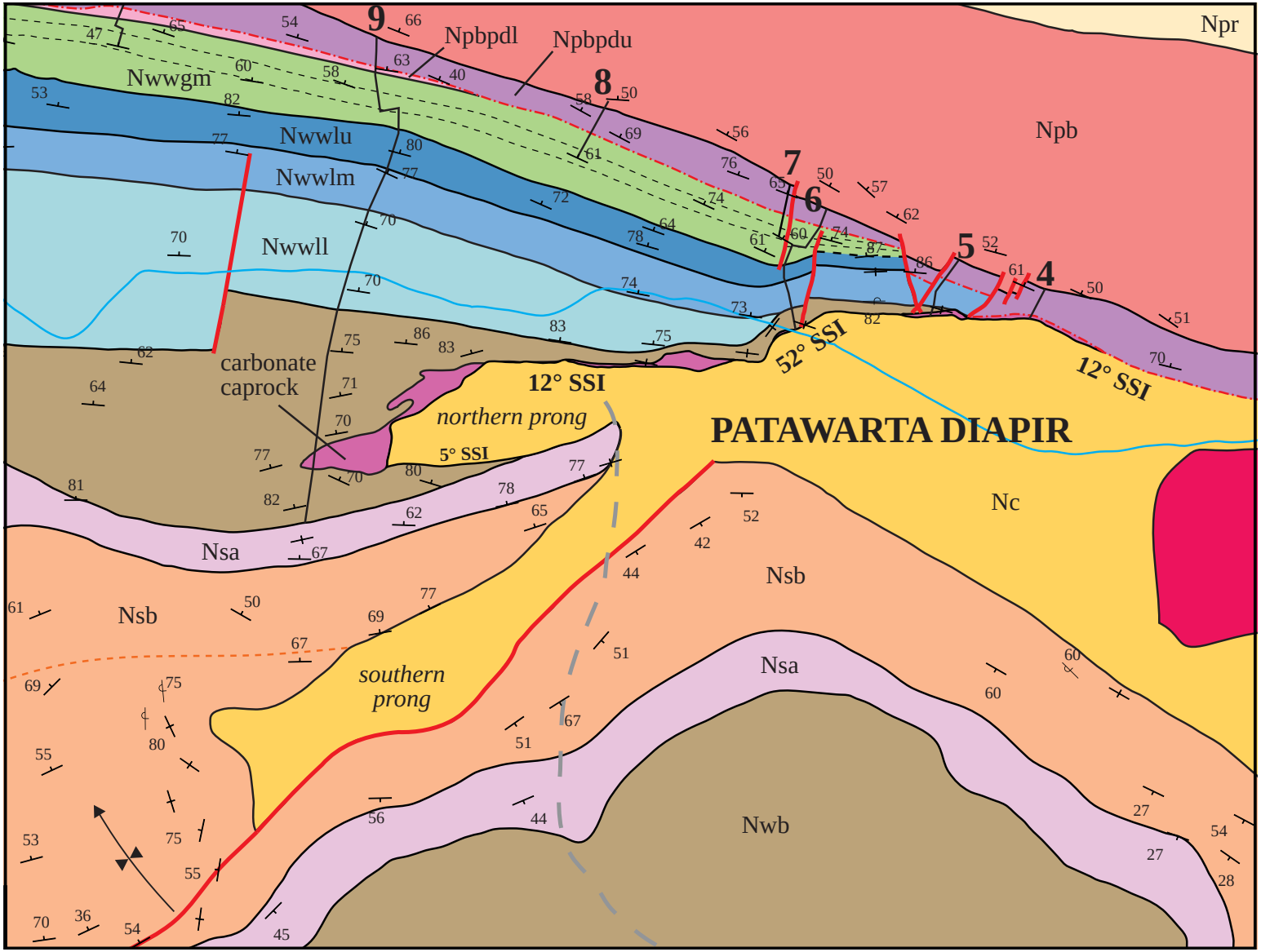

Figure 33. Detailed geologic map of the northwestern end of Patawarta diapir showing the two structural domains or prongs and calculated orientations of the salt-sediment interface (SSI) indicated along the top salt surface; map unit colors match explanation from Plate 1; modified from Coats (1973, 2009), Kernen (2011), Kernen et al. (2012), Hearon (2013), and Hearon et al. (2014).

Bunyeroo Formation against diapiric breccia (Figure 33). The restored depositional stratal geometries of suprasalt units display dominantly low-angle onlap and gradual thinning on to a shallowly dipping top of Patawarta diapir with some local truncation over distances of 3-6 km from the northwest to the southeast (Figure 32). Halokinetic upturn of suprasalt stratigraphy at the salt-sediment interface is restricted to a small zone of Bunyeroo Formation at the locally steep (52°) top salt surface (Figure 33).

4.5 Depositional Sequence Stratigraphy

Within the lower of two major regressive cycles in Wilpena Group stratigraphy, the Bunyeroo and Wonoka formations and Patsy Hill Member of the Bonney Sandstone form parts of two distinct 3rd-order depositional sequences (Coats, 1964; von der Borch et al., 1982, 1988; Haines, 1990; Preiss, 1987, 2000; Kernen et al., 2012). The formational contact between the ABC Range Quartzite and Bunyeroo Formation is interpreted as the sequence boundary (SB) of the lower depositional sequence based on the abrupt non-Waltherian facies shift from progradational shoreface shallow marine sandstones to offshore basinal shales (Christie-Blick et al., 1988; von der Borch, et al., 1988; Haines, 1990; Posamentier et al., 1992; Preiss, 2000). The previously interpreted maximum flooding surface (*mfs*) at the deep-water Wearing Dolomite Member of the overlying Wonoka Formation records sediment starvation in the basin (Haines, 1990; Preiss, 2000). However, the Wearing Dolomite Member was not identified in the suprasalt minibasin at Patawarta diapir, so the *mfs* is placed at the formational contact of the Bunyeroo and Wonoka formations. The Bunyeroo Formation forms the Transgressive Systems Tract (TST) of the lower depositional sequence in the suprasalt minibasin (Figure 34; Catuneanu, 2006).

The lower, middle, and upper limestone and green mudstone members of the Wonoka Formation in the suprasalt minibasin at Patawarta diapir indicate normal regression of depositional facies assemblages from outer shelf to shoreface, foreshore, and lagoonal environments (Figures 20 and 34, Plate 2). The lower dolomite beds of the Patsy Hill Member of the Bonney Sandstone record continued normal regression of the suprasalt depositional system from lagoonal to subtidal and intertidal environments (Figures 20 and 34, Plate 2). The Wonoka Formation and lower dolomite beds of the Patsy Hill Member

Stratigraphy			Map Unit	Depositional Environment	Depositional Sequence Stratigraphy	Halokinetic Sequence Stratigraphy
Bonney Sandstone			Npb	middle shelf lower shoreface	**Transgressive-Highstand Systems Tracts**	No halokinetic deformation
Bonney Sandstone	Patsy Hill Member	unit 11	Npbpdu	lagoon with washover fans & flood tidal deltas	*Transgressive Surface* **Lowstand Systems Tract**	Minibasin-scale folding and thinning only
Bonney Sandstone	Patsy Hill Member	unit 10	Npbps	barrier island		
Bonney Sandstone	Patsy Hill Member	unit 9	Npbpdl	intertidal tidal flat	*Sequence Boundary*	*CHS Boundary*
Wonoka Formation		unit 8	Nwwgm	lagoon & subtidal to intertidal upper shoreface to foreshore	**Highstand Systems Tract**	**Tapered CHS**
Wonoka Formation		units 6-7	Nwwlu	foreshore upper shoreface		
Wonoka Formation		unit 5	Nwwlm	upper shoreface lower to middle shoreface		
Wonoka Formation		units 1-4	Nwwll	lower shoreface outer shelf	*Maximum Flooding Surface*	*CHS Boundary*
Bunyeroo Formation			Nwb	offshore deep basin to outer shelf	**Transgressive Systems Tract**	**Tapered CHS**

Figure 34. Compilation of depositional environments and comparison of depositional and halokinetic sequence stratigraphy for suprasalt minibasin strata at Patawarta diapir; correlative regional stratigraphy from Haines' (1990) Wonoka Formation units 1-11 are shown.

constitute the Highstand Systems Tract (HST) of the lower depositional sequence in the suprasalt minibasin (Figure 34, Plate 2; Catuneanu, 2006).

The lower dolomite beds of Patsy Hill Member in the suprasalt minibasin are unconformably overlain by the sandstone beds in diapir-distal settings and the upper dolomite beds in diapir-proximal settings (Plate 1). This sharp, erosional contact is interpreted as the sequence boundary (SB) separating the lower and upper depositional sequences (Figure 34, Plate 2). Therefore, the upper half of the Patsy Hill Member records an abrupt non-Waltherian facies shift from deposition of the lower dolomite beds in an intertidal setting to the sandstone beds as an isolated barrier bar and the upper dolomite beds in a lagoonal environment (Figures 20 and 34, Plate 2; Posamentier et al., 1992). The sandstone and upper dolomite beds of the Patsy Hill Member form the Lowstand Systems Tract (LST) of the upper depositional sequence in the suprasalt minibasin (Figure 34, Plate 2; Catuneanu, 2006).

The formational contact between the Patsy Hill Member and the overlying undifferentiated Bonney Sandstone is a major flooding surface that marks a transition from a mixed carbonate and siliciclastic lagoonal setting to a siliciclastic-dominated shallow marine environment (Figure 34; Forbes, 1971; Kernen et al., 2012). It is interpreted as a transgressive surface (ts) and a transgressive lag is recorded locally within the suprasalt minibasin by a thin, laterally discontinuous conglomeratic sandstone bed (Figure 34, Plate 2). The undifferentiated Bonney Sandstone represents the Transgressive Systems Tract (TST) to Highstand Systems Tract (HST) of the upper depositional sequence (Figure 34; Catuneanu, 2006; Kernen et al., 2012).

4.6 Halokinetic Sequence Stratigraphy

Structural analysis of the Wonoka Formation and Patsy Hill Member of the Bonney Sandstone preserved in the suprasalt minibasin flanking Patawarta diapir documents the gradual fanning of stratal attitudes from proximal to distal settings. Dips in suprasalt Bunyeroo and Wonoka strata are vertical to 82°W overturned in diapir-proximal settings and shallow away from the diapir to 25°-68°E in the diapir-distal syncline axis. Dips in suprasalt Patsy Hill strata are 70°-86°E in diapir-proximal settings and shallow away from the diapir to 25°-55°E in the diapir-distal syncline axis (Plate 1). Complexity in the dips

obtained from the diapir-distal syncline axis is likely due to the structural overprint of the Delamerian Orogeny.

The overall shallow (12°) dip of the original top salt-sediment interface and the gradual shallowing of stratal dips both away from the diapir and through time indicate the formation of a broad, open fold on top of the allochthonous salt body over distances of 3-6 km with significant thinning but only minor halokinetic upturn at the salt-sediment interface (Plate 3). Therefore, the suprasalt minibasin at Patawarta diapir was primarily subject to minibasin-scale folding and thinning (Figure 34) characteristic of a synclinal minibasin subsiding into allochthonous salt (Figure 3; Giles and Rowan, 2012).

However, angular discordance indicating stratal truncation was documented at two significant surfaces (Figure 32; Plates 1 and 3). The halokinetically upturned Bunyeroo Formation and the Wonoka lower limestone member are truncated at the basal contact of the overlying Wonoka middle limestone member near the locally steeper suprasalt-sediment interface. A depositional sequence boundary juxtaposes upper Wonoka (Nwwlm, Nwwlu, and Nwwgm) and lower Patsy Hill (Npbpdl) stratal units unconformably against upper Patsy Hill (Npbps and Npbpdu) stratal units. The Patsy Hill Member upper dolomite beds above this surface are preserved along the top of salt for a significantly greater distance than the underlying stratal units (Figure 32; Plates 1 and 3). Angular unconformities such as these adjacent to a salt body constitute halokinetic sequence boundaries (Giles and Rowan, 2012). Therefore, the basal contact of the Wonoka middle limestone member and the depositional sequence boundary within the Patsy Hill Member are interpreted as composite halokinetic sequence (CHS) boundaries.

Enhanced thinning of suprasalt strata on to the allochthonous salt body occurs approximately 1-1.5 km from the salt-sediment interface (Plate 1). The Wonoka lower limestone member represents increasing sedimentation rates with the initiation of the HST, which were presumably maintained throughout deposition of the Wonoka Formation and lower dolomite beds of the Patsy Hill Member. Based on the broad zone of thinning, high sedimentation rates, and absence of dramatic facies changes, suprasalt strata form two tapered CHS on the shallowly dipping top salt surface (Figure 34; Giles and Rowan, 2012). The lower CHS consists of the Bunyeroo Formation and lower limestone member of the Wonoka Formation. The upper CHS contains the middle and upper limestone and green mudstone member of the

Wonoka Formation and the lower dolomite beds of the Patsy Hill Member. Development of stacked tapered CHS in the suprasalt minibasin suggests that the relative diapir rise rate was outpaced by the transition to higher sedimentation rates from the TST to HST in Bunyeroo, Wonoka, and lower Patsy Hill strata (Giles and Rowan, 2012). The overlying Patsy Hill sandstone and upper dolomite beds do not form CHS and instead represent only minibasin-scale folding and thinning. The formation of a depositional sequence boundary within Patsy Hill strata at the base of the LST, which coincides with the upper CHS boundary, marks a shift to depositional rates that greatly outpaced local diapir rise and that did not allow for halokinetic folding and thinning at the margin of the allochthonous salt sheet.

4.7 Correlation to Subsalt Minibasin Stratigraphy

The suprasalt minibasin at Patawarta diapir was correlated to the subsalt minibasin using a revised depositional sequence stratigraphic framework interpreted for the Bunyeroo and Wonoka formations and the Patsy Hill Member of the Bonney Sandstone (Figure 35). The depositional sequence stratigraphic framework provides the context to compare and contrast depositional and diagenetic facies, stratal thickness trends, structural style and stratal geometries, and halokinetic sequence architecture from one side of Patawarta diapir to another.

4.7.1 Depositional Facies

Wonoka strata show overall consistent stratigraphic trends in facies distribution and depositional setting from the suprasalt to subsalt minibasin, whereas Patsy Hill strata vary significantly in trends in facies distribution between the minibasins. It is important to note that the stratal section on top of Patawarta diapir (Sections 1-5) was originally interpreted by Kernen (2011) as a condensed section of suprasalt Wonoka carapace (Figure 16). This strata is reinterpreted here as the upper dolomite beds (Npbpdu) of the Patsy Hill Member of the Bonney Sandstone (Plates 1, 2, and 3).

Wonoka Formation

The lower, middle, and upper limestone members of the Wonoka Formation preserved in the suprasalt minibasin at Patawarta diapir display consistent depositional facies trends to coeval subsalt strata

<table>
<tr><th colspan="3" rowspan="2">Stratigraphy</th><th rowspan="2">Map Unit</th><th colspan="2">Depositional Environment</th><th colspan="2">Depositional Sequence Stratigraphy</th><th colspan="2">Halokinetic Sequence Stratigraphy</th></tr>
<tr><th>Suprasalt Minibasin
(Gannaway, 2014)</th><th>Subsalt Minibasin
(Kernen et al., 2012)</th><th>Suprasalt Minibasin
(Gannaway, 2014)</th><th>Subsalt Minibasin
(Kernen et al., 2012)</th><th>Suprasalt Minibasin
(Gannaway, 2014)</th><th>Subsalt Minibasin
(Kernen et al., 2012)</th></tr>
<tr><td rowspan="6">Bonney Sandstone</td><td rowspan="3">Patsy Hill Member</td><td></td><td>Npb</td><td colspan="2">middle shelf
lower shoreface</td><td colspan="2">Transgressive-Highstand Systems Tracts
Transgressive Surface</td><td>No halokinetic deformation</td><td>No halokinetic deformation</td></tr>
<tr><td>unit 11</td><td>Npbpdu</td><td>lagoon with washover fans & flood tidal delta</td><td>lagoon/bay</td><td rowspan="2">Lowstand Systems Tract</td><td rowspan="2">Lowstand Systems Tract</td><td rowspan="2">Minibasin-scale folding and thinning only</td><td>CHS Boundary</td></tr>
<tr><td>unit 10</td><td>Npbps</td><td>barrier island</td><td>barrier bar</td><td rowspan="4">Tapered CHS</td></tr>
<tr><td>unit 9</td><td>Npbpdl</td><td>intertidal tidal flat</td><td>main tidal channel inlet</td><td>Sequence Boundary</td><td>Proposed Sequence Boundary</td><td>CHS Boundary</td></tr>
<tr><td rowspan="4">Wonoka Formation</td><td>unit 8</td><td>Nwwgm</td><td>lagoon & subtidal to intertidal
upper shoreface to foreshore</td><td>coastal plain</td><td rowspan="3">Highstand Systems Tract</td><td rowspan="3">Highstand Systems Tract</td><td rowspan="2">Tapered CHS</td></tr>
<tr><td>units 6-7</td><td>Nwwlu</td><td>foreshore
upper shoreface</td><td>foreshore
upper shoreface</td></tr>
<tr><td>unit 5</td><td>Nwwlm</td><td>upper shoreface
lower to middle shoreface</td><td>foreshore
lower to upper shoreface</td><td>CHS Boundary</td></tr>
<tr><td>units 1-4</td><td>Nwwll</td><td>lower shoreface
outer shelf</td><td>lower shoreface
outer shelf</td><td rowspan="2">Tapered CHS</td><td>CHS Boundary</td></tr>
<tr><td colspan="3">Bunyeroo Formation</td><td>Nwb</td><td colspan="2">offshore deep basin</td><td colspan="2">Maximum Flooding Surface
Transgressive Systems Tract</td><td>Tapered CHS</td></tr>
</table>

Figure 35. Compilation of depositional environments and comparison of depositional and halokinetic sequence stratigraphy for suprasalt and subsalt minibasin strata; interpretations compiled from this study and Kernen et al. (2012); note that the sequence boundary in the subsalt minibasin is reinterpreted within this study to be at the Npbpdl-Npbps contact; correlative regional stratigraphy from Haines' (1990) Wonoka Formation units 1-11 are shown.

(Figure 35; Kernen et al., 2012). However, the green mudstone member of the Wonoka Formation differs significantly in facies distribution and depositional setting from the suprasalt minibasin to the subsalt minibasin. Depositional facies assemblages in both the suprasalt and subsalt minibasin fill indicate normal regression from outer shelf to shoreface and foreshore environments. Ongoing regression resulted in the development of a coastal plain environment in the subsalt minibasin, whereas the suprasalt minibasin developed barrier bar complexes associated with lagoonal and subtidal to intertidal environments (Figures 13 and 20).

Suprasalt Wonoka facies suggest overall deposition in slightly deeper water than that recorded for subsalt facies (Plate 2; Appendix A). The suprasalt Wonoka lower limestone member (Nwwll) includes fine-grained turbidites and slumping not found in the correlative subsalt strata (Figure 20). The litharenite in the Wonoka upper limestone member (Nwwlu) is finer-grained in the suprasalt minibasin than the subsalt minibasin. The suprasalt Wonoka green mudstone member (Nwwgm) displays various sedimentary structures indicative of upper shoreface to foreshore deposition (Figure 20), whereas the correlative subsalt strata are devoid of sedimentary structures, suggesting deposition in a coastal plain environment (Figure 13; Kernen et al., 2012). Despite these slight differences in the minibasin depositional profile, correlation of the Wonoka Formation at Patawarta diapir indicates deposition in similar outer shelf to shoreface and foreshore environments in the coeval suprasalt and subsalt minibasins (Figures 13, 20, and 35).

Variations in facies distribution and depositional setting of the green mudstone member of the Wonoka Formation include an expanded suprasalt section with respect to the correlative subsalt and regional stratal units and the presence of diapir-proximal conglomerate beds in the subsalt minibasin related to the erosional unroofing of Wonoka diapir roof strata (Kernen et al., 2012). Both the subsalt and suprasalt Wonoka green mudstone member contain siltstone and shale interbedded with lime to silty-lime mudstone in the lower part of this unit. However, in the middle to upper part of this unit the suprasalt strata are intimately interbedded with stromatolitic boundstone, lithoclastic wackestone, calcareous sandstone, and rare oolitic (-peloidal) packstone to grainstone beds, which are not present in the subsalt minibasin (Plate 2; Appendix A). Based on the distribution of these lithofacies, the suprasalt minibasin

preserved an expanded section of the uppermost Wonoka green mudstone member from deposition in a foreshore to lagoonal and subtidal to intertidal environment (Figure 35).

The subsalt Wonoka green mudstone member contains twelve intercalated conglomeratic litharenite to sublitharenite beds in the diapir-proximal setting interpreted as a diapir unroofing sequence (Kernen et al., 2012). The subsalt conglomerate beds are composed entirely of intraclasts derived locally from the former diapir roof, which consisted of older Wonoka strata (Kernen et al., 2012). In contrast, the suprasalt Wonoka green mudstone member contains a single conglomeratic litharenite, which contains polymict, granule-sized lithic extraclasts and intraclasts that reflect a more regional source rather than just the underlying Wonoka stratigraphy (Plate 2; Appendix A). Based on the composition and distribution of conglomerate beds in the Wonoka green mudstone member, the erosional unroofing of Patawarta diapir was primarily recorded in the subsalt minibasin.

Patsy Hill Member

The Patsy Hill Member of the Bonney Sandstone varies significantly in regard to depositional facies between the suprasalt and subsalt minibasins flanking Patawarta diapir (Figure 35). Stromatolitic boundstone is present throughout the Patsy Hill Member in both suprasalt and subsalt minibasin strata. However, suprasalt Patsy Hill strata also includes lithoclastic wackestone to packstone in the lower dolomite beds and oolitic-lithoclastic-peloidal packstone to grainstone in the upper dolomite beds, which are not present in correlative subsalt Patsy Hill strata. Diapir-derived pebble conglomerates are present in both the Patsy Hill lower and upper dolomite beds in the subsalt minibasin, but are restricted to only the upper dolomite beds in the suprasalt minibasin where they form a significant part of the stratal section (Plate 2; Appendix A).

4.7.2 Diagenetic Facies

The Rim Dolomite carbonate caprock facies (Giles et al., 2012) is preserved in the suprasalt minibasin as highly fractured and brecciated, thin (avg. <10 m) isolated lenses that are oriented parallel to the suprasalt-sediment interface of Patawarta diapir. On the subsalt side, the Rim Dolomite forms a thicker (up to 100m thick), relatively continuous diagenetic interval along the margin of the diapir. Internal fabrics are similar in both minibasins where they form massive, laminated, brecciated, and/or silicified carbonate

caprock assemblages (Figure 28; Giles et al., 2012). In both minibasins, the development of carbonate caprock is directly linked to the overlying Bunyeroo stratigraphy, which contains clasts of eroded Rim Dolomite. The subsalt Rim Dolomite caprock is erosionally terminated at a tapered-CHS boundary between the Bunyeroo and Wonoka formations. The suprasalt Rim Dolomite caprock extends farther along the top salt-sediment interface and is in contact with and onlapped by Patsy Hill upper dolomite beds (Plate 1). Additionally, subsalt caprock occurs as a laterally extensive (>10 km) unit along the minibasin margin, but suprasalt caprock occurs as laterally discontinuous exposures along the top salt surface. The Rim Dolomite in the subsalt minibasin represents the rotation of crestal caprock into a lateral position along the steep southwestern margin of Patawarta diapir by the same mechanisms that halokinetically drape-folded the associated Bunyeroo roof strata (Figure 17). In contrast, the Rim Dolomite in the suprasalt minibasin reflects minimal rotation or halokinetic drape-folding and has remained essentially *in situ,* instead displaying attenuation of the caprock unit along the shallowly dipping top salt surface.

4.7.3 Stratal Thickness Trends

All map units of the Wonoka Formation and Patsy Hill Member of the Bonney Sandstone are thicker in the suprasalt minibasin than the correlative units in the subsalt minibasin (Figures 31, 36, and 37; Kernen et al., 2012). Suprasalt Bunyeroo, Wonoka, and Patsy Hill strata display an upward decreasing trend in the percentage of thinning of individual map units through time with the exception of the youngest unit of the Patsy Hill Member (Npbpdu) (Figure 36). In contrast, the subsalt minibasin displays no systematic stratigraphic trends in percentage of thinning.

The thicker stratigraphic section in the suprasalt minibasin relative to the subsalt minibasin reflects greater creation of long-term accommodation in the suprasalt minibasin. Greater long-term accommodation was likely created by greater subsidence of the suprasalt minibasin into the Patawarta salt sheet by load-induced evacuation when compared to the regional subsidence associated with subsalt minibasin accommodation trends. The decrease in the amount of stratal thinning over the diapir through time on the suprasalt side suggests that the differential topographic relief over the diapir decreased through

Stratigraphy		Map Unit	SUPRASALT MINIBASIN (Gannaway, 2014)						SUBSALT MINIBASIN (Kernen et al., 2012)					
			Thickest Section (m)	Location of Thickest Section	Thinnest Section (m)	Location of Thinnest Section	Lateral Distance of thinning toward diapir	Percentage of thinning	Thickest Section (m)	Location of Thickest Section	Thinnest Section (m)	Location of Thinnest Section	Lateral Distance of thinning toward diapir	Percentage of thinning
Bonney Sandstone		Npb							40	remains relatively constant	25	remains relatively constant	covers entire field area	remains relatively constant
Bonney Sandstone	Patsy Hill Member	Npbpdu	105	11	20	1	5.8 km	81	55	H	15	B	2 isolated lens	73
Bonney Sandstone	Patsy Hill Member	Npbps	156	12*	69	11	isolated lens	56	40	I	9	B	590 m	78
Bonney Sandstone	Patsy Hill Member	Npbpdl	43	11	19	9	2.1 km	55	40	I	18	J	isolated lens	55
Wonoka Formation		Nwwgm	230	12	97	4	3.0 km	58	130	E	7	B	323 m	95
Wonoka Formation		Nwwlu	246	12	36	6	3.3 km	85	80	E	20	A	457 m	75
Wonoka Formation		Nwwlm	383	12	30	6	3.8 km	92	215	E	20	A	457 m	91
Wonoka Formation		Nwwll	779	12	247	9	4.2 km	96	550	E	70	A	457 m	87
Bunyeroo Formation		Nwb	1588	12	32	5	5.0 km	98						

Figure 36. Stratigraphic unit thicknesses and locations relative to Patawarta diapir with calculated percentages of thinning for suprasalt and subsalt stratal units; *indicates estimated thickness at Sec. 12 from projected attitudes; data compiled from this study and Kernen et al. (2012).

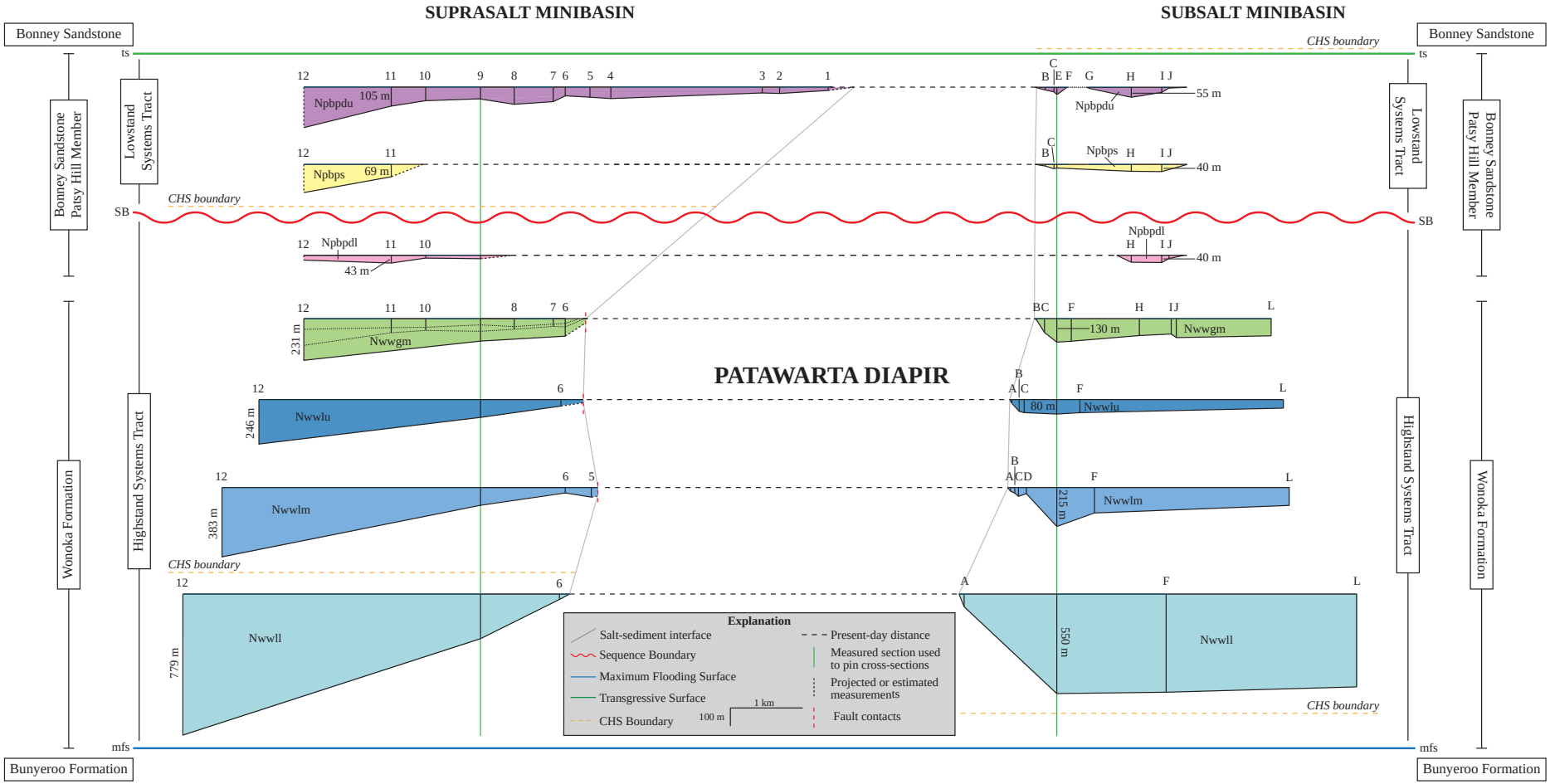

Figure 37. Interval thickness cross-sections of individual Wonoka and Patsy Hill stratal units constructed for suprasalt and subsalt minibasins; note that distances over which strata thin for suprasalt and subsalt minibasin fills are ~3-6 km and 560 m, respectively; distances shown between minibasins represent present-day, meters are thickest section measured for stratal units (see Figure 36); data compiled from this study and Kernen et al. (2012).

time (Giles and Rowan, 2012). The lack of a stratigraphic trend in stratal thinning over the diapir on the subsalt side suggests that the topographic relief over the diapir was highly variable through time.

4.7.4 Structural Style and Stratal Geometry

Subsalt Wonoka and Patsy Hill stratal geometries record a monoclinal drape-fold adjacent to Patawarta diapir expressed in oblique map view as a syncline-anticline pair (Plate 1; Kernen et al., 2012). Subsalt Wonoka strata preserve an east-west trending syncline with a shallowly dipping diapir-distal limb (20-30º) and more steeply dipping diapir-proximal limb (50º to overturned). Subsalt Wonoka and Patsy Hill strata preserve a southeast-northwest trending anticline with steeply dipping diapir-distal (50º to vertical) and diapir-proximal limbs (vertical to 80º overturned). All thinning of the subsalt Wonoka Formation and Patsy Hill Member occurs between the syncline-anticline pair over a distance of approximately 560 m from the diapir margin (Figures 36 and 37). The subsalt stratal geometries indicate this thinning occurs by a combination of onlap, stratal convergence, and low-angle erosional truncation (Kernen et al., 2012). This highlights an important distinction between the structural styles and stratal geometries preserved in suprasalt and subsalt minibasin fill adjacent to Patawarta diapir. Although thinning occurs in similar ways across the coeval minibasins, Wonoka and Patsy Hill strata experienced two very different styles of folding on top of and at the toe of the allochthonous salt body. The suprasalt minibasin fill developed a broad, open fold with minor halokinetic upturn at the salt-sediment interface, whereas the subsalt minibasin fill developed a tighter fold with significant halokinetic upturn at the advancing front of Patawarta diapir (Kernen et al., 2012).

4.7.5 Depositional Sequence Stratigraphy

Analogous to the suprasalt minibasin at Patawarta diapir, subsalt Wonoka Formation and Patsy Hill Member of the Bonney Sandstone also comprise parts of two 3rd-order depositional sequences (Coats, 1964; von der Borch et al., 1982, 1988; Preiss, 1987, 2000; Kernen et al., 2012). However, the depositional sequence stratigraphic framework applied at Patawarta diapir highlights several similarities and differences between the stratigraphic fill of coeval minibasins adjacent to allochthonous salt. Based on the correlation of depositional facies assemblages and stratigraphic relationships of the Wonoka Formation and Patsy Hill Member across the suprasalt and subsalt minibasins, a comparison can be made of the

stratigraphic units that form the Highstand and Lowstand Systems Tracts of the lower and upper depositional sequences, respectively.

The lower, middle, and upper limestone and green mudstone members of the Wonoka Formation display consistent trends between suprasalt and subsalt minibasin fills in lithofacies assemblages, depositional environments, and associated depositional sequence stratigraphic interpretations. In both the suprasalt and subsalt minibasins, the depositional facies of the Wonoka Formation record normal regression from an outer shelf to shoreface and foreshore environments (Figure 35; Kernen et al., 2012). These coeval progressively shallowing upward successions denote a prograding depositional system with high sedimentation rates, which also reflects the regional signature of a storm-dominated carbonate shelf prograding from west to east (Haines, 1990; Kernen et al., 2012). Correlative Wonoka suprasalt and subsalt strata therefore comprise the majority or all of the Highstand Systems Tract (HST), respectively, of the lower depositional sequence preserved adjacent to Patawarta diapir (Figure 35; Kernen et al., 2012).

However, the suprasalt minibasin fill at Patawarta diapir records deposition of an expanded section of the Wonoka green mudstone member with respect to both the correlative subsalt minibasin and regional stratigraphy (Haines, 1990; Kernen et al., 2012). The expanded Wonoka section contains interbedded stromatolitic boundstone, lithoclastic wackestone, calcareous sandstone, and rare oolitic (-peloidal) packstone to grainstone in the suprasalt minibasin only (Plate 1). Therefore, the suprasalt minibasin preserved ongoing deposition of the Wonoka green mudstone member at the end of the HST in lagoonal and subtidal to intertidal environments (Figure 35), whereas subsalt deposition had ceased after early deposition in a coastal plain environment. This suggests that subsidence of the suprasalt minibasin into underlying salt continued from Bunyeroo through Wonoka time, which created the necessary accommodation increase for deposition of the expanded section of the Wonoka green mudstone member.

The interpreted stratigraphic position of the sequence boundary (SB) varies between the suprasalt and subsalt minibasins (Figure 35). The sequence boundary is placed at the erosional basal contact of the Patsy Hill Member sandstone beds in the suprasalt minibasin, whereas it is placed at the erosional basal contact of the Patsy Hill Member lower dolomite beds in the subsalt minibasin. Based on better exposure in the suprasalt minibasin and correlation to the regional stratigraphic framework, the sequence boundary

in the subsalt minibasin is reinterpreted here to be at the contact between Patsy Hill lower dolomite and sandstone beds. Therefore, the lower dolomite beds of the Patsy Hill Member were deposited in a channelized tidal flat setting within the intertidal zone and form the latest HST. Regional erosion and formation of a sequence boundary was followed by deposition of the sandstone and upper dolomite beds of the Patsy Hill Member in a barrier island-lagoonal complex, which comprise the LST in both the suprasalt and subsalt setting.

4.7.6 Halokinetic Sequence Stratigraphy

As emphasized by the differences in structural styles and stratal geometries, an important difference between the suprasalt and subsalt minibasins flanking Patawarta diapir is the halokinetic sequence stratigraphy of the coeval minibasin fills (Figure 35). Subsalt Wonoka and Patsy Hill strata form the upper part of two stacked tapered composite halokinetic sequences at the toe of the advancing Patawarta allochthonous salt sheet. The lower CHS boundary is within the Wonoka lower limestone member and the upper CHS boundary coincides with the formational contact with the Patsy Hill Member and the Bonney Sandstone. Significant folding and thinning of subsalt strata occurred within 560 m of the salt-sediment interface as the original top of salt was rotated, along with its onlapping Wonoka and Patsy Hill strata, into a base-salt position dipping 62º inward (Plates 1 and 3; Kernen et al., 2012; Hearon et al., 2014).

In contrast, suprasalt minibasin strata record primarily minibasin-scale folding and thinning with two composite halokinetic sequence (CHS) boundaries at the suprasalt-sediment interface. Overall, Bunyeroo, Wonoka, and Patsy Hill strata form a broad, open fold that thins over 3-6 km on the shallowly dipping (12º) top of the allochthonous salt body (Figure 33; Plates 1 and 3). However, two significant angular unconformities at the suprasalt-sediment interface, which are interpreted as tapered CHS boundaries, are present at the basal contact of the Wonoka middle limestone member and the sequence boundary within the Patsy Hill Member (Plates 1 and 3). Enhanced thinning of suprasalt strata occurs over 1-1.5 km with dominantly gradational facies changes, which resulted in two stacked tapered CHS. Bunyeroo and lower Wonoka (Nwwll) strata form the lower CHS, while upper Wonoka (Nwwlm, Nwwlu, and Nwwgm) and lower Patsy Hill (Npbpdl) strata comprise the upper CHS (Figure 34). Upper Patsy Hill

(Npbps and Npbpdu) strata did not develop CHS, but instead represent minibasin-scale folding and thinning only.

Correlation of the depositional sequence stratigraphy suggests that Patawarta diapir and the flanking suprasalt and subsalt minibasins experienced similar sedimentation rates for accumulation of Bunyeroo, Wonoka, and Patsy Hill strata. Therefore, the development of halokinetic sequence boundaries at different stratigraphic levels in the coeval minibasins is interpreted to be due to local variations in relative diapir rise rate through time. This suggests that no prediction can be made based on halokinetic sequence stratigraphy in coeval minibasins adjacent to allochthonous salt.

Characteristic pebble conglomerates in the Patsy Hill Member adjacent to Patawarta diapir are interpreted as evidence for periods of exposure of the allochthonous salt sheet and diapir caprock and subsequent erosion into diapir-proximal halokinetic growth strata (Plate 1). The pebble conglomerates contain diagnostic meta-igneous and silicified carbonate clasts, which were derived from diapiric breccia and associated diagenetic caprock, respectively, as well as lithic siltstone, chert, quartzite, and shale clasts (Figure 27b). They occur in varying Patsy Hill lithostratigraphic units in the suprasalt and subsalt minibasins. Diapir-derived pebble conglomerates are present in the subsalt Patsy Hill lower dolomite beds, but absent in the correlative suprasalt map unit. The subsalt conglomerates have erosional basal scour surfaces and display imbrication of the pebble clasts, which suggests that their incorporation into the subsalt Patsy Hill lower dolomite beds is due to erosion associated with the tidal channel inlet depositional setting. In contrast, the suprasalt Patsy Hill lower dolomite beds were deposited in a tidal flat environment that was not subject to the erosion necessary to shed diapir-derived detritus into the depositional system. The Patsy Hill upper dolomite beds contain diapir-derived pebble conglomerates throughout the stratal unit in both suprasalt and subsalt settings, which indicates Patawarta diapir experienced repeated exposure and erosion in late Patsy Hill time. Despite the lack of correlation in the halokinetic sequence stratigraphy as detailed above, the correlatability of suprasalt and subsalt pebble conglomerates suggest erosional events not directly linked to the development of halokinetic sequence boundaries are relevant temporal indicators for the stratigraphic fill of coeval minibasins.

Chapter 5: Discussion

The stratigraphic and structural relationships of the suprasalt minibasin fill at Patawarta diapir reflect deposition on a shallowly dipping allochthonous salt sheet, which can be correlated to coeval subsalt minibasin strata folded beneath a steep to overturned salt-sediment interface at the ramping salt front. The distribution of depositional facies in Wilpena Group stratigraphy at Patawarta diapir highlights the impacts of salt-modified bathymetry on shallow marine depositional environments adjacent to allochthonous salt, as well as the complicated relationships between the depositional and halokinetic sequence stratigraphy.

Depositional facies in the Bunyeroo form broad, linear facies belts that display good lateral correlation throughout the suprasalt minibasin (Plate 2). The absence of lateral facies variability suggests that salt-modified bathymetry had minimal impact on the Bunyeroo Formation deposition in an outer shelf environment. However, there must have been significant topographic relief over the diapir at this time in order to generate the high percentage of stratal thinning recorded.

The Rim Dolomite represents diagenetic carbonate caprock formation associated with the Bunyeroo Formation directly adjacent to Patawarta diapir, where carbonate caprock assemblages developed at the salt-sediment interface in adjacent minibasin fills. The diagenetic fabrics of massive, laminated, brecciated, and/or silicified dolomite are interpreted to be the result of the complex interactions between the salt body and undersaturated waters and the migration of hydrocarbons carrying sulfate-reducing anaerobic bacteria (Giles et al., 2012). Although genetically linked to the same stratigraphic unit, the present orientation and lateral continuity of Bunyeroo-age caprock assemblages reflects differences in subsalt and suprasalt minibasin development. Halokinetic drape-folding of subsalt Rim Dolomite and overlying Bunyeroo roof strata from a crestal to a lateral position resulted in a laterally extensive (>10 km) unit along most of the western margin of Patawarta diapir (Giles et al., 2012). In contrast, suprasalt Rim Dolomite remained essentially *in situ* in a crestal position on top of the allochthonous salt body, but was strongly attenuated into irregular pods along the top salt surface at the northwestern end of Patawarta diapir. Therefore, in the subsalt setting it may be more likely to encounter a laterally continuous carbonate caprock unit along the steep salt-sediment interface that will characteristically terminate at CHS

boundaries. However, carbonate caprock units in the suprasalt setting are likely to have a more irregular distribution along the salt margin as they are not rotated from a crestal position, but instead attenuated into laterally discontinuous units along the shallowly dipping top of salt during inflation of allochthonous salt.

Depositional facies in the lower, middle, and upper limestone members of the Wonoka Formation form linear facies belts that display good lateral correlation throughout the suprasalt minibasin as well as to coeval subsalt strata (Plate 2). Conversely, depositional facies in the green mudstone member of the Wonoka Formation display several differences in facies distribution and depositional setting. The absence of dramatic lateral facies variability in all but the uppermost Wonoka strata suggests that salt-modified bathymetry had minimal impact on deeper water deposition in progressively shallowing upward outer shelf to foreshore environments. Based on the restriction of differences in Wonoka facies distribution to the green mudstone member, the presence of thick underlying allochthonous salt became more influential in shallow water deposition near the end of Wonoka deposition in adjacent coastal plain, lagoonal, and subtidal to intertidal environments.

Siltstone and shale of the Wonoka green mudstone member in the subsalt minibasin are interbedded with lime to silty-lime mudstone at the base and diapir-proximal conglomerate beds at the top of this unit. Conversely, the correlative suprasalt unit contains interbedded lime to silty-lime mudstone at the base, stromatolitic boundstone, lithoclastic wackestone, and rare oolitic (-peloidal) packstone to grainstone in the middle, and calcareous sandstone at the top of this unit (Plate 2; Appendix A). The subsalt Wonoka green mudstone member records deposition in a coastal plain environment, whereas the correlative suprasalt unit records deposition in upper shoreface to foreshore, lagoonal, and subtidal to intertidal environments (Figure 35). The variable facies distribution and associated environments of deposition reflect the preservation of an expanded section of the uppermost Wonoka green mudstone member in the suprasalt minibasin. This suggests that an accommodation increase occurred locally in the suprasalt minibasin as it continued to subside into the underlying Patawarta allochthonous salt sheet, while deposition filled the subsalt minibasin early and was followed by the development of a bypass surface towards the end of the HST.

The subsalt diapir-proximal conglomerates document the erosional unroofing of Patawarta diapir and have important implications for understanding the timing of salt sheet inflation and dispersal of recycled roof material (Kernen et al., 2012). Preservation of the diapir unroofing sequence only in the subsalt Wonoka green mudstone member is interpreted as a result of coeval salt sheet inflation and relatively slower deposition associated with the late HST transition from foreshore to coastal plain setting (Kernen et al., 2012). Pinned inflation of the allochthonous salt sheet at the advancing front due to rapid deposition during the HST created a steep to overturned subsalt-sediment interface (Plate 3; Hearon et al., 2014). Continued salt inflation in turn halokinetically drape-folded older Wonoka roof strata and formed a topographic high directly adjacent to the subsalt minibasin (Kernen et al., 2012; Hearon et al., 2014). In contrast, the suprasalt-sediment interface maintained a shallow dip with low-angle onlap of the suprasalt Wonoka green mudstone member deposited in a foreshore to lagoonal and subtidal to intertidal environment. Therefore, shoreface erosion of the topographic high of the locally inflated salt sheet preferentially shed roof material into the subsalt minibasin, whereas little to no erosion of roof strata occurred in the suprasalt minibasin where Patawarta diapir had minimal topographic expression. These observations suggest that the late HST is more prone to locally derived conglomerates of diapiric roof material, as pinned inflation and a resultant diapiric high are created. Additionally, this implies that conglomerates of reworked diapir roof strata may preferentially be deposited in the adjacent subsalt minibasin where strata are ultimately halokinetically drape-folded beneath ramping allochthonous salt, rather than recycled from the top of salt with less topographic expression into an adjacent suprasalt minibasin.

In contrast to the underlying Bunyeroo and Wonoka linear facies belts, depositional facies in the Patsy Hill Member of the Bonney Sandstone form a facies mosaic with gross correlation in depositional environment trends within the suprasalt minibasin and in comparison to the subsalt minibasin (Plate 2). Several suprasalt depositional facies are absent from correlative subsalt lithostratigraphic units, such as lithoclastic wackestone to packstone (Npbpdl) and oolitic-lithoclastic-peloidal packstone to grainstone (Npbpdu). Barrier island and lagoonal systems inherently create depositional facies mosaics such as are preserved in Patsy Hill strata (Scholle et al., 1983). However, the differences in suprasalt to subsalt

distribution of Patsy Hill depositional facies implies salt-modified bathymetry exhibited strong control on deposition in very shallow water, which created isolated micro-environments. The restriction of wackestone, packstone, and grainstone to only suprasalt strata suggest that the bathymetric high of Patawarta diapir set up a depositional barrier within the more regional barrier island-lagoonal complex to isolate environments and prevent widespread distribution of lithoclasts, ooids, and peloids.

Within the subsalt and suprasalt minibasin fill, Bunyeroo strata forms the TST, which represents slower sedimentation rates during base level rise (Figure 35; Catuneanu, 2006; Kernen et al., 2012). In the subsalt minibasin, upper Bunyeroo strata preserve the lower of two stacked tapered CHS (Hearon et al., 2014). The formation of composite halokinetic sequence boundaries are often associated with low sedimentation rates, diapir inflation, and local angular unconformities (Giles and Rowan, 2012). In an offshore basinal to outer shelf depositional system, those conditions are common during formation of the *mfs* at the end of the TST because sedimentation rates are low relative to the HST or LST (Catuneanu, 2006; Kernen et al., 2012). In the suprasalt minibasin, this youngest Bunyeroo strata display the only minor halokinetic upturn documented at the suprasalt-sediment interface (Plate 1). Based on the correlation of Bunyeroo facies, sedimentation rates in the suprasalt minibasin were also relatively low. The minor halokinetic upturn of Bunyeroo strata is interpreted as inflation of Patawarta diapir coincident with slow sedimentation, and ultimately, draping of thin roof strata on a shallow but locally irregularly top salt. Therefore, the development of a CHS boundary in subsalt Bunyeroo strata and minor halokinetic upturn in suprasalt Bunyeroo strata are interpreted as correlative responses to the depositional sequence stratigraphy, regardless of the differences in halokinetic sequence stratigraphy.

Within the subsalt and suprasalt minibasins, the Wonoka Formation and lower Patsy Hill Member form the HST, which reflects relatively rapid sediment accumulation during late base level rise and the start of base level fall (Figure 35; Catuneanu, 2006, Kernen et al., 2012). As expected in a HST sedimentary package, Wonoka and lower Patsy Hill strata record normal regression from outer shelf through shoreface and foreshore to tidal channel depositional environments in the subsalt minibasin and lagoonal and subtidal to intertidal environments in the suprasalt minibasin (Figure 35; Catuneanu, 2006; Kernen et al., 2012). The progressively shallowing upward successions documented in coeval minibasin

fills represent regionally prograding depositional systems with high sedimentation rates characteristic of the HST. The Wonoka lower limestone member displays the greatest amount of stratal thinning adjacent to Patawarta diapir, which suggests the initiation of HST deposition, and the associated high sedimentation rates, greatly outpaced diapir rise and resulted in minibasin fill that strongly reflect depositional onlap and overlap onto inherited diapir topography (Figures 36 and 37). The stratal thinning trends documented in Bunyeroo through Wonoka time suggest accommodation was gradually decreasing through these stages in the development of the suprasalt minibasin, further supporting the interpretation that these stratal packages represent the TST and HST, respectively (Figure 36).

The Patsy Hill sandstone and upper dolomite beds form the LST within both the subsalt and suprasalt minibasin where depositional facies reflect a non-Waltherian shift as the depositional systems abruptly step basinward along the depositional profile (Figure 35; Catuneanu, 2006, Kernen et al., 2012). After deposition of the Patsy Hill lower dolomite beds in a channelized tidal flat setting, lenticular, detached barrier islands developed in the coeval minibasins (Npbps), followed by the onset of lagoonal conditions (Npbpdu) characterized by exposure of the adjacent allochthonous salt sheet and erosion and recycling of diapiric breccia and diagenetic caprock.

The preservation of a barrier bar and lagoonal complex during the LST conflicts with models based on Holocene examples that suggest that this depositional system is typical of the TST developed along passive margins (Demarest and Kraft, 1987; Nummedal and Swift, 1987). However, in the case of deposition adjacent to Patawarta diapir, local subsidence of the subsalt and suprasalt minibasins into the underlying allochthonous salt produced a local rise in relative sea-level. Therefore, the creation of local accommodation in the coeval minibasins allowed for the preservation of barrier bar and lagoonal facies during the LST rather than erosion by the transgressive surface during the subsequent TST.

The key differences in the depositional sequence stratigraphic framework of Patawarta diapir are restricted to the late HST and the LST (Figure 35; Plate 2). This has important implications on the stratigraphic and structural relationships of coeval minibasin fill because these intervals coincide with fundamental stages in the development of the allochthonous salt sheet. The interbedded conglomerates in the subsalt Wonoka green mudstone member occur because Patawarta diapir developed a topographic

high through Wonoka time with a flanking subsalt minibasin. An expanded suprasalt section of the Wonoka green mudstone member was deposited as accommodation was created by the ongoing subsidence of the suprasalt minibasin into the underlying allochthonous salt sheet. The absence of suprasalt depositional facies in the correlative subsalt Patsy Hill stratal units, such as wackestone, packstone, and grainstone, suggest that Patawarta diapir formed a bathymetric high in a very shallow marine setting, which set up a depositional barrier to isolate the barrier island-lagoonal complex environments and prevent widespread distribution of lithoclasts, ooids, and peloids to the subsalt minibasin. Finally, the distribution of diapir-derived pebble conglomerates in the upper Patsy Hill Member records successive periods of exposure and erosion of the diapir breccia and associated diagenetic caprock into both flanking minibasins shortly before allochthonous salt breakout.

The correlation of subsalt and suprasalt minibasin characteristics highlight broad similarities in Wonoka and Patsy Hill depositional sequence stratigraphy with several key differences, particularly in the upper Wonoka and Patsy Hill strata (Figure 35). Kernen et al. (2012) documented the upper of two stacked tapered CHS adjacent to Patawarta diapir, whereby the geometric relationships in subsalt minibasin fill and the interpreted halokinetic sequence stratigraphy are inherently related to the depositional history of Wonoka and Patsy Hill stratigraphy. High sedimentation rates in the HST resulted in pinned inflation at the advancing toe of Patawarta diapir and development of a tapered CHS. However, in the suprasalt minibasin presumably experiencing similar sedimentation rates in the depositional sequence stratigraphic framework, Wonoka and Patsy Hill strata form primarily a broad, open fold with gradual thinning and minor upturn at the salt-sediment interface, as well as two tapered CHS near the diapir margin. The formation of halokinetic sequence boundaries at Patawarta diapir occurred at different times in the depositional histories of the subsalt and suprasalt minibasins, which suggests that halokinetic deformation adjacent to allochthonous salt is influenced by local differences in diapir rise rate rather than just the regional depositional framework. Because of these variations in halokinetic deformation from one side Patawarta diapir to the other due to local diapir rise rates, the predictive capability of using suprasalt minibasin attributes as indicators for subsalt reservoir characteristics is deemed unsuccessful.

Chapter 6: Conclusions

6.1 Depositional Environments

The stratigraphic fill of the suprasalt minibasin flanking Patawarta diapir comprises the Bunyeroo and Wonoka formations and the Patsy Hill Member of the Bonney Sandstone. The Wonoka Formation was subdivided into four informal lithostratigraphic units. They comprise, in ascending stratigraphic order, (1) lower limestone member, (2) middle limestone member, (3) upper limestone member, and (4) green mudstone member. The Patsy Hill Member of the Bonney Sandstone was subdivided into three informal lithostratigraphic units. They comprise, in ascending stratigraphic order, (1) lower dolomite beds, (2) sandstone beds, and (3) upper dolomite beds.

Bunyeroo, Wonoka, and Patsy Hill strata in the suprasalt minibasin at Patawarta diapir were deposited in outer shelf to shallow marginal marine environments. The suprasalt Bunyeroo Formation was deposited in an offshore basinal to outer shelf environment and thins from 1588 m to 32 m toward the diapir. The lower limestone member of the suprasalt Wonoka Formation was deposited in an outer shelf to lower shoreface environment and thins from 779 m to 247 m toward the diapir. The middle limestone member of the suprasalt Wonoka Formation was deposited in a lower and middle shoreface environment and thins from 383 m to 30 m toward the diapir. The upper limestone member of the suprasalt Wonoka Formation was deposited in an upper shoreface to foreshore environment and thins from 246 m to 36 m toward the diapir. The green mudstone member of the suprasalt Wonoka Formation was deposited in an upper shoreface to foreshore environment that transitioned upward to a lagoonal and subtidal to intertidal environment and thins from 230 m to 97 m toward the diapir. The Wonoka Formation in the suprasalt minibasin at Patawarta diapir was deposited in an outer shelf to foreshore, lagoonal, and subtidal to intertidal environment.

The lower dolomite beds of the suprasalt Patsy Hill Member were deposited in a tidal flat environment in the intertidal zone and thin from 43 m to 19 m toward the diapir. The sandstone beds of the suprasalt Patsy Hill Member were deposited in a barrier island environment and thin from a projected thickness of 159 m to 69 m before abruptly pinching out towards the diapir. The upper dolomite beds of the suprasalt Patsy Hill Member were deposited in a lagoonal environment with washover fans and flood

tidal deltas and thin from 105 m to 20 m toward the diapir. The Patsy Hill Member of the Bonney Sandstone in the suprasalt minibasin at Patawarta diapir was deposited in a barrier island-lagoonal complex environment.

6.2 Depositional Sequence Stratigraphy

Suprasalt strata flanking Patawarta diapir form parts of two 3rd-order depositional sequences. The offshore basinal shales of the Bunyeroo Formation comprise the Transgressive Systems Tract of the lower depositional sequence. The formational contact between the Bunyeroo and Wonoka formations is interpreted at the maximum flooding surface. The lower, middle, and upper limestone and green mudstone members of the Wonoka Formation represent the progressive shallowing from outer shelf to shoreface, foreshore, lagoonal, and subtidal to intertidal depositional environments. The lower dolomite beds of the Patsy Hill Member of the Bonney Sandstone record ongoing normal regression to tidal flat settings within the intertidal zone. Therefore, the Wonoka Formation and lower Patsy Hill Member form the Highstand Systems Tract of the lower depositional sequence. The sharp, erosional contact between the Patsy Hill Member lower dolomite and sandstone beds is interpreted as the sequence boundary between the lower and upper depositional sequences. The sandstone and upper dolomite beds of the Patsy Hill Member record a non-Waltherian shift to more basinward deposition within the barrier island-lagoonal complex. The upper Patsy Hill Member form the Lowstand Systems Tract of the upper depositional sequence. The formational contact between the Patsy Hill Member and undifferentiated Bonney Sandstone is interpreted as the transgressive surface.

6.3 Halokinetic Sequence Stratigraphy

Suprasalt Bunyeroo, Wonoka, and Patsy Hill strata adjacent to Patawarta diapir thin gradually, but dramatically from ~3500 to 20 m over distances of 3-6 km. They display low-angle onlap and depositional thinning on to the shallowly dipping (12°) top salt-sediment interface with local angular truncations. Halokinetic upturn of suprasalt strata is restricted to the locally steeper (52°) top salt surface near the stratigraphic termination of the Bunyeroo Formation and associated diagenetic caprock against diapiric

breccia. These stratigraphic and structural characteristics indicate suprasalt Bunyeroo, Wonoka, and Patsy Hill strata form primarily a broad, open fold above the allochthonous salt sheet with significant thinning but only minor halokinetic upturn, which represents minibasin-scale folding and thinning. Additionally, angular unconformities at the basal contact of the Wonoka middle limestone member and at the sequence boundary within the Patsy Hill Member are interpreted as composite halokinetic sequence boundaries adjacent to the suprasalt margin, and Bunyeroo, Wonoka, and lower Patsy Hill strata comprise two stacked tapered composite halokinetic sequences.

6.4 Correlation to Subsalt Minibasin Stratigraphy

The suprasalt minibasin fill adjacent to Patawarta diapir was correlated to the previously studied subsalt stratigraphy of Kernen et al. (2012) utilizing the depositional sequence stratigraphic framework. Characteristic stratigraphic and geometric relationships were highlighted within this framework with the goal of developing a depositional and halokinetic model that could utilize suprasalt stratigraphy to predict coeval subsalt depositional facies, stratal thickness trends, and structural styles and stratal geometries.

The informal map units of Kernen (2012) for the Wonoka Formation display consistent depositional facies trends between the coeval subsalt and suprasalt minibasin fills in regards to both facies distribution and depositional setting except in the uppermost Wonoka green mudstone member. Variations in Wonoka facies distribution and depositional settings include: 1) deposition in overall slightly deeper water in each of the Wonoka stratal units in the suprasalt minibasin; 2) an expanded suprasalt section of the green mudstone member; and 3) presence of a series of granule to pebble-bearing conglomerate beds in the green mudstone member in the subsalt minibasin only, which were interpreted by Kernen et al. (2012) to represent progressive erosional unroofing of diapir roof strata.

The informal map units of the Patsy Hill Member of the Bonney Sandstone vary significantly in regards to facies distribution between the coeval subsalt and suprasalt minibasin fills. Important differences in Patsy Hill facies distribution and depositional settings include the following: 1) occurrence of lithoclastic wackestone to packstone in the suprasalt lower dolomite beds and oolitic-lithoclastic-peloidal packstone to grainstone in the suprasalt upper dolomite beds, but not in their correlative subsalt

stratal units and 2) presence of diapir-derived conglomerate beds in the subsalt lower and upper dolomite beds, but only in the suprasalt upper dolomite beds, which record different periods of diapir exposure and erosion.

Bunyeroo, Wonoka, and Patsy Hill strata in the coeval minibasins at Patawarta diapir comprise parts of two 3rd-order depositional sequences. In both minibasins, the Bunyeroo Formation forms the TST, which is bound at the base by a SB at the formational contact with the underlying ABC Range Quartzite and at the top by a *mfs* at the formational contact with the overlying Wonoka Formation. The Wonoka Formation and lower dolomite beds of the Patsy Hill Member form the HST. The SB is reinterpreted based on this study and is placed at the erosional contact between the Patsy Hill lower dolomite and sandstone beds. The Patsy Hill sandstone and upper dolomite beds form the LST, which is bound at the top by a ts at the formational contact with the overlying undifferentiated Bonney Sandstone.

The subsalt minibasin fill at Patawarta diapir developed two stacked CHS, whereby significant folding and thinning of Bunyeroo, Wonoka, and Patsy Hill strata occurred within 560 m of the subsalt-sediment interface. In contrast, the suprasalt minibasin fill recorded primarily minibasin-scale folding and thinning with two stacked tapered CHS. Bunyeroo, Wonoka, and Patsy Hill strata form a broad, open fold that thins gradually, but dramatically over 3-6 km on to the shallowly dipping top of allochthonous salt Stratal truncation near the diapir margin at two significant angular unconformities combined with enhanced thinning over approximately 1-1.5 km reflect the formation of tapered CHS in suprasalt strata. However, despite analogous high sedimentation rates across Patawarta diapir, CHS boundaries developed in different stratigraphic levels in the subsalt and suprasalt minibasins, which reveals the strong control of local differences in diapir rise rate on when and where halokinetic growth strata develop. Therefore, correlation based on a halokinetic sequence stratigraphic framework was unsuccessful in developing predictions of subsalt geometries and facies from suprasalt relationships.

The analysis of suprasalt stratigraphy at Patawarta diapir and correlation to the subsalt stratigraphy strongly suggest that, despite many similarities, the depositional and halokinetic history of coeval minibasin fills do not display characteristic, predictable relationships. Stratigraphic trends reflected in suprasalt and subsalt minibasins can be correlated within a depositional sequence stratigraphic framework,

but the strong local influences of vertical and lateral salt movement on stratal architecture renders attempts to correlate within a halokinetic stratigraphic framework futile. While this negates the applicability of a predictive model for the characteristics of subsalt minibasin fill based on correlative suprasalt strata, further documentation of outcrop examples of halokinetic growth strata adjacent to allochthonous salt, such as Patawarta diapir, continues to add to the catalogue of petroleum system possibilities, limiting the risks involved with pre-drill prediction of subsalt minibasin reservoir exploration.

References

Bouma, A.H., 1962, Sedimentology of some Flysch deposits: A graphic approach to facies interpretation: Elsevier, Amsterdam, 168 p.

Callot, J.-P., Ribes, C., Kergaravat, C., Bonnel, C., Temiz, H., Poisson, A., Vrielynck, B., Salel, J.-F., and Ringenbach, J.-C., 2014, Salt tectonics in the Sivas Basin (Turkey): crossing salt walls and minibasins: Bulletin de la Société Géologique de France, v. 185, no. 1, p. 33-42.

Catuneanu, O., 2006, Principles of Sequence Stratigraphy: Elsevier, Amsterdam, 375 p.

Christie-Blick, N., Grotzinger, J.P., and von der Borch, C.C., 1988, Sequence stratigraphy in Proterozoic successions: Geology, v. 16, p. 100-104.

Christie-Blick, N., von der Borch, C.C., and DiBona, P.A., 1990, Working hypothesis for the origin of the Wonoka Canyons (Neoproterozoic), South Australia: American Journal of Science, v. 290, p. 295-332.

Christie-Blick, N., Dyson, I.A., and von der Borch, C.C., 1995, Sequence stratigraphy and the interpretation of Neoproterozoic earth history: Precambrian Research, v. 73, p. 3-26.

Coats, R.P., 1964, Large scale Precambrian slump structures, Flinders Ranges, Quarterly Geologic Notes: Geological Survey of South Australia, v. 11, p. 1-2.

Coats, R.P., 1973, COPLEY, South Australia: Adelaide, South Australia Geological Survey, Geological Series Explanatory Notes, sheet SH 54-9, 1:250 000, 1 sheet.

Coats, R. P., 2009, ANGEPENA, South Australia: Adelaide, South Australia Geological Survey, sheet 6636, scale 1:100 000, 1 sheet.

Coe, A.L., ed., 2002, The Sedimentary Record of Sea-Level Change: Cambridge University Press.

Dalgarno, C.R. and Johnson, J.E., 1964, The Wilpena Group, *in* Thomson, B.P., et al., eds., Precambrian rock groups in the Adelaide Geosyncline: a new subdivision, Quarterly Geological Notes, Geological Survey of South Australia, v. 20, p. 12-15.

Dalgarno, C.R. and Johnson, J.E., 1966, PARACHILNA, South Australia: Adelaide, South Australia Geological Survey, sheet SH54-13, scale 1:250 000, 1 sheet.

Demarest, J.M., II, and Kraft, J.C., 1987, Stratigraphic record of Quaternary sea levels: Implications for more ancient strata, *in* Nummedal, D., Pilkey, O.H., and Howard, J.D., eds., Sea-Level Fluctuation and Coastal Evolution: Society of Economic Paleontologists and Mineralogists, Special Publication 41, p. 223-239.

Dyson, I.A., 1996, A new model for diapirism in the Adelaide Geosyncline: Division of Mines and Energy Resources of South Australia (MESA) Journal, v. 3, p. 41-48.

Dyson, I.A., 2003, A new model for the Wonoka canyons in the Adelaide Geosyncline: Division of Mines and Energy Resources of South Australia (MESA) Journal, v. 31, p. 49-58.

Dyson, I.A., 2004, Geology of the Eastern Willouran Ranges – evidence for the earliest onset of salt tectonics in the Adelaide Geosyncline: Division of Mines and Energy Resources of South Australia (MESA) Journal, v. 35, p. 48-56.

Dyson, I.A. and Rowan, M.G., 2004, Geology of a welded diapir and flanking mini-basins in the Flinders Ranges of South Australia: *in* Post, P.J., Olson, D.L., Lyons, K.T., Palmes, S.L., Harrison, P.F., and Rosen, N.C., eds., Salt-sediment interactions and hydrocarbon prospectivity: Concepts,

applications, and case studies for the 21st century: 24th Annual Gulf Coast Section SEPM Foundation Bob F. Perkins Research Conference, p. 69-89.

Eickhoff, K.H., von der Borch, C.C., and Grady, A.E., 1988, Proterozoic canyons of the Flinders Ranges (South Australia): submarine canyons or drowned river valleys?: Sedimentary Geology, v. 58, p. 217-235.

Enos, J.S. and Kyle, J.R., 2002, Diagenesis of the Carrizo Sandstone at Butler Salt Dome, East Texas Basin, U.S.A.: Evidence for fluid-sediment interaction near halokinetic sequences: Journal of Sedimentary Research, v. 72, no. 1, p. 68-81.

Forbes, B.G., 1971, Stratigraphic subdivision of the Pound Quartzite (late Precambrian, South Australia): Transactions of the Royal Society, Southern Australia, v. 95, p. 219-225.

Giddings, J.A., Wallace, M.W., Haines, P.W., and Mornane, K., 2010, Submarine origin for the Neoproterozoic Wonoka canyons, South Australia: Sedimentary Geology, v. 223, p. 35-50.

Giles, K.A. and Lawton, T.F., 2002, Halokinetic sequence stratigraphy adjacent to the El Papalote Diapir, northeastern Mexico: American Association of Petroleum Geologists Bulletin, v. 86, p. 823-840.

Giles, K.A., Lawton T.F., and Rowan, M.G., 2004, Summary of halokinetic sequence characteristics from outcrop studies of La Popa Salt Basin, northeastern Mexico *in* Post, P.J., Olson, D.L., Lyons, K.T., Palmes, S.L., Harrison, P.F., and Rosen, N.C., eds., Salt-sediment interactions and hydrocarbon prospectivity: Concepts, applications, and case studies for the 21st century: 24th Annual Gulf Coast Section SEPM Foundation Bob F. Perkins Research Conference, p. 1045-1062.

Giles, K.A., Lawton, T.F., Shock, A.L., Kernen, R.A., Hearon IV, T.E., and Rowan, M.G., 2012, A Halokinetic Drape-Fold Model for Caprock in Diapir-Flanking and Subsalt Positions: American Association of Petroleum Geologists Annual Convention and Exhibition.

Giles, K.A. and Rowan M.G., 2012, Concepts in halokinetic-sequence deformation and stratigraphy, *in* Alsop, G.I., Archer, S.G., Hartley, A.J., Grant, N.T., and Hodgkinson, R., eds., Salt Tectonics, Sedimentation and Prospectivity, Geological Society of London Special Publications, v. 363, p. 7-31.

Gostin, V.A. and Jenkins, R.J.F., 1983, Sedimentation of the early Ediacaran, Flinders Ranges, South Australia [abs]: 6th Australian Geological Convention, Canberra, Geological Society Australia, v. 9, p. 196-197.

Haines, P.W., 1987, Carbonate shelf and basin sedimentation, late Proterozoic Wonoka Formation, South Australia: Ph.D. thesis, University of Adelaide, unpublished, 269 p.

Haines, P.W., 1990, A late Proterozoic storm-dominated carbonate shelf sequence: The Wonoka Formation in the central and southern Flinders Ranges, South Australia, *in* Jago, J.B. and Moore, P.S., eds., The Evolution of a Late Precambrian-Early Paleozoic Rift Complex: Adelaide Geosyncline, Geological Society of Australia, Special Publication, v. 16, p. 177-198.

Hall, D., Both, R.A., and Daily, B., 1986, Copper mineralization in the Patawarta Diapir, northern Flinders Ranges, South Australia: Bulletin of Australasian Institute of Mining and Metallurgy, v. 291, no.7, p. 55-60.

Hart, W. and Albertin, M., 2001, Subsalt trap archetype classification: A diagnostic tool for predicting and prioritizing Gulf of Mexico subsalt traps [abs] *in* Fillon, R.H., Rosen, N.C., Weimer, P., Lowrie, A., Pettingill, H., Phair, R.L., Roberts, H.H., van Hoorn, B., eds., Petroleum systems of

deep-water basins: Global and Gulf of Mexico experience: 21st Annual Gulf Coast Section SEPM Foundation Bob F. Perkins Research Conference, p.44.

Hart, W., Jaminski, J., and Albertin, M., 2004, Recognition and exploration significance of supra-salt stratal carapaces *in* Post, P.J., Olson, D.L., Lyons, K.T., Palmes, S.L., Harrison, P.F., and Rosen, N.C., eds., Salt-sediment interactions and hydrocarbon prospectivity: Concepts, applications, and case studies for the 21st century: 24th Annual Gulf Coast Section SEPM Foundation Bob F. Perkins Research Conference, p.166-199.

Hearon IV, T.E., 2013, Analysis of salt-sediment interaction associated with steep diapirs and allochthonous salt: Flinders and Willouran Ranges, South Australia, and the deepwater northern Gulf of Mexico: Ph.D. thesis, Colorado School of Mines, unpublished, 178 p.

Hearon, T. E., IV, Rowan, M.G., Giles, K.A., Kernen, R.A., Gannaway, C.E., Lawton, T.F., and Fiduk, J.C., 2014, Allochthonous salt initiation and advance in the Flinders and Willouran Ranges, South Australia: using outcrops to test subsurface-based models from the northern Gulf of Mexico: American Association of Petroleum Geologists Bulletin.

Hudec, M.R. and Jackson, M.P.A., 2006, Advance of allochthonous salt sheets in passive margins and orogens: American Association of Petroleum Geologists Bulletin, v. 90, no. 10, p. 1535-1564.

Hudec, M.R. and Jackson, M.P.A., 2011, The salt mine: a digital atlas of salt tectonics: The University of Texas at Austin, Bureau of Economic Geology, Udden Book Series No. 5, American Association of Petroleum Geologists Memoir 99, 305 p.

Hudec, M.R., Jackson, M.PA., and Schultz-Ela, D.D., 2009, The paradox of minibasin subsidence into salt: Clues to the evolution of crustal basins: Geological Society of America Bulletin, v.121, no. 1/2, p. 201-221.

Jackson, M.P.A. and Talbot, C.J., 1991, A glossary of salt tectonics: The University of Texas at Austin, Bureau of Economic Geology Geological Circular, 91-4, 44 p.

Jackson, M.P.A., 1995, Retrospective salt tectonics, *in* Jackson, M.P.A., Roberts, D.G., and Snelson, S., eds., Salt Tectonics: a global perspective: American Association of Petroleum Geologists Memoir 65, p. 1-28.

Jackson, M.P.A. and Harrison, J.C., 2006, An allochthonous salt canopy on Axel Heiberg Island, Sverdrup Basin, Arctic Canada: Geology, v. 34, p. 1045-1048.

Jackson, M.P.A., Warrin, O.N., Woad, G.M., and Hudec, M.R., 2003, Neoproterozoic allochthonous salt tectonics during the Lufilian orogeny in the Katangan copper belt, Central Africa: Geological Society of America Bulletin, v. 115, p. 314-330.

Jenkins, R.J.F., 1990, The Adelaide fold belt: tectonic reappraisal, *in* Jago, J.B. and Moore, P.S., eds., The Evolution of a Late Precambrian-Early Paleozoic Rift Complex: Adelaide Geosyncline, Geological Society of Australia, Special Publication, v. 16, p. 396-420.

Kernen, R.A., 2011, Halokinetic sequence stratigraphy of the Neoproterozoic Wonoka Formation at Patawarta Diapir, Central Flinders Ranges, South Australia: M.S. thesis, New Mexico State University, unpublished, 132 p.

Kernen, R.A., Giles, K.A., Rowan, M.G., and Hearon IV, T.E., 2011, Identification of a Neoproterozoic shelfal suprasalt carapace and correlation to a tapered composite halokinetic sequence at Patawarta Diapir, Central Flinders Ranges, South Australia [abs]: American Association of Petroleum Geologists Annual Convention and Exhibition.

Kernen, R.A., Giles, K.A., Rowan, M.G., Lawton, T.F., and Hearon IV, T.E., 2012, Depositional and halokinetic-sequence stratigraphy of the Neoproterozoic Wonoka Formation adjacent to Patawarta allochthonous salt sheet, Central Flinders Ranges, South Australia *in* Alsop, G.I., Archer, S.G., Hartley, A.J., Grant, N.T., and Hodgkinson, R., eds., Salt Tectonics, Sedimentation and Prospectivity, Geological Society of London Special Publications, v. 363, p. 81-105.

Kyle, J.R. and Posey, H.H., 1991, Halokinesis, Cap Rock Development, and Salt Mineral Resources, *in* Melvin, J.L., eds., Developments in Sedimentology: Evaporites, Petroleum, and Mineral Resources, v. 50, p. 428-491.

Lemon, N.M., 1988, Diapir recognition and modelling with examples from the late Proterozoic Adelaide Geosyncline, Central Flinders Ranges, South Australia: Ph.D. thesis, University of Adelaide, unpublished.

Lemon, N.M., 2000, A Neoproterozoic fringing stromatolite reef complex, Flinders Ranges, South Australia: Precambrian Research, v. 100, p. 109-120.

Mawson, D., 1938, Cambrian and sub-Cambrian formations at Parachilna Gorge: Transactions of the Royal Society, Southern Australia, v. 62, p. 255-262.

Mawson, D., 1939, The late Proterozoic sediments of South Australia: Report of the Australian and New Zealand Association for the Advancement of Science, v. 24, p. 79-88.

Mawson, D., 1941, The Wilpena pound formation and underlying Proterozoic sediments: Transactions of the Royal Society, Southern Australia, v. 65, p. 295-303.

Mawson D. and Segnit, E.R., 1949, Purple slates of the Adelaide System: Transactions of the Royal Society, Southern Australia, v. 72, p. 276-280.

Moore, D., Snyder F.C., Rutkowski, S., 1995, Supra-salt stacked condensed section (SCS): Potential indicators of subsalt stratigraphy [abs] *in* Travis, C.J., Harrison, H., Hudec, M.R., Vendeville, B.C., Peel, F.J., and Perkins, B.F., eds., Salt, sediment, and hydrocarbons: 16th Annual Gulf Coast Section SEPM Foundation Bob F. Perkins Research Conference, p. 195-196.

Nummedal, D., and Swift, D.J.P., 1987, Transgressive stratigraphy at sequence-bounding unconformities: Some principles derived from Holocene and Cretaceous examples, *in* Nummedal, D., Pilkey, O.H., and Howard, J.D., eds., Sea-Level Fluctuation and Coastal Evolution: Society of Economic Paleontologists and Mineralogists, Special Publication 41, p. 240-260.

Plint, A.G., 2010, Wave- and Storm-Dominated Shoreline and Shallow-Marine Systems, *in* James, N.P. and Dalrymple, R.W., eds., Facies Models 4, GEOtext 6, Geological Association of Canada, p. 167-199.

Posamentier, H.W., Allen, G.P., James, D.P., and Tesson, M., 1992, Forced regressions in a sequence stratigraphic framework: concepts, examples, and exploration significance: American Association of Petroleum Geologists Bulletin, v. 76, no. 11, p. 1687-1709.

Preiss, W.V., 1987, The Adelaide Geosyncline – late Proterozoic stratigraphy, sedimentation, paleontology and tectonics: Geological Survey of South Australia Bulletin, v. 53, 438 p.

Preiss, W.V., 2000, The Adelaide Geosyncline of South Australia and its significance in Neoproterozoic continental reconstruction: Precambrian Research, v. 100, p. 21-63.

Reid, P.W., and Preiss, W.V., 1999, PARACHILNA (second ed.), South Australia: Adelaide, South Australia Geological Survey, sheet SH54-13, scale 1:250 000, 1 sheet.

Ringenbach, J.-C., Salel, J.-F., Kergaravat, C., Ribes, C., Bonnel, C., and Callot, J.-P., 2014, Salt tectonics in the Sivas Basin, Turkey: outstanding seismic analogues from outcrops: First Break, v. 31, p. 57-65.

Rowan, M.G., Lawton, T.F., Giles, K.A., and Ratliff, R.A., 2003, Near-salt deformation in La Popa Basin, Mexico, and the northern Gulf of Mexico: a general model for passive diapirism: American Association of Petroleum Geologists Bulletin¸ v. 87, no. 5, p. 733-756.

Rowan, M.G. and Vendeville, B.C., 2006, Foldbelts with early salt withdrawal and diapirism: physical model and examples from the Northern Gulf of Mexico and the Flinders Ranges, Australia: Marine and Petroleum Geology, v. 23, p. 871-891.

Sherkati, S., Molinaro, M., de Lamotte, D.F., and Letouzey, J., 2005, Detachment Folding in the Central and Eastern Zagros fold-belt (Iran): salt mobility, multiple detachments, and late basement control: Journal of Structural Geology, v. 27, p. 1680-1696.

Shock, A.L., 2012, Origin and implications of Permian and Triassic diagenetic carbonate caprock adjacent to diapiric salt walls, Paradox Basin, Utah: M.S. thesis, New Mexico State University, unpublished, 115 p.

Scholle, P.A., Bebout, D.G., and Moore, C.H., eds., 1983, Carbonate Depositional Environments: American Association of Petroleum Geologists Memoir 33, 708 p.

Schulz-Ela, D.D. and Jackson, M.P.A., 1996, Relation of subsalt structures to suprasalt structures during extension: American Association of Petroleum Geologists Bulletin, v. 80, no. 12, p. 1896-1924.

Selwyn, A.R.C., 1860, Geological notes of a journey in South Australia from Cape Jervis to Mount Serle: Parliamentary Paper South Australia, no. 20.

Sprigg, R.C., 1952, Sedimentation in the Adelaide Geosyncline and the formation of the continental terrace, *in* Glaessner, M.F. and Rudd, E.A., eds., Sir Douglas Mawson Anniversary Volume, University of Adelaide, Adelaide, p. 153-159.

von der Borch, C.C., Smit, R., and Grady, A.E., 1982, Late Proterozoic submarine canyons of Adelaide Geosyncline, South Australia: Petroleum Exploration Society of Australia Journal, v. 19, p. 332-347.

von der Borch, C.C., Christie-Blick, N., and Grady, A.E., 1988, Depositional sequence analysis applied to Late Proterozoic Wilpena Group, Adelaide Geosyncline, South Australia: Australian Journal of Earth Sciences, v. 35, p. 59-71.

Warren, J.K., 2006, Evaporites: Sediments, Resources and Hydrocarbons: Springer, Berlin-Heidelberg-New York, 1050 p.

Appendix A

Measured stratigraphic sections from the suprasalt minibasin at Patawarta diapir detailing lithology, grain size, grain type, color, sedimentary structures, bed thickness, and interpreted depositional sequence stratigraphy. Note that vertical scales vary between sections. Map units and colors reference explanation from Plate 1. Locations of Section 1-12 are indicated on Plate 1.

Measured Section Explanations

Sedimentary Structures and Grain Types

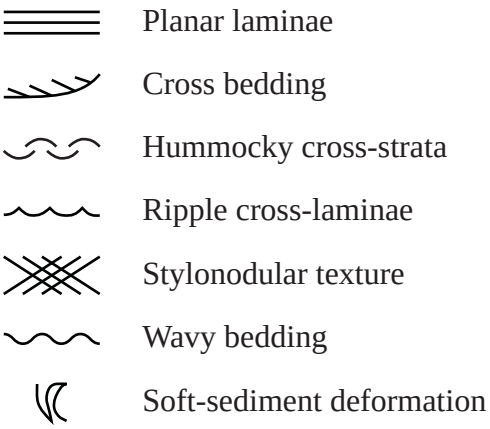

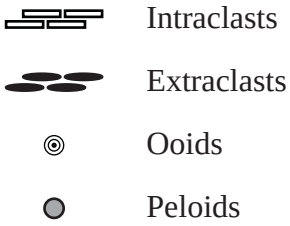

Lithologic Symbols

Carbonate Facies

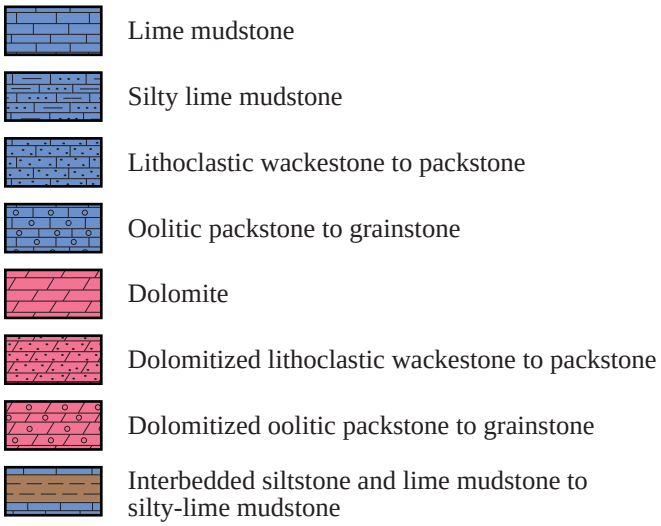

Siliciclastic Facies

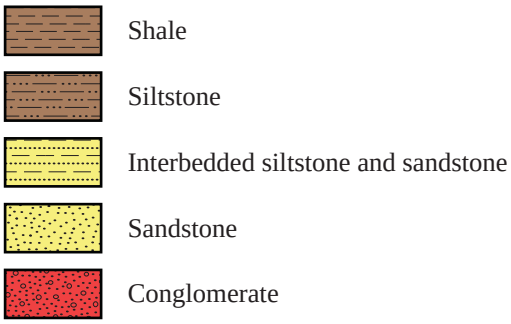

Diagenetic Facies

Depositional Sequence Stratigraphy

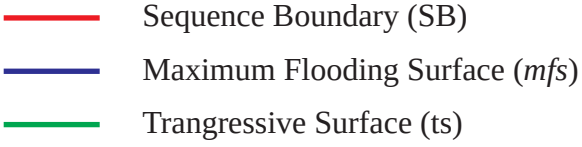

Measured Section 1

Start 0278206 6574385
End 0278220 6574401

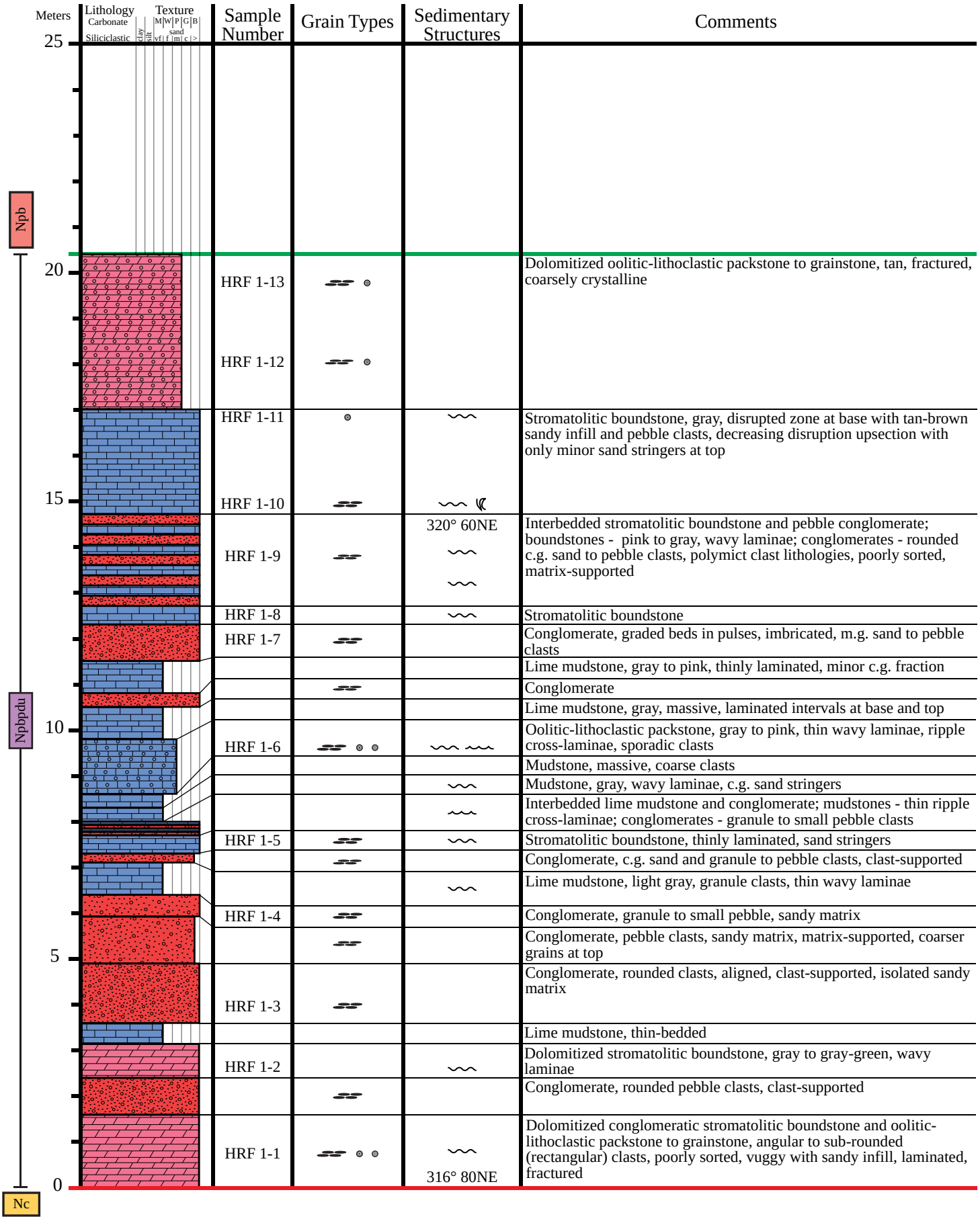

Sample Number	Grain Types	Sedimentary Structures	Comments
HRF 1-13			Dolomitized oolitic-lithoclastic packstone to grainstone, tan, fractured, coarsely crystalline
HRF 1-12			
HRF 1-11			Stromatolitic boundstone, gray, disrupted zone at base with tan-brown sandy infill and pebble clasts, decreasing disruption upsection with only minor sand stringers at top
HRF 1-10			
HRF 1-9		320° 60NE	Interbedded stromatolitic boundstone and pebble conglomerate; boundstones - pink to gray, wavy laminae; conglomerates - rounded c.g. sand to pebble clasts, polymict clast lithologies, poorly sorted, matrix-supported
HRF 1-8			Stromatolitic boundstone
HRF 1-7			Conglomerate, graded beds in pulses, imbricated, m.g. sand to pebble clasts
			Lime mudstone, gray to pink, thinly laminated, minor c.g. fraction
			Conglomerate
			Lime mudstone, gray, massive, laminated intervals at base and top
HRF 1-6			Oolitic-lithoclastic packstone, gray to pink, thin wavy laminae, ripple cross-laminae, sporadic clasts
			Mudstone, massive, coarse clasts
			Mudstone, gray, wavy laminae, c.g. sand stringers
			Interbedded lime mudstone and conglomerate; mudstones - thin ripple cross-laminae; conglomerates - granule to small pebble clasts
HRF 1-5			Stromatolitic boundstone, thinly laminated, sand stringers
			Conglomerate, c.g. sand and granule to pebble clasts, clast-supported
			Lime mudstone, light gray, granule clasts, thin wavy laminae
HRF 1-4			Conglomerate, granule to small pebble, sandy matrix
			Conglomerate, pebble clasts, sandy matrix, matrix-supported, coarser grains at top
HRF 1-3			Conglomerate, rounded clasts, aligned, clast-supported, isolated sandy matrix
			Lime mudstone, thin-bedded
HRF 1-2			Dolomitized stromatolitic boundstone, gray to gray-green, wavy laminae
			Conglomerate, rounded pebble clasts, clast-supported
HRF 1-1		316° 80NE	Dolomitized conglomeratic stromatolitic boundstone and oolitic-lithoclastic packstone to grainstone, angular to sub-rounded (rectangular) clasts, poorly sorted, vuggy with sandy infill, laminated, fractured

Measured Section 2

Start 0277839 6574884
End 0277891 6574891

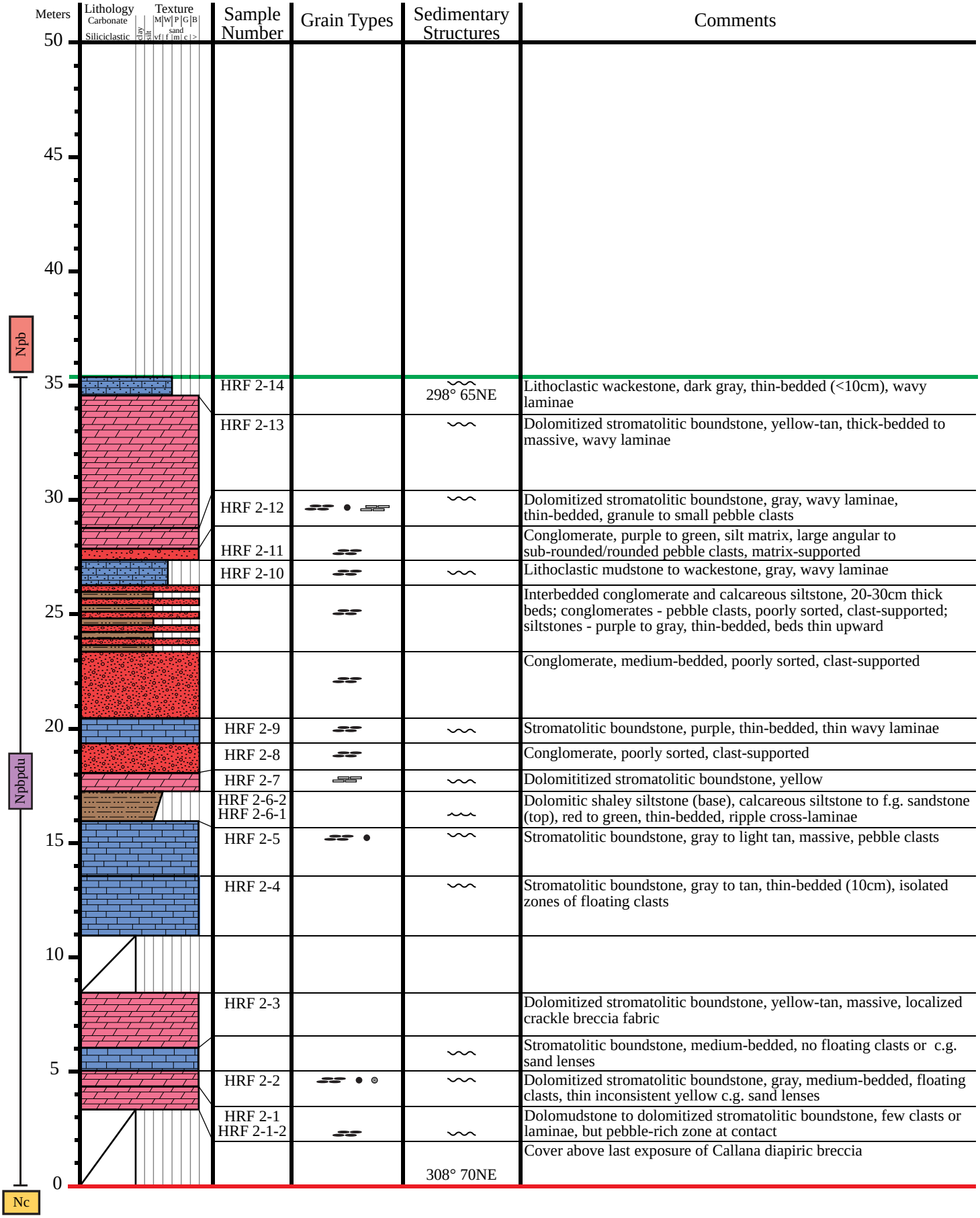

Sample Number	Grain Types	Sedimentary Structures	Comments
HRF 2-14		298° 65NE	Lithoclastic wackestone, dark gray, thin-bedded (<10cm), wavy laminae
HRF 2-13			Dolomitized stromatolitic boundstone, yellow-tan, thick-bedded to massive, wavy laminae
HRF 2-12			Dolomitized stromatolitic boundstone, gray, wavy laminae, thin-bedded, granule to small pebble clasts
HRF 2-11			Conglomerate, purple to green, silt matrix, large angular to sub-rounded/rounded pebble clasts, matrix-supported
HRF 2-10			Lithoclastic mudstone to wackestone, gray, wavy laminae
			Interbedded conglomerate and calcareous siltstone, 20-30cm thick beds; conglomerates - pebble clasts, poorly sorted, clast-supported; siltstones - purple to gray, thin-bedded, beds thin upward
			Conglomerate, medium-bedded, poorly sorted, clast-supported
HRF 2-9			Stromatolitic boundstone, purple, thin-bedded, thin wavy laminae
HRF 2-8			Conglomerate, poorly sorted, clast-supported
HRF 2-7			Dolomititized stromatolitic boundstone, yellow
HRF 2-6-2 HRF 2-6-1			Dolomitic shaley siltstone (base), calcareous siltstone to f.g. sandstone (top), red to green, thin-bedded, ripple cross-laminae
HRF 2-5			Stromatolitic boundstone, gray to light tan, massive, pebble clasts
HRF 2-4			Stromatolitic boundstone, gray to tan, thin-bedded (10cm), isolated zones of floating clasts
HRF 2-3			Dolomitized stromatolitic boundstone, yellow-tan, massive, localized crackle breccia fabric
			Stromatolitic boundstone, medium-bedded, no floating clasts or c.g. sand lenses
HRF 2-2			Dolomitized stromatolitic boundstone, gray, medium-bedded, floating clasts, thin inconsistent yellow c.g. sand lenses
HRF 2-1 HRF 2-1-2			Dolomudstone to dolomitized stromatolitic boundstone, few clasts or laminae, but pebble-rich zone at contact
		308° 70NE	Cover above last exposure of Callana diapiric breccia

Measured Section 3

Start 0277706 6575070
End 0277754 6575080

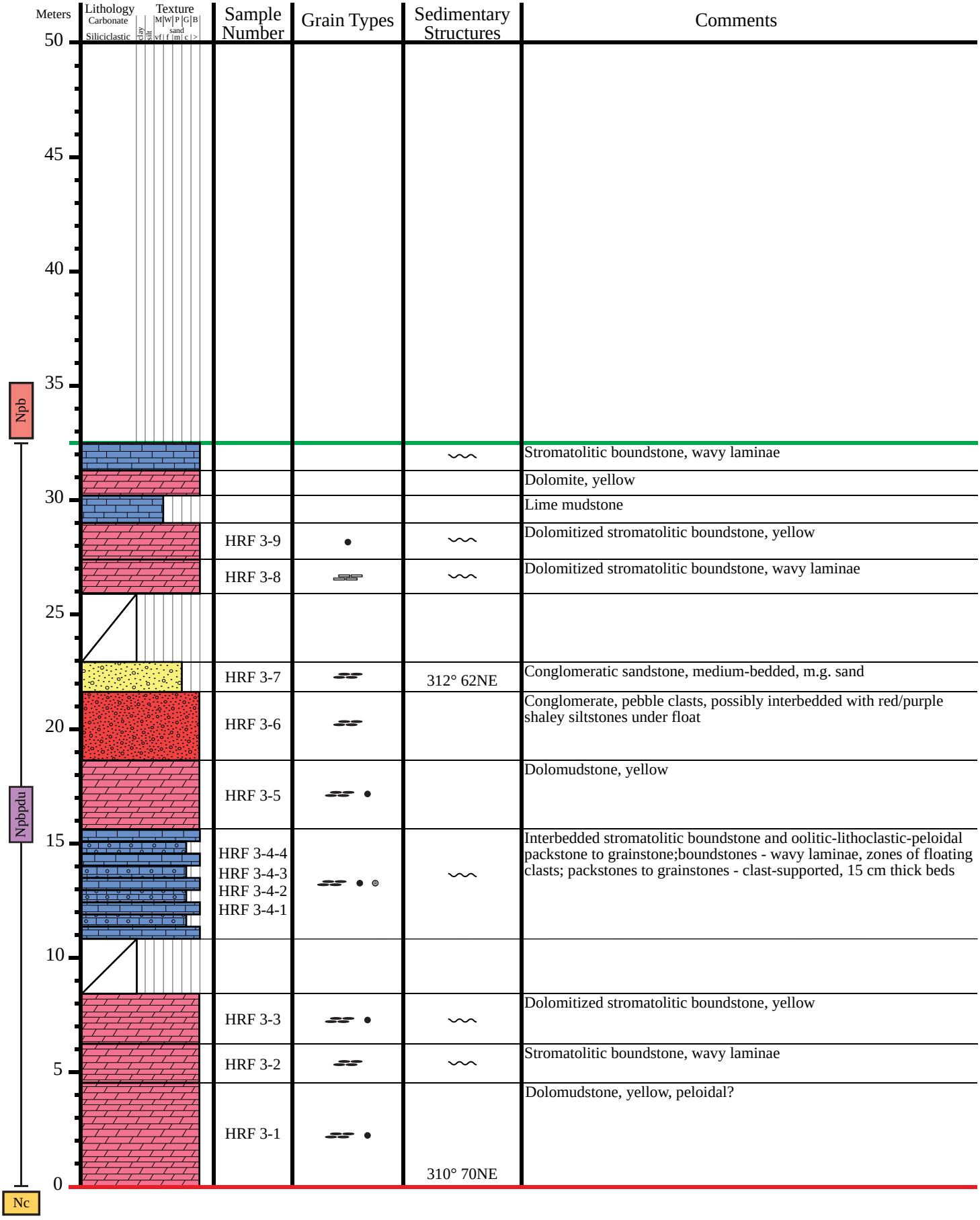

Measured Section 4

Start 0276724 6576801
End 0276790 6576821

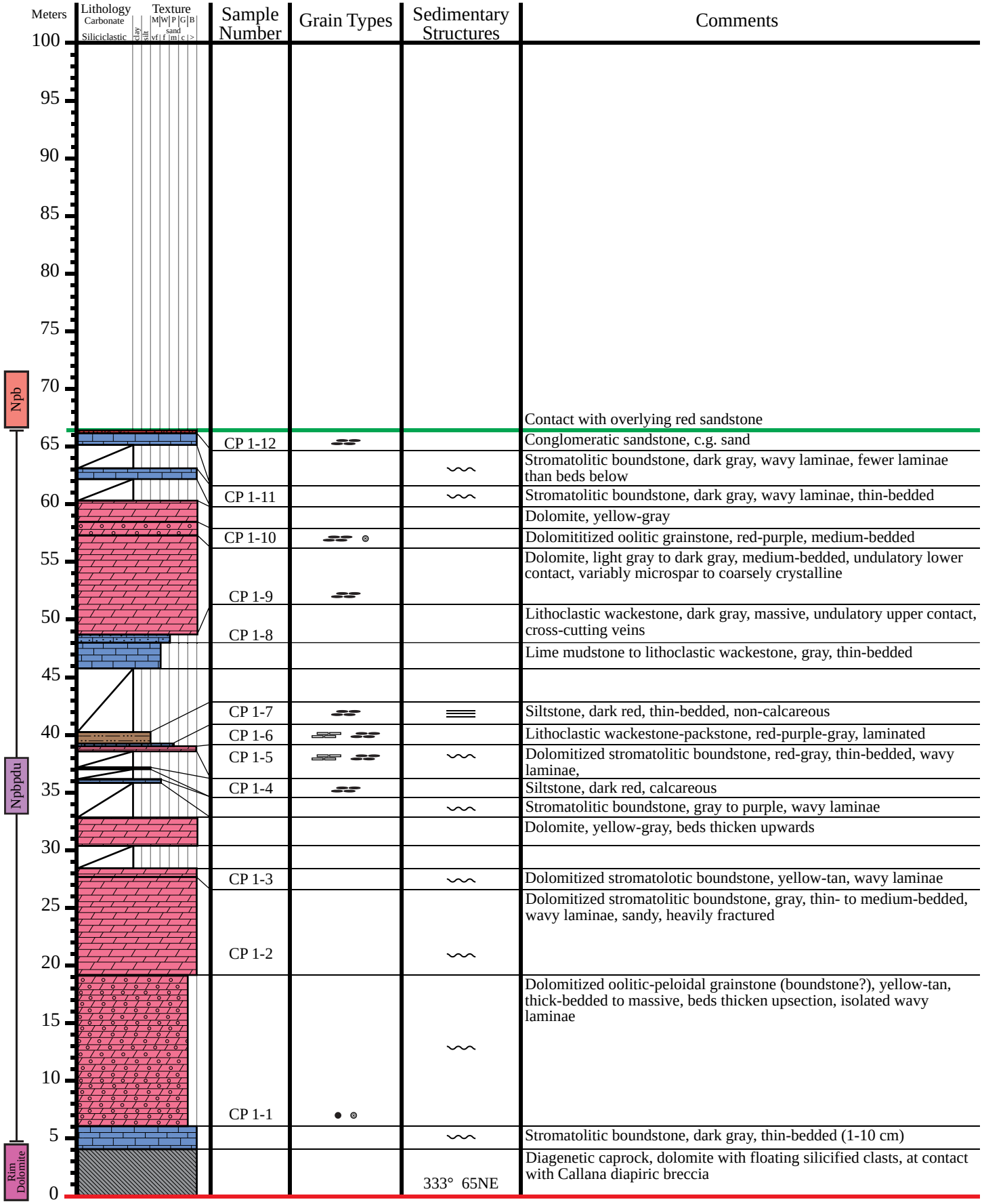

Measured Section 5 (pg. 1)

Start 0276564 6576987
End 0276698 6577029

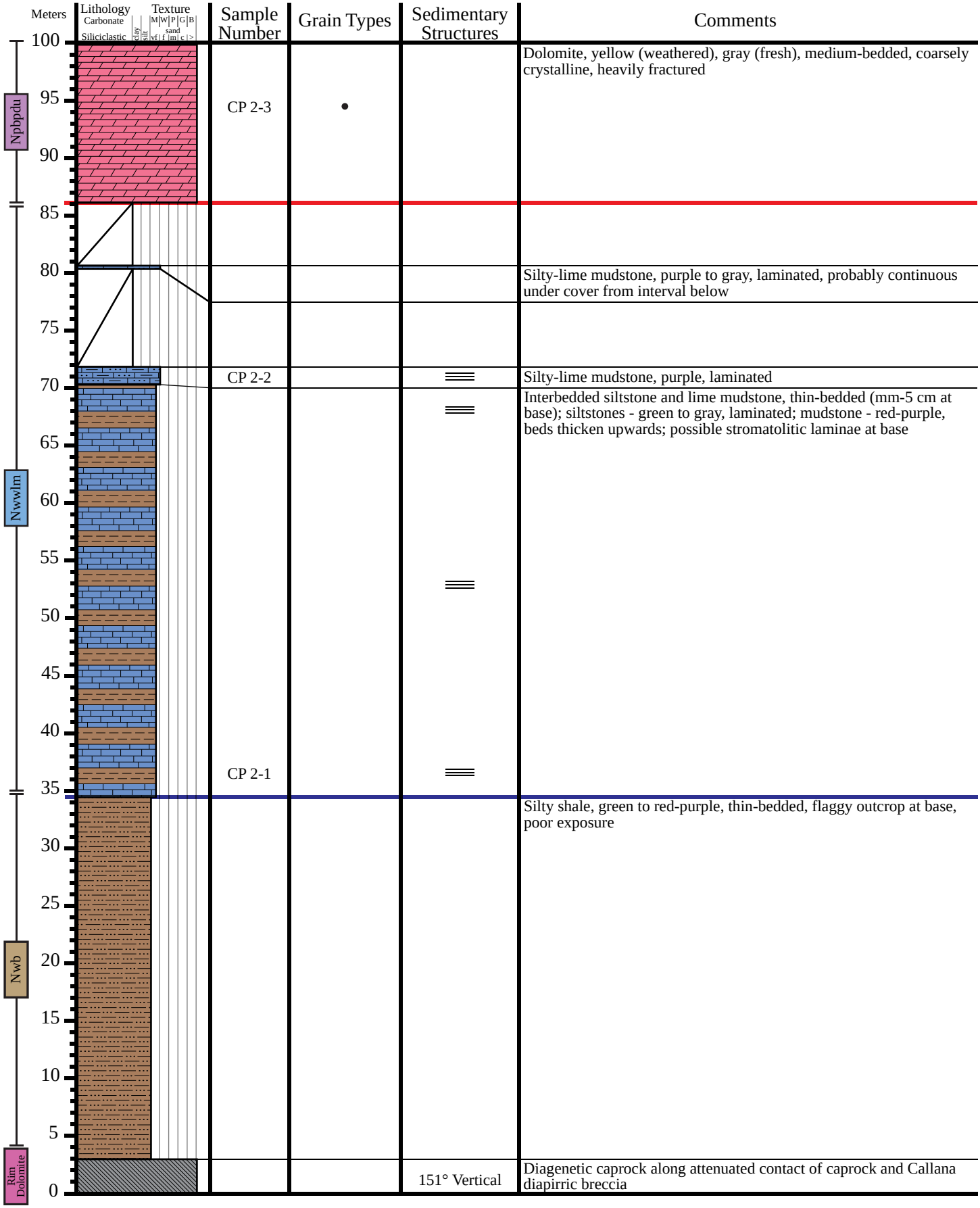

Sample Number	Grain Types	Sedimentary Structures	Comments
CP 2-3	•		Dolomite, yellow (weathered), gray (fresh), medium-bedded, coarsely crystalline, heavily fractured
			Silty-lime mudstone, purple to gray, laminated, probably continuous under cover from interval below
CP 2-2		≡	Silty-lime mudstone, purple, laminated
		≡	Interbedded siltstone and lime mudstone, thin-bedded (mm-5 cm at base); siltstones - green to gray, laminated; mudstone - red-purple, beds thicken upwards; possible stromatolitic laminae at base
		≡	
CP 2-1		≡	
			Silty shale, green to red-purple, thin-bedded, flaggy outcrop at base, poor exposure
		151° Vertical	Diagenetic caprock along attenuated contact of caprock and Callana diapirric breccia

Measured Section 5 (pg. 2)

Start 0276564 6576987
End 0276698 6577029

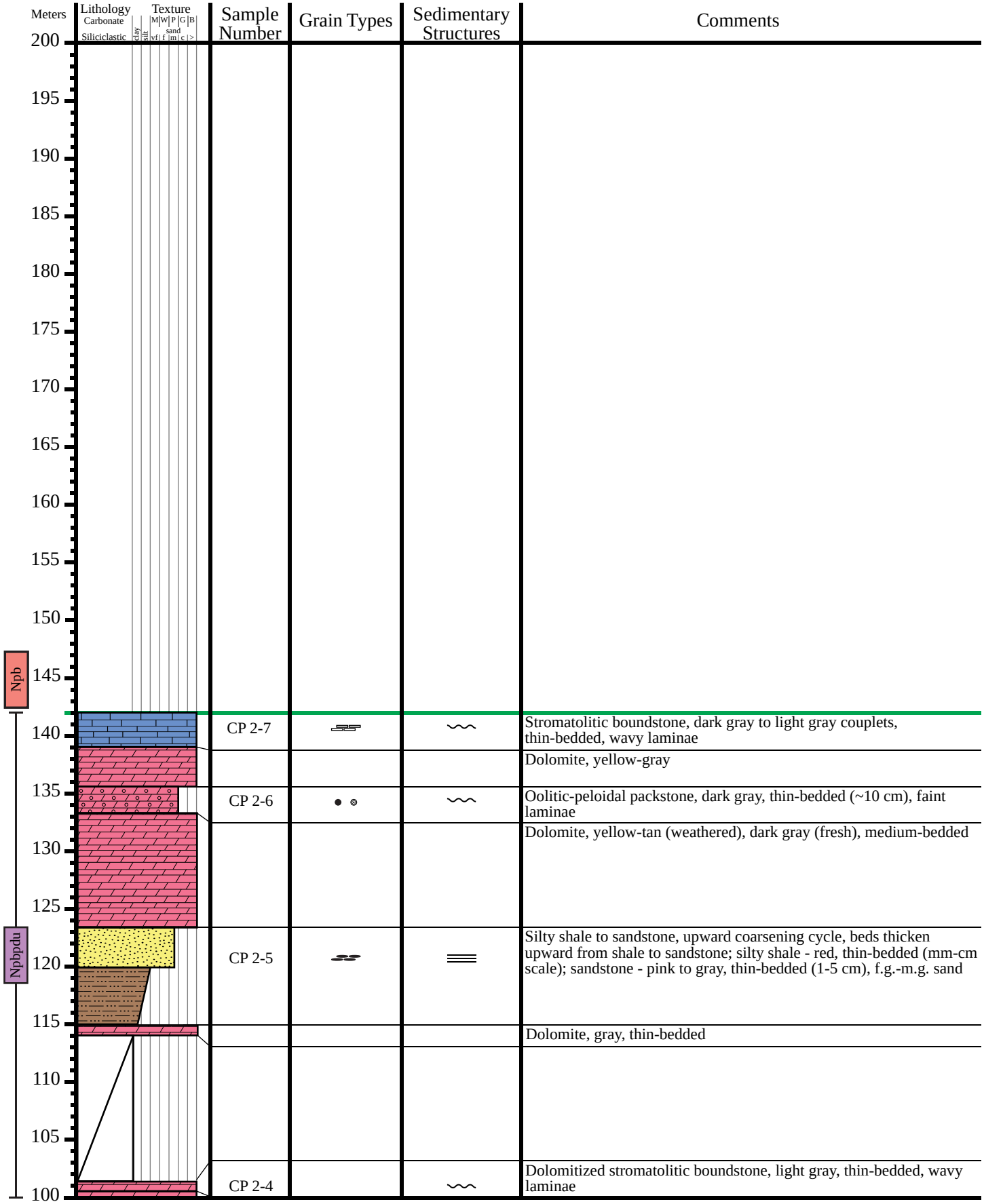

Measured Section 6 (pg. 1)

Start 0276306 6577215
End 0276568 6577389

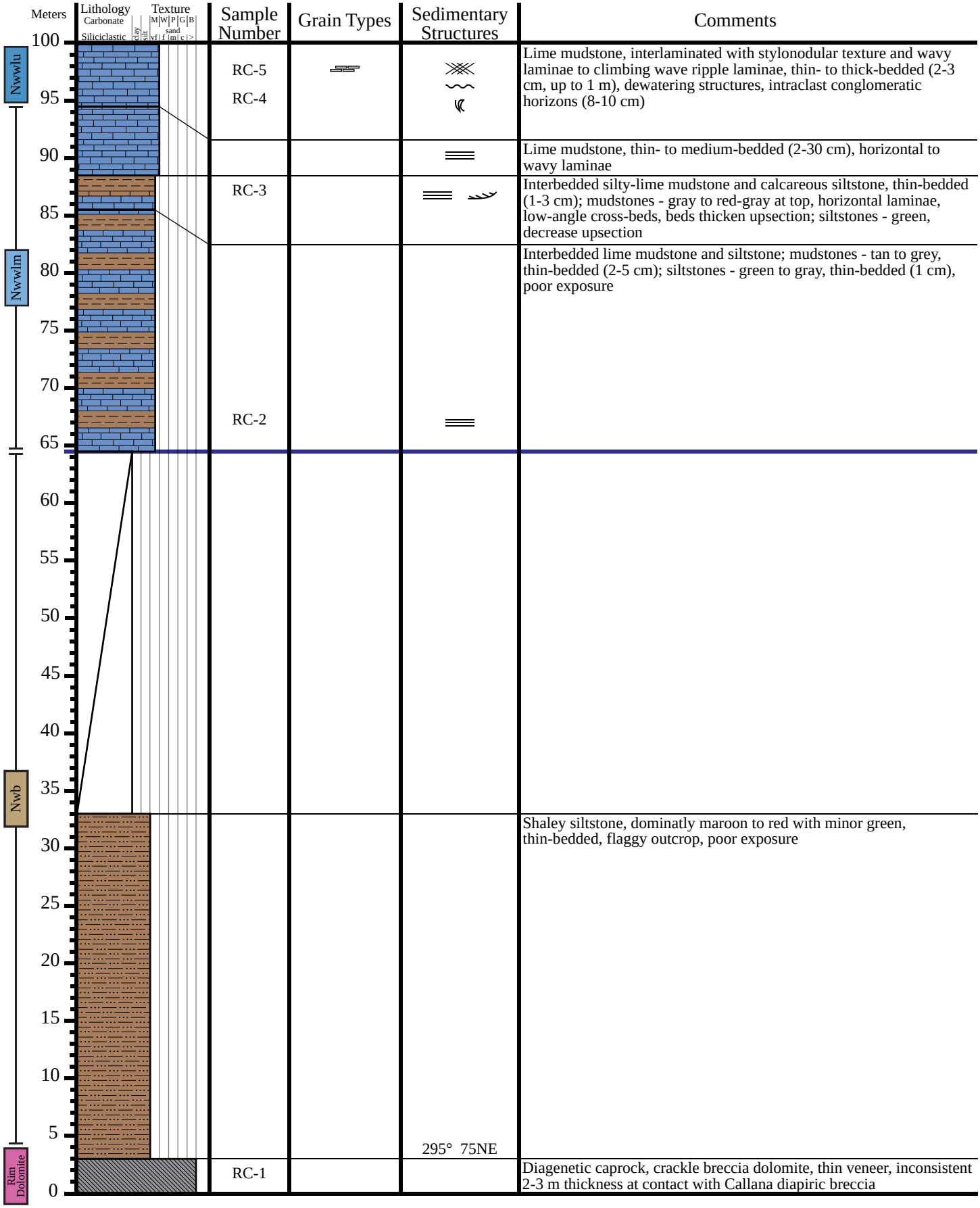

Measured Section 6 (pg. 2)

Start 0276306 6577215
End 0276568 6577389

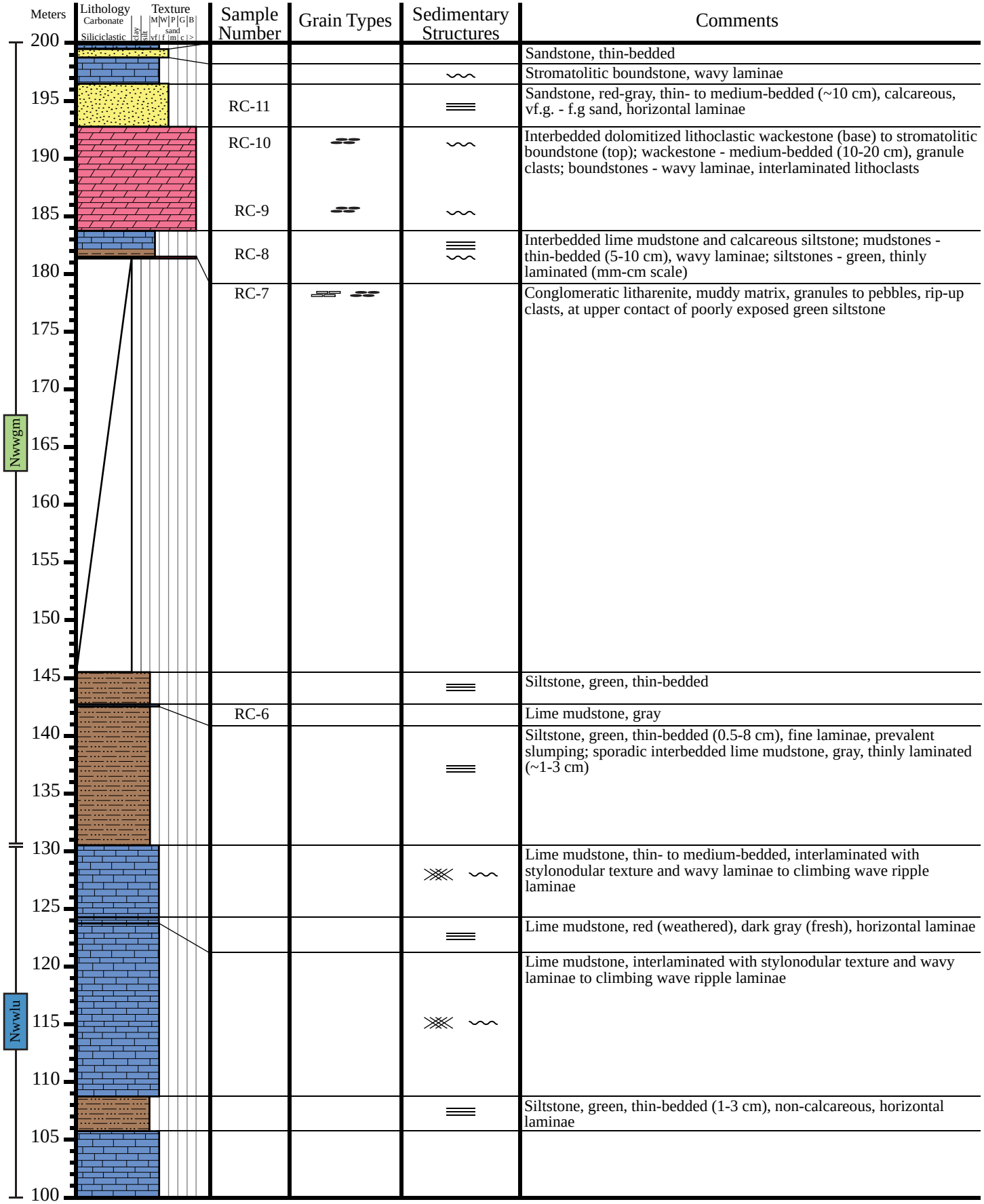

Measured Section 6 (pg. 3)

Start 0276306 6577215
End 0276568 6577389

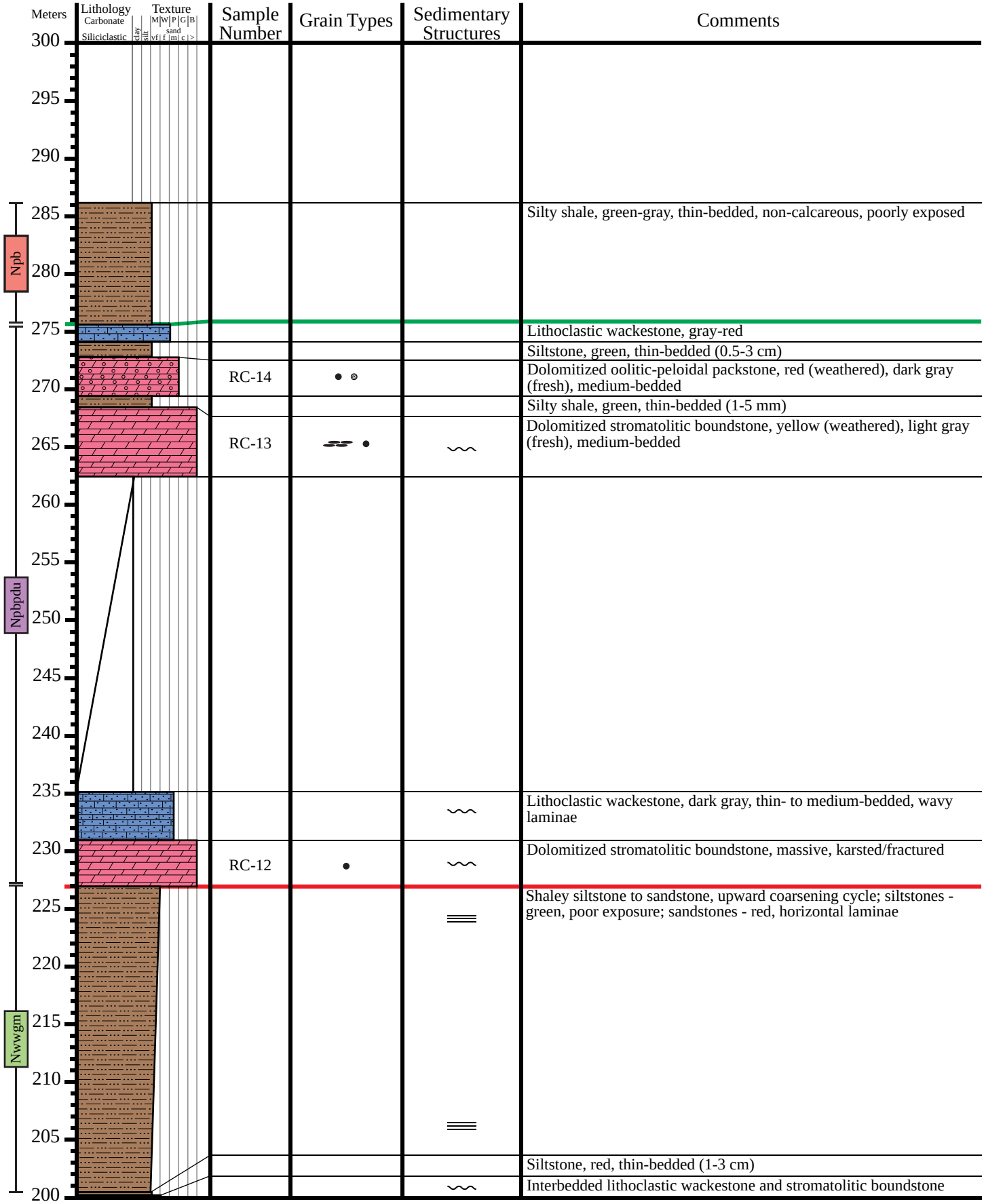

Measured Section 7 (pg. 1)

Start 0276416 6577407
End 0276525 6577502

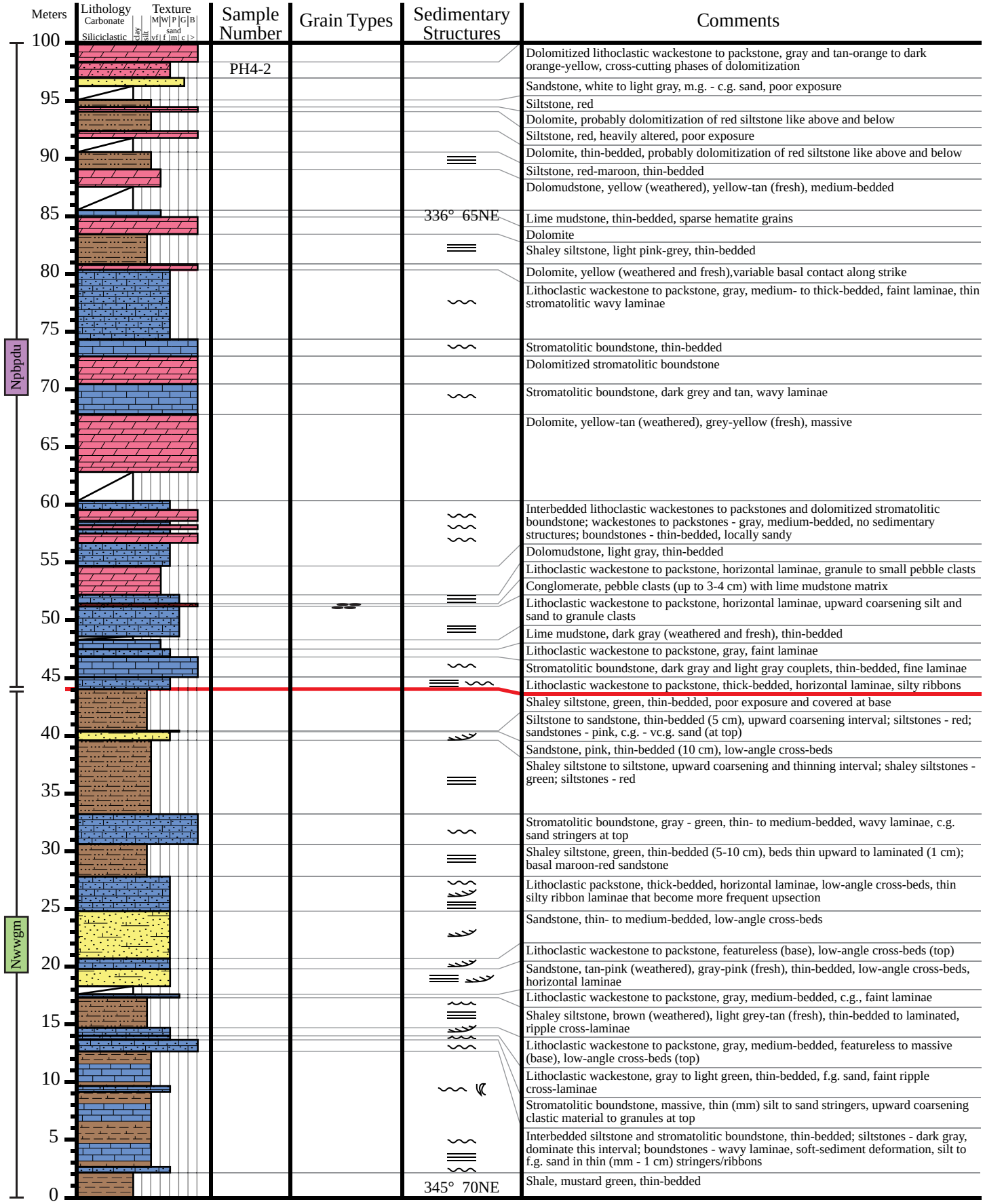

Measured Section 7 (pg. 2)

Start 0276416 6577407
End 0276525 6577502

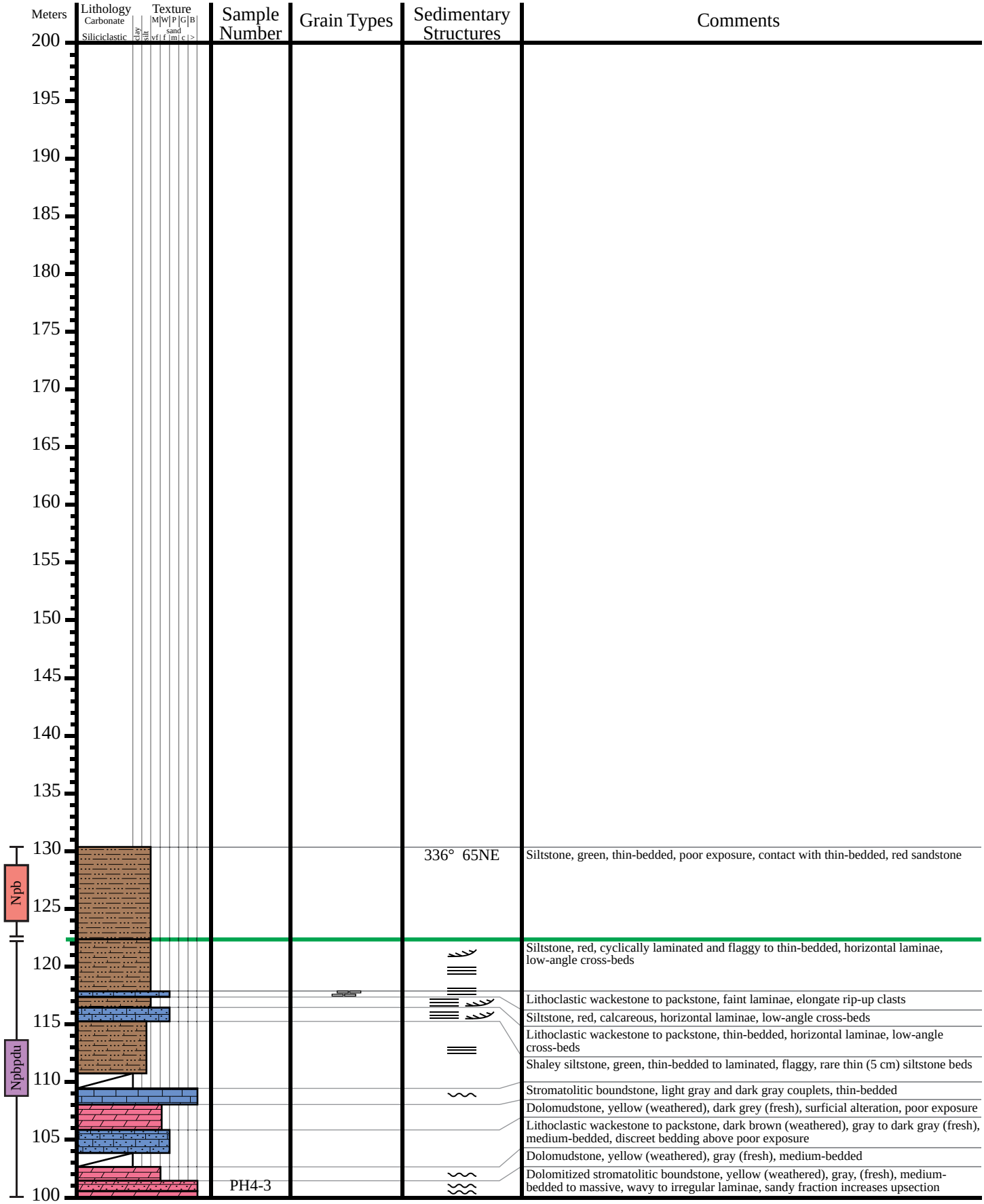

Measured Section 8 (pg. 1)

Start 0276201 6577952
End 0276360 6577990

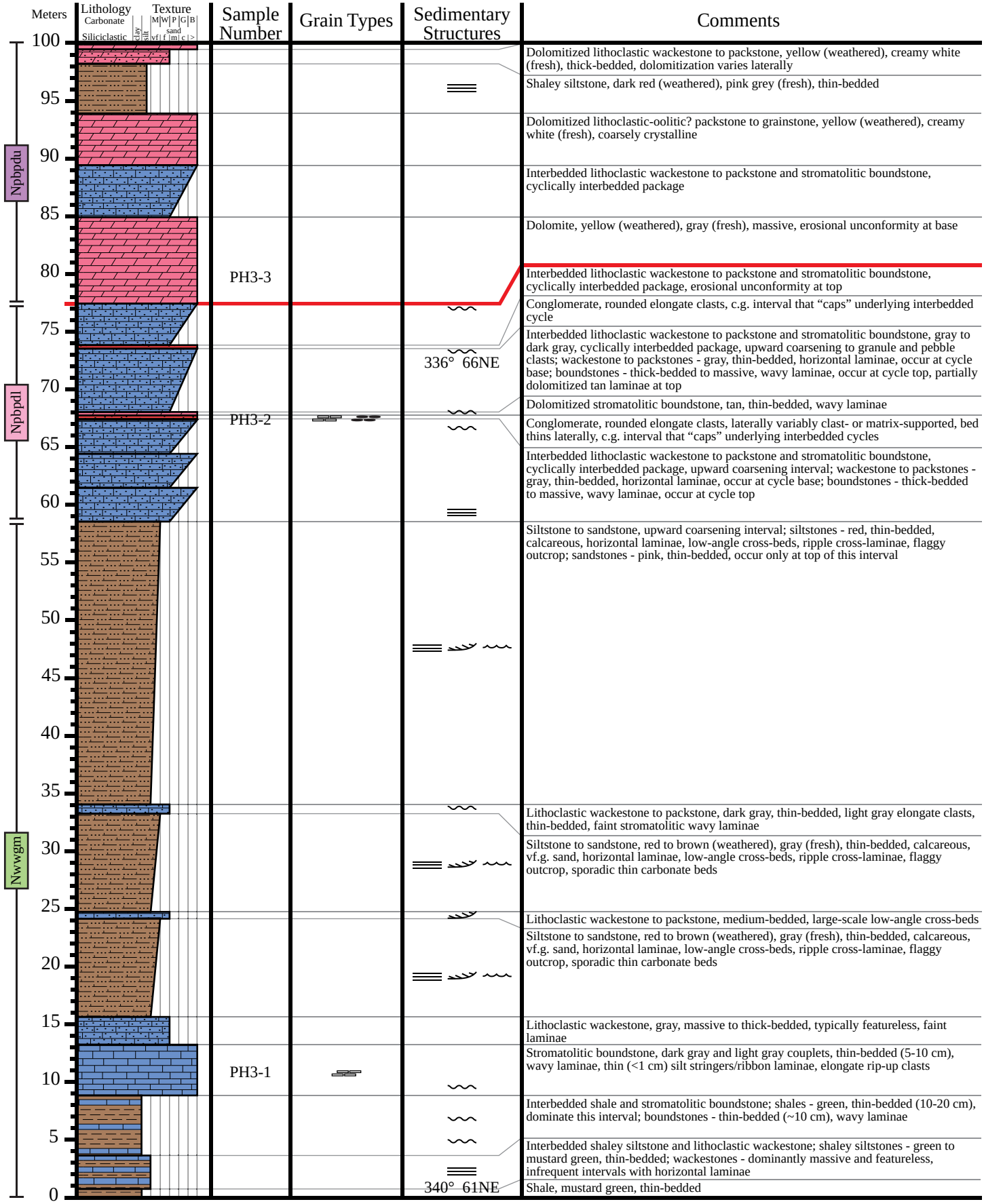

Measured Section 8 (pg. 2)

Start 0276201 6577952
End 0276360 6577990

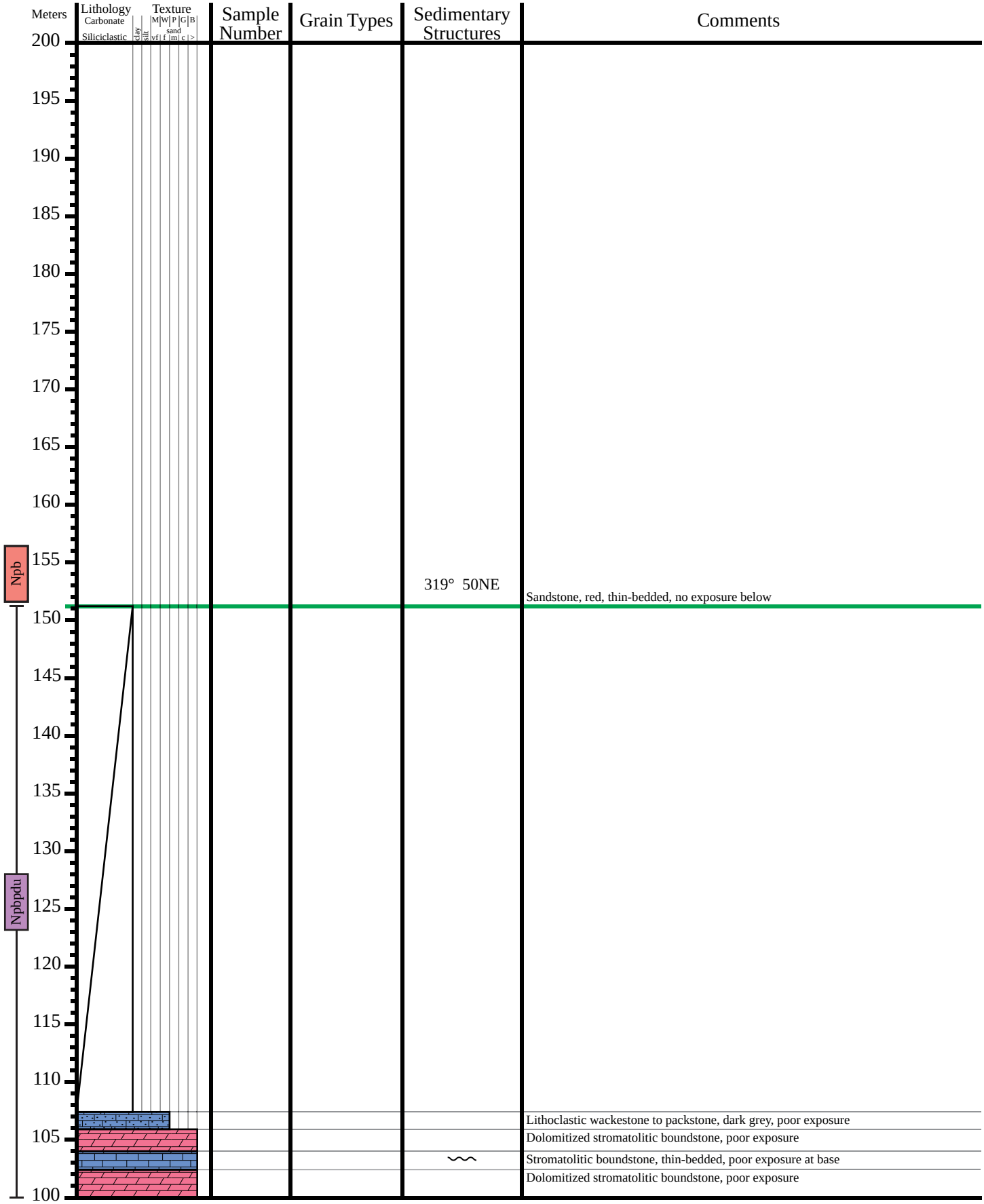

Measured Section 9 (pg. 1)

Start 0275129 6577712
End 0276083 6578533

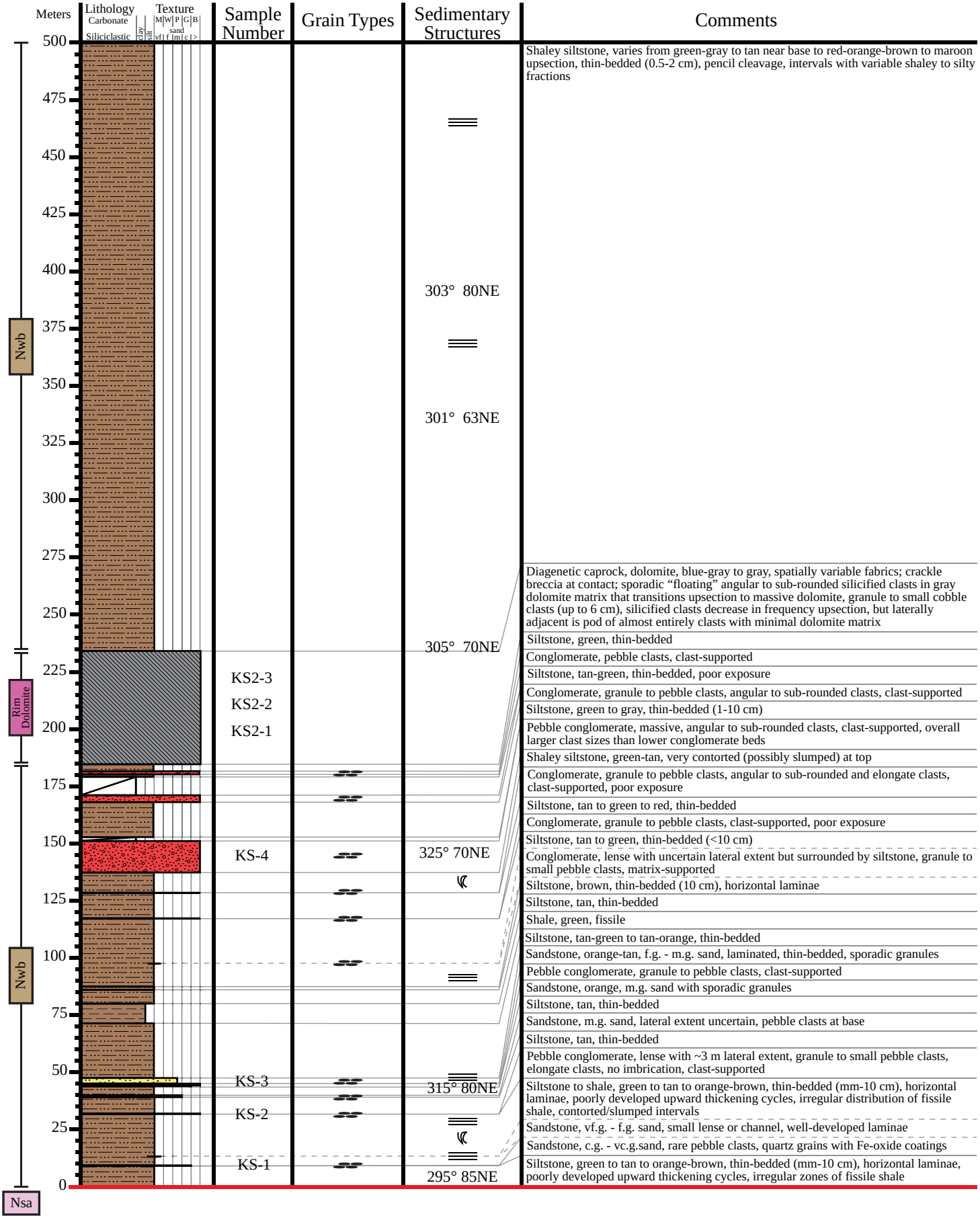

Measured Section 9 (pg. 2)

Start 0275129 6577712
End 0276083 6578533

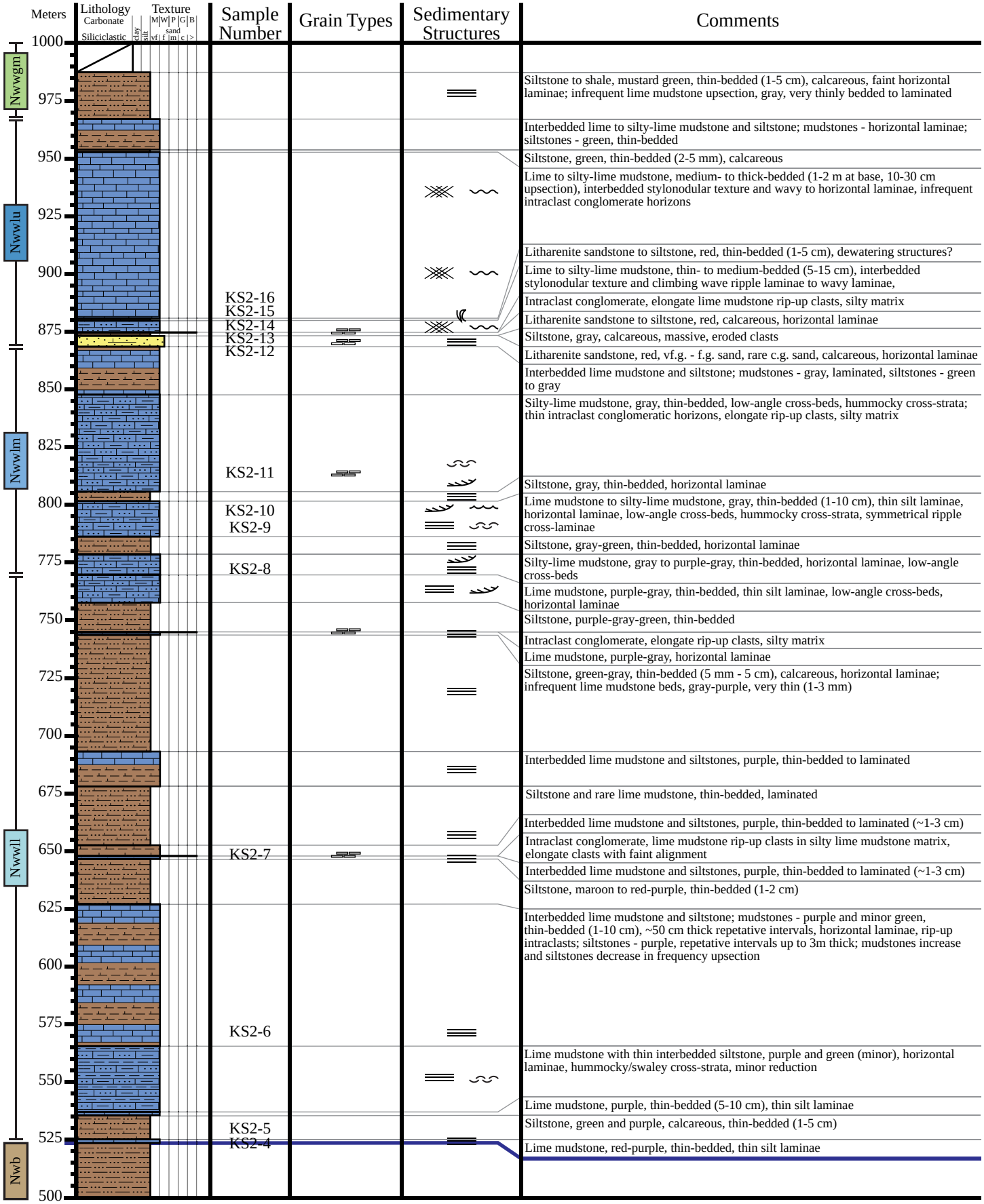

Measured Section 9 (pg. 3)

Start 0275129 6577712
End 0276083 6578533

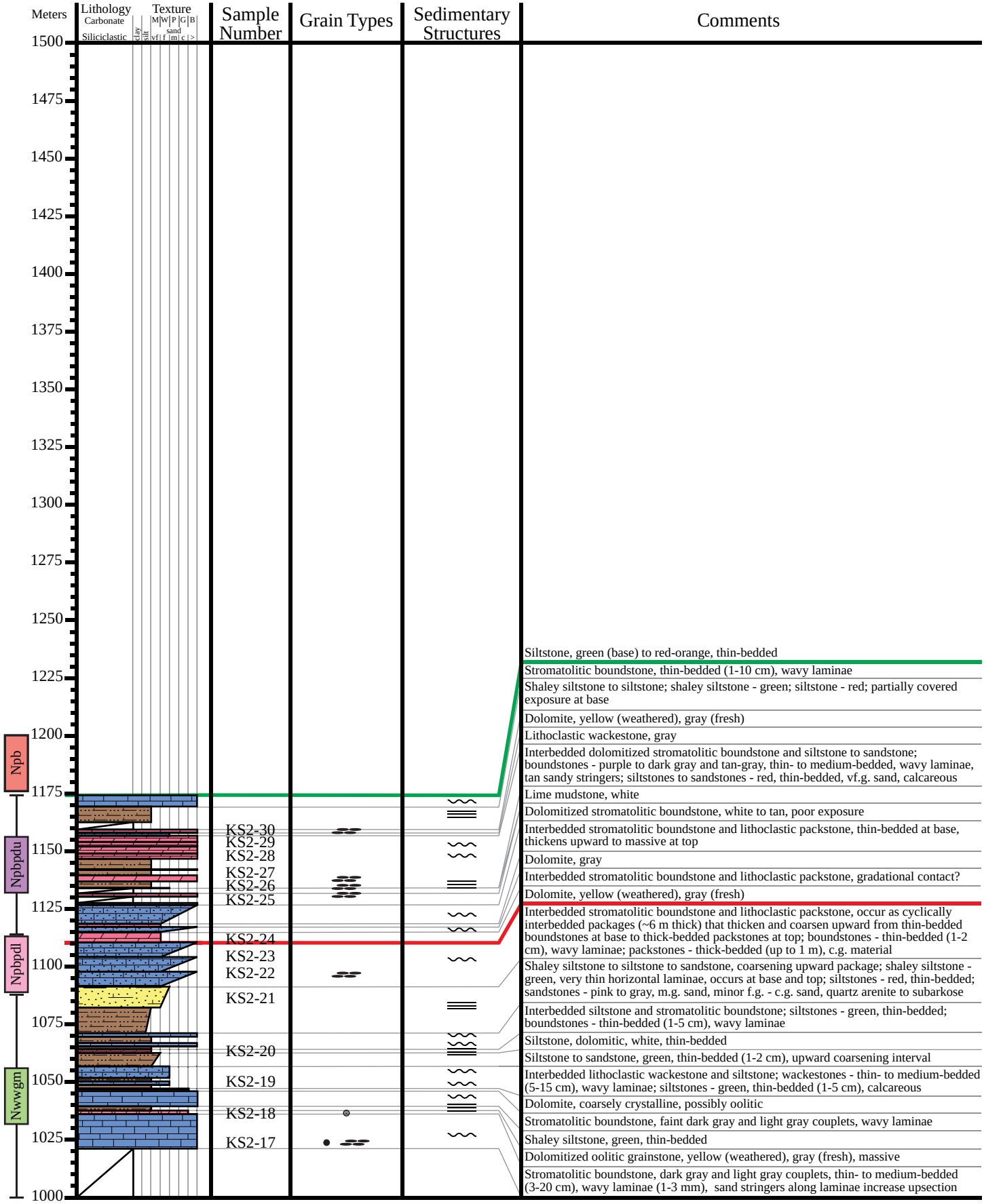

Measured Section 10 (pg. 1)

Start 0275611 6579021
End 0275839 6579160

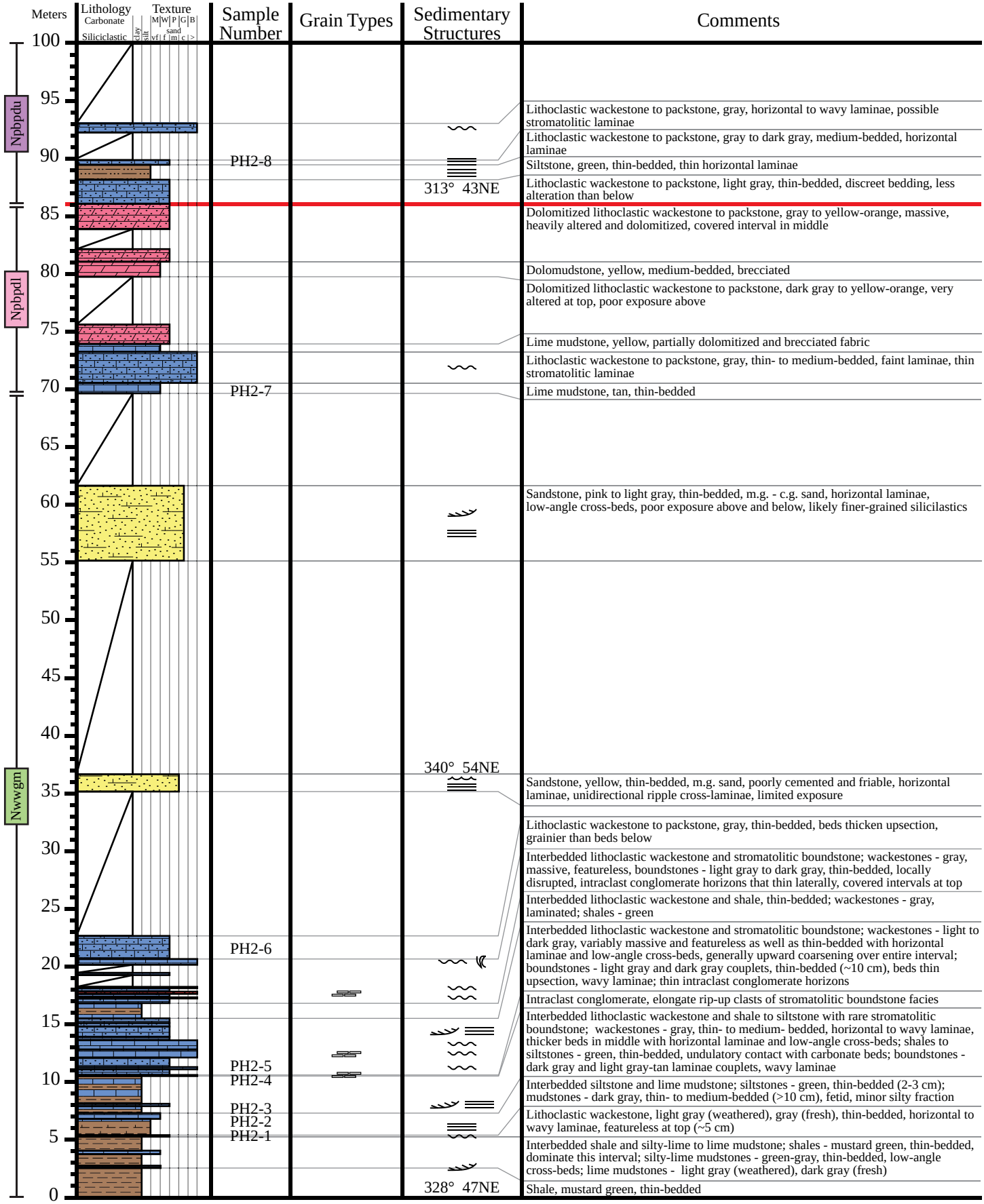

Measured Section 10 (pg. 2)

Start 0275611 6579021
End 0275839 6579160

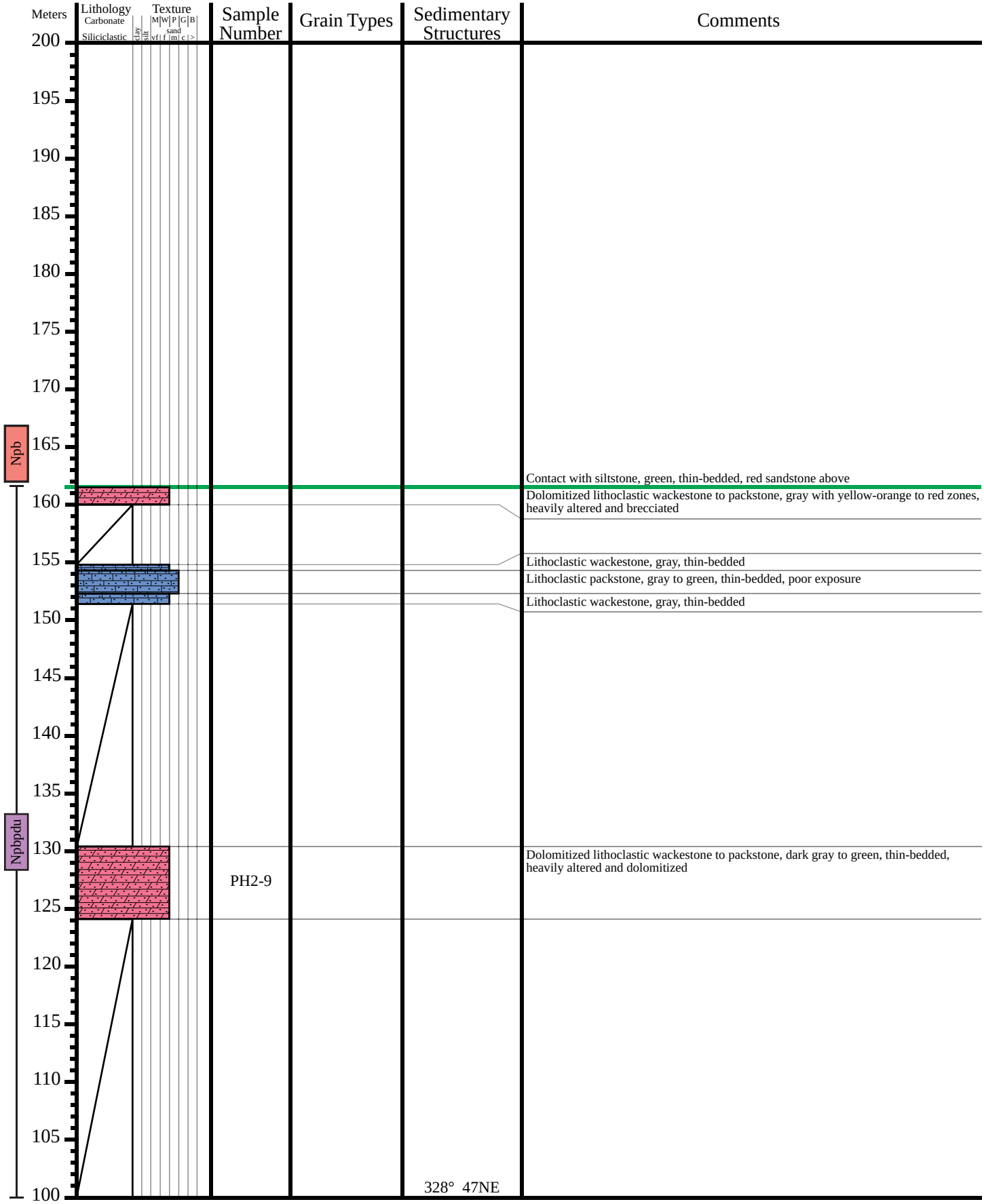

Measured Section 11 (pg. 1)

Start 0275201 6579589
End 0275811 6579349

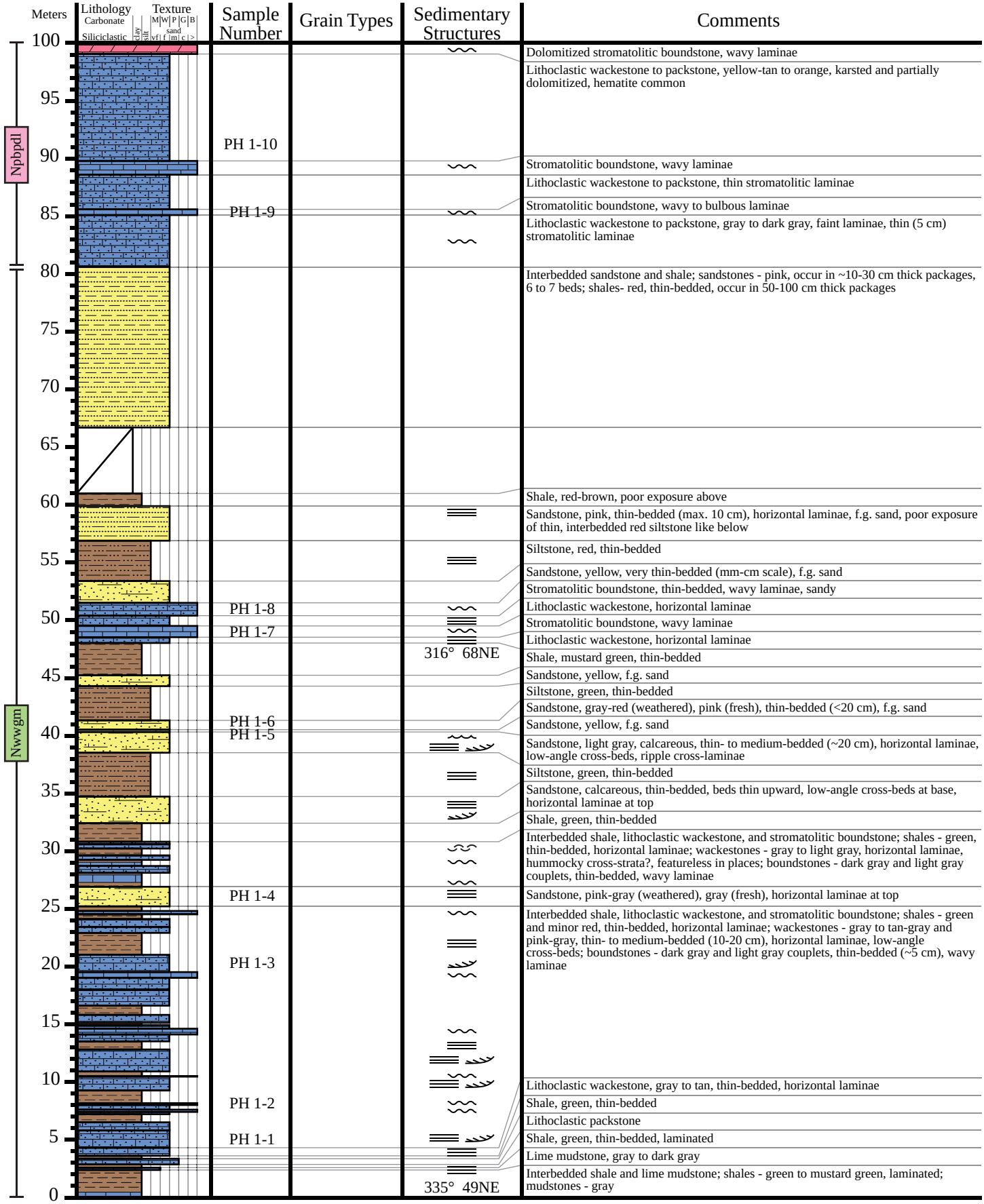

Measured Section 11 (pg. 2)

Start 0275201 6579589
End 0275811 6579349

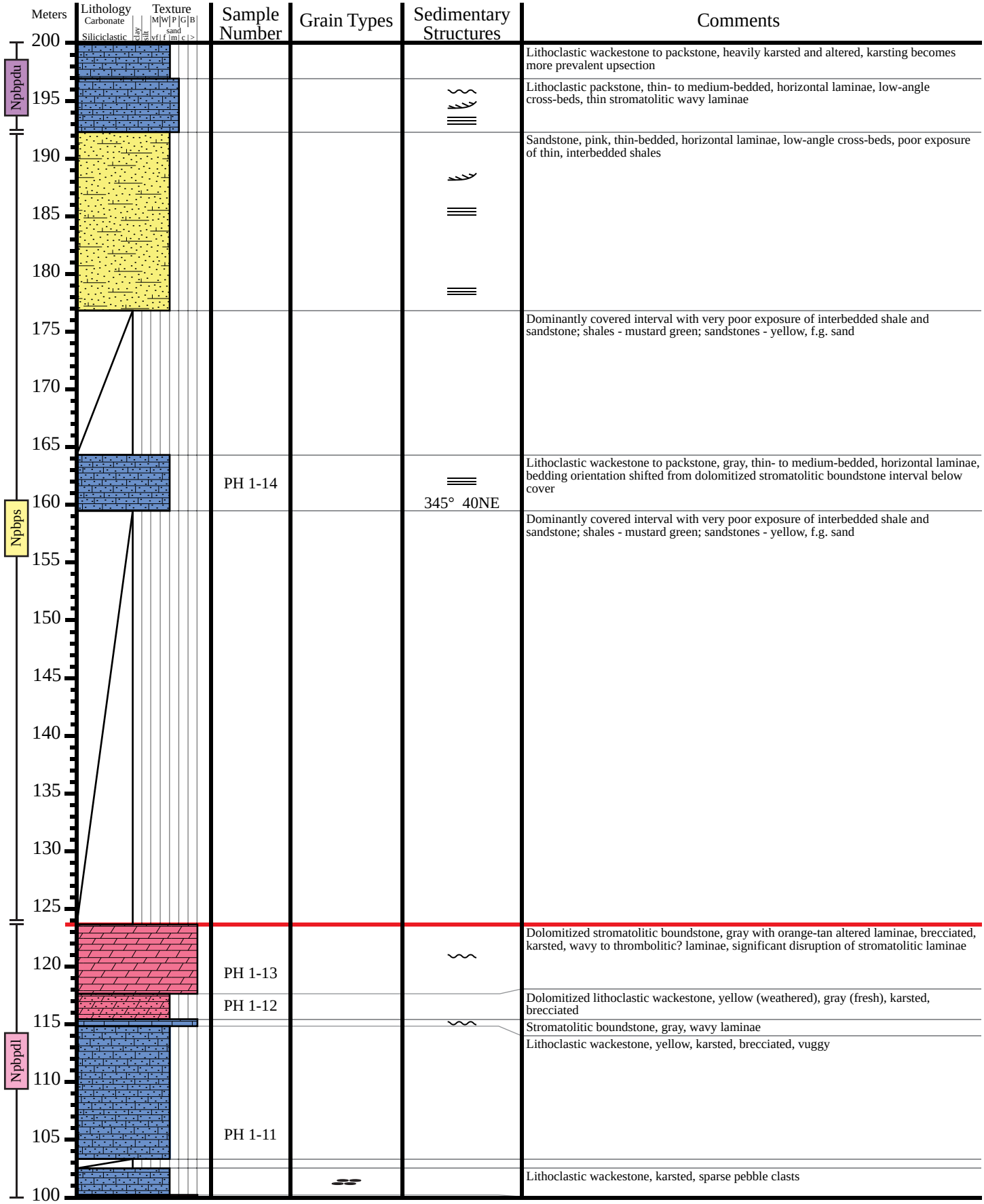

Measured Section 11 (pg. 3)

Start 0275201 6579589
End 0275811 6579349

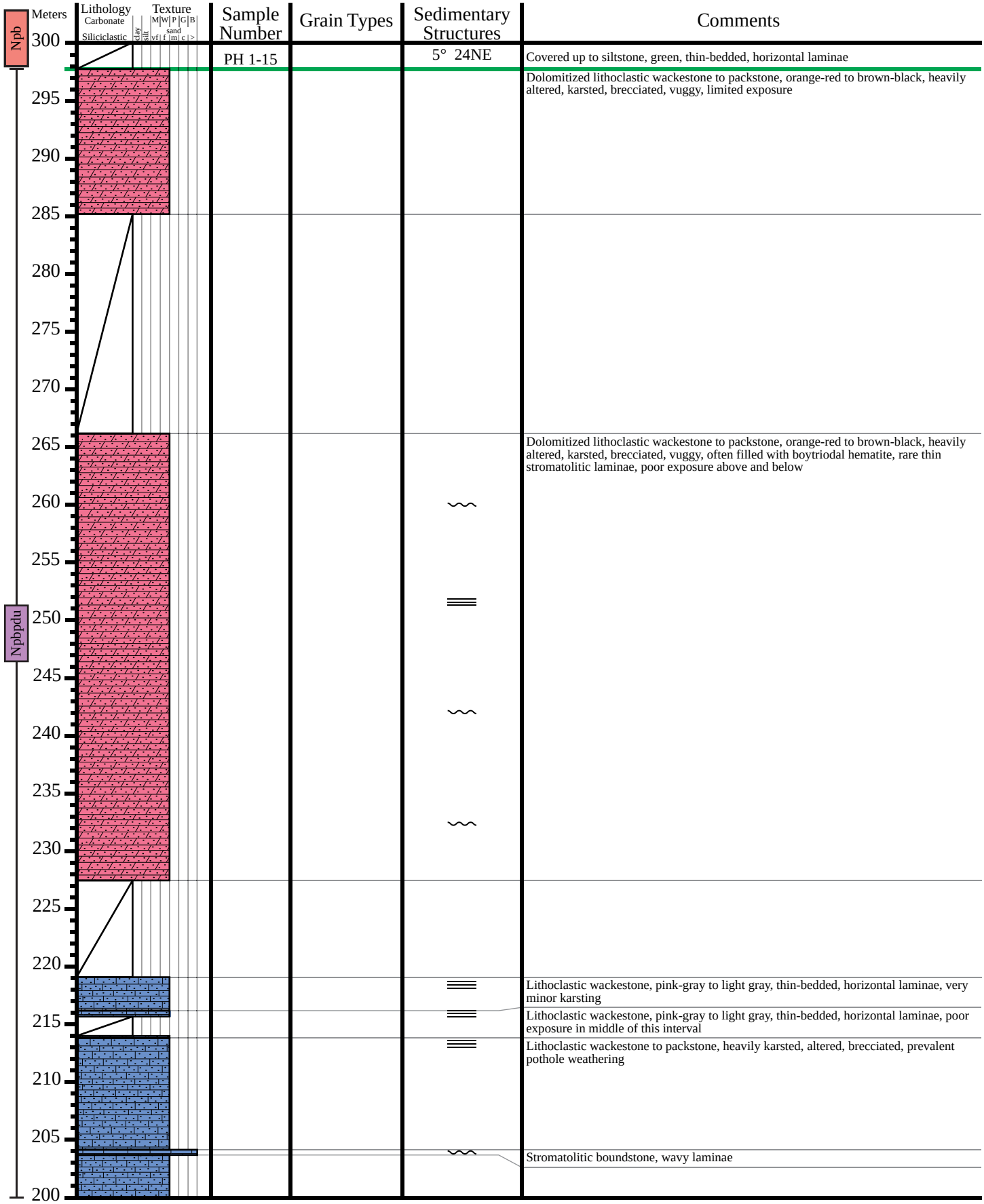

Measured Section 12 (pg. 1)

Start 0271978 6580167
End 0275268 6579946

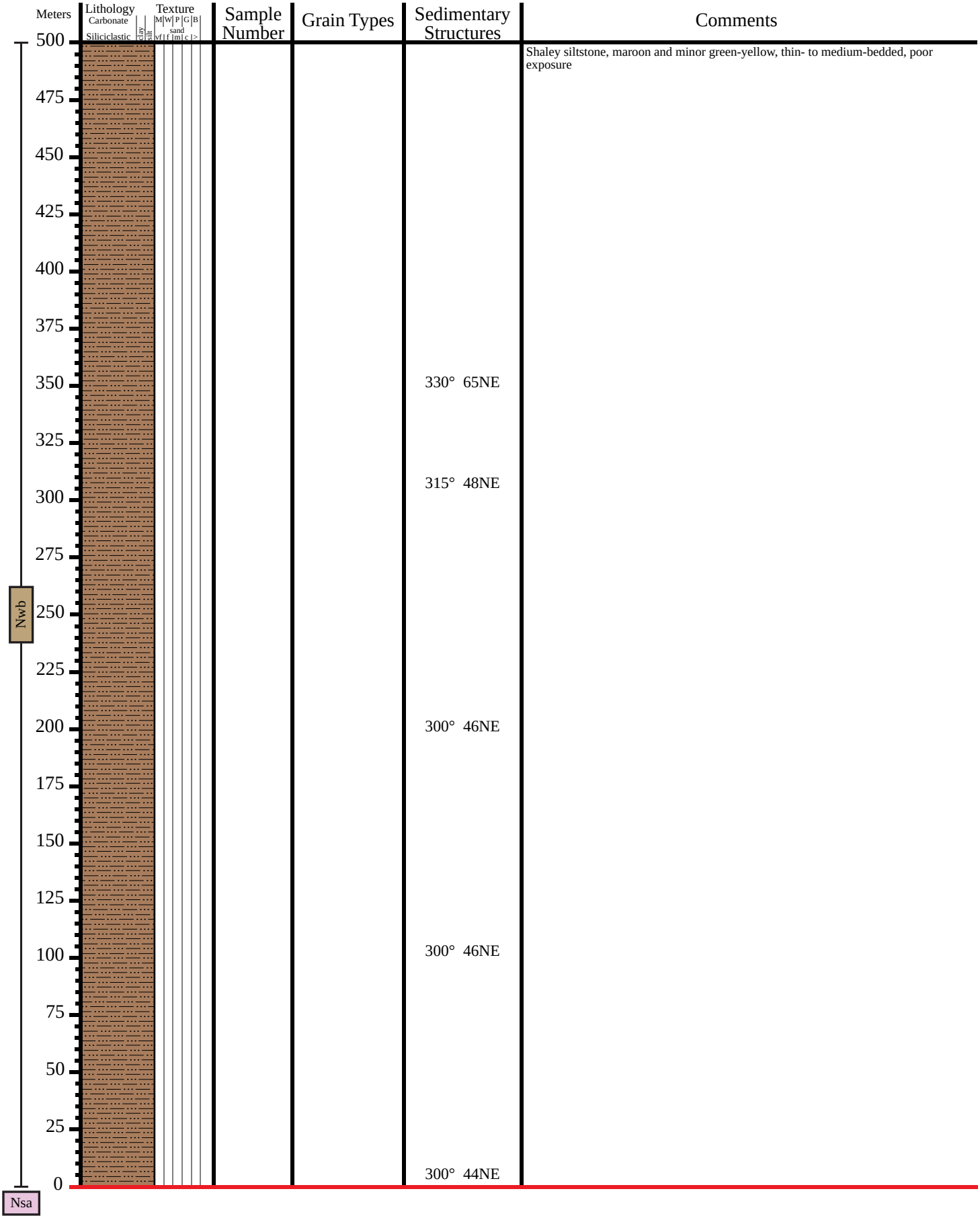

Measured Section 12 (pg. 2)

Start 0271978 6580167
End 0275268 6579946

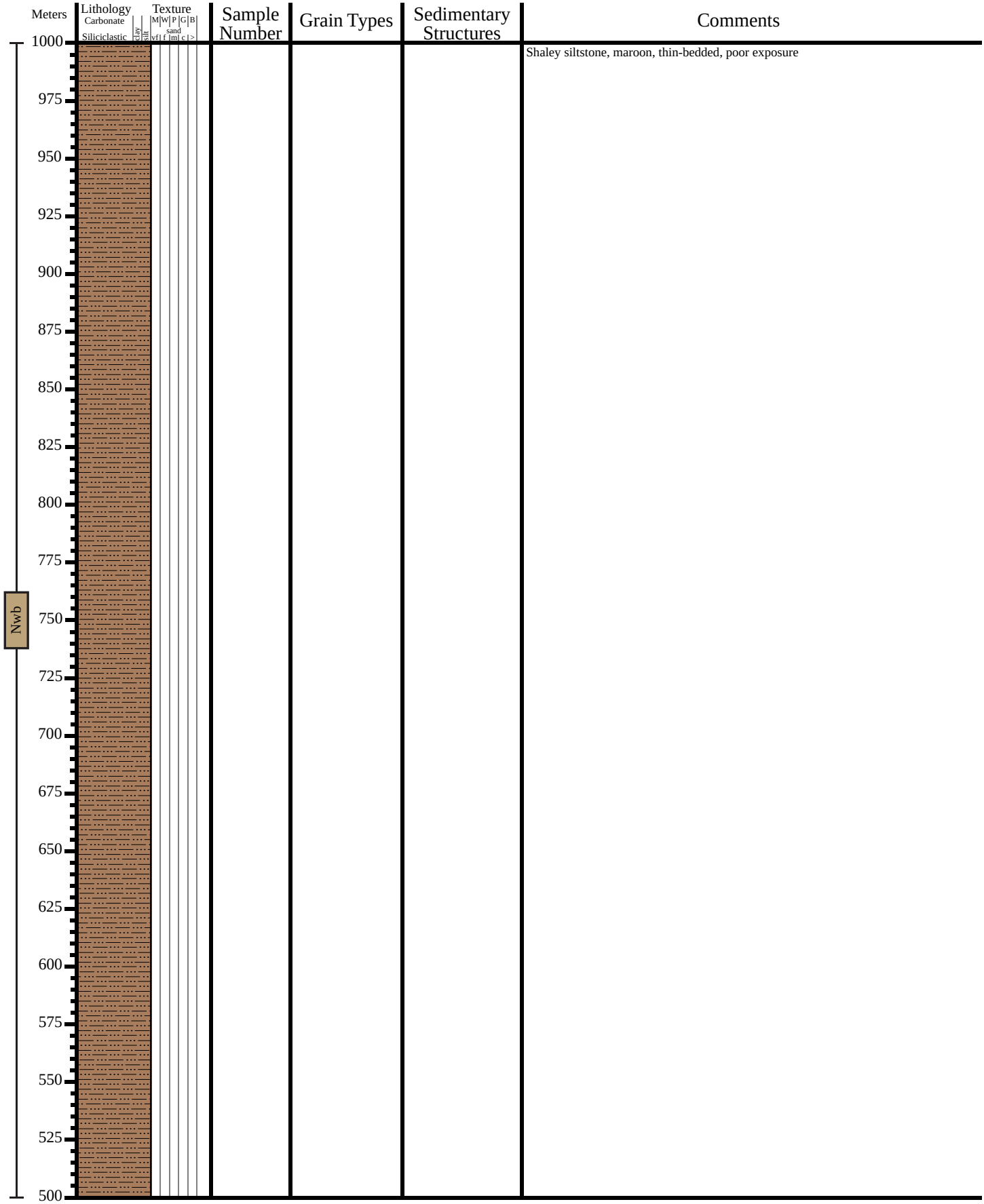

Sample Number	Grain Types	Sedimentary Structures	Comments
			Shaley siltstone, maroon, thin-bedded, poor exposure

Measured Section 12 (pg. 3)

Start 0271978 6580167
End 0275268 6579946

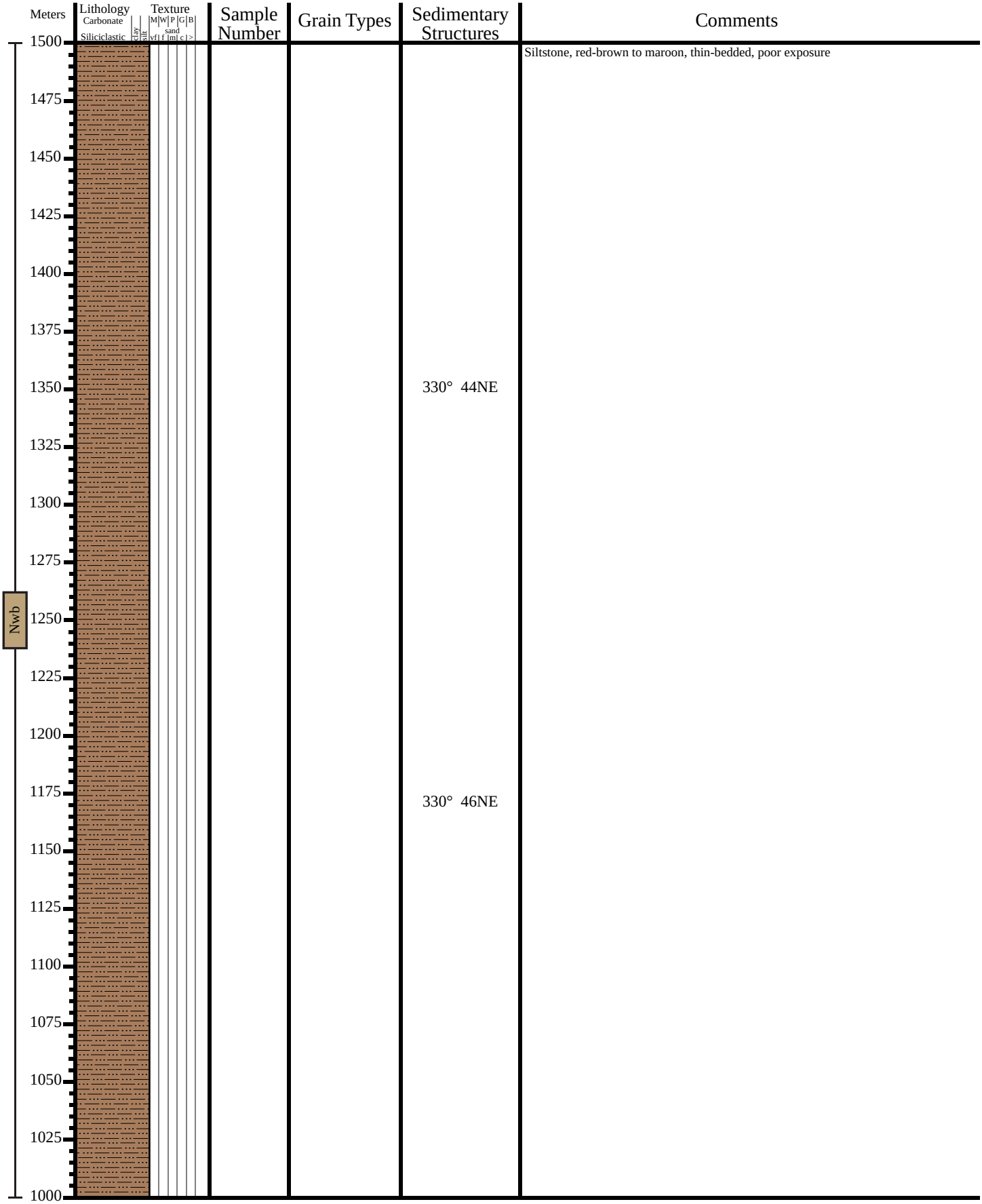

Measured Section 12 (pg. 4)

Start 0271978 6580167
End 0275268 6579946

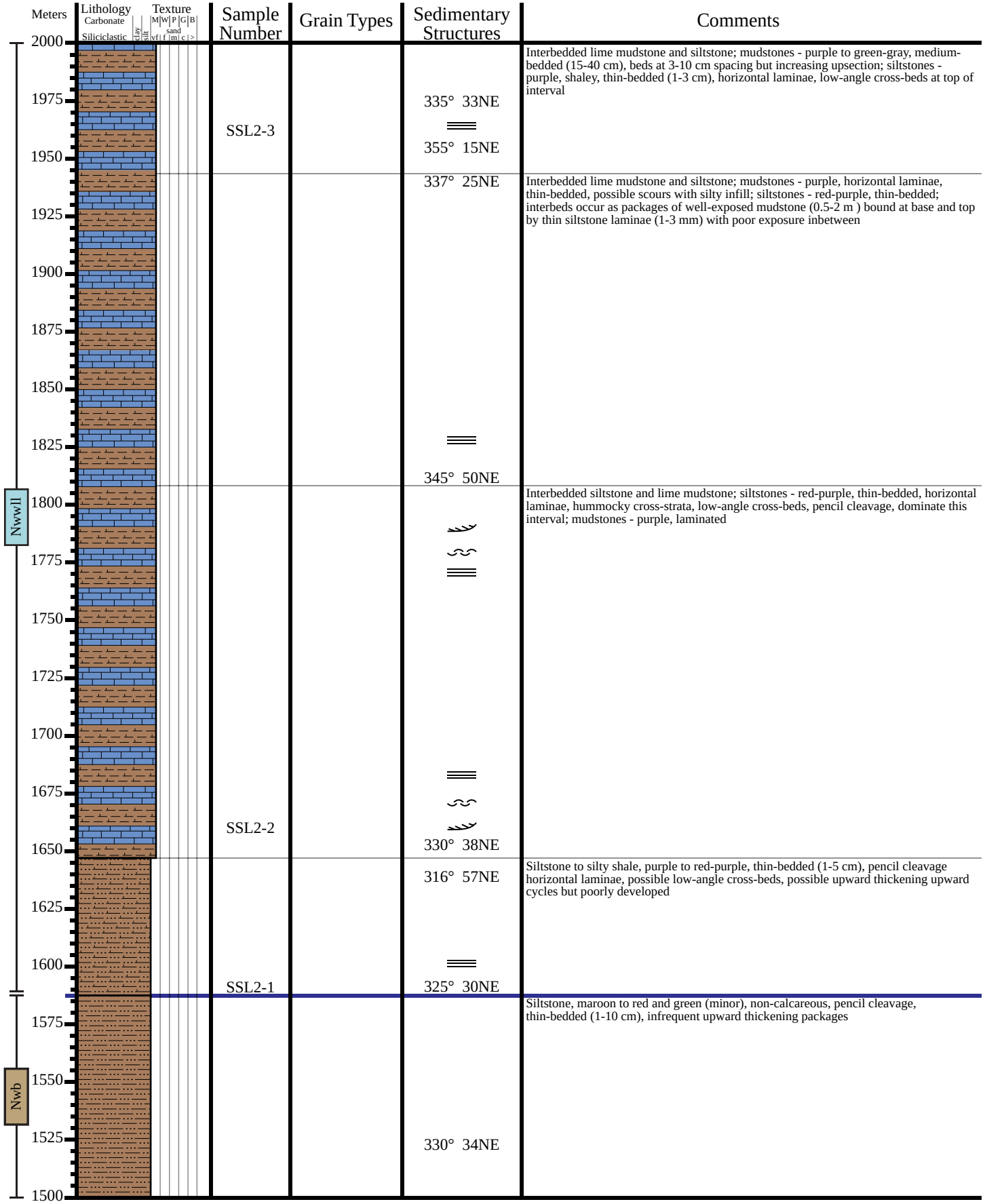

Measured Section 12 (pg. 5)

Start 0271978 6580167
End 0275268 6579946

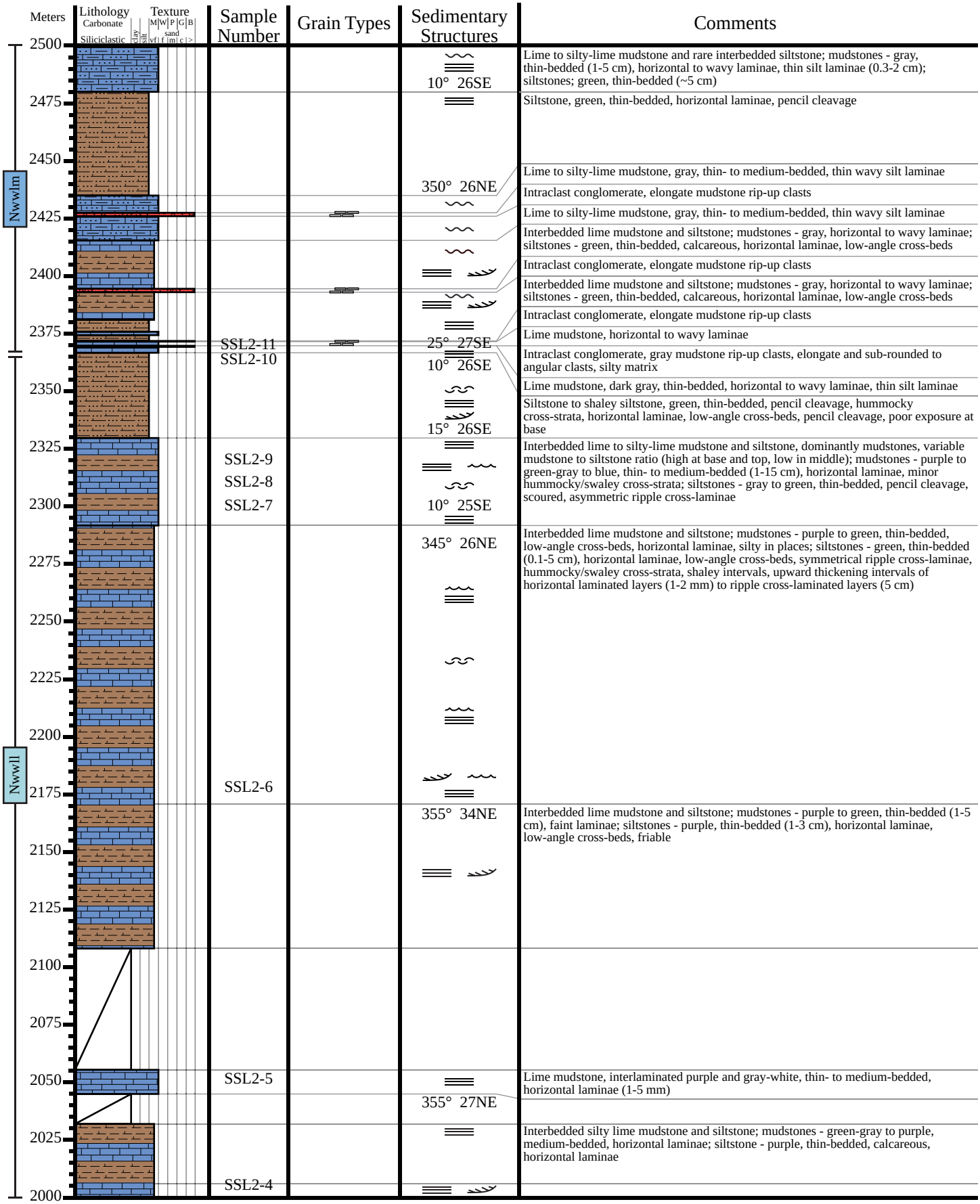

Measured Section 12 (pg. 6)

Start 0271978 6580167
End 0275268 6579946

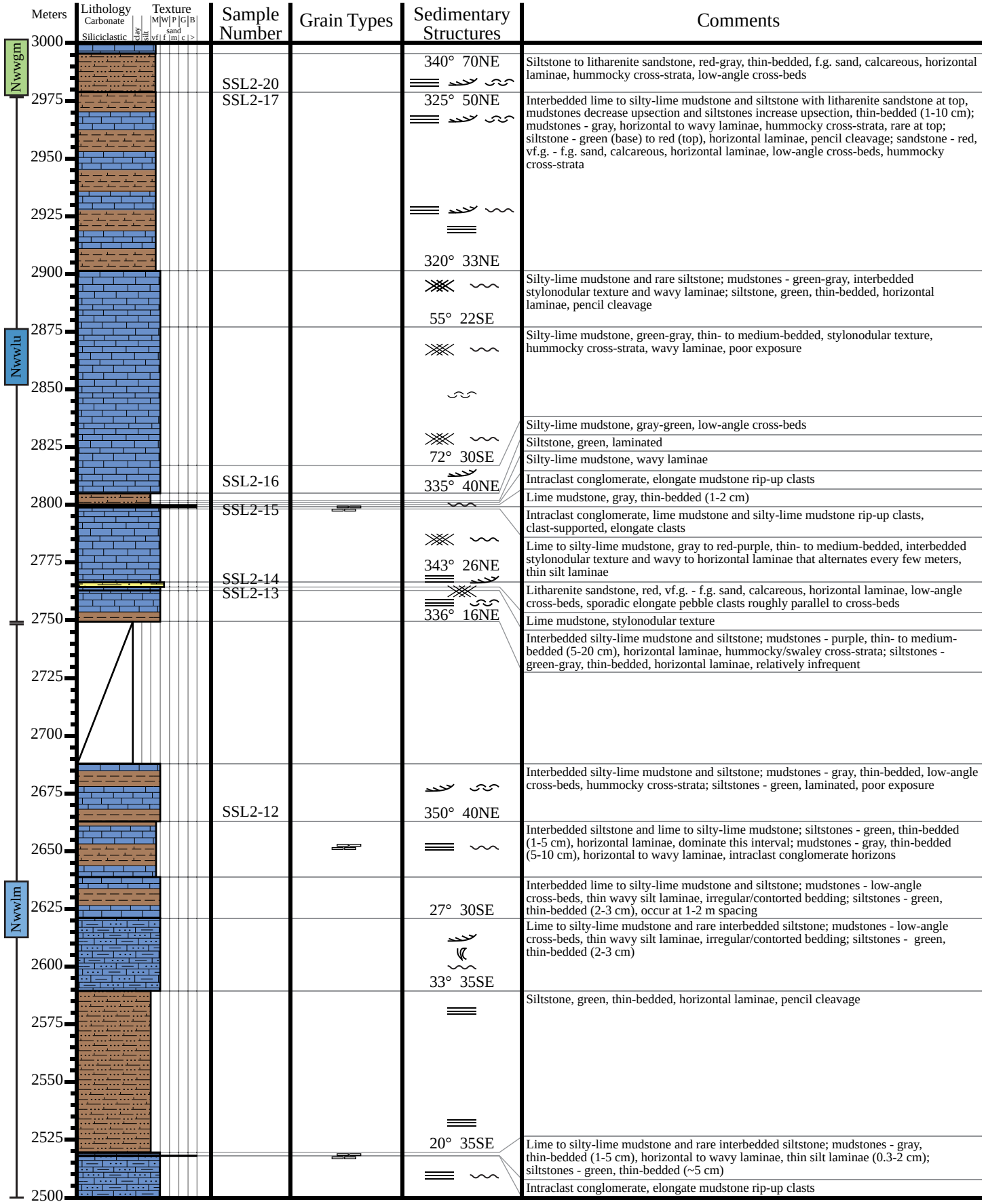

Siltstone to litharenite sandstone, red-gray, thin-bedded, f.g. sand, calcareous, horizontal laminae, hummocky cross-strata, low-angle cross-beds

Interbedded lime to silty-lime mudstone and siltstone with litharenite sandstone at top, mudstones decrease upsection and siltstones increase upsection, thin-bedded (1-10 cm); mudstones - gray, horizontal to wavy laminae, hummocky cross-strata, rare at top; siltstone - green (base) to red (top), horizontal laminae, pencil cleavage; sandstone - red, vf.g. - f.g. sand, calcareous, horizontal laminae, low-angle cross-beds, hummocky cross-strata

Silty-lime mudstone and rare siltstone; mudstones - green-gray, interbedded stylonodular texture and wavy laminae; siltstone, green, thin-bedded, horizontal laminae, pencil cleavage

Silty-lime mudstone, green-gray, thin- to medium-bedded, stylonodular texture, hummocky cross-strata, wavy laminae, poor exposure

Silty-lime mudstone, gray-green, low-angle cross-beds

Siltstone, green, laminated

Silty-lime mudstone, wavy laminae

Intraclast conglomerate, elongate mudstone rip-up clasts

Lime mudstone, gray, thin-bedded (1-2 cm)

Intraclast conglomerate, lime mudstone and silty-lime mudstone rip-up clasts, clast-supported, elongate clasts

Lime to silty-lime mudstone, gray to red-purple, thin- to medium-bedded, interbedded stylonodular texture and wavy to horizontal laminae that alternates every few meters, thin silt laminae

Litharenite sandstone, red, vf.g. - f.g. sand, calcareous, horizontal laminae, low-angle cross-beds, sporadic elongate pebble clasts roughly parallel to cross-beds

Lime mudstone, stylonodular texture

Interbedded silty-lime mudstone and siltstone; mudstones - purple, thin- to medium-bedded (5-20 cm), horizontal laminae, hummocky/swaley cross-strata; siltstones - green-gray, thin-bedded, horizontal laminae, relatively infrequent

Interbedded silty-lime mudstone and siltstone; mudstones - gray, thin-bedded, low-angle cross-beds, hummocky cross-strata; siltstones - green, laminated, poor exposure

Interbedded siltstone and lime to silty-lime mudstone; siltstones - green, thin-bedded (1-5 cm), horizontal laminae, dominate this interval; mudstones - gray, thin-bedded (5-10 cm), horizontal to wavy laminae, intraclast conglomerate horizons

Interbedded lime to silty-lime mudstone and siltstone; mudstones - low-angle cross-beds, thin wavy silt laminae, irregular/contorted bedding; siltstones - green, thin-bedded (2-3 cm), occur at 1-2 m spacing

Lime to silty-lime mudstone and rare interbedded siltstone; mudstones - low-angle cross-beds, thin wavy silt laminae, irregular/contorted bedding; siltstones - green, thin-bedded (2-3 cm)

Siltstone, green, thin-bedded, horizontal laminae, pencil cleavage

Lime to silty-lime mudstone and rare interbedded siltstone; mudstones - gray, thin-bedded (1-5 cm), horizontal to wavy laminae, thin silt laminae (0.3-2 cm); siltstones - green, thin-bedded (~5 cm)

Intraclast conglomerate, elongate mudstone rip-up clasts

Measured Section 12 (pg. 7)

Start 0271978 6580167
End 0275268 6579946

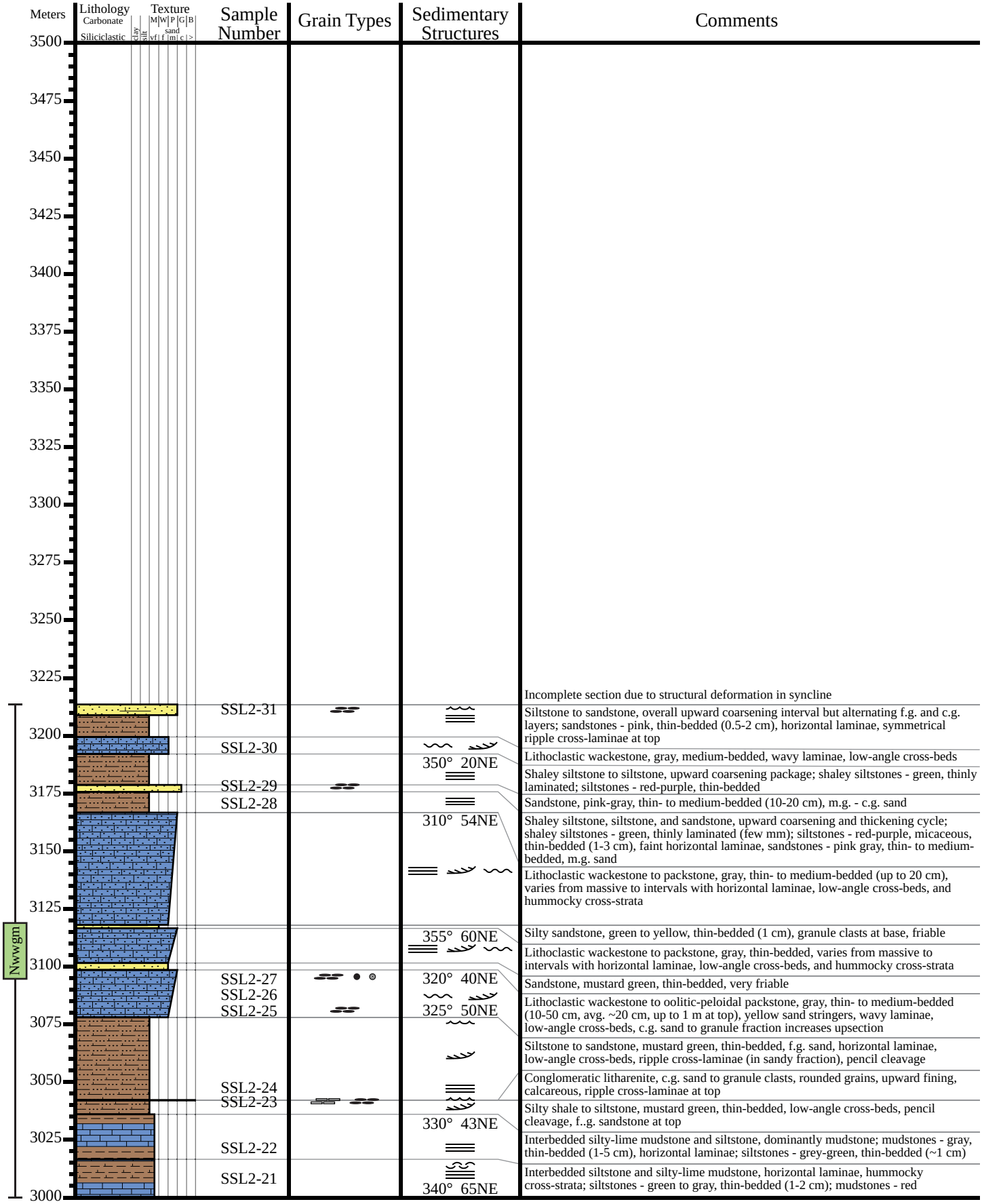

Appendix B

Petrographic analysis of depositional facies in the suprasalt minibasin at Patawarta diapir detailing sample lithology, grain type and abundance, matrix percentage, cements, diagenetic fabrics, and sedimentary structures. Map units and colors reference explanation from Plate 1. All sample locations are indicated on measured stratigraphic sections (Appendix A).

Petrography Chart Explanations

Grain Abundance


0-10%


10-50%


50-90%


90-100%

Matrix


0-10%


10-50%


50-90%


90-100%

Cements

f = fracture

ff = fenestral fabric

Fe = iron-rich

Table 1. Petrographic analysis of depositional facies in the Bunyeroo Formation from the suprasalt minibasin adjacent to Patawarta diapir.

SAMPLE NO.	MAP UNIT	LITHOLOGY	GRAIN TYPES																				MATRIX	CEMENT																	DIAGENETIC FABRIC										SEDIMENTARY STRUCTURES									NOTES
																								Calcite																															
			Calcite	Dolomite	Quartz	Feldspars	Muscovite	Opaques	Fe-oxides	Clays	Cyanobacteria	Ooid	Peloid	Intraclast	Extraclast	Siltstone	Chert	Quartzite+sandstone	Strained/fused quartz	Shale	Meta-igneous	Silicified CO3 (caprock?)		Fibrous	Bladed	Equant	Blocky	Isopachous	Meniscus	Overgrowth	Poikalotopic	Dolomite	Quartz	Chalcedony	Chert	Hematite	Cementation	Micritization	Recrystallization	Replacement	Authigenic crystal growth	Compaction	Dissolution	Dolomitization	Horizontal laminae	Low-angle cross-beds	Hummocky cross-strata	Ripple cross-laminae	Stylonodular texture	Wavy bedding	Fenestral fabric	Mudcracks	
KS-4	Nwb	Pebble conglomerate																										f?																													Pebble clasts >20mm, clast-supported, elongate/tabular clasts, minor sand+shale matrix, dominantly shale clasts
KS-3	Nwb	Pebble conglomerate																										?																													Pebble clasts 15mm max, rounded, elongate/tabular clasts, some ovoid, clast-supported with minor sand+shale matrix
KS-2	Nwb	Pebble conglomerate															?					?																																			Pebble clasts 10mm max, rounded, elongate/tabular clasts, clast-supported, dominantly siltstone clasts
KS-1	Nwb	Sandstone (c.g-vc.g)																																																						Rounded, moderately well-sorted, some early quartz overgrowth cements, but primarily Fe-oxide cements, irregular grain boundaries

Table 2. Petrographic analysis of depositional facies in the Wonoka Formation from the suprasalt minibasin adjacent to Patawarta diapir.

SAMPLE NO.	MAP UNIT	LITHOLOGY	GRAIN TYPES																				MATRIX	CEMENT													DIAGENETIC FABRIC								SEDIMENTARY STRUCTURES								NOTES
																								Calcite																													
			Calcite	Dolomite	Quartz	Feldspars	Muscovite	Opaque minerals	Fe-oxides	Clays	Cyanobacteria	Ooid	Peloid	Intraclast	Extraclast	Siltstone	Chert	Quartzite+sandstone	Strained/fused quartz	Shale	Meta-igneous	Silicified CO3 (caprock?)		Fibrous	Bladed	Equant	Blocky	Isopachous	Meniscus	Overgrowth	Poikalotopic	Dolomite	Quartz	Chalcedony	Chert	Hematite	Cementation	Micritization	Recrystallization	Replacement	Authigenic crystal growth	Compaction	Dissolution	Dolomitization	Horizontal laminae	Low-angle cross-beds	Hummocky cross-strata	Ripple cross-laminae	Stylonodular texture	Wavy bedding	Fenestral fabric	Mudcracks	
SSL2-31	Nwwgm	Sublitharenite (calcareous)																																										p									Vf.g-m.g sand with some silt and c.g. sand, poorly sorted, angular to sub-rounded, partially dolomitized, cyanobacterial?
SSL2-30	Nwwgm	Lithoclastic wackestone (silty)																																										p									Silt, angular-subangular, stylolites
SSL2-29	Nwwgm	Quartz arenite to subarkose (m.g-c.g.)																																																			Dominantly m.g-c.g. sand, minor f.g. component, sub-rounded to rounded, moderately-well sorted, quartz overgrowth cements
SSL2-28	Nwwgm	Micaceous siltstone																																																			Silt - vf.g. sand, angular to sub-angular, non-calcareous, elongate clay and mica-rich seams
SSL2-27	Nwwgm	Oolitic-peloidal packstone																																										p									Variety of ooid types (ooids, superficial, composite, deformed), cores of c.g. dolomite spar, m.g. calcite spar, or extraclasts
SSL2-26	Nwwgm	Lithoclastic- peloidal? wackestone (silty)																							f	f																										Dominantly f.g.-m.g. silt, minor c.g. sand fraction of authigenic quartz and feldspar, patchy micrite vs. spar - peloids
SSL2-25	Nwwgm	Lithoclastic wackestone (silty to sandy)																							f	f									f																	Sub-angular silt, sub-rounded m.g.- c.g. sand, silt=quartz, sand=quartz, feldspar, lithics, matrix entirely recrystallized to calcite spar
SSL2-24	Nwwgm	Calcareous siltstone																							f	f																										M.g. -c.g. silt
SSL2-23	Nwwgm	Calcareous conglomeratic litharenite																																																		Polymict, c.g. sand-granule, sub-angular
SSL2-22	Nwwgm	Silty-lime mudstone																																										p									Alternating laminae of dense micrite mud and microspar
SSL2-21	Nwwgm	Silty-lime mudstone																																										p								?	Matrix recrystallized to calcite microspar, f.g. silt, dolomitization along silt-rich laminae
SSL2-19	Nwwgm	Silty-lime mudstone																							f	f																		p									M.g. silt, possibly graded, dolomitized matrix?
SSL2-20	Nwwlu	Litharenite																																																			Sub-angular to sub-rounded, f.g. coarse calcite grains (recrystallized lime mudstone), distinct black matrix - hematite?
SSL2-18	Nwwlu	Lime mudstone & siltstone (cyanobacterial?)									?																																	p									Laminae of dense, dark micrite vs. c.g. spar with quartz silt, cyanobacterial?
SSL2-17	Nwwlu	Litharenite																							f	f																										Graded, sub-rounded, vf.g.-f.g. coarse calcite spar grains (recrystallized lime mudstone), f.g. quartz sand
SSL2-16	Nwwlu	Silty-lime mudstone																							f	f																		p									F.g. silt, dolomitization concentrated in silt-rich laminae
SSL2-15	Nwwlu	Intraclast conglomerate																																								?											Heterogenous clast size, intraclasts (lime mudstone dominantly, silty lime mudstone)
SSL2-14	Nwwlu	Litharenite																																																			Sub-rounded, vf.g.-f.g. grains of recrystallized calcite lime mudstone, silt-f.g. sand grains of quartz and feldspars
SSL2-13	Nwwlu	Lime mudstone																																								?	?	p									Silt and clays isolated to stylonodular meshwork
SSL2-12	Nwwlm	Silty-lime mudstone																																										p									Patchy recrystallization of mud to microspar, f.g. silt
SSL2-11	Nwwll	Intraclast conglomerate																																								?											Clast-supported, intraclasts (lime mudstone, silty lime mudstone)
SSL2-10	Nwwll	Lime mudstone																																										p									Minor silt laminae, dolomitization only along silt laminae
SSL2-9	Nwwll	Silty-lime mudstone & calcareous siltstone																																										p									Irregular laminae, thin interbeds, calciturbidite
SSL2-8	Nwwll	Calcareous siltstone																																																			Micaceous, f.g. silt, Fe-rich calcite cement
SSL2-7	Nwwll	Lime mudstone																																										p									Calcite mud, dolomitization on silt laminae
SSL2-6	Nwwll	Lime mudstone																																										p									Silty, micaceous
SSL2-5	Nwwll	Lime mudstone																																										p									Micaceous, graded, calciturbidite
SSL2-4	Nwwll	Calcareous siltstone & silty-lime mudstone																																										m									Calciturbidite
SSL2-3	Nwwll	Lime mudstone																							f	f									f																	Faint laminae, micaceous
SSL2-2	Nwwll	Lime mudstone																																										m									Silt along laminae
SSL2-1	Nwwll	Micaceous siltstone																																										m									Non-calcareous, iron staining
SSL1-3	Nwwll	Lime mudstone																							f	f									?								p									Calciturbidite, micaceous
SSL1-2	Nwwll	Lime mudstone & calcareous siltstone																																	f																	Calciturbidite
SSL1-1	Nwwll	Dolomudstone																																	f																	Patchy distribution of voids filled with calcite spar
KS2-21	Nwwgm	Quartz arenite to subarkose																																?																		Dominantly m.g. sand with f.g.-c.g. component, sub-rounded, poorly sorted, quartz overgrowth cements
KS2-20	Nwwgm	Dolomitized siltstone																																																			Sub-angular c.g. silt, dolomicrite clasts - peloids/intraclast rip-ups
KS2-19	Nwwgm	Lithoclastic-peloidal? wackestone (sandy)																																										p?									Silt - f.g. sand, angular quartz/feldspar, c.g. dolomite grains (diagenetic cores?), irregular/ragged grain edges
KS2-18	Nwwgm	Oolitic grainstone																							Fe	Fe					f				f																	Ooids and superficial ooids, some c.g. saddle dolomite
KS2-17	Nwwgm	Stromatolitic boundstone																																																			Angular to sub-angular silt, wavy cyanobacterial laminae of calcite microspar vs. f.g. spar
KS2-16	Nwwlu	Lime mudstone to silty-lime mudstone																							f	f																?	?	p									Patchy dolomitization
KS2-15	Nwwlu	Silty-lime mudstone																							f	f																		p									Dolomitized only along quartz silt laminae, c.g. fraction primarily authigenic quartz growth
KS2-14	Nwwlu	Intraclast conglomerate																							f	f																										Clast-supported, intraclasts (lime mudstone, silty lime mudstone, heterogenous clast size up to large pebble
KS2-13	Nwwlu	Calcareous siltstone																																																			Angular quartz silt
KS2-12	Nwwlu	Litharenite																																																			Sub-rounded to sub-angular, vf.g.-f.g. calcite grains (recrystallized lime mudstone), heterogenous clast size, rare intraclast, graded
KS2-11	Nwwlm	Silty-lime mudstone																																													?						Erosional scour?
KS2-10	Nwwlm	Silty-lime mudstone																																										m									Dolomitization only along silt-rich laminae
KS2-9	Nwwlm	Lime mudstone																							f	f																		p									Calcite microspar, minor dolomitization of silt-rich laminae, Fe-rich calcite cements
KS2-8	Nwwlm	Silty-lime mudstone																							f	f																		p									Calcite microspar (with dolomite?), Fe-rich calcite cements
KS2-7	Nwwll	Intraclast conglomerate & silty-lime mudstone																																																			Lime mudstone intraclasts, disrupted laminae and convolute bedding, calciturbidite
KS2-6	Nwwll	Lime mudstone																																										p									Calciturbidite, Fe-oxide rich, partially dolomitized
KS2-5	Nwwll	Dolomudstone																							f	f																										Patchy calcite due to dolomitization
KS2-4	Nwwll	Lime mudstone																																										?									Micaceous, recrystallized micrite to microspar

Table 2. Petrographic analysis of depositional facies in the Wonoka Formation from the suprasalt minibasin adjacent to Patawarta diapir.

SAMPLE NO.	MAP UNIT	LITHOLOGY	GRAIN TYPES																				MATRIX	CEMENT																	DIAGENETIC FABRIC										SEDIMENTARY STRUCTURES								NOTES
																								Calcite																																
			Calcite	Dolomite	Quartz	Feldspars	Muscovite	Opaque minerals	Fe-oxides	Clays	Cyanobacteria	Ooid	Peloid	Intraclast	Extraclast	Siltstone	Chert	Quartzite+sandstone	Strained/fused quartz	Shale	Meta-igneous	Silicified CO3 (caprock?)		Fibrous	Bladed	Equant	Blocky	Isopachous	Meniscus	Overgrowth	Poikalotopic	Dolomite	Quartz	Chalcedony	Chert	Hematite	Cementation	Micritization	Recrystallization	Replacement	Authigenic crystal growth	Compaction	Dissolution	Dolomitization	Horizontal laminae	Low-angle cross-beds	Hummocky cross-strata	Ripple cross-laminae	Stylonodular texture	Wavy bedding	Fenestral fabric	Mudcracks	
RC-11	Nwwgm	Calcareous subarkose (vf.g-f.g)																							Fe	Fe						Fe																						Sub-angular to sub-rounded, vf.g - f.g. sand, minor quartz overgrowth cements
RC-10	Nwwgm	Stromatolitic boundstone (dolomitized)																			?																																	Angular/sub-angular, c.g. silt - c.g. sand, up to pebble, cyanobacterial mat with storm events, intraclasts (silty/sandy wackestone)
RC-9	Nwwgm	Lithoclastic wackestone (sandy)																							f	f																													Sand, minor clay seam
RC-8	Nwwgm	Lime mudstone & calcareous siltstone																																																			Angular silt, rare rounded grains up to m.g. sand, interlaminated mudstone and calcareous siltstone
RC-7	Nwwlu	Litharenite conglomeratic sandstone																																																			Silt to granule clasts, angular to sub-angular extraclasts, rounded intraclasts (lime mudstone, dolomudstone, c.g. Fe-dolomite)
RC-6	Nwwlu	Lime mudstone																							f	f																													p		
RC-5	Nwwlu	Intraclast conglomerate																																																			Clast-supported, small pebble-granule, intraclasts (lime mudstone, silty lime mudstone), clay matrix
RC-4	Nwwlu	Lime mudstone																																																			Minor authigenic quartz growth, insolubles along stylonodular mesh
RC-3	Nwwlm	Silty-lime mudstone to calcareous siltstone																																																			Isolated "stringers" of opaques
RC-2	Nwwlm	Lime mudstone																																																			Minor dolomitization
CP 2-2	Nwwlm	Silty-lime mudstone																							f	f																													p		Angular f.g. silt
CP 2-1	Nwwlm	Calcareous siltstone & dolomudstone																							f	f								?																				Interlaminated dolomite microspar/spar + Fe oxide-cemented quartz silt, thin zones with calcite cement, irregular laminae

Table 3. Petrographic analysis of depositional facies in the Patsy Hill Member of the Bonney Sandstone from the suprasalt minibasin adjacent to Patawarta diapir.

SAMPLE NO.	MAP UNIT	LITHOLOGY	GRAIN TYPES: Calcite	Dolomite	Quartz	Feldspars	Muscovite	Opaque minerals	Fe-oxides	Clays	Cyanobacteria	Ooid	Peloid	Intraclast	Extraclast	Siltstone	Chert	Quartzite+sandstone	Strained/fused quartz	Shale	Meta-igneous	Silicified CO3 (caprock?)	MATRIX	CEMENT: Calcite: Fibrous	Bladed	Equant	Blocky	Isopachous	Meniscus	Overgrowth	Poikalotopic	Dolomite	Quartz	Chalcedony	Chert	Hematite	DIAGENETIC FABRIC: Cementation	Micritization	Recrystallization	Replacement	Authigenic crystal growth	Compaction	Dissolution	Dolomitization	SEDIMENTARY STRUCTURES: Horizontal laminae	Low-angle cross-beds	Hummocky cross-strata	Ripple cross-laminae	Stylonodular texture	Wavy bedding	Fenestral fabric	Mudcracks	NOTES
KS2-30	Npbpdu	Stromatolitic boundstone (dolomitized)																																															?		Cyanobacterial mat with storm events, peloid clusters /grapestones
KS2-29	Npbpdu	Stromatolitic boundstone (dolomitized)																								f	f																	p						?		Very irregular thin laminae, f.g. silt fraction, possible ooid
KS2-28	Npbpdu	Stromatolitic boundstone (dolomitized)																								f	f						Fe										p	?							Quartz silt , isolated zone of dolomitization at top and bottom, heavily fractured
KS2-27	Npbpdu	Stromatolitic boundstone (dolomitized)																																									p								Angular silt, up to m.g. sand, very irregular laminae, possibly rip-up clasts
KS2-26	Npbpdu	Calcareous siltstone - sandstone (vf.g.)																																																	Angular to sub-angular silt to vf.g. sand, rounded/ovoid dolomicrite clasts, thin dolomite rim cements?
KS2-25	Npbpdu	Stromatolitic boundstone (dolomitized)									?															f	f						Fe	f																	Fe-dolomite with zoning, heavily fractured
KS2-24	Npbpdu	Dolomudstone																								f	f						Fe				?															Possible faint peloidal fabric, coarse-grained Fe-dolomite fills fractures
KS2-23	Npbpdl	Stromatolitic boundstone (dolomitized)																								f	f																	p								Angular to sub-angular quartz silt, silt-rich laminae dolomitized, calcite grains with dolomite rims
KS2-22	Npbpdl	Lithoclastic packstone (sandy)																								?	?																	p								Minor dolomicrite clasts - intraclasts (or peloids?), isopachous dolomite cements
RC-14	Npbpdu	Oolitic-peloidal packstone																								f	f						f				f													Ghosted ooid grains (small), dense dolomicrite ovoids - peloids
RC-13	Npbpdu	Stromatolitic boundstone (dolomitized)																								f	f					f	Fe	f																	Sub-angular quartz silt, styolite boundary separates distinct microspar - c.g. spar transition, hexagonal opaques
RC-12	Npbpdu	Stromatolitic boundstone (dolomitized)																																			f														Laminae of dolomicrite and microspar, peloids, karsting/very fractured, opaques isolated to dolomicrite laminae
CP 2-7	Npbpdu	Stromatolitic boundstone																																																Angular f.g. silt, stromatolite with mm-cm scale relief, rare sand=authigenic quartz
CP 2-6	Npbpdu	Oolitic-peloidal packstone																																Fe																	Angular c.g. silt, ghosted ooids/coated grains
CP 2-5	Npbpdu	Sandstone (f.g.-m.g.)																																Fe																	F.g. - m.g sand, sub-rounded to rounded, moderately sorted, cements (1) quartz overgrowth cements + (2) Fe-dolomite
CP 2-4	Npbpdu	Stromatolitic boundstone (dolomitized)																								f	f							f	f		f												?	Sub-rounded silt, Fe-staining, irregular c.g. dolomite patches - possible fenestral fabric
CP 2-3	Npbpdu	Dolomite (c.g.)																								f	f					f	f				f													Stoyolites, dolomicrite clasts (peloids + peloid clusters), m.g dolomite spar, heavily fractured
CP 1-12	Npbpdu	Conglomeratic sandstone (c.g.)																																?																	Sub-angular silt to rounded c.g. sand, granule-small pebble, poorly sorted, intraclasts (wackestone, dolomudstone, lime mudstone)
CP 1-11	Npbpdu	Stromatolitic boundstone																																																Angular to sub-angular silt
CP 1-10	Npbpdu	Oolitic wackestone (c.g. dolomite)																								f	f						?				?													Ghosted small ooids, c.g. dolomite with Fe-staining rhomb boundaries
CP 1-9	Npbpdu	Dolomite (microspar-c.g.)																								f	f						f	f			f													Very disting microspar vs c.g. spar boundary, rounded c.g. sand, hexagonal opaques
CP 1-8	Npbpdu	Lithoclastic wackestone (silty)																							f	f	f						f																	Angular to sub-angular silt, patchy recrystallization, fracture with bladed calcite+equant/blocky calcite+saddle dolomite+hematite
CP 1-7	Npbpdu	Non-calcareous siltstone																																																Angular to sub-angular silt, rare rounded m.g. sand, clay seams/matrix
CP 1-6	Npbpdu	Lithoclastic wackestone-packstone (sandy)																																																Silt-m.g. sand, sub-rounded, polymict
CP 1-5	Npbpdu	Stromatolitic boundstone (dolomitized)																														?				?	?													Significant disruption of irregular laminae, polymict, poorly sorted
CP 1-4	Npbpdu	Calcareous siltstone																																																Angular to sub-angular silt, minor f.g. sand
CP 1-3	Npbpdu	Stromatolitic boundstone (dolomitized)																								f	f						f																	Irregular laminae with mm-cm scale relief of dense dolomicrite (60%) vs calcite spar (40%) with angular quartz silt
CP 1-2	Npbpdu	Stromatolitic boundstone (dolomitized)																								f	f																	m								Sub-angular silt, sand grains=authigenic quartz, cyanobacterial?
CP 1-1	Npbpdu	Oolitic-peloidal grainstone (boundstone?)																																																Mixed ooid types (ooids+superficial+composite), poorly sorted, coarsening-inward dolomite cement
HRF 3-9	Npbpdu	Stromatolitic boundstone (dolomitized)											?													f	f							f										p								Less laminar than below, very patchy dolomite
HRF 3-8	Npbpdu	Stromatolitic boundstone (dolomitized)																								f	f							f																	Sub-angular silt - f.g. sand, very irregular laminae, rare c.g. dolomite
HRF 3-7	Npbpdu	Conglomeratic sandstone (m.g.)																																			?															Polymict, poorly sorted, rounded to sub-rounded, f.g - c.g. sand
HRF 3-6	Npbpdu	Pebble conglomerate																				?														?															Polymict, non-calcareous, rounded c.g. sand to elongate pebble clasts, clast-supported
HRF 3-5	Npbpdu	Dolomudstone																																																	Sub-angular silt, patchy/irregular dolomicrite vs. microspar
HRF 3-4-4	Npbpdu	Lithoclastic-oolitic-peloidal packstone																																																	Coated grains, silt to granule and small pebble clasts (max >5mm)
HRF 3-4-3	Npbpdu	Stromatolitic boundstone																																																	Sub-angular silt, intraclast (mudstone)
HRF 3-4-1	Npbpdu	Lithoclastic-oolitic-peloidal? grainstone																										?																								C.g. coated grains, mixed ooid types (ooids+superficial+composite), elongate to tabular pebble extraclasts
HRF 3-3	Npbpdu	Stromatolitic boundstone (dolomitized)																																	?																	Irregular laminae with dense dolomicrite vs. peloid-dominated zones
HRF 3-2	Npbpdu	Stromatolitic boundstone																																																	Sub-rounded silt
HRF 3-1	Npbpdu	Peloidal? dolomudstone																																			f															Fractured/karsted, evidence of microbial coating/peloids, void cements=(1) silica, (2) calcite, (3) hematite
HRF 2-14	Npbpdu	Lithoclastic wackestone (silty)																																														?				Sub-angular f.g. silt, wavy laminae - cyanobacterial?
HRF 2-13	Npbpdu	Stromatolitic boundstone (dolomitized)																								ff?	ff?																	m								Irregular laminae - calcite vs. dolomitized f.g. silt
HRF 2-12	Npbpdu	Stromatolitic boundstone (dolomitized)																																											p								Alternating wavy laminae and ooids, mixed ooid types (ooids+superficial+composite, small-large), elongate/tabular extraclasts
HRF 2-11	Npbpdu	Pebble conglomerate																																			?	?														Matrix-supported, calcareous siltstone matrix, up to large pebble clasts, ooid-sandy wackestone intraclast, needle-like silica cements
HRF 2-10	Npbpdu	Lithoclastic mudstone-wackestone (silty-pebbly)																																										m								Sub-rounded to rounded c.g. sand, sub-rounded to sub-angular silt, possibly graded
HRF 2-9	Npbpdu	Stromatolitic boundstone																																										p								Angular (to sub-angular) c.g. silt and rare sand
HRF 2-8	Npbpdu	Pebble conglomerate																				?													?															Poorly sorted, clast-supported, polymict, granule to pebble, elongate to tabular clasts, f.g. - c.g. sand, intraclasts (dolomicrite, shale)
HRF 2-7	Npbpdu	Stromatolitic boundstone (dolomitized)																								f	f							f																	Angular to sub-angular silt, disrupted irregular laminae
HRF 2-6-2	Npbpdu	Calcareous siltstone (c.g.) - sandstone (f.g.)																																			?															Very poorly sorted, angular to sub-angular, c.g. silt - granule, ragged grain boundaries=dolomite rhomb replacement?
HRF 2-6-1	Npbpdu	Dolomitic shaley siltstone																																																	F.g. silt to shale
HRF 2-5	Npbpdu	Stromatolitic boundstone										?																																											Disrupted and irregular laminae, possible peloids, silt to pebble clasts
HRF 2-4	Npbpdu	Stromatolitic boundstone																																																	Irregular laminae of micrite vs. spar with sub-angular silt, rare c.g. sand

Table 3. Petrographic analysis of depositional facies in the Patsy Hill Member of the Bonney Sandstone from the suprasalt minibasin adjacent to Patawarta diapir.

SAMPLE NO.	MAP UNIT	LITHOLOGY	GRAIN TYPES																				MATRIX	CEMENT: Calcite								CEMENT					DIAGENETIC FABRIC								SEDIMENTARY STRUCTURES								NOTES
			Calcite	Dolomite	Quartz	Feldspars	Muscovite	Opaque minerals	Fe-oxides	Clays	Cyanobacteria	Ooid	Peloid	Intraclast	Extraclast	Siltstone	Chert	Quartzite+sandstone	Strained/fused quartz	Shale	Meta-igneous	Silicified CO3 (caprock?)		Fibrous	Bladed	Equant	Blocky	Isopachous	Meniscus	Overgrowth	Poikilotopic	Dolomite	Quartz	Chalcedony	Chert	Hematite	Cementation	Micritization	Recrystallization	Replacement	Authigenic crystal growth	Compaction	Dissolution	Dolomitization	Horizontal laminae	Low-angle cross-beds	Hummocky cross-strata	Ripple cross-laminae	Stylonodular texture	Wavy bedding	Fenestral fabric	Mudcracks	
HRF 2-3	Npbpdu	Stromatolitic boundstone (dolomitized)																								f	f																										Very irregular laminae, sub-angular silt
HRF 2-2	Npbpdu	Stromatolitic boundstone (dolomitized)																																										p									Irregular laminae of dolomicrite vs calcite microspar-spar, ooids with micrite rim and sparry center
HRF 2-1-2	Npbpdu	Stromatolitic boundstone (dolomitized)																								f	f					Fe				f																	Faint disrupted/irregular laminae, heavily fractured, fenestral fabric filled with Fe-dolomite cements
HRF 2-1-1	Npbpdu	Dolomudstone																								f	f									f																	Dominantly dolomite microspar, heavily fractured
HRF 1-13	Npbpdu	Oolitic-lithoclastic packstone-grainstone																																										p									Mixed ooid types and sizes (ooids+superficial+composite), c.g. dolomite spar in ooid cores
HRF 1-12	Npbpdu	Oolitic packstone-grainstone																														Fe				f																	Baroque c.g. Fe-dolomite spar with zoning, irregular spar vs. microspar fabric - ghosted ooids
HRF 1-11	Npbpdu	Stromatolitic boundstone																																										p								?	Disrupted laminae, ooids vs sub-angular to sub-rounded f.g. - c.g. sand, mixed ooid types (ooid+superficial+composite+deformed)
HRF 1-10	Npbpdu	Stromatolitic boundstone																								ff	ff																									?	Irregular/disrupted laminae, dominantly f.g. sub-angular silt and rare c.g. sand
HRF 1-9	Npbpdu	Pebble conglomerate																				?																																	Matrix-supported, sub-rounded silt - rounded c.g. sand, up to pebble clasts, polymict, poorly sorted
HRF 1-8	Npbpdu	Stromatolitic boundstone																							?	ff	ff																								?		Disrupted laminae, sub-angular f.g. silt, voids with coarsening-inward calcite cement - fenstral fabric or just recrystallization?
HRF 1-7	Npbpdu	Pebble conglomerate																				?																																	Clast-supported, poorly sorted, polymict, m.g. sand-pebble, unusual alteration minerals
HRF 1-6	Npbpdu	Oolitic-lithoclastic packstone																																																			Patchy micrite/microspar vs spar - ghosted ooids
HRF 1-5	Npbpdu	Stromatolitic boundstone																		?																																	Alternating wavy laminae of calcite spar and clast-rich (sand stringers), f.g. silt - pebble clasts
HRF 1-4	Npbpdu	Pebble conglomerate																		?																																	Clast-supported, poorly sorted, polymict, f.g. sand - small pebble clasts, unusual alteration minerals
HRF 1-3	Npbpdu	Pebble conglomerate																																																			Clast-supported, polymict, poorly sorted, m.g. silt - pebble clasts, unusual feathery opal? cement
HRF 1-2	Npbpdu	Stromatolitic boundstone (dolomitized)																																										p									Disrupted laminae (dolomicrospar - dolomite/calcite microspar - calcite microspar/spar), angular to sub-angular f.g. silt
HRF 1-1D	Npbpdu	Oolitic-lithoclastic grainstone																				?																																	Less laminar than below, polymict, tabular to elongate pebble clasts, mixed ooid types (ooids+superficial+composite+deformed?)
HRF 1-1C	Npbpdu	Lithoclastic-oolitic packstone-grainstone																				?																						m									Similar to above but with smaller ooid fraction, mixed ooid types and sizes
HRF 1-1B	Npbpdu	Lithoclastic-oolitic-stromatolitic boundstone																									f																	m									More laminar than above, more f.g. material, cyanobacterial mat, silt with rare c.g. sand, unusual alteration mineral
HRF 1-1A	Npbpdu	Conglomeratic stromatolitic boundstone																																										p									Pebble clasts, polymict, very poorly sorted, intraclasts (sandy wackestone, c.g.dolomite, dolomudstone)

Curriculum Vita

Cora Evelyn (Evey) Gannaway was born and raised in Collierville, Tennessee. The fourth of five children of Jim and Cass Gannaway, she graduated from Collierville High School in 2005 and enrolled at Sewanee: The University of the South, Sewanee, Tennessee. While pursuing a Bachelor of Science degree in geology, she worked as an intern for SCS Environmental Group during semester breaks from 2006 to 2009 and conducted undergraduate research as a Keck Geology Consortium Project Fellow in 2008. She was a member of the Order of the Gownsmen academic honor society from 2007 to 2009, qualified for the Dean's List in 2008 and 2009, and received the Allen Farmer Award for outstanding senior leadership in the Forestry and Geology Department in 2009. Evey was also a four-year starter for the Sewanee women's soccer team, with whom she received numerous awards including Southern Collegiate Athletic Conference Academic Honor Roll from 2005 to 2008, NSCAA/adidas All-Region Second Team in 2008, and SCAC Co-Offensive Player of the Year in 2008. After graduating *magna cum laude* from Sewanee in 2009, she was a Fulbright Scholar in geological sciences at Technische Universität München-Weihenstephan, Freising, Germany until 2010. She enrolled at New Mexico State University, Las Cruces, New Mexico in the fall of 2011 before transferring to The University of Texas as El Paso in the fall of 2012 to pursue a Master of Science degree in geological sciences. While a graduate student, she received research grants from the Geological Society of America and the American Association of Petroleum Geologists, worked as a teaching assistant for numerous classes at NMSU and UTEP, and completed an internship with ConocoPhillips in Houston, Texas.

Contact information: 4111 Westcity Court
Apt. 206
El Paso, TX 79902
Or
cegannaway@miners.utep.edu

This thesis was typed by Cora Evelyn Gannaway.